Processing and trafficking of Shiga-like toxin 1 in eukaryotic cells.

Submitted for the degree of

Philosophical Doctorate

Nicholas Lea (B.Sc. Hons.)

University of Warwick.

February 1996

Contents

Section 5 References

Acknowledgment.

During my time at Warwick I have received assistance and encouragement from a huge number of people. Without this help I would never have reached this stage.

Dr. Lynne Roberts has provided me with constant and expert guidance, without which I would certainly have been lost. My greatest thanks must go to her for providing me with an opportunity to achieve this much.

Thanks to Professor Mike Lord who has shown an interest throughout my work and has been a source of inspiration and specialist advice during this study. Professor David Crout and Dr. Detter Muller for providing me with globotriose without which this work would have taken considerably longer. Thank you to Professor Arthur Donohue-Rolfe for anti ST serum.

To undoubtedly the richest source of practical and technical support and, when their backs were turned, solutions I thank the members of Plant Biochemistry II. Thank you PBL II for all your handy and not so handy hints and tips and moreover thanks for making PBL II a friendly environment to work in. Special thanks should go to Dr. John Chaddock who was prepared to drop anything to advise me on my latest problem.

Finally I would like to thank Rachel and my family and for all their considerable encouragement and support.

Figure index

Declaration.

Research presented in this thesis was obtained by the author unless specifically indicated in the text. The research presented in this thesis has not been submitted for any previous degree. All sources of information used in the preparation of this thesis are indicated by reference.

Nicholas Lea.

Abbreviations.

Amp	ampicillin
ATP	adenosine triphosphate
BCPIP	disodium 5,-bromo-4-chloro-3-indolyl phosphate
BFA	brefeldin A
BSA	bovine serum albumin
CHO	Chinese hamster ovary
CIP	calf intestine phosphatase
CT	cholera toxin
DMEM	Dulbecco modified eagles medium
ds	double stranded
DT	diphtheria toxin
DTT	dithiothreitol
EDTA	disodium ethylenediaminetetra acetate.
Gb_3	globotriosylceramide
GuHCl	Guanidine hydrochloride
HRP	horse radish peroxidase
IC_{50}	50% cytotoxic dose
IPTG	isopropyl-β-D-thiogalactopyranoside
LB	Luria broth
mRNA	messenger RNA

NBT	nitro blue tetrazolium chloride
PA	anthrax toxin protective antigen
PAGE	polyacrylamide gel electrophoresis
PBS	phosphate buffered saline
PCR	polymerase chain reaction
PE	*Pseudomonas* exotoxin A
PMSF	phenyl methyl sulphonyl fluoride
RIP	ribosome inactivating protein
RTA	ricin toxin A subunit
rRNA	ribosomal RNA
rSLT 1	recombinant Shiga-like toxin 1
SDS	sodium dodecyl sulphate
ss	single stranded
SSC	saline sodium citrate
ST	Shiga toxin
SLT	Shiga-like toxin
TCA	trichloro acetic acid
TPCK	Nα-p-tosyl-L-phenylalanine chloromethyl ketone
TLCK	Nα-p-tosyl-L-lysine chloromethyl ketone
X-gal	5-Bromo-4-chloro-3-indolyl-β-D-galactoside

Section 1

Introduction

Summary

Shiga toxin (ST) and the *Escherichia coli* Shiga-like toxins (SLTs) are type II ribosome inactivating proteins (RIPs). All members of this group exhibit specific RNA N-glycosidase activity, the prototype being the plant toxin ricin. ST and the SLTs are bipartite toxins composed of a catalytic A subunit and a pentamer of cell binding B subunits. These toxins show overall structural similarities to ricin, which is also a bipartite toxin with a catalytic A chain and a single cell binding B chain. The A chains of ST and SLT 1 show homology to ricin A chain, particularly in the active site region, and appear identical in their enzymatic mechanism. The respective B chains however are structurally very different and interact with quite different cellular components.

In this study, the role of intracellular proteolytic activation of SLT 1 is addressed using a molecular biological approach. The biological characteristics of several mutant SLTs has been investigated both *in vitro,* by addition of exogenous protease, and *in vivo* by comparing the relative cytotoxicities of mutant and wild type proteins in Vero cells. The intracellular processing of these mutant toxins has also been examined. In parallel, the biological properties of a ricin A chain SLT 1 chimeric protein has been investigated. The ultimate aim of this study was to extend our knowledge of the proteolytic processing requirements of SLT 1 and it has led to the conclusion that proteolytic removal of the A2 portion of SLT 1 is not an essential prerequisite for intoxication of Vero cells with SLT 1.

1.1 History and Disease

In 1898 , after an epidemic of dysentery in Japan, Kiyoshi Shiga first described the causative agent of a dysentery which was distinct to that of amoebic dysentery and named it *Bacillus dysenteriae*. This was latter named *Shigella dysenteriae* and the disease it caused shigellosis. Shiga toxin was first described by (Conradi (1903)) where it was reported that intravenous inoculation of a lysate of the bacillus *Shigella dysenteriae* paralyzed and killed rabbits. It was this observation which led researchers at the time to consider ST as a neurotoxin. It was later shown that ST acts on various animal species with variable consequences but that only the rabbit and mouse show neurological disorders (Cavanagh *et al* (1956)). Shiga toxin does not act directly on the neurons but can cause secondary neurological disorders by its action on the vascular system of the brain (Howard (1955); Baldini *et al* (1983)). In 1972 Keusch *et al* reported that inoculation of Shiga toxin in ligated rabbit ileal loops caused inflammatory enteritis and resulted in net fluid accumulation.

Konawalchuk *et al* (1977) first described a toxin from *E.coli* which was toxic to Vero cells and was distinct from the heat labile and heat stable toxins from the same organism. This observation led to this toxin being named Vero toxin (VT). Antibody neutralization and molecular biology studies showed that these cytotoxins are

antigenically and genetically related to Shiga toxin (O'Brien et al (1982); Strockbine *et al* 1986,1988)). These observations resulted in the renaming of the toxins to the Shiga-like toxins (SLTs). Further studies of *E.coli* 0157:H7 strain 933 revealed the presence of two toxin-converting phages 933J and 933W (O'Brien *et al* (1984)). These phages carry the structural genes for two distinct cytotoxins (Scotland *et al* (1985)), one of which is neutralized by anti Shiga toxin antisera and one which is not. These two toxins are designated Shiga-like toxin 1 and Shiga-like toxin II respectively. The genes for these two toxins and those of Shiga toxin have been cloned and the nucleotide sequences determined (Calderwood *et al* (1987); Strockbine *et al* (1988); Jackson, *et al* (1987)). The predicted amino acid sequences have shown that SLT 1 is virtually identical to ST and SLT II is 56% homologous to ST. The *E.coli* Shiga-like toxins have been shown to be identical or similar in biological activities to that of ST including receptor specificity (Waddel *et al* (1988); Cohen *et al* (1987)) and enzymatic action (Endo *et al* (1988)). Hence it is proposed that Shiga toxin is the prototype for a family of toxins termed the Shiga-like toxins.

The role that ST and SLTs have in disease is unclear and the method by which these toxins are administered to the host has served to complicate studies. *Shigella dysenteriae* invades and multiplies within the epithelial cells during infection (Sansonetti (1991)). This makes it difficult to distinguish between the responses due to invagination and those attributed to free toxin. Studies in which a toxin-deletion

mutant of *S. dysenteriae* type 1 (Fontaine *et al* (1988)) was used to infect primates, showed that they retained their ability to produce intestinal disease, albeit less severe than disease caused by the wild type tox+ strain. However these data are complicated by the fact that these mutants still produce toxin under certain *in vitro* conditions. The presence of the functional Shiga toxin gene is associated with severe lesions of the colon in rhesus monkey infections not seen with the tox- mutant. The situation with *E.coli* infection is more simple. Infection with SLT-producing *E.coli* does not result in invasion of the epithelial cells. These toxin producing strains have been classed as enterohaemorrhagic *E.coli* (EHEC) and are able to adhere to colonic epithelia and colonize the gut. Numerous outbreaks of haemorrhagic colitis (HC) and the haemolytic uraemic syndrome (HUS) have established a link between these disorders and infection with SLT-producing *E.coli* (Karmali *et al* (1983); Bopp *et al* (1987); Carter *et al* (1987)). Epidemiological studies have demonstrated that *E.coli* serotype 0157:H7 was associated with severe instances of bloody diarrhoea in the United States and Canada (Johnson *et al* (1983); O'Brien *et al* (1983); Riley *et al* (1983); Wells *et al* (1983)). Evidence in favor of a toxin effect *in vivo* is that non invasive EHEC 0157:H7, which produce large quantities of both SLT 1 and SLT II, cause colonic damage from inflammation and ulceration to exacerbation of ulcerative colitis (Hunt *et al* (1989); Ljungh *et al* (1988); Von Wulfen *et al* (1989)). No animal model for HUS or HC has been developed. Rabbit intestine is often used as an *in vivo* model and results using this assay have shown that the effects from ST and SLT from *E.coli* 0157:H7 are similar (Keenan *et al* (1986)).

1.2 Structure and function of ST/SLT 1

SLT is a bipartite toxin composed of a single catalytic A subunit non-covalently associated with five receptor binding B subunits (Donohue-Rolfe *et al* (1984, 1989); Olsnes *et al* (1981)). Comparison of deduced amino acid sequences between ST and SLT has shown that the two toxins are identical (Takao *et al* (1988)) or differ by a single amino acid at position 45 (threonine in ST and serine in SLT 1) (Calderwood *et al* (1987); DeGrandis *et al* (1987) and Strockbine *et al* (1988)). The mature A chain is composed of 293 amino acids with a molecular weight of 32,217 Da and the B chain 69 amino acids molecular weight 7692 Da (Calderwood *et al* (1987); Strockbine *et al* (1988)) Figure 1.3 shows a schematic representation of the SLT 1 structure.

The SLT 1/ST B chain is responsible for receptor binding. The B chain pentamer binds to the cell surface glycolipids with the carbohydrate sequence Galα1-4Galβ (galabiose). Lingwood *et al* (1987) isolated the natural receptor for SLT from Vero cells and showed it to be a glycolipid-globotriosylceramide containing the carbohydrate sequence galactose α1-4galactoseβ1-4glucose-ceramide often referred to as Gb_3 or CD77. Figure1.1 shows the structure of the carbohydrate moitey of the Gb_3 receptor.

Figure 1.1 The structure of globotriose, the carbohydrate component of the Shiga-like toxin 1 receptor globotriosylceramide.

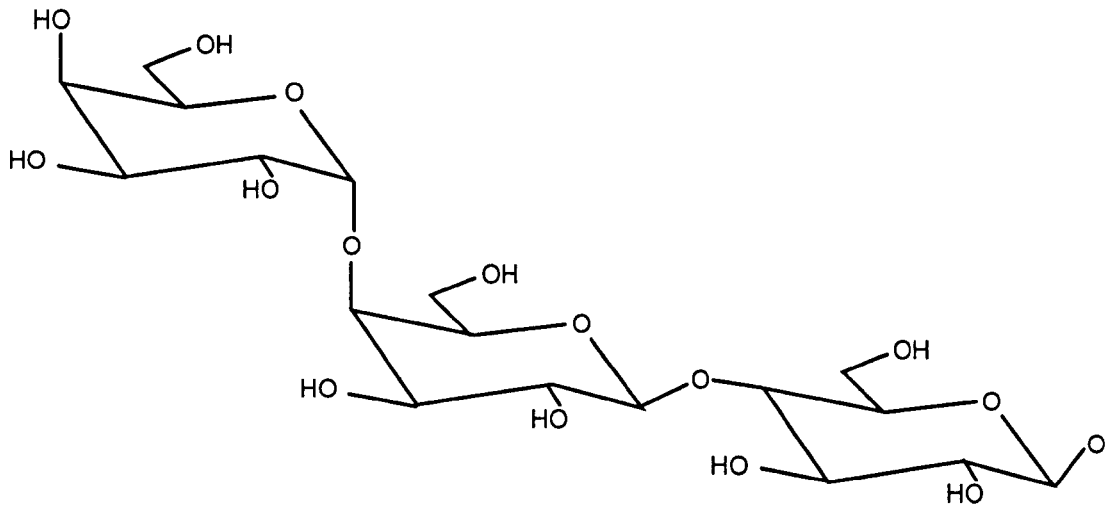

Figure 1.1 The carbohydrate portion of the SLT 1/ST receptor globotriosylceramide is a trisaccharide galactose α1-4galactoseβ1-4glucose. This trisaccharide is (1→1) linked to ceramide to form globotriosylceramide.

SLT 1 B chain has been crystallized (Hart *et al* (1991)) and the structure determined by X-ray analysis (Stein *et al* (1992)). From these studies it was confirmed that the B chain associates as a pentamer. Each monomer of 69 amino acids is comprised of two three-stranded antiparallel β-sheets and an α-helix. β-sheets from adjacent pairs of monomers form six stranded antiparallel β-sheets at the outer surface of the pentamer and the five helices line a pore-like structure in the center of the pentamer. The pore is reported to be 11 Å in diameter and is lined with neutral and non-polar residues. In this study they proposed that the carbohydrate binding site lay within a cleft formed by the β-sheets of adjacent monomers. This cleft is occupied by polar and acidic side chains which it is proposed could make hydrogen-bond interactions with polar groups of the carbohydrate. A schematic representation of the subunit composition of SLT 1 is given in figure 1.3. Several mutagenic studies of SLT/ST B chain are in good accordance with these data. Jackson *et al* (1990) demonstrated that the residues Asp 17 and Lys 53 were important for receptor binding both of which are found in the proposed carbohydrate binding cleft. Mutation of residues Gln64→Glu and Lys66→Gln in SLT IIv (VTE) (a variant of SLT II which is specific for binding to globotetraosylceramide (Gb_4) with terminal GalNAcβ1-3Galα1-4Gal is seen to disrupt Gb_4 binding and allow binding to Gb_3, effectively changing the specificity of SLT IIv to that of SLT 1 (Tyrrell *et al*(1992)). Residues 64 and 66 are located at the lower portion of the carbohydrate binding site proposed by Stein *et al* (1992). Phaedria *et al* (1994) investigated the binding of SLT 1 B

subunit to the trisaccharide [methyl 4-O-(4-O-α-D-galactopyranosyl)-4-O-β-D-galactopyranosyl-β-D-glucopyranoside] and its constituent disaccharides. By Scatchard analysis of binding data they determined that the SLT 1 B pentamer has five identical non-interacting binding sites. On the basis of the thermodynamics of binding, optical spectroscopy and binding-induced protein aggregation they propose a model of SLT 1 membrane interaction which relies on protein-carbohydrate interaction for specificity and protein-lipid interaction for tight binding.

The fatty acid content of the ceramide group of the Gb_3 receptor is important in determining SLT 1 binding. The study of the requirements for toxin binding are complicated by the fact that heterogeneous mixtures of GB_3 molecules with mixed chain lengths appear to bind SLT 1 more effectively than any one homogeneous synthetic receptor (as measured by the TLC overlay assay) (Pellizzari *et al* (1992)). It is postulated by Pellizzari and colleages that the increased affinity is due to cooperative binding of isoreceptors present in Gb_3 of mixed fatty acid content. These mixed isoreceptors would present a non-planar 'receptor surface' which may be a better fit for the three dimensional configuration of the pentameric binding site of the SLT 1 holotoxin. Changes in fatty acid composition can also change the overall orientation of the terminal carbohydrate moiety, which it is speculated, may profoundly affect its receptor function. The actual requirements for effective toxin receptor binding are still not fully understood although it also appears that the lipid

environment in which the receptor molecule resides is also important (Kiarash *et al* (1994)).

The A chain of ST/SLTs can be separated into two domains by a trypsin-sensitive region. Trypsin treatment generates two fragments-A1 approximately 27,000Da and A2 approximately 4000Da, joined by a disulphide bond (O'Brien and LaVeck (1983)). The A1 fragment has catalytic activity (Brown (1980)) and residues within the A2 fragment are required for association with the B chain pentamer (Haddad and Jackson (1993)).

The crystal structure of ST holotoxin has been solved at 2.5 Å resolution (Fraser *et al* (1994)) (shown in figure 1.2). The arrangement of all six subunits is seen. The C-terminus of the A subunit lies in the center of the ring of B subunits. The residues 279-286 form an α-helix which is packed antiparallel to the five helices of the B subunits. The helix is initiated at residue Asp278 at the helix cap position. The first three residues of the helix lie above the B subunit pentamer, the next six residues (occupying 11A) penetrate the 20 Å pore. The last six residues (Arg288-Ser293) could not be seen in the structure. A mutagenic study of residues required for holotoxin assembly was conducted by Haddad and Jackson (1993) which also revealed the importance of residues 279-287 in stabilizing the holotoxin structure.

The disulphide bond which links the A1 and A2 fragments after mild trypsin treatment was confirmed to be between Cys 242 and 261. As seen in figure 1.2 a portion of the A2 fragment lies on top of the B subunit pentamer.

The major contacts between A chain and the B chain pentamer are residues of A2 and a β-hairpin structure from A1. Half of the residues buried in the B subunit pentamer are from the C-terminal helix and this constitutes an area of about 1000Å^2. These data exclude any contacts made by the residues 288-293 for which density was not seen. Interaction between the A chain and the B pentamer is not symmetrical, the majority of the contacts between the pentamer and the A1 portion of the A chain are primarily with just 3 of the five subunits. The residues involved in cleavage of toxin are thought to lie within a loop subtended by a disulphide bond. However the residues of this loop are not seen in the crystal structure. The reason for this is that either the loop is disordered and hence has no definable structure, or that during crystallization, the toxin became nicked. The disulphide loop is placed close to the active site since methionine residue 260 is seen to lie in the active site cleft.

Figure 1.2 Ribbon diagrams of Shiga toxin.

The six subunits of the hexomeric ST holotoxin are shown with the A subunit in yellow above the five B subunits. The carboxy and amino terminals are labelled C and N respectively. The positions of the two cysteine residues Cys 242 and 261 are marked. The approximate position of residues Arg 220 and Arg 223 are also marked. The diagram was reproduced with the kind permission of Marie Fraser,University of Alberta, Edmonton, Alberta, Canada. T6G 2H7

Figure 1.2 Ribbon diagrams of Shiga toxin.

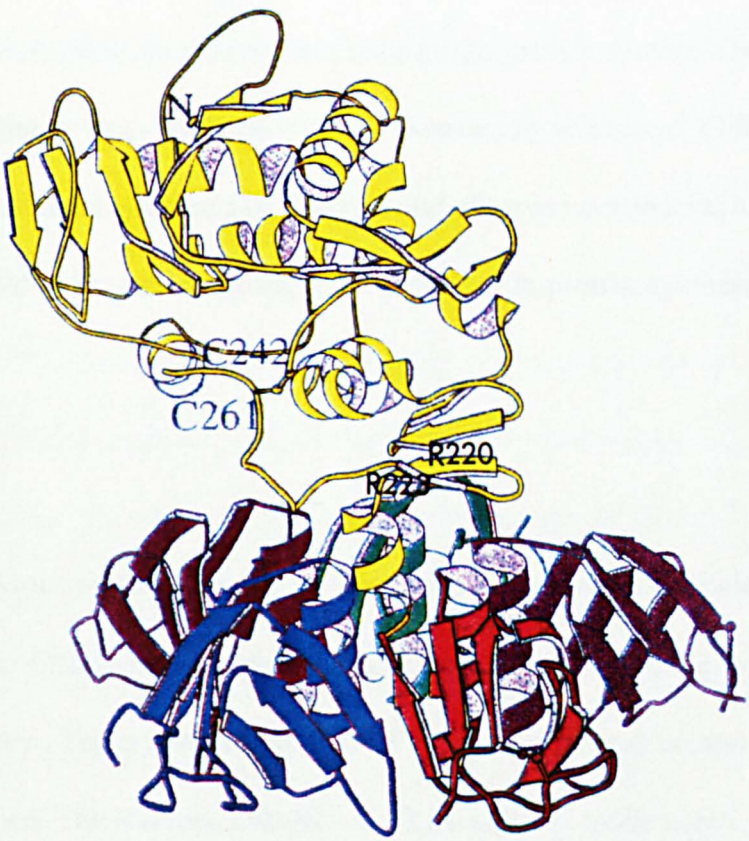

The residues which form the active site are highlighted in the SLT 1 sequence in appendix 5. These include glutamic acid 167, tyrosine 114, tyrosine 77, alanine 168, arginine 170 and tryptophan 203. The active site was identified by using information from other ribosome inactivating proteins such as ricin A chain. The active site residues of Shiga toxin were identified prior to the X-ray crystal structure by sequence alignment and computer modelling (see appendix 1)(Calderwood (1987); Deresiewicz *et al* (1992)) and by specific site-directed mutagenesis. Hovde *et al* (1988) found that mutation of glutamic acid 167, a residue conserved in the active site of ricin A chain, to aspartic acid reduced the protein synthesis inhibition activity of SLT 1 (taken from crude periplasmic extracts) by a factor of 1000. Deresiewicz *et al* (1993) mutated tyrosine 114 to serine and observed a reduction in activity of 500 to 1000 fold as judged by testing (crude) extracts in protein synthesis inhibition assays.

Many previous studies with ST/SLT have shown that proteolytic cleavage and separation of the two domains of the A chain is necessary for the full activity of the toxin *in vitro*. The crystal structure of ST provides a clear structural basis for this phenomenon. The residues 258-262 of A2 lie adjacent to the active site cleft and the side chain of methionine 260 is inserted into the active site of the enzyme. This structural feature explains why removal of the A2 portion of SLT/ST, including residue 260, results in an elevation in enzyme activity.

1.3 Purification of Shiga toxin and the Shiga-like toxins

The purification of ST and the SLTs has been critical in the biochemical characterisation of these toxins and the role they play in the onset of disease caused by *Shigella dysenteriae* and Shiga-like toxin-producing *E.coli*. Numerous methods have been described for their purification both from producer strains and from genes cloned into laboratory strains of *E.coli*. These protocols are of two main types.

Early methods for toxin purification were based on multiple chromatography purifications. One such method described by Donohue-Rolfe *et al* (1984) was used for the purification of ST from a non-pathogenic strain of *S. dysenteriae* type 1 strain 60R (Dubos and Geiger (1946)) This method used bacteria grown to the stationary phase at 37°C in iron-depleted syncase broth. A sonic lysate of the bacteria is subjected to Cibacron Blue F3G-A-Sepharose chromatography followed by chromatofocussing where Shiga toxin elutes in buffer pH 7.0-7.1. The final step of the purification scheme is molecular sieve chromatography with Bio-Gel P-60. Using this method, a yield of 1mg from a 4 liter starting culture was obtained, with a 1300 fold increase in toxin specific activity.

More recently methods for the purification of ST and SLTs have been described which take advantage of the specific binding of ST/SLTs to carbohydrates via the B

chain pentamer. Ryd *et al* (1989) describe the production and subsequent use of α-D-galactose-(1→4)-β-D-galactose-(1→4)-β-D-glucose-(1→) (globotriose or Gb_3) linked to polyacryl/polyvinyl (Fractogel) for the purification of ST from *Shigella dysenteriae* type 1 strain 114Sd. A yield of 36mg of toxin from 12 liters of culture was purified in a single step by this method. A second receptor affinity method reported at the same time (Donohue-Rolfe *et al* (1989)) used P1 glycolipid isolated from the hydatid cyst fluid of sheep infected with *Echinococcus granulosus*. This glycolipid contains galactose α1→4 galactose (to which ST could to bind (Jacewicz *et al* (1986)), linked to activated Sepharose 4B. In a similar method to that of Ryd *et al* (1989), they purified large quantities of ST in a single step. Analog affinity methods of ST/SLT purification prove very successful in the purification of these toxins, they are simple and relatively quick methods which yield highly pure preparations.

1.4 Catalytic action of Shiga toxin and the Shiga-like toxins

ST/SLTs have potent RNA N-glycosidase activity comparable with that of the plant toxin ricin (Endo *et al* (1988)). Once located within the cytosol of a eukaryotic cell this action leads to inhibition of protein synthesis followed by cell death. Thompson

et al (1976) provided the first evidence that ST inhibits protein synthesis in a cell free system using a partially purified ST preparation. Brown *et al* (1980) demonstrated that a pure preparation of Shiga toxin inhibits protein synthesis directly by studies using cell free protein synthesis systems. Since they saw elevated activity in the cell free system after treatment with strong denaturants and reducing agents it was proposed that Shiga toxin is synthesized as a proform. A 70 fold increase in ST activity was seen after treatment with 8M urea and 10mM DTT, they concluded that toxin requires activation prior to exerting its full activity. Reisbig (1981) demonstrated that Shiga toxin or a fragment of it could inactivate salt-washed ribosomes in simple buffered solutions at a rate of 40 ribosomes/minute. Ribosome inactivation does not appear to have a cofactor requirement since addition of 500μM NAD, ATP, NADP and NADH or addition of pH5 supernatant from salt washed ribosomes (containing elongation factors and aminoacyltransferases) did not increase the activity of toxin *in vitro*. Addition of antitoxin during these assays prevented any further inactivation but did not rescue activity already lost indicating that ribosome inactivation is irreversible. Endo *et al* (1988) determined the exact site of action of SLT II and ST. They observed that treatment of eukaryotic ribosomes with either toxin causes release of a 400 nucleotide fragment generated from the 28S ribosomal RNA when the isolated rRNA was treated with acetic-aniline. Analysis of the 3' fragment from cleaved rRNA showed that the adenine base at position 4324 is removed. They also demonstrated that treatment of rat liver ribosomes with toxin resulted in a loss of adenine as judged by thin layer chromatography. Depurination of

rRNA was correlated to inhibition of protein synthesis and of binding of elongation-factor-1-dependent amino acyl-tRNA to ribosomes. They conclude that both SLT II and ST inactivate 60S ribosomal subunits by cleaving the N-glycosidic bond at adenine 4324 in 28S rRNA of the 60S ribosomal subunits. Furutani *et al* (1992) compared the modes of action of SLT and ricin and concluded that they are identical. Osborn and Hartley (1990) examined the effects of ricin A chain (RTA) on the partial reactions of translation of globin messenger RNA (mRNA) in a reticulocyte lysate system. They have shown that the primary block by RTA is the elongation factor 2-dependent stage. Since ST/SLT and ricin are thought to inhibit protein synthesis in an identical manner this is thought to be the mode of action of ST/SLTs also.

1.5 Common features of selected bacterial and plant toxins.

The Shiga toxin family share many structural elements with other bacterial and plant toxins. This feature is important in structural studies of SLT as it allows predictions to be made about the function of structural elements of SLT by analogy with other toxins.

The most striking similarities with SLT are between cholera toxin (CT) and *E.coli* heat labile enterotoxin (LT). Since cholera toxin is considered to be the prototype for the heat labile enterotoxins (Finkelstein (1988)), only this toxin will be considered here. Like SLT, cholera toxin is a bipartite toxin comprised of a single catalytic A chain and a pentamer of cell binding B subunits. Cholera toxin has been crystallized (Spangler (1989)) and the high resolution structure published (Zhang *et al* (1995)). With the structures of CT and LT available (Sixma *et al* (1991) ; (1992)) the structure of the holotoxin and the receptor binding sites can be seen. The overall structural arrangement of the six subunits of CT is identical to that of SLT. Like SLT, CT is proteolytically processed at the junction of the A1-A2 domains. The location at which this processing occurs however is different, CT being nicked by a protease produced by *V. cholerae* hemagglutinin / protease (Booth *et al* (1984)). Hence under normal conditions, the toxin only encounters target cells in the nicked form. This is in contrast to SLT which is secreted to the *E.coli* periplasm in the unnicked form and is thought to be processed later during transport in the target cell (Burgess and Roberts (1993); Garred *et al* (1995a)). As with SLT, CT A interacts with its cell binding pentamer via an A2 domain which inserts into a pore formed by the B chain pentamer. Studies have shown that treatment of the nicked holotoxin with reducing and mild denaturing agents can remove the CT A1 portion leaving, the CT A2-B5 portion intact (Mekalanos *et al* (1979)). This demonstrates that the CT A1 is not required to maintain the non-covalent interaction between the A2 domain and

the B chain pentamer. In a later study the A2 portion of CT was expressed as a fusion with bacterial alkaline phosphatase (BAP), maltose binding protein (MAP) or β-lactamase (BLA) and all three fusion proteins were able to bind to G_{M1} ganglioside (the CT receptor) and the enzyme markers retained activity. This provides further evidence that the A2 portion of CT is responsible for the interaction with its B chain and that the A1 portion is not required to form any of the essential non-covalent contacts (Jobling and Holmes (1992)). When these fusion proteins are expressed in *Vibrio cholerae* they are found in the periplasm rather than being exported as normal to the external medium. This suggests that the A1 domain may be involved in toxin transport across the bacterial outer membrane. However, the possibility that the foreign protein domains fused to CT prevents membrane translocation is also probable. The function of the catalytic domain of CT is different to that of ST. CT A1 catalyses the ADP ribosylation of Gsα, and GTP-binding protein that functions to regulate a component of the plasma membrane adenylate cyclase system, and ultimately acts to activate adenylate cyclase (Gilman (1984)). Despite their difference in function and receptor specificity, the overall structural arrangements of SLT and CT are extremely similar. A detailed comparison of the B chain pentamers of SLT and heat labile enterotoxin was carried out by Sixma *et al* (1993). Despite an almost complete absence of sequence homology between the two pentamers, structural features are highly conserved, with seven out of eight secondary structure elements of the pentamers being retained in the two toxins.

Pseudomonas exotoxin A is a bipartite A-B structure toxin from *Pseudomonas aeruginosa,* the three dimensional structure for which was solved by Allured *et al* (1986). PE is translated as a single polypeptide that has both catalytic and cell binding domains. During toxin entry the protein is separated into two domains by proteolytic activation at a protease sensitive site which remain linked by a disulphide bond (Ogata *et al* (1990)). Numerous mutagenic studies have identified the functional domains of PE. Residues 1-252 (domain Ia) constitutes the cell binding domain, deletion of these residues prevented binding to cells (Hwang *et al* (1987)). Domain II residues 253-364 contains a disulphide-bonded loop in which two trypsin-sensitive arginines lie (Ogata *et al* (1990)). Mutation of these Arg residues reduces cytotoxicity by preventing intracellular processing of the toxin and release of a catalytic portion capable of membrane translocation. A second site within domain II is thought to be responsible for membrane translocation of a catalytic fragment across an internal membrane. Alanine residues 339 and 343 are implicated in this function because mutation to glycines still results in the generation of a catalytic fragment during target cell entry but cytotoxicity is eliminated suggesting that the mutant catalytic fragment can not reach its cytosolic target (Siegall *et* al (1991)). Furthermore fusion of domains I and II of PE with the ribonuclease barnase results in a cytotoxic fusion protein presumably capable of translocation to the cytosol (Prior *et* al 1992).The C-terminal domain of PE contains catalytic activity. Its function is the ADP-ribosylation of cytosolic EF-2 thus preventing host cell protein synthesis (Carroll and Collier 1987). The structural elements of PE described can be seen to

have analogous elements in the SLT structure. For example, a cell binding domain analogous to that of the SLT B pentamer and a catalytic domain which must be cleaved away from other elements of the toxin in order to be fully cytotoxic similar to the A1 domain in SLT. A translocation domain for SLT has not been identified.

Diphtheria toxin (DT) provides another example of a bipartite A-B structure toxin. Like PE, DT is translated as a single polypeptide 62,000 Da (Gill and Dinius (1971); Collier and Kandel (1971)). DT, like other A-B toxins, can be cleaved into two at a surface exposed protease-sensitive loop subtended by a disulphide bond. The loop contains three arginine residues and is sensitive to nicking by trypsin and bacterial proteases (Michel *et al* (1972); DeLange *et al* (1976)). Sandvig and Olsnes (1981) demonstrated that DT required proteolytic cleavage in order to express its full cytotoxicity. The DT structure consists of three domains, the N-terminal catalytic domain (C-domain), the transmembrane domain (T-domain) and the C-terminal receptor binding domain (R-domain) (Choe *et al* (1992); Bennett *et al* (1994)). The C-domain is the portion which enters the cytosol and ADP-ribosylates the side chain of the residue diphthamide, a post-translationally-modified histidine of EF-2 (Van Ness *et al* (1980)). After secretion from *Corynebacterium diphtheriae* and possible extracellular cleavage within the disulphide bonded loop between the C and T domains, DT binds to the DT receptor at the surface of target cells via a β-hairpin loop in the R domain (Shen *et al* (1994)). Internalization to the acidic endosome follows (Morris *et al* (1985)) and the T domain facilitates the translocation of the C

domain across the membrane. From solution of the crystal structure at 2.5 Å (Choe *et* al (1991)) a model for membrane translocation has been proposed. It is thought that the T domain is able to penetrate the membrane in such a way as to form a pore structure through which the catalytic domain can translocate. The charge of two helices within the T domain is highly pH dependent, in the low pH environment of the endosome two of the helices in the T domain become neutral in charge due to partial protonation. It is proposed that following exposure to low pH the tips of these two helices become "membrane soluble daggers" which lead the apolar helix pairs into the membrane. Further experimental evidence for this model was provided by Johnson *et al* (1993) where mutation of proline 345, a residue known to undergo a cis/trans isomerization reaction and thus thought to play a role in conformational changes seen when DT enters a low pH environment, was seen to reduce the cytotoxicity of the toxin by 100 fold.

The plant toxin ricin is a potent cytotoxin found in castor oil plant seeds (Stillmark (1888)). Ricin is isolated as a heterodimer, consisting of a 32 000Da A chain glycoprotein linked by a disulphide bond to a 32 000Da B chain glycoprotein (Olsnes and Pihl (1976)). The B chain of ricin has lectin activity and can bind cell surface galactosides (Olsnes and Pihl (1982)). The A chain has catalytic activity and is responsible for the RNA N-glycosidase activity of ricin (Endo *et al* (1987)) identical to that of ST/SLT 1. The crystal structure of ricin was solved at 2.8 A by

Montfort *et al* (1987) and more recently refined by Rutenber *et al* (1991) to 2.5 Å. The A chain of ricin has some homology to that of SLT 1 (appendix 1 contains an alignment of the active site residues of SLT and ricin). The region of homology lies between the active sites of the two proteins. In a stretch of 73 amino acids, the two proteins have identical residues in 32% of positions and either identical or chemically similar residues in 53% of positions. Using the Chou-Fasman algorithm, virtually identical secondary structure predictions for the two proteins in the active site region were made (Calderwood *et al* (1987)). Interestingly this was one early indication of evolutionary relationships between prokaryotic and eukaryotic toxin genes. The B chains of ricin and SLT 1 have no sequence homology. However both serve the function of binding the toxin moiety to different cell surface molecules and may also be involved in later translocation events. Proteolytic processing of mature ricin A chain (RTA) has been reported by (Fiani *et al* (1993)) in macrophages. However, this work has not been repeatable (Argent (1995)) and it is considered in the absence of other data that RTA remains intact during intoxication. Ricin provides another example of the bipartite A-B family of toxins to which SLT 1 conforms.

Several experiments have demonstrated that isolated domains from bacterial toxins have specific functions. These isolated domains can be transferred from one protein to another. For example the translocation domain of PE, domain II, was fused with the ribonuclease barnase. This protein fusion was potently cytotoxic and thus it was

proposed that domain II of PE was sufficient for translocation of toxin into the cytosol of target cells (Prior *et al* (1992)). In a similar experiment Guidi-Rontani (1992) fused domain II of PE with the catalytic A domain of DT. This chimeric toxin was cytotoxic demonstrating that domain II of PE is sufficient to direct and translocate an enzymatically active heterologous polypeptide segment into the cytosol of sensitive cells and that the A fragment of DT alone contains the catalytic function. In SLT 1 residues involved in carbohydrate recognition were identified by mutation of specific residues of SLT 1 B to the equivalent residues in SLT IIv B (Tyrrell *et al* (1992)). The resultant mutant SLT 1 toxin became specific for binding to the trisaccharide Gb_4 as opposed to the natural SLT 1 receptor Gb_3. These experiments and those discussed previously highlight the similarities between a diverse group of toxins. By studying the toxins as a group a general theme emerges. All the toxins discussed contain cell binding domains analogous to SLT 1 B and a catalytic domain analogous to SLT A1. In addition in several cases a translocation domain has also been identified. By analogy with the toxins discussed it seems reasonable to assume that a translocation domain for SLT / ST is also present, however such a domain has not yet been delineated.

Figure 1.3 Schematic representation of the subunit compositions of selected bacterial and plant toxins.

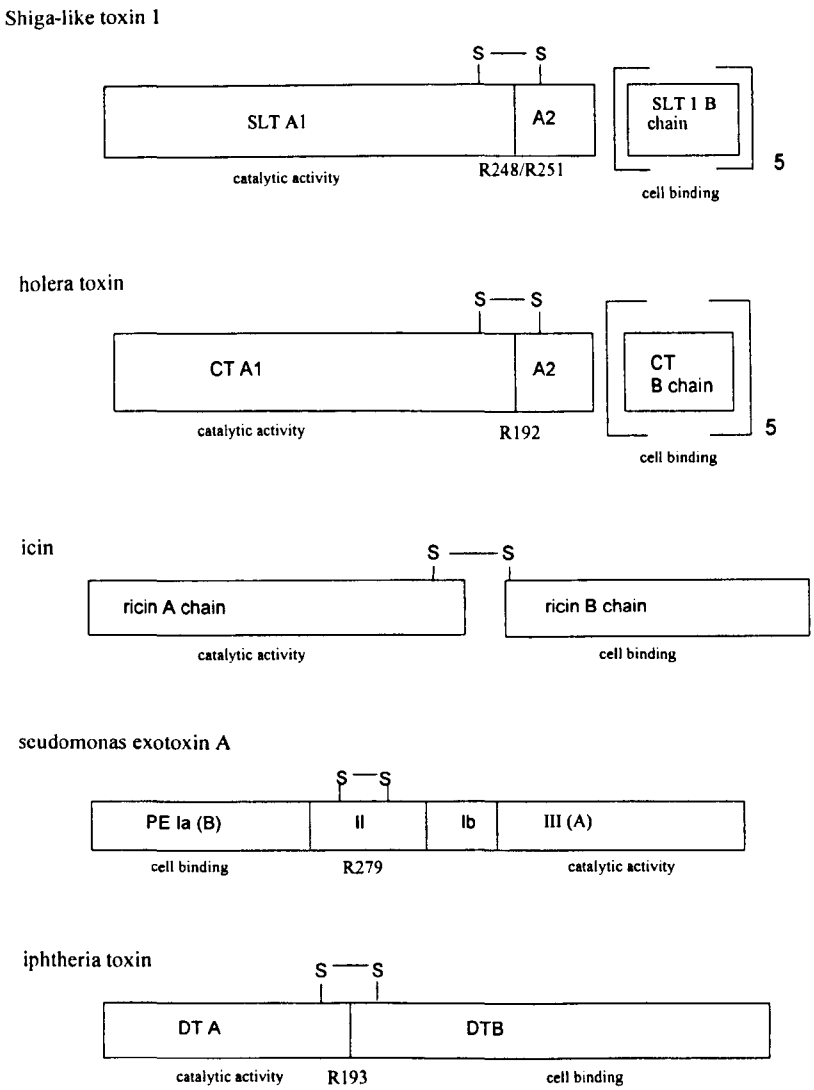

Arginine residues within the trypsin sensitive regions are indicated.

: not to scale

1.6 Proteolytic processing of SLT/ST: Possible analogy with other bipartite toxins.

All the toxins discussed in section 1.5 with the notable exception of ricin, which is cleaved in the seed to the mature form, appear to show an absolute requirement for proteolytic processing in order to generate a catalytic fragment which presumably is capable of translocating an internal membrane. The need for proteolytic processing of SLT 1 is the main area of investigation in the present study. The study of intracellular processing during intoxication with bacterial toxins has been a field of considerable interest in recent years. Observations that many of the bacterial toxins isolated included at least a proportion of nicked toxin led to the hypothesis that these toxins were extremely sensitive to proteases. Improved methods of purification and advances in recombinant protein expression have led to the production of unnicked samples of bacterial toxins and this has allowed their detailed study with respect to the need for proteolytic activation. With the exception of cholera toxin, a single mammalian protease has been implemented in the processing events which take place during intoxication of eukaryotic target cells with bacterial toxins. The protease responsible is the ubiquitous, subtilisin-like endoprotease furin (for review see Barr (1991a)).

Furin has a broad pattern of tissue expression and is conserved amongst eukaryotic species (Schalken *et al* (1987); Barr *et al* (1991b)). The role of furin is to cleave mammalian prohormones and proproteins such as human proinsulin and chicken proalbumin (Brennan and Peach (1991)). It is a dibasic endoprotease which cleaves after the sequence R X R/K R (Barr (1991a)) with a minimum requirement for RXXR (Watanabe *et al* (1993)). Furin has been localized primarily to the trans-Golgi (Bresnahan *et al* (1990); Misumi *et al* (1991)) however other reports indicate that furin has a more extensive cellular location (Tsuneoka *et al* (1993); Klimpel *et al* (1992)).

One well studied example of bacterial toxin processing is that of *Pseudomonas* exotoxin A. Native PE is a proenzyme and to detect its ADP-ribosylation activity in biochemical assays it has to be treated with urea and dithiothreitol to partially unfold the protein (Leppla *et al* (1989); Lory and Collier (1980)). A study by Ogata *et al* (1990) used radiolabelled PE to track the processing events which occur during intracellular uptake and translocation to the cytosol. Their results showed that PE is cleaved within domain II near Arg 279. This cleavage site is within the disulphide loop region and reduction is seen to follow proteolysis. A 37,000 Da fragment is released when Swiss 3T3 cells are incubated with radiolabelled toxin. They determined that this fragment is generated from the C-terminus by comparing the fragments produced by cells following intoxication with N-terminally and C-

terminally labelled toxin. A mutant form of PE where Arg 276 is changed to Gly is 1000 fold less toxic to cells. Incubation of this mutant with cells revealed that it is not proteolytically processed to the 37 kDa size. Further investigation showed that the 37 kDa fragment is the only PE-related fragment which can be detected in the cytosol following wild type PE intoxication. They conclude that proteolytic processing of PE is required for cellular intoxication. This processing was said to occur after Arg residues within the disulphide loop of domain II and, following proteolysis, a 37 kDa fragment was believed to translocate to the cytosol.

More recent studies have revealed that furin is the proteolytic enzyme involved in PE processing. Fryling *et al* (1992) showed that the protease responsible is associated with membranes and is stimulated by divalent ions. This protease is independent of ATP and has a pH optimum of 5.5. Inocencio *et al* (1994) have demonstrated that a Chinese hamster ovary cell line resistant to PE is mutated within the furin gene. This cell line can be made susceptible to PE by transfection of a mouse furin expressing cDNA gene (Moehring *et al* 1993).

Diphtheria toxin has an identical catalytic mechanism to that of PE. Its activity *in vitro* relies on proteolytic cleavage and separation of a 21kDa fragment from the rest of the toxin (Collier and Kandel (1971)). Sandvig and Olsnes (1981) purified

unnicked DT and were able to show that nicked DT is more toxic and that it inhibits protein synthesis more quickly than unnicked toxin. Furin-cleavage of DT was demonstrated by Tsuneoka *et al* (1993), providing evidence that DT can be cleaved *in vitro* by soluble furin. The cleavage site for furin is proposed to be between Arg 193-Ser 194. This site conforms to the minimal consensus recognition sequence for furin (Watanabe *et al* (1992)) and is located in a disulphide loop shown in the crystal structure to be exposed on the protein surface (Choe *et al* (1992)). Furthermore, using an approach similar to that of Moehring with PE (Moehring *et al* (1993)), LoVo cells, a human colon carcinoma cell line which lack functional furin, were incubated with DT. LoVo cells were known to be resistant to intoxication with DT whereas LoVo cells transfected with a mouse furin expressing cDNA were susceptible. It has been reported that DT can also be nicked by furin at the cell surface and in the culture medium in addition to nicking in endosomes (Tsuneoka *et al* (1993)). These results challenge previous studies which indicate that furin is located primarily in the trans-Golgi Network (Bresnahan *et al* (1990); Misumi *et al* (1991)) though it is not clear whether such external enzyme represents a very minor fraction of furin which has escaped the TGN.

Perhaps the first evidence of the involvement of furin in toxin activation was provided by the study of anthrax toxin protective antigen (PA). The causative agent of anthrax is *Bacillus anthracis.* It produces three proteins which, when combined

appropriately, form two toxins. PA and edema factor combine to form edema toxin and PA and lethal factor form lethal toxin. The two toxins are known collectively as anthrax toxin and both conform to the A-B structure toxin model (Leppla (1991)). For intoxication to take place, PA must bind to the cell surface where it is processed by proteolytic cleavage. The bound, activated PA is then able to form ion-conducting channels in cells (Milne and Collier (1993)). Release of a 20kDa fragment allows binding of LF or EF to form ET or LT (Leppla *et* al (1988)) which is then internalized by receptor-mediated endocytosis (Freidlander (1986); Gordon *et al* (1988)). The cleavage of PA occurs after the sequence Arg164-Lys-Lys-Arg167 (Singh *et al* (1989)). Mutagenesis revealed that the toxin must contain the sequence R-X-X-R i.e. Arg residues in the -1 and -4 positions in order to be cytotoxic (Klimpel *et al* (1992)). In the same study it was demonstrated that PA is a substrate for furin *in vitro* and known inhibitors of furin prevent cell surface cleavage of PA. The processing events described are thought to occur at the cell surface, another indication that furin has a ubiquitous cellular location. They concluded that PA is proteolytically-processed by a protease indistinguishable from furin.

A recent study by Gordon *et al* (1995) has provided evidence that PA and DT are cleaved by at least one protease other than furin. It was showed that in contrast to the work of Tsuneoka *et al* (1993), LoVo cells are sensitive to DT using longer incubation periods than studied previously. A mutant CHO cell line (FD11) which is

furin-deficient, is also sensitive to DT and PA but not to a PA mutant with the wild-type cleavage sequence R-K-K-R mutated to R-A-A-R (a cleavage site which does not contain a paired dibasic sequence). They conclude that the sensitivity of this mutant and of DT is due to proteolytic processing by a second enzyme distinct to that of furin which is capable of recognizing paired dibasic sequences. So, although DT can be cleaved by furin *in vitro*, furin may not exclusively nick this toxin *in vivo*.

Cholera toxin has a similar structure to that of heat labile enterotoxin from *Escherichia coli* with a 80% homology between the A chains (Dallas and Falkow (1980)). Despite a lack of sequence homology between CT/LT and SLT these two toxins share remarkable homology with the tertiary structure of SLT 1. Both toxins are seen to require proteolytic cleavage prior to target cell intoxication (Fisherman (1982); Clements and Finkelstein (1979)). However, in contrast to *Escherichia coli* heat labile enterotoxin, cholera toxin is secreted from the bacterium in a cleaved form (Booth *et al* (1984)), whereas *Escherichia coli* heat labile enterotoxin (LT) is produced largely in the unnicked form. By analogy with CT, studies have been conducted to compare the activity of unnicked LT with that of nicked LT. It is reported that nicked LT has greater activity in the skin permeability test than unnicked toxin (Rappaport *et al* (1976)). Experiments with LT intoxication of cells have produced conflicting results. Unnicked toxin appears less toxic to Y1 adrenal cells than nicked toxin (Donta *et al* (1982)) but not to CHO cells (Tsuji *et al* (1984)).

This evidence may suggest that Y1 cells are disabled in their ability to process LT. A more recent study demonstrates that mutation of Arg 192 to Gly (the residue thought to be susceptible to trypsin cleavage *in vitro*) does not reduce the cytotoxicity to CHO cells by a large amount. A slight decrease in the rate of intoxication and a 4 fold reduction in cytotoxicity between unnicked R192-G protein and trypsin nicked wild-type protein was observed (Grant *et al* (1994)). These results do not rule out processing which may occur at a site other than Arg192. In fact LT contains a furin consensus motif at amino acid residues 141-146 which is highly conserved amongst all LT variants (Pickett *et al* (1989)). The data regarding proteolytic activation of LT remains ambiguous and more *in vivo* experiments are required to clarify its role in toxin activation.

As discussed in section 1.4, ST and SLT 1 only display full protein synthesis inhibition activity after separation of the cell binding B subunits and the A2 region away from the catalytic A1 domain. Like many other bacterial toxins, ST/SLT 1 display the structural features of typical A-B toxins. By analogy with other bacterial toxins it seems reasonable to suggest that ST/SLT 1 also have a requirement for proteolytic activation. In common with PE, DT, PA and LT, SLT/ST have disulphide-bonded protease-sensitive loops which contain minimal furin recognition sequences. Kongmuang *et al* (1988) investigated the effect of nicking of SLT 1 on toxicity to Vero cells. Trypsin-treated and intact SLT 1 were incubated with Vero

cells, however no increase in cytotoxic activity between nicked and unnicked toxin was reported. Whether toxin was nicked intracellulary however was not investigated. SLT 1 contains the sequence R248-V-A-R251 in the exposed loop region. Burgess and Roberts (1993) made a mutant SLT 1 R248, R251→G248,G251 which is more resistant to trypsin *in vitro* but is only 10 fold less toxic to Vero cells than the wild type when incubated with cells for 3 hours or less. It was found that if the incubation period is extended the mutant appears as toxic as wild-type protein. Garred *et al* (1995a) mutated the same loop arginine residues of ST and converted them to histidines. They demonstrated by direct visualisation that the mutant ST is still cleaved during Vero cell intoxication and that the A1-sized fragment generated appears identical in size to that generated from the wild-type toxin. In contrast to the processing of ST wild-type, the mutant is not processed in cells pretreated with the fungal metabolite brefeldin A. Brefeldin A (BFA) causes disassembly of the Golgi apparatus and thus prevents transport through the Golgi (Fujiwara *et al* (1988); Lippincott-Schwartz *et al* (1989)). They concluded that the mutant protein is processed more slowly and that for this to occur the toxin must reach a later cellular compartment. They also observed that the mutant toxin is not processed in the presence of the membrane-permeable calpain inhibitor I where as the wild-type toxin is unaffected by treatment of cells with this inhibitor. From these data they conclude that in the absence of the most likely cleavage site in ST, the protein can still be processed by an alternative protease which is inhibited by calpain inhibitor I. It isn't clear from the current literature as to what structural features are recognised by the

ubiquitous Ca^{2+}-requiring enzyme, calpain, nor is the cellular location of this enzyme confirmed, though it is generally believed to be cytosolic (for a recent review see Suzuki *et al* (1995)). From the intoxication time-points used in the study by Garred *et al* (1995a), namely two and four hours, it is conceivable that toxin has by this stage reached the cytosol. That cleavage by calpain might occur in the cytosol to activate the reduced A1 fragment by causing its release from the A2-B_5 complex, suggests that holotoxin itself might be capable of translocating an internal membrane. In the present investigation, shorter incubation times of toxin mutants with cells have been used in an attempt to distinguish any processing in the endocytic pathway from possible processing in the cytosol.

In a separate study by Samuel and Gordon (1994), the loop arginines in SLT IIv were mutated to glutamic acid or histidine residues, toxin labelled with ^{125}I was used to trace toxin processing in target cells. Since the mutant toxins made in this study remained cytotoxic but were processed less efficiently they concluded that proteolytic toxin activation can be mediated by proteases with different specificities to those which cleave the wild-type protein and that efficient cleavage is not required for toxicity.

Garred *et al* (1995b) demonstrated that wild-type ST can be a substrate for furin *in vitro* and that LoVo cells nicked wild-type ST more slowly than LoVo cells transfected with a furin expressing cDNA. LoVo cells pretreated with BFA or calpain inhibitor I were not able to nick mutant ST (Garred *et al* (1995b)). This report clearly demonstrates that furin is the enzyme normally responsible for efficient cleavage of ST in LoVo cells but that other cellular proteases can also cleave the toxin, albeit less efficiently.

In a report by Takao *et al* (1988) the molecular structures of SLT 1 and ST were compared. By performing Edman degradation of trypsin-generated fragments of ST it was observed that the toxin is nicked between Ala 253 and Ser 254. Since this nicking could not have been performed by trypsin they concluded that the ST preparation was pre-nicked at this site. The fragments generated by this nicking were linked by a disulphide bond. Since mutation of the residues Arg 248 and Arg 251 (Garred *et al* (1995a)) did not result in a protein totally resistant to proteolytic attack it is hypothesized that the Ala Ser residues in the loop region may constitute sites for alternative processing . The disulphide loop of SLT 1 contains two pairs of Ala-Ser residues either side of the proposed nicking site Arg248-Arg251. In this study the possible relevance of these residues in the proteolytic activation of SLT 1 is addressed by mutating them to glycine and serine residues. In addition, a second

potential furin-recognition site located upstream at residues Arg 220-Arg223 is also investigated.

Clearly in comparison with other bacterial toxins the number of reports on SLT/ST processing are limited. The only report where protease-resistant mutants have been constructed, expressed and visualized in cells has shown that the mutant protein remains sensitive to host cell proteases (Garred *et al* (1995a). This report, and others using either similar SLT mutants (Burgess and Roberts (1993); Samuel and Gordon (1994)) or using protease-deficient cells (Garred *et al* (1995b)), have yielded information about the physiological events which may occur during target cell intoxication. However there is no literature to address whether the proteolytic separation of the A2 domain away from A1 is a absolute requirement for intoxication and whether the A2 domain provides an efficient block to activity *in vivo*. In the present study mutant SLT 1 proteins which are apparently resistant to host cell proteases are described. The mutant proteins remain cytotoxic in the apparent absence of intracellular proteolytic cleavage. The implications of this for the membrane translocation of SLT 1 and ricin are discussed.

1.7 Endocytosis, intracellular trafficking and membrane translocation of SLT/ST and ricin.

ST/SLT and ricin enter cells via receptor-mediated endocytosis (Sandvig *et al* (1989); van Deurs *et al* (1986); van Deurs *et al* (1988)). Receptor binding sites for ST are located randomly on the cell surface. However following treatment of target cells with ST at 37°C the binding sites become localized in coated pits. Horse radish peroxidase conjugates and colloidal gold conjugates have been used to trace toxin endocytosis and transport. Ricin appears to be endocytosed by clathrin-dependent and clathrin-independent endocytosis (Sandvig *et al* (1982)) whereas ST appears to be internalized exclusively by the clathrin-dependent mechanism (Sandvig *et al* (1989)). The reason for ST being endocytosed by the clathrin-dependant mechanism only is unclear. However this may be due to interactions of the multivalent receptor binding sites on ST with the glycolipid receptors and with underlying coat and plasma membrane proteins. These interactions may be strong enough to ensure that the toxin remains in coated pits. The mechanisms by which clathrin-independent endocytosis occurs are still unclear. A complete understanding of these processes will inevitably reveal the significance between the two mechanisms.

Transport to or through the Golgi complex appears to be important for intoxication of target cells with ST/SLT and ricin. Following endocytosis, toxin conjugates are seen in endosomes, lysosomes and in the Golgi region (van Deurs *et al* (1986); Sandvig (1989)). In the case of ricin the pattern of labelling can be dependent on the type of conjugate used. For example, ricin conjugated to HRP (ricin-HRP) in

polyvalent complexes or ricin conjugated to gold (ricin-Au) is not seen in the Golgi, whereas monovalent complexes of ricin-HRP and native ricin are seen in the Golgi. There are several other lines of evidence which suggest a role for the Golgi complex in ricin and ST/SLT intoxication. Youle and Colombatti (1987) demonstrated that a hybridoma cell line expressing anti ricin B chain antibodies is less susceptible to intoxication by ricin than a hybridoma which does not express the anti ricin IgG. By ruling out cell surface neutralization with a series of controls they conclude that ricin must meet the antibody on the secretory pathway presumably at a point where secretory and endocytic pathways converge, possibly the trans-Golgi network. Transport to the Golgi is inhibited at 18°C (Sandvig *et al* (1986); Deurs *et al* (1987)). and cells are protected from both ricin and ST at this temperature (Deurs *et al* (1987); Sandvig *et al* (1989)) but are not protected from DT which is known to enter the cytosol from acidified endosomes (Sandvig *et al* (1984)). Perhaps more compellingly, brefeldin A (BFA), which disrupts the Golgi stack in Vero cells preventing transport from the TGN to the Golgi stacks and ER, protects cells from ricin and ST (Sandvig *et al* (1991); Yoshida *et al* (1991)). Since it is conceivable that BFA has, as yet ill defined pleiotropic effects, an even better approach has been to block specific transport steps using trans-dominant interfering mutants. Simpson *et al* (1995a) disrupted ER to Golgi trafficking by expressing mutants of Sar 1, intra-Golgi trafficking by expressing mutants of ARF 1 and early Golgi trafficking by expressing mutants of Rab 1. In all cases a significant protection against ricin was observed. *E.coli* SLT 1 likewise was also protected (unpublished data). These data

together suggest that ricin and ST/SLT must either travel to or through the Golgi stack or that they must receive a secreted component while they are located within the TGN, possibly a molecule to assist translocation from the TGN. It has been postulated that transport through the Golgi stack and delivery to the ER is required for ricin, PE, ST and SLTs (Pelham *et al* (1992) .This begs the question can these toxins ever be seen within this compartment?

Visualization of toxins in the ER has proven difficult presumably because in so many cases so little toxin is expected to reach this organelle. In several reports (Sandvig *et al* (1992); Sandvig *et al* (1994)) ST has been demonstrated visually in the ER. In the first description of this, A431 cells had been sensitized to ST with (2mM) butyric acid. Butyric acid sensitizes some insensitive cell lines to ST by altering the composition of fatty acid chains in the ST receptor (Sandvig *et al* (1994)). ST-HRP complexes were clearly seen in endosomes, Golgi, endoplasmic reticulum and in the nuclear envelope following intoxication of A431 cells pretreated with butyric acid (Sandvig *et al* (1992)) The fact that this appearance of toxin in the ER was correlated with acquisition of toxin sensitivity led to the belief that for ST at least , the ER was the translocation compartment. In the later study both ST-HRP and the ST B chain-HRP alone were observed in the ER following intoxication of A431 cells pretreated with butyric acid or with cAMP. These data suggest that the ST B chain is capable of transport from the cell surface to the ER in a retrograde manner in the absence of the

A chain, and that this transport is regulated by fatty acid composition of the receptor molecule and by physiological signals.

Ricin has not been visualized in the large volume of the ER by the same methods and this may reflect the quantity of toxin reaching this destination compared with ST. However there is evidence which supports the hypothesis that ricin like ST requires transport in a retrograde manner to the ER in order to translocate to the cytosol. The data includes that described above (BFA effects and protection against intoxication by mutants of early regulators of secretory vesicle transport). As stated earlier however, these data only suggest a routing of ricin through the Golgi. They can also be interpreted to mean that for ricin, a factor must reach it in the TGN by normal anterograde transport, a process disrupted by BFA and the trans-dominant mutants. For ricin to reach the ER it presumably needs to interact with a recycling component. The most well defined recycling component is the KDEL-receptor, first identified in yeast as the erd2 gene product (Semenza *et al* (1990); Lewis *et al* (1990)), the human homologue of which was described by Lewis and Pelham (1990). The KDEL-receptor has been located throughout the Golgi and is present, albeit in very small amounts, even within the TGN. It is known to retrieve escaped ER residents throughout the Golgi stack (Pelham (1988); Pelham (1990)). One of these retrieved proteins appears to be CaBP3-calreticulin which is galactosylated (Peter *et al* (1992)). There may be other examples of galactosylated ER residents that remain to

be discovered. It has therefore been hypothesised that ricin in the TGN may encounter many newly galactosylated proteins, some of which, like calreticulin, may be ER escapees that are retrieved by the circulating KDEL-receptor and returned to the ER. A very small proportion of the TGN-located ricin may therefore piggy-back to the ER using a carrier (like calreticulin) bound to the KDEL receptor. It has been observed that intracellular galactose-binding is important for full cytotoxicity of ricin (Newton *et al* (1992)), a finding compatible with this model. Of course,not all toxins may need such an indirect association with the KDEL-receptor. PE has a C-terminal tail (REDLK) which, if the C-terminal K is processed intracellularly, resembles the endoplasmic reticulum retention sequence KDEL (Munro and Pelham (1987)). This REDLK sequence is essential for toxicity and is thought to mediate transport of the toxin through the Golgi to the ER via a direct interaction with the KDEL receptor (Chaudhary *et al* (1990)). Interestingly, CT and LT have C-terminal KDEL and RDEL sequences respectively and may use the same strategy to reach the ER. Addition of a KDEL sequence to either whole ricin (Wales *et al* (1992)) or to the A chain (Wales *et al* (1993)) increases its cytotoxicity suggesting that ricin is at least capable of transport to the Golgi where it can be "seen" by the KDEL receptor and that it possibly travels to the ER via an indirect association with this membrane component. The findings here also suggest that the TGN is probably not the site of ricin translocation. If the TGN was the site of toxin entry to the cytosol then addition of a KDEL tag leading to a presumed retrieval to the ER, should result in a decreased rather than an increased potency. Therefore of the two interpretations mentioned

earlier, the model of ricin moving through the Golgi to the ER remains the current favourite.

The ER is an attractive compartment for membrane traversal since it contains cellular machinery which may aid the translocation of a toxic fragment. This organelle is known to contain the enzyme protein disulphide isomerase (Freedman (1989)) which could effect disulphide bond reduction, as well as molecular chaperones (Gething and Sambrook (1992)) and a complete apparatus for translocation of nascent proteins and peptides. It has been proposed that these factors may be required for the reverse translocation of certain toxins (Pelham *et al* (1992)).

Domains responsible for translocation of an internal membrane have been identified in PE and DT. The best studied of these examples is DT which translocates the endosomal membrane to reach its cytosolic target (Sandvig *et al* (1984)). The low pH environment of the endosome is important for the insertion of the DT B-fragment into the membrane (Moskaug *et al* (1991)). Translocation of DT can be mimicked at the plasma membrane by exposing cells to low pH (Sandvig and Olsnes (1980)). Exposure to low pH is seen to induce partial unfolding of the toxin molecule (Dumont and Richards (1988); Jiang *et al* (1991)). Consistent with this idea, it has been found that internal disulphide bonds introduced to the A fragment of DT, to

prevent unfolding, resulted in a significant reduction in the level of translocation either after endocytosis or when surface bound toxin is exposed to low pH (Falnes *et al* (1994)), data which suggests that the low pH-induced unfolding is physiologically relevant to membrane traversal. In addition to unfolding, low pH is thought to be responsible for the insertion of α-helical domains into the membrane which its proposed initiates membrane translocation (Gray *et al* (1993); Moskaug *et al* (1991)). The intense study of the translocation of DT has led to a good understanding of the mechanisms involved in membrane traversal. However, DT appears to be a unique case since it translocates from the endosome and simply requires a low pH to induce the relevant conformational changes. As previously described, other well studied bacterial and plant toxins do not translocate from the endosome but may translocate from more distal intracellular compartments. These proteins, like ST,SLT and ricin cannot be induced to translocate the plasma membrane by exposure to low pH. For these reasons caution must be used in extrapolating results obtained with DT to ST/SLT and ricin.

A translocation domain in PE has been roughly delineated (Siegall *et al* (1991); Prior *et al* (1992)). In the later report, domains I and II of PE are shown to be capable of translocation of the ribonuclease protein barnase into cells which have the PE receptor. Its suggested that this fusion protein binds to target cells via the cell binding domain I. Translocation is attributed to domain II. However no direct

evidence of membrane translocation is presented other than the measurement of cytotoxicity of this fusion.

Specific translocation signals or domains as yet have not been identified for ST/SLT and ricin although some recent work has indicated the importance of certain C-terminal residues of ricin A chain that appear to impede the translocation event (Simpson *et al* (1995b)). However it is always difficult in the absence of a direct translocation assay to be certain that protein stability, routing etc. have not been affected and that any reduction in cytotoxicity observed is exclusively due to a block in membrane transport. The situation is further complicated by the fact that some of these toxins may translocate an active fragment from the ER possibly with the help of their cell binding B subunits. Results presented in a previous study (Garred *et al* (1995a); Garred (1995b)) have suggested that proteolytic release of an A1 fragment from the ST/SLT holotoxin is potentially very important for full toxicity. From work with immunotoxins and other ricin A chain fusions it would appear that toxicity and translocation of ricin can occur in the absence of the B chain a finding in apparent contradiction to results with ricin containing a galactose-binding deficient B chain (Newton *et al* (1992)). Finally, there is the attractive possibility that all these proteins may exploit in reverse, transport machinery already in place for the translocation of nascent polypeptides from the cytosol to the ER. Study in this area is in its infancy. In the absence of a direct membrane translocation assay, studies to determine the

precise structural and factor requirements for translocation of SLT, ST ricin and PE are extremely difficult. Whether ricin, PE and ST/SLT translocate membranes by similar mechanisms and how such toxins are unfolded and rendered competent for this process are piquant questions which as yet remain unresolved.

This present study therefore aims to resolve the absolute need for proteolytic processing of SLT 1 (and, by analogy, ST) as a prelude to other studies on membrane translocation. Using a source of unnicked SLT 1 cellular processing events have been followed.

Project aims

1: To test a new analogue affinity chromatography matrix for purification of unnicked, biologically active SLT 1.

2: To clone the coding sequence for SLT 1 into an expression vector and devise a quick efficient method for the expression and purification of SLT 1 holotoxin and mutant derivatives.

3: To introduce specific mutations into the A chain of SLT 1 at sites potentially involved in intracellular processing. To express and purify these mutant proteins in order to characterize them *in vitro* and *in vivo* in an attempt to examine further the importance of proteolytic processing for SLT 1 cytotoxicity.

4: To produce a chimeric fusion protein which incorporates the A chain of the plant toxin ricin with the C-terminal A2 portion of SLT 1 and the cell binding B subunits of SLT 1. The entry characteristics and the requirements for processing of this chimeric holotoxin are examined to determine more about the need for proteolytic processing.

Section 2

Materials and Methods

2.1. Suppliers and reagents

2.1.1 Suppliers.

The majority of analytical grade chemicals used were obtained from either BDH Chemicals Ltd. Or FSA / Fisons where available. The sources of other specific reagents are detailed below.

Amersham International PLC, Amersham, Buckinghamshire.

Amplify ™

[α^{35}S] dATP (10mci/ml, 1200ci/mmol)

L-[^{35}S] methionine (15mci/ml, 1000ci / mmol)\

Hybond™-C; nitrocellulose membrane, Hybond™-N; nitrocellulose membrane.

BIO 101 Inc. Lajolla, USA

Genelean II kit

Bio-Rad Laboratories Ltd. Hemel Hempstead, Herfordshire.

Pre-stained mid-range molecular weight markers.

Boehringer Mannheim (UK) Ltd., Lewes, East Sussex

calf intestinal phosphatase, creatine phosphate (CIP), sequencing grade trypsin, calpain inhibitor 1.

Cruachem, Glasgow, UK.

PCR primer PSDO

DIFCO Laboratories, Basingstoke, Hampshire.

Bacto-agar, Bacto-tryptone, yeast extract.

Becton Dickinson Labware, New Jersey, USA.

Falcon disposable tissue culture centrifuge tubes, Falcon 3002 60X15 and 3003 100x20 tissue culture dishes.

GIBCO / BRL Life technologies Ltd., Paisley Renfrewshire, Scotland.

T4 DNA ligase, T7 RNA polymerase, deoxyribonucleotides. Taq DNA polymerase, restriction enzymes, T4 polynucleotide kinase

New England BioLabs, Beverley, USA

Msc 1restriction endonuclease, $Vent_R$ DNA polymerase.

Nunclon, Roskilde, Denmark.

175cm^2 tissue culture flasks.

Paterson, Hertfordshire, England

All darkroom reagents.

Pharmacia., Milton Keynes, Buckenhamshire.

M^7G(5')ppp(5')G, Sodium (CAP)

Pierce and Warner (UK) Ltd. Chester, England.

Disposable 5ml columns, Iodogen (1,3,4,6,-tetrachloro-3α-6α-diphenylglycouril) iodination catalyst.

Polaroid, Cambridge, USA.

Polaroid 665 positive and negative, Polaroid positive 665 film.

Promega, Biotechnology P&S Biochemical Ltd., Liverpool Merseyside.

Rnasin, Rabbit reticulocyte lysates, protein molecular weight markers, Plasmid pGEM2

QIAGEN Inc., Chatsworth, USA.

QIApre-spin plasmid purification kit.

Sigma Chemical company Ltd., Poole, Dorset.

Ampicillin, bovine serum albumin (BSA), Coomasie blue G250, dithiothreitol (DTT), ethidium bromide, L-amino acids, phenylmethylsulphonyl fluoride (PMSF) peptide protease inhibitors, TLCK, brefeldin A (BFA). Cell culture media.

United States Bioscience, Cambridge Bioscience, Cambridge.

Sequenase™ DNA sequencing kit version 2.0, T7-GEN™ *in vitro* mutagenesis kit,

2.1.2 Reagents.

2.1.2 Coomassie blue G250 stain.

Coomassie blue G250 stain was prepared by dissolving Coomassie blue G250 in hot distilled water to a final concentration of 0.025% w/v with stirring on a hot plate. When the dye was completely dissolved the solution was allowed to cool and perchloric acid was added to a final concentration of 3.8% v/v.

2.1.2 Aniline reagent.

iAniline was prepared from aniline which had been distilled twice. 1ml of this aniline was mixed with 7ml of autoclaved distilled water and 0.5ml glacial acetic acid in a sterile glass universal. The pH of the aniline was adjusted to 4.5 by addition of more glacial acetic acid and the final volume made up to 11ml. Aniline reagent was stored in the dark at 4°C.

2.1.3 Kirby buffer.

Kirby buffer was prepared by dissolving 6g 4-aminosalicylic acid in 4x Tris-HCl/KCl (Tris-HCl 200mM pH7.6, KCl 40mM). To this solution was added 10ml of 10% Tri isopropylnaphaline-sulphonic acid-Na salt (TNS) w/v. On addition of TNS the solution becomes cloudy, Tris saturated phenol was then added drop wise until the solution cleared. Following addition of phenol the solution was made up to 50ml and stored in aliquots at -20°C.

2.2. Growth and maintenance of bacteria and eukaryotic cells.

2.2.1 Growth and maintenance of bacteria.

All DNA manipulations were performed using *E.coli* strain TG2 with the exception of M13 mutagenesis which requires transformation of mutant single stranded DNA into SDM2. JM105 was used for expression of recombinant proteins.

TG2- SupE hsdΔ 5 thiΔ (lac-proAB) Δ(srl-recA)306::Tn10(tet^r)

F' [traD36 $proAB^+$ $lac\ I^q$ lacZ M15]

JM105- SupE endA sbcB15 hsdR4 rpsL thi Δ(lac-proAB)

F' [traD36 proAB+ lac^q lacZ ΔM15]

SDM2- ϕ80Δ lac Z Δ M15 mcrA Δ(mrr hsd RMS mcrBC) Δ(lac-proAB) Δ(rec A 1398) deoR rpsL srl thi

F'[traD36 proAB+ lac I^q lacZ ΔM15]

Bacterial strains were maintained on minimal medium agar plates consisting of 1× M9 salts (12.8% (w/v) $Na_2HPO_4.7H_2O$, 3% (w/v) KH_2PO_4, 0.5% (w/v) NaCl, 1% (w/v) NH_4Cl), 2μg/ml thiamine, 4% (w/v) glucose, 0.1 M $CaCl_2$, 10mM $MgCl_2$, 10 mM $MgSO_4$ for up to one month before re-streaking onto fresh plates.

Liquid culture of both TG2 and JM105 was performed in L-broth (Luria Berani medium:1% (w/v) NaCl, 1% (w/v) bactotryptone, 0.5% (w/v) yeast extract).

Selection pressure for the retention of plasmids in *E.coli* was provided by including ampicillin to a final concentration of 100μg/ml in both plates (L_{amp}) and liquid media ($L\text{-broth}_{amp}$)

2.2.2 Preparation of competent cells.

Competent cells were prepared by calcium chloride treatment. 1ml from a 10ml overnight culture of *E.coli* in L-broth was used to inoculate 40ml of L-broth. This culture was incubated at 37°C 200rpm until the optical density at 600nm reached 0.9. Cells were harvested by centrifugation at 2000 × g for 10 minutes at 4°C, the cell pellet was resuspended in 10ml of ice cold 0.1M $MgCl_2$ and the cells immediately centrifuged. The washed cell pellet was resuspended in 2.5ml of ice cold 0.1M $CaCl_2$ and incubated on ice for at least 2 hours. Cells were then used within 24 hours or were frozen as 200µl aliquots in 50% glycerol at -70°C.

2.2.3 Growth and maintenance of Vero cells.

Vero cells were routinely grown in 175 cm^2 vented Nunclon tissue culture flasks with Dulbecco Modified Eagle's Medium (DMEM) (DME plus 5% heat inactivated foetal calf serum, 2mM glutamine, 50 IU/ml penicillin, 300µg/ml streptomycin) in a 5% CO_2 incubator. Vero cells were stored frozen in freezing mix (50% heat inactivated foetal calf serum v/v, 40% DMEM v/v, 10% DMSO v/v) under liquid nitrogen.

2.3 Manipulation of nucleic acids.

2.3.1 Transformation of plasmid DNA

100µl of fresh competent cells or 200µl of frozen cells were used in each DNA transformation. Plasmid DNA was added to the cells and mixed gently. The cells were held on ice for 45 minutes then exposed to heat shock, 2 minutes 42°C. The transformed cells were returned to ice briefly prior to plating on dry L_{amp} plates. Plates were incubated overnight at 37°C

2.3.2 Transformation of M13 DNA.

100µl of fresh or 200µl of frozen competent cells were used in each DNA transformation. M13 DNA (double or single stranded) was incubated with competent cells on ice for 45 minutes. The cells were exposed to heat shock for 2 minutes at 42° C and returned to ice. 3ml of B-top (0.8% (w/v) bactotryptone, 0.5% (w/v) NaCl, 0.6% (w/v) bactoagar), 100µl log phase TG2, 10 µl 100mM IPTG and 25µl X-GAL (50mg/ml) were added to sterile universals and maintained at 42°C . The transformed cells were added to the molten agar, mixed and poured onto dry B-agar plates (0.8% (w/v) bactotryptone, 0.5 % (w/v) NaCl, 2% (w/v) bactoagar) and incubated overnight at 37°C.

2.3.3 Purification and concentration of nucleic acids from aqueous solution.

Phenol extraction

To a protein contaminated DNA solution an equal volume of phenol/chloroform was added. The sample was vortexed briefly and centrifuged at 13 000 x g for 1 minute. The upper aqueous phase was transferred to a clean tube.

Ethanol precipitation

To an aqueous solution of DNA a one tenth volume of 3M sodium acetate and 2 volumes of ice cold ethanol was added. The sample was mixed and held on dry ice for 15 minutes. DNA was pelleted by centrifugation at 15 000 x g for 20 minutes at 4 °C. The pellet was rinsed in cold 70% ethanol, vacuum dried and resuspended in TE buffer (10mM Tris HCl pH 7.4, 1mM EDTA pH 8.0).

2.3.4 Separation of nucleic acids by agarose gel electrophoresis.

0.8% w/v agarose gels were routinely used for separation, visualisation and isolation of DNA fragments.

0.8g of agarose was melted in a microwave oven in 100mls of 1× TBE (900mM Tris HCl, 900mM Boric acid, 25 mM EDTA). 10µl of ethidium bromide (10mg/ml) was

added, the gel cast, placed in a horizontal electrophoresis tank and covered with 1 litre of 1× TBE buffer. Samples were loaded in 1× loading buffer (10× TBE, 50% (v/v) glycerol, 0.01% bromophenol blue). A 60mA current was applied to the gel and migration was monitored by visualising under a long wave UV source.

Formamide - Agarose gels.

Resolution of aniline-treated ribosomal RNA was achieved using 1.2% w/v agarose in 0.1 x TPE buffer (3.6mM Tris, 3mM NaH_2PO_4, 0.2mM EDTA), 50% formamide. 100ml in a 15x15cm gel former. Aniline treated RNA was heated to 65°C for 5 min and cooled briefly on ice and sample buffer (50% v/v glycerol, 0.1% w/v bromophenol blue) 3 µl was added to 10µl of sample. Prior to loading all wells were filled with 60% formamide in 0.1x TPE. RNA samples were loaded on to the gel and the apparatus filled with 0.1x TPE just enough buffer not to submerge the gel was added and the gel run 20mA for approximately 2 hours. Gels were stained by immersing in 1 litre of ethidium bromide solution 20µg /ml for 30 min followed by de-staining in water for approximately 1 hour with several changes in wash. RNA was visualised by UV illumination.

2.3.5 DNA polyacrylamide gel electrophoresis.

[^{32}P]-labelled oligonucleotides were separated on 16% polyacrylamide urea gels. A gel mix was made and stored at 4°C.

Gel mix:, 80ml 40% acrylamide w/v 2% bisacrylamide w/v, 20ml 10×TBE, 92g urea, made upto 200ml with water.

A single gel was made by polymerisation of 45ml gel mix with 90µl 25% APS w/v and 90µl TEMED. Gels were run at 40mAmps constant current for the appropriate period of time. Gels were then dried and exposed to Fuji RX x-ray film at -70°C with an intensifying screen.

7.2% w/v polyacrylamide urea gels were used for the separation of sequencing products.

Gel mixture: 9ml 40% w/v acrylamide 2% bisacrylamide w/v, 6ml 10×TBE, 25.2g urea, 25ml water, 140µl 25% APS w/v, 140µl TEMED. Gels were then dried and exposed to Fuji RX x-ray film at room temperature.

2.3.6 Preparation of plasmid DNA

Small scale preparations of plasmid DNA from *E.coli* were made using the QIAprep spin miniprep kit (a modification of the alkaline lysis method of Birnboim and Doly 1979) according to the manufacturers instructions. Briefly the method involves lysis of an overnight culture of *E.coli* followed by precipitation of contaminating protein and chromosomal DNA. The resulting plasmid DNA solution is then adsorped onto a DNA binding membrane washed and eluted with low TE buffer (10mM Tris HCl, 0.1 mM EDTA).

Large scale DNA preparation was performed using a modification of the alkaline lysis method of Birnbiom and Doly (1979). *E.coli* transformed with the plasmid of interest were grown overnight in 40ml of L-broth$_{amp}$ with shaking (200 rpm). Cells were pelleted 2000 × g 10 minutes 4°C. The cell pellet was resuspended in 2ml of ice cold SET (25mM Tris HCl pH 8.0, 10mM EDTA, 15 % sucrose). To this cell suspension 0.2ml lysozyme (20mg/ml) was added and placed on ice for 5 minutes. 4ml lysis mix (0.2M NaOH, 1% SDS w/v) was added whilst vortexing and placed on ice for 10 minutes. 3ml of 3M sodium acetate (pH 4.8) was added whilst vortexing and placed on ice for 15 minutes. Cell debris was removed by centrifugation at 17,500 ×g for 20 minutes at 4°C. The supernatant was extracted twice with phenol/chloroform and precipitated as in (2.3.3)

2.3.7 Preparation of single stranded M13 DNA

M13 DNA consists of two strands + and -, single stranded + form DNA was prepared for use in mutagenesis reactions or for single stranded sequencing by exploiting the life cycle of the M13 phage.

To sterile universals 3.5ml L-broth was added, 100µl of overnight TG2 culture and a plaque plug (taken from an agar plate with a sterile Gilson tip) from an M13 transformation (2.3.2). This culture was incubated at 37°C with shaking (300 rpm) for 6 hours. 1.5ml of this culture was centrifuged at 13 000 × g at room temperature for 5 minutes. The supernatant was transferred to a clean tube (the pellet was used to

make double stranded DNA using the QIAprep method (2.3.6) (if required). To the supernatant was added 150µl (20% (w/v) PEG 6000, 2.5M NaCl), mixed and incubated at room temperature for at least 20 minutes. The aggregated virus was pelleted by centrifugation 13 000 × g at room temperature and the PEG solution removed. The tubes were re-centrifuged and the remaining PEG solution removed by aspiration. The pellet was resuspended in 120 µl TE buffer and the viral proteins removed by extraction with 50µl of phenol and DNA precipitated from the aqueous phase (2.3.3). The dried pellet was resuspended in 20µl TE and stored at -20 C.

2.3.8 Preparation of double stranded M13 DNA.

25µl of log phase TG2 was used to inoculate 10ml of L-broth into which was added a plaque plug from an M13 transformation (2.3.2). This culture was incubated overnight at 37°C with shaking (200 rpm). 40ml of L-broth was inoculated with 1 ml of a 10ml L-broth TG2 overnight culture and incubated with shaking (200rpm) until the optical density at 600nm reached 0.5. 100µl from the M13 containing culture was added and the culture incubated at 37°C with shaking (300rpm) for 4 hours. The cells from this culture were pelleted and viral DNA isolated using the alkaline lysis method (2.3.6).

2.3.9 Gel isolation of DNA fragments.

Restricted plasmid vector DNA, excised DNA fragments and PCR products were purified prior to subsequent cloning steps using the Geneclean II kit (Bio 101 Inc.). DNA fragments are first separated by agarose gel electrophoresis (2.3.4). The band of interest is excised from the gel and dissolved in NaI. A DNA binding resin is added which binds DNA under conditions of high ionic strength. The resin is then washed and pure DNA is eluted using low salt buffers such as TE or low TE.

2.3.10 Enzymatic modification of DNA

All enzymatic modifications to DNA were made as directed by manufactures unless stated otherwise.

2.3.11 Phosphorylation of oligonucleotides.

Oligonucleotides used for site directed mutagenesis were phosphorylated prior to use. Several oligonucleotides were also phosphorylated in the presence of gamma [^{32} P]-ATP in order to visualise and assess the integrity of DNA or for use as a probe in Northern blot analysis (by phosphorylation of the 5' terminus of the DNA with radioactive phosphate and visualising by polyacrylamide gel electrophoresis (2.3.5).

A kinase buffer was prepared to 10× working concentration; 1M Tris HCl pH 8.0, 100mM $MgCl_2$, 70mM DTT, 10mM ATP (ATP was omitted when labelling DNA with radioactive phosphate) and stored at -20°C. Phosphorylation reaction: 2.5µl oligonucleotide (5 OD_{260nm} units/ml) was added to 3µl 10× kinase buffer, 24µl water and 0.5µl T4 polynucleotide kinase. For the preparation of radioactive oligonucleotides, 0.5µl (10µCi) $\gamma[^{32}P]$-ATP was added. The reaction mixture was incubated at 37°C for 15 minutes followed by inactivation by incubation at 70°C for 10 minutes.

2.3.12 Oligonucleotide Site directed mutagenesis.

The USB T-7 GEN *in vitro* mutagenesis system was used for the preparation of mutant M13 DNA. The system functions by binding a mismatch oligonucleotide to the template to be mutated, this oligonucleotide is then extended in the presence of 5-methyl dCTP producing a double stranded hetroduplex DNA in which the mutant strand is methylated. The parental strand is then nicked and destroyed by exonuclease activity leaving only the mutant strand which is then transformed into competent SDM2 cells. The kit was used as directed by the manufacturers instructions. Transformants were screened by DNA sequencing (2.3.13).

2.3.13 DNA sequencing.

Single stranded M13 DNA (2.3.7) was sequenced using Sequenase® T7 DNA Polymerase kit version 2.0 (United States Biochemical) using oligonucleotide primers complementary to the sequence of interest. This kit exploits the chain termination DNA sequencing method (Sanger *et al* 1977). The kit was used in accordance with the manufactures instructions. Products of the sequencing reactions were separated on high resolution polyacrylamide gels (2.3.5) and visualised by autoradiography.

2.3.14 DNA quantitation.

DNA was quantified by reading absorbance at 260nm Maniatis *et al* (1989).

2.3.15 Polymerase chain reaction amplification.

Specific mutagenic PCR methods are discussed in subsequent sections. All reactions were carried out using a Hybaid thermocycler. PCR products were purified by phenol extraction and ethanol precipitation (2.3.3) followed by gel isolation (2.3.9) prior to all enzyme treatments.

2.3.16 Preparation of rabbit reticulocyte ribosomes.

Rabbit reticulocyte ribosomes were prepared from rabbit reticulocyte lysate (non-nuclease treated) (Promega). 1ml of rabbit reticulocyte lysate was centrifuged through a 1ml ice cold 1M sucrose pad in 1x ENDO buffer (25mM Tris-HCl pH7.6, 25mM KCl, 5mM $MgCl_2$) at 100 000 x g for 1hr at 4°C. The supernatant was poured off, 2ml of ice cold 1x ENDO buffer was added to the tube and immediately poured off. The resulting partially purified ribosome pellet was resuspended in 1ml of ice cold 1x ENDO buffer on ice with a glass rod. The ribosomes were re-pelleted by centrifugation at 100 000 x g for 1 hour and the supernatant discarded. The ribosome pellet was resuspended in 100µl of 1x ENDO buffer. The ribosome concentration was estimated by spectrophotometery using the formula that 1mg/ml of ribosomes is equivalent to 12.5 OD units at 260nm. Ribosomes were stored in small aliquots at -70°C.

2.3.17 Northern blot analysis.

Northern blot analysis was used to visualise the specific 400 nucleotide RNA species produced by cleavage of modified rRNA on aniline treatment (2.7.3). The primer CL580 with the sequence 5'CAT AAT CCC ACA GAT GG 3' end labelled with [^{32}P]-γATP (2.3.11) was used as probe in these analysis.

Following separation of RNA (2.3.4) on denaturing formamide gels, rRNA was transferred to a nitro-cellulose membrane (Hybond-N). The gel was first soaked in 0.05M NaOH for 20 min then rinsed briefly in distilled water and then immersed with agitation on a rotating platform in 20x SSC (NaCl 175.32g/l, Tri sodium citrate:$2H_20$ 88.2g/l pH7.0). Following equilibration with 20x SSC the gel and a piece of nitro-cellulose pre-soaked in 20xSSC were assembled in a vacuum blotting apparatus (vacugene, Pharmacia) according to the manufacturers instructions and transferred for 60min. When transfer was complete the apparatus was disassembled and the membrane rinsed in 6x SSC to remove gel debris. The air dried membrane was fixed by UV irradiation using a Stratalink set on autolink (1200 joules).

Northern blots could be stored at this stage or probed directly. Northern blots were pre-hybridized by incubation at 37°C for 2 hours in pre-hybridization buffer (6x SSC, 0.3% SDS, 5x Denhardts solution (100x Denhardts 20g/l Ficoll type 400,20g/l polyvinylpyrridine, 20g/l bovine serum albumin), 90μg heat denatured sonicated salmon sperm DNA (Pharmacia)) using a hybridization oven (Hybaid). When pre-hybridization was complete 50pmoles of labelled CL580 oligonucleotide (2.311), precipitated in the presence of 30 μg sonicated salmon sperm DNA, was added in 10 ml of fresh pre-hybridization buffer by passage through a Dynoguard filter. Hybridization was achieved by incubation overnight at 37°C. The following morning the membrane was washed once in 2x SSC at room temperature then twice at 37°C for 30 min. The membrane was then removed from the bottle, wrapped in cling film

and exposed to pre-flashed RX x-ray film with an intensifying screen overnight at -70°C

2.4 *in vitro* Transcription / Translation.

2.4.1 *In vitro* transcription

Recombinant SLT 1 A coding DNA was cloned into pGEM 2 vector and orientated such that transcription *in vitro* could be driven by the viral promoter T7. Prior to transcription reactions, plasmids were linerised at convenient restriction sites. Transcription was carried out by the method of Maniatis et al (1989).

2.4.2 Wheat germ lysate *in vitro* translation.

Wheat germ lysate was a kind gift from Dr J. Chaddock and Dr A. Messiah (Warwick). Wheatgerm translations were carried out using standard methods Maniatis et al (1989). Translations were carried out in the presence of [^{35}S]-methionine and the products separated on 15% SDS polyacrylamide gels (2.7.7).

2.4.3 Rabbit reticulocyte lysate *in vitro* translation.

(i) Double translation assay.

Rabbit reticulocyte lysate (Promega) translations were carried out in the presence of [^{35}S] methionine as directed in the manufacturers instructions. However to detect the expression of a protein with potentially N-glycosidase activity, the ability of a rabbit reticulocyte *in vitro* translation reaction to translate a second message was examined. Following expression of a potentially toxic protein 30 min at 30°C a second non-toxic messenger RNA (yeast prepro-alpha factor) was added to the reaction for a further 30 min 30°C. The translation products were then separated on 15% SDS polyacrylamide gels (2.7.7).

(ii) Examination of ribosomal RNA following *in vitro* translation.

In order to detect small quantities of potentially toxic proteins translated *in vitro*, ribosomal RNA can be extracted from a standard rabbit reticulocyte translation reaction and examined for characteristic depurination. A rabbit reticulocyte *in vitro* translation reaction using a mRNA coding a potentially toxic protein was set up using the manufacturers instructions. Radioactive label is substituted for unlabelled methionine. Following translation of the test mRNA, ribosomal RNA is extracted (2.7.3), treated with aniline (2.7.3) and separated on a denaturing formamide gel (2.3.4).

2.5 *In vivo* expression of recombinant proteins.

Expression of all recombinant proteins was performed in *Escherichia coli* JM105. All recombinant *in vivo* expression plasmids were constructed in pUC19 incorporating the amp^r gene. Expression was driven by the IPTG inducible promoter laq^Z. The SLT 1 B chain expression plasmid pSBC32 Calderwood *et al* (1990) contains the SLT 1 B coding sequence in the plasmid pKK233.2 under the trc promoter and was a kind gift from Dr S. Calderwood (Boston, USA).

2.5.1 Expression of unlabelled recombinant proteins.

Plasmids coding for the protein of interest were transformed into JM105 (2.3.1). A single colony was used to inoculate a 10ml LB_{amp} overnight culture. The following day 1 litre of LB_{amp} was inoculated with 10ml of overnight culture. The culture was grown with shaking at 37°C 250rpm until the optical density at 600nm reached 0.6. The culture was then induced by addition of IPTG to a final concentration of 1mM and shaking incubation was continued for a further 3 hours. All the recombinant holotoxin protein expression and periplasm extraction was carried out in a category III containment laboratory.

2.5.2 Preparation of periplasm extracts

Following growth and induction of transformed Escherichia coli, cells were harvested by centrifugation at 700 x g at 4°C for 30 min. The resulting cell pellet was gently resuspended in 20ml Tris/Sucrose (0.3M Tris pH8.0, 1mM EDTA, 0.5 mM $MgCl_2$ 200g/l Sucrose) and incubated at room temperature for 10 min. Cells were then re-centrifuged at 4 400 x g at 4°C for 5 min. The supernatant was carefully removed from the cell pellet and discarded. The cell pellet was then resuspended in 10ml of ice cold 1mM Tris pH7.5 and incubated on ice for 10 min before removing cell debris by centrifugation 31 000 x g at 4°C for 15 min. The resultant supernatant containing the periplasmic fraction was filter sterilised before removal from the category III laboratory and subsequent purification.

2.6 Protein purification.

2.6.1 Purification of recombinant proteins.

Galα1→4Galβ1→4Glc (globotriose) linked to activated Sepharose 4B via a 6(CH_2) linker (Gb_3-Seph.) was a kind gift from Dr D. Muller (Warwick). This matrix was used for the affinity purification of SLT 1 and mutants, it was also used in the purification of RTASTA2 and SLT 1 B chain alone.

A 1ml column of Gb_3-Seph. was equilibrated with 0.5M NaCl in PBS. 10ml of periplasm extract from an SLT expression (2.4.1) was applied to the column at a flow rate of 0.4 ml/min. The column was then washed with approximately 40 column volumes of 0.5M NaCl in PBS to remove all traces of non-specifically binding *Escherichia coli* proteins. Elution of pure fractions of SLT 1 was achieved by addition of 6M Guanidine HCl pH6.7 at 0.4 ml/min. 0.5 ml fractions were collected in Ependorff tubes preloaded with 0.5 ml of 6M Guanidine HCl pH6.7 to immediately dilute protein 2 fold. After collection of approximately 15 fractions the absorbance of each fraction was determined at 280nm in a spectrophotometer. Fractions in the peak were immediately dialysed against PBS, with buffer changes after 1, 3 and 12 hours, overnight. All purification procedures were carried out at 4°C in a cold room. Purified proteins were analysed by SDS PAGE and quantified as described in (2.7.1)

2.6.2 Purification of Native SLT 1 from *Escherichia coli* 026:H11, strain E3787

Escherichia coli 026:H11 strain E3787 was obtained from the National Type culture collection on the advice of Dr S M Scotland (Public Health Laboratory Service, Collingdale). This was then grown under category II containment at PHLS CAMR, Porton Down using the method of O'Brein *et al* (1982b). The resulting cell paste from 2x 10 liter cultures was a kind gift from Dr B Burgess, Warwick.

Purification was a modification of the method of Ryd *et al* (1989). Approximately 4g of cell paste was re-suspended in 20ml PBS and sonicated using an MSE Soniprep 150 sonicator 10x 20 sec bursts at amplitude setting 22. Centrifugation at 10 000 x g for 45 min at 4°C was used to remove cell debris. The supernatant was then precipitated with ammonium sulphate to 60% saturation (Petric *et al* (1987)) for 1 hour with stirring at 4°C. Precipitated proteins were separated by centrifugation at 10 000 x g for 10 min at 4°C. The precipitated protein pellet was then resuspended in 20ml PBS and dialysed against PBS overnight at 4°C. This protein preparation was filter sterilised and applied to a 1ml Gb_3-Seph. column. Further purification steps were as in (2.6.1).

2.6.3 Storage of recombinant proteins

Recombinant SLT 1 holotoxins and fusion proteins were stored for short periods of time in PBS at 4°C, if proteins were likely to be stored for more than one month small aliquots were kept in PBS at -70°C. Recombinant ricin A chain (ICI) and native ricin holotoxin (Sigma) were routinely stored at 4°C. SLT 1 B chain was stored in PBS at -20°C. [^{125}I] labelled proteins were stored in small aliquots in PBS at -70°C.

2.6.4 [^{125}I]-labelling of recombinant proteins.

Recombinant proteins were radiolabelled using an iodination catalyst, Iodogen according to the manufactures instructions. 50μg of recombinant protein was labelled in each case.

2.6.5 Expression and purification of SLT 1 B subunit

pSBC32 in *Escherichia coli* JM105 was a kind gift from Dr S B Calderwood (Boston, USA). It was grown and expressed as described by Calderwood *et al* (1990). Following expression a periplasmic extract was prepared using the method described in section 2.5.2. Purification was achieved by binding to a Gb_3-Sepharose affinity matrix column as described in section 2.6.1.

2.6.6 Metabolic labelling of RASTA2

RASTA2 was labelled with [^{35}S]-methionine during expression in *Escherichia coli* JM105. pRASTA2 in JM105 was grown on M9 minimal media amp agar plates prior to liquid culture. Transformed cells were grown overnight in 100mls of M9 minimal media with 100μg/ml ampicillin (in a 250ml flask) at 37°C with shaking at 250rpm. The following morning 100ml of fresh prewarmed M9 minimal media plus 100μg/ml amp (in a 1000ml flask) was inoculated to a starting optical density at 600nm of 0.2.

Escherichia coli were grown at 37°C with shaking until the optical density at 600nm reached ≈ 0.6. Protein expression was then induced by addition of IPTG to a final concentration of 1mM. 1mCi of [^{35}S]-methionine was also added and the flask was incubated with shaking for a further 3 hours at 30°C. An *Escherichia coli* periplasmic extract was made (section 2.5.2) and protein was purified as described in section 2.6.1. All bacterial manipulations were carried out under category III biological containment conditions.

2.7 Protein analysis and Characterisation.

2.7.1 Determination of protein concentration.

The concentration of recombinant SLT 1 holotoxins was determined by spectrophotometry using a Shimadzu UV 160 A. Optical density values at 280nm were converted to protein concentrations from a calculated extinction co-efficient of 0.984 from the formula:

$$A280nm = \frac{12.075x[N^{o}\ Try + (5xN^{o}\ Trp)]}{\text{Total } N^{o} \text{ Amino acids.}}$$

The concentration of RASTA2 fusion protein was determined by scanning densitometry of Western blots. Samples of ricin A chain of known concentration were run against RASTA2 samples on 15% PAGE (2.7.7). Proteins were transferred

to nitro-cellulose membranes and probed with anti RTA antibodies (2.7.2). The optical density of RTA standards was used to create a calibration curve which was used to quantify the concentration of unknown samples. This method was used since the RASTA2 protein was highly contaminated with free SLTB. The method described quantifies chimeric A chain alone which is directly proportional to the concentration of holotoxin present.

2.7.2 Western blot analysis

Western blot analysis was used to identify specific proteins on polyacrylamide gels. Rabbit anti-ST antibodies were a kind gift from Prof. A Donohue-Rolfe. Following separation of proteins by SDS PAGE (2.7.7) proteins were transferred to nitro-cellulose membranes (Hybond-C). Gel, nitro-cellulose and blotting paper (Whatman) soaked in transfer buffer (1.44% w/v glycine, 0.3% w/v Tris, 20% methanol v/v) were assembled in a semi-dry transblot apparatus according to the manufactures instructions. Following transfer the nitro-cellulose membrane was agitated in blocking solution 20% w/v dried milk (Marvel) in TBS (10mM Tris pH8.0, 150mM NaCl) plus 0.1% v/v Tween 20 for 30 min. Primary antibody was applied in 10ml of blocking solution and agitated for a minimum of 3 hours. The membrane was then washed four times 5 min TBS + 0.1% v/v Tween 20. Secondary antibody conjugated to alkaline phosphatase was applied in 10ml of blocking solution and agitated for 1 hour. After incubation of the second antibody the membrane was washed twice with

TBS+0.1% v/v Tween 20 followed by two washes with TBS. The membrane was allowed to air dry and was then developed in developing solution (100mM Tris-HCl, pH9.5, 100mM NaCl, 5mM $MgCl_2$ plus 33µl 50mg/ml BCPIP in dimethyl formamide and 66µl 50mg/ml NBT per 10ml). When colour development was complete the reaction was stopped by addition of 50ml stop solution (20mM Tris-HCl pH8.0, 5mM EDTA).

2.7.3 RNA N-glycosidase activity

Endo *et al* (1988) first described the cleavage of ricin A chain modified rRNA. This method was modified by May *et al* (1989). Potential toxins were incubated with 30µg of rabbit reticulocyte ribosomes (2.3.16) in a 30µl reaction in 1x ENDO buffer (25mM Tris/HCl pH7.6, 25mM KCl, 5mM $MgCl_2$) plus β-mecaptoethanol 6mM and 6.5mM vanadyl ribonuclease complex (VRC), for 30 min. Reactions were stopped by addition of 100 µl 2x Kirby buffer (2.1.3) plus 100 µl water on ice. Following two rounds of phenol extraction (2.3.3) rRNA was precipitated with ethanol (2.3.3).
To 4-5µg of modified rRNA 20µl of acetic aniline (1M aniline-acetic acid pH 4.5 (2.1.2)) was added and incubated for 2 min at 60°C followed by addition of 2.6 µl 7M Ammonium acetate and 65 µl ethanol at -20°C. rRNA was precipitated on dry ice for 30 min followed by centrifugation at 4°C for 30 min 15 000 x g. Pelleted RNA was washed by addition of 2 x 100 µl 70% ethanol and dried under vacuum. Dry RNA pellets were resuspended in 60% formamide in 0.1 x TPE prior to gel electrophoresis and held on dry ice or stored at -70°C.

2.7.4. Cytotoxic action of recombinant proteins to Vero cells.

Vero cells were plated out in flat bottomed 96 well tissue culture plates at density of $1.5x10^4$ cells per well in Dulbecco Modified Eagle's Medium (DMEM) (DME plus 5% v/v heat inactivated foetal calf serum, 2mM glutamine, 50IU/ml penicillin 300μg/ml streptomycin). Following incubation overnight at 37°C in a 5% CO_2 incubator cells formed a confluent monolayer. Media was removed and plates were washed with PBS. Toxin diluted in 100μl DMEM was added to appropriate wells and incubated at 37°C in a 5% CO_2 incubator for a specified period of time less 30 min. Following toxin incubation the cells were washed with PBS and 1μCi of [^{35}S]-methionine in 100μl of PBS was added to each well. Plates were incubated once more at 37°C in a 5% CO_2 incubator for 30 min. Following labelling the [^{35}S]-methionine was shaken off and monolayers were washed 3 times with 5% ice cold trichloroacetic acid and once with PBS. Addition of 100μl of 0.5M NaOH to each well solubilized TCA precipitated protein and after a 30 min incubation the contents of each well was transferred to a liquid scintillation vial containing 4ml of scintillation fluid. Quantitation of [^{35}S]-methionine incorporated into cells was achieved by scintillation counting. For each time point or toxin concentration four identical wells were set-up. Percentage incorporation was measured against the radioactivity in 6 untreated wells. Results from this assay were plotted as the mean of counts in test quadruplicates as a percentage of the mean of the no toxin controls, against toxin concentration to give IC_{50} values or against time to give $t_{1/2}$ values.

2.7.5 *In vivo* cleavage of SLT 1 and Mutants.

Recombinant SLT 1 and mutants were labelled with [^{125}I] using the Iodogen method (2.6.4) to a specific activity of approximately 25 000 cpm/ng. Vero cells were grown in 6 well plates in DMEM at a density of approximately 5.0X10^5 cells per well. After washing with PBS 100ng/ml [^{125}I]-labelled toxin was added to each well in 1.5 ml DMEM and cells were incubated for the specified period of time. Following toxin incubation the cells were washed three times with PBS and lysed in cell lysis buffer, 1% Triton X-100, 150mM NaCl, 50mM Tris pH 7.4, leupeptin 210μM, chymostatin 82μM, elastatinol 6μM, pepstatin A 1.6μM, aprotinin 0.3μM, PMSF 1mM, EDTA 1mM. Cellular debris and nuclei were removed by centrifugation 7 500 x g at 4°C for 5 min and protein precipitated by addition of acetone followed by centrifugation at 15 000 x g for 15 min at 4°C. The resulting protein pellets were dried under vacuum, resuspended in SDS PAGE loading buffer and run on 15% gels (2.7.7).

2.7.6 *In vitro* protease treatment.

The sensitivity of mutant proteins to trypsin or proteinase K was assessed by treatment *in vitro* with sequencing grade trypsin (Boehringer) or proteinase K (Sigma). 1μg of mutant proteins in PBS was digested with varying concentrations of protease. All trypsin digests were performed at 37°C for 7 min in a 30μl reaction. Proteinase K digestions were performed either at 37°C for 7 min or at 0°C for 40

min. The products of protease digestions were separated on 15% SDS PAGE (2.7.7) and stained with coomassie G250 or transferred to nitro-cellulose membranes (Hybond-C) for Western blot analysis (2.7.2).

2.7.7 SDS-Polyacrylamide gel electrophoresis (SDS PAGE).

Proteins were routinely separated on 15% polyacrylamide gels. By the method of Laemmli (1970) under reducing or non-reducing conditions. The latter was achieved by omission of β-mercaptoethanol from the sample loading buffer (0.06M Tris-HCl pH6.8, 0.2% SDS w/v, 20% glycerol v/v, 0.05% β-mercaptoethanol v/v, 0.1% bromo-phenol blue). Protein was visualised in several ways.

(i) Visualisation of radio-labelled proteins.

[^{125}I]-labelled proteins were visualised by exposure of dried gels to preflashed Fuji RX x-ray film with an intensifying screen at -70°C. Where [^{14}C]-labelled molecular weight markers were used, gels were fluorographed with Amplify (Amersham) prior drying and exposure to Fuji RX x-ray film.

[^{35}S]-methionine labelled proteins were visualised using fluorography by immersing gels in Amplify prior to drying and exposure to Fuji RX x-ray film at -70°C (no screen).

(ii) Silver staining.

Gels were silver stained as described by Merril *et al* (1981).

(iii) Coomassie blue G250 staining.

Gels were stained by immersing in Coomassie blue G250 stain reagent (0.025% coomassie blue G250, 3.8% perchloric acid) at 80°C for 30 min or room temperature overnight. Developing is achieved by 3 rounds of heating in distilled water in a microwave oven on high for 5 min with fresh changes of distilled water.

Section 3 Results and Discussion.

Chapter 1.

3.1 Cloning, expression and purification of wild-type Shiga-like toxin 1.

Introduction

Previous work at Warwick involving expression and purification of SLT 1 had relied upon separate expression of SLT 1 A and B chains followed by purification of B chain using a commercially available affinity matrix provided by BioCarb (Gb_3-Fractogel). Following reassociation of impure SLT 1 A chain with pure SLT 1 B chain, holotoxin and unreassociated SLT 1 B chain were co-purified on the Gb_3-Fractogel column. This method has several disadvantages. It was time consuming, results in very low yields of holotoxin, and resultant holotoxin is contaminated with unassociated excess B chain. Since this study was to involve the production of several toxins mutated in the A chain, and large quantities of these mutant toxins were required for biochemical analysis, it was decided to design a new expression system which would not have these technical difficulties. In addition the cost of the affinity matrix was prohibitively expensive and is in very short supply since its manufacture has been ceased. Dr. D. Muller (Warwick) chemically synthesized the trisaccharide globotriose (galactose α1-4galactoseβ1-4glucose) (figure 1.1) and immobilization of this sugar via a six carbon spacer arm ($(CH_2)_6$) onto cyanogen bromide-activated Sepharose (see appendix 2) provided a means by which the biological properties of this compound could be tested as an affinity matrix for SLT

1. The new expression system and method of purification presented here were designed to allow rapid expression and purification of large quantities SLT 1 wt and variants. The purification protocol described is based on the method of Ryd *et al* (1989) (section 1.2)

3.1.1 Cloning

The genes coding for the SLT 1 operon including the associated Shine-Dalgarno and periplasmic targeting sequences were amplified by PCR from *Escherichia coli* 026:H11 cell paste (a strain which produces SLT 1 only). Two primers were designed which anneal to the 5' and 3' ends of the sequence and in addition to the complementary sequence, a *Pst*1 site was incorporated in the 5' end of the 5' primer and a *EcoR*1 site in the 5' end of the 3' primer (Figure 3.1.1). Amplification was achieved by 25 cycles of PCR in the presence of Taq DNA polymerase in a 100 µl reaction volume.

PCR conditions: 1X reaction buffer, 1.5mM $MgCl_2$, 100pmoles primers (ESTO3' and PSTO5'), 0.2 mM dNTPs, 0.05 U/µl Taq DNA polymerase. 94°C 1 min, 39°C 1 min, 72°C 1.5 min.

The PCR generated two fragments one of approximately 1300 base pairs and a smaller fragment which runs just above the unincorporated primer band on a 0.8% agarose gel (figure 3.1.2). The larger fragment is the amplified SLT 1 coding

sequence and this was established by restriction analysis. Digestion of the PCR reaction with *Nru*I or *Ssp*I cleaves the 1300 base pair fragment to two smaller fragments with the predicted sizes (figure 3.1.2). The 1300 base pair fragment was gel isolated (2.3.9) phenol extracted (2.3.3) and cut overnight at 37°C with *EcoR* I and *Pst* I. The cut PCR fragment was then gel isolated again and ligated into M13 mp18 previously cut with *EcoR*I and *Pst*I, gel isolated and treated with calf intestine phosphatase (CIP) to create M13SLTwt. The ligated plasmid DNA was then transformed into *E.coli* strain TG2 (2.3.2). A single white plaque was used to make single stranded DNA (2.3.7) which was used for DNA sequencing (2.3.13) and subsequent mutagenesis. The sequence of the PCR amplified DNA in M13 mp18 was confirmed by DNA sequencing prior to subcloning into the expression vector.

Double stranded M13SLTwt DNA was prepared (2.3.8) and digested overnight with *EcoR* I and *Pst* I. Digested DNA was phenol extracted and the SLT 1 coding 1300 base pair fragment gel isolated. pUC19 plasmid DNA was also digested with *EcoR* I and *Pst* I and gel isolated. Cut plasmid DNA was treated with CIP before being ligated with the 1300 base pair fragment from M13SLTwt to create pSLTwt. Ligated DNA was transformed into TG2 and transformants screened for insert by *Hind* III digestion of mini prep plasmid DNA. *Hind* III digestion releases a diagnostic 580 base pair fragment from pSLTwt. The cloning of M13SLTwt and pSLTwt are described schematically in figure 3.1.3

Figure 3.1.1 Sequence of oligonucleotide primers ESTO3' and PSTO5' used for amplification of SLT 1 from *Escherichia coli* 026:H11 cell paste.

ESTO3'

*EcoR*I Complementary sequence

5'-GCT AGA ATT CTC AAC GAA AAA TAA CTT-3'

PSTO5'

*Pst*I Complementary sequence

5'-CGG AAC TGC AGC AAG GAG TAT TGT GTA ATA T-3'

Figure 3.1.1 shows the sequence of the primers used in the PCR of the SLT 1 coding sequence from *Escherichia coli* cell paste. ESTO3' contains DNA complementary to the 3' end of the SLT 1 operon. This primer adds an *EcoR* I site to the 3' end of the SLT 1 coding sequence. PSTO5' contains sequence complementary to the 5' end of the SLT 1 coding sequence including the Shine-Dalgarno-sequence. This primer adds a *Pst* I site to the 5' end of the SLT 1 coding sequence.

Figure 3.1.2 Agarose gel electrophoresis of amplified SLT 1 DNA from *Escherichia coli* 026:H11 and subsequent restriction analysis.

Figure 3.1.2 shows the PCR amplified fragments from *Escherichia coli* (serotype 026:H11 strain H19) cell paste. The reaction generated two fragments one which has a size consistent with that of the full length SLT 1 operon (1271 base pairs) and a second smaller fragment presumably generated by non-specific priming and amplification. Restriction analysis was performed in order to confirm the identity of the amplified fragment *Nru* I cuts at position 1136 and produces two fragments of approximately 850 and 450 base pairs. *Ssp* I cuts at position 1219 and produces two fragments of approximately 900 and 320 base pairs. Both restriction digests confirm that the larger fragment produced in the PCR reaction described is the amplified SLT 1 operon sequence. Numbering is from the sequence published by Calderwood *et al* (1987).

Lane 1/ λ DNA digested with *EcoR* I and *Hind* III

Lane 2/ 3µl uncut PCR reaction.

Lane 3/ 3µl *Nru* I digested PCR reaction.

Lane 4/ 3µl *Ssp* I digested PCR reaction.

Figure 3.1.2 Agarose gel electrophoresis of amplified SLT 1 DNA from *Escherichia coli* 026:H11 and subsequent restriction analysis.

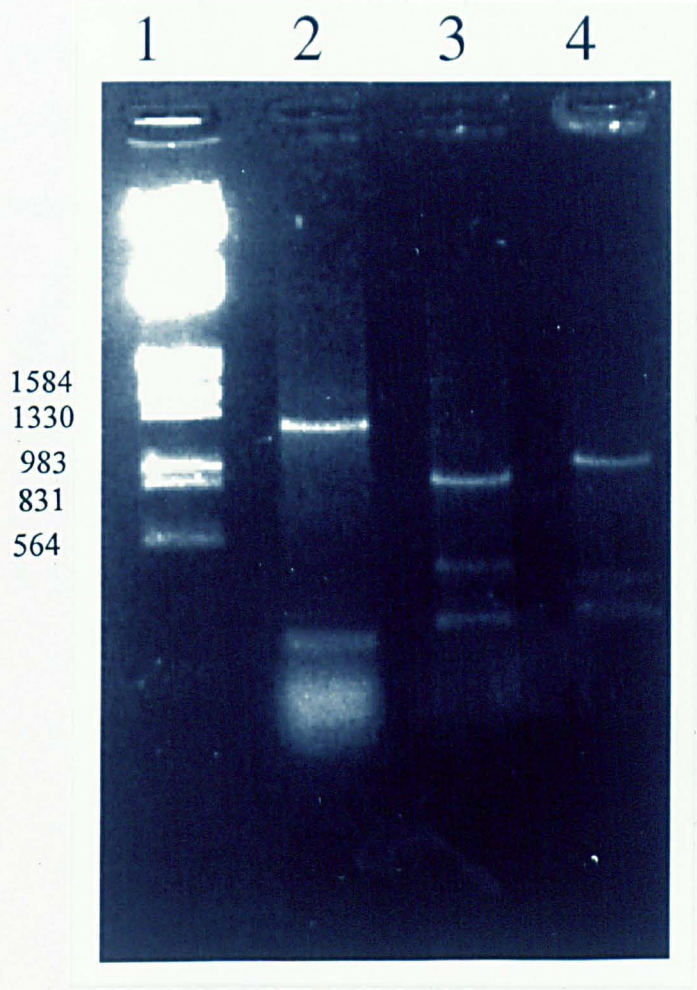

Figure 3.1.3 Cloning steps used for the production of M13SLTwt and pSLTwt.

Figure 3.1.3 shows a schematic diagram of the steps used to clone a DNA fragment coding for the full length SLT 1 operon generated by PCR from *Escherichia coli* 026:H11 cell paste. The positions of *Ssp* 1 and *Nru* 1 used for restriction analysis of the PCR fragment are marked. The PCR fragment was digested with *Pst* 1 and *EcoR* 1 and ligated into M13 mp18 digested similarly to generate M13SLTwt. M13SLTwt was used to generate single stranded DNA for sequencing. Double stranded M13SLTwt was cut with *Pst* 1and *EcoR* 1 to release a fragment of approximately 1300 base pairs (bp) which was ligated into pUC19 similarly digested to generate pSLTwt.

Figure 3.1.3 Cloning steps used for the production of M13SLTwt and pSLTwt.

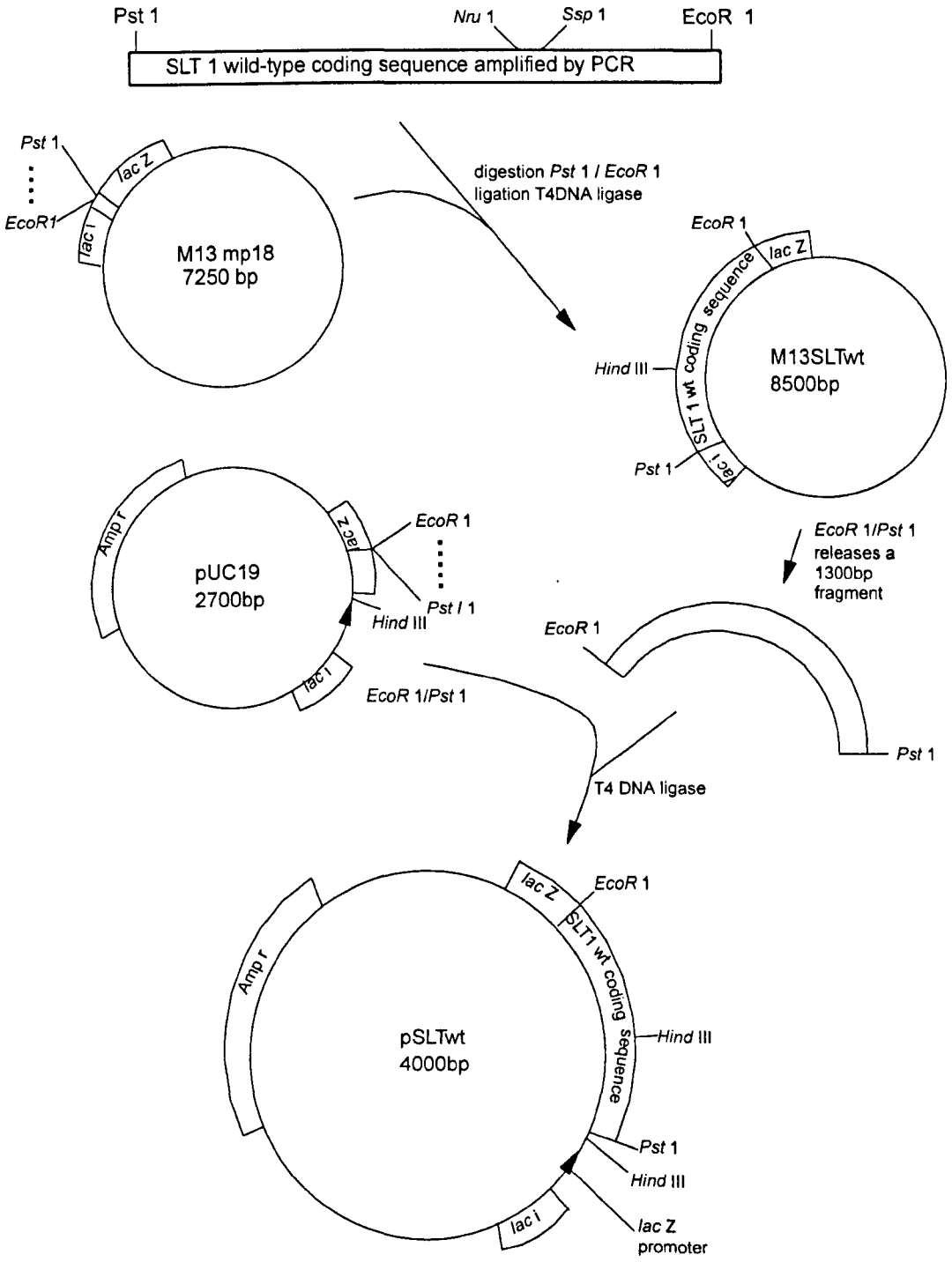

3.1.2 Expression/purification of SLT 1 wt.

pSLTwt was expressed in *Escherichia coli* JM105 (as in section 2.5.1). Following expression the periplasm was extracted (section 2.5.2) and recombinant protein was purified using a receptor analogue affinity matrix column (section 2.6.1). 0.5 ml fractions were collected on addition of denaturing 6M guanidine hydrochloride (850 mM Tris HCl pH6.7, 6MGuHCl pH6.7). These fractions were collected in Eppendorf tubes pre-loaded with 0.5 ml of 6MGuHCl pH6.7. The reason for this is that in previous experiments some fractions collected from the Gb_3 -Sepharose column were often highly concentrated and protein precipitated in these fractions. After collection of 20 0.5 ml fractions, samples were analyzed by reading their absorbance at 280nm. The absorbance values were plotted against fraction number to give a peak. The peak fractions were immediately dialyzed against PBS in order to remove the denaturing GuHCl as soon as possible and thus prevent damage to the sample. Figure 3.1.4 shows a typical elution profile obtained from plotting A280nm against fraction number. Following extensive dialysis, protein was quantified (2.7.1) and analyzed by SDS PAGE (2.7.7). Purification of SLT 1 wt using the method described routinely resulted in the production of approximately 1mg of pure SLT 1 from a 1 liter starting culture. Figure 3.1.5 shows the purification of SLT 1 wt analyzed by SDS PAGE.

Figure 3.1.4 Profile of SLT 1 wt protein eluted with guanidine hydrochloride from a 1ml Gb_3-Sepharose column.

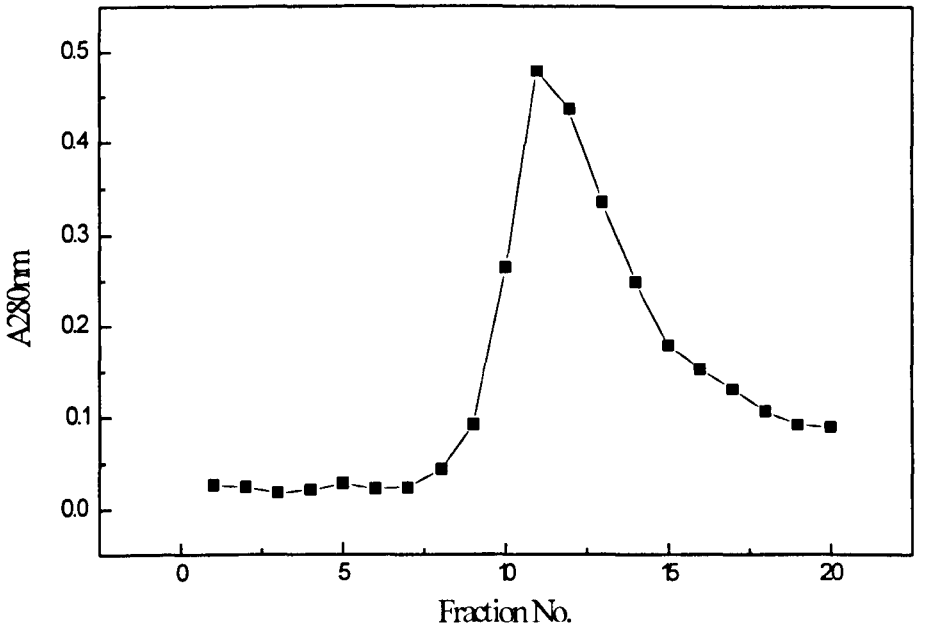

Figure 3.1.4 shows the elution profile of SLT wt from a 1ml Gb_3-Sepharose column. Periplasm containing SLT 1 wt was bound to a 1ml Gb_3-Sepharose column and washed with 40 column volumes of 0.5M NaCl in phosphate buffered saline (PBS). 0.5ml fractions were eluted with 6M GuHCl pH6.7 and collected in tubes containing 0.5ml 6M GuHCl pH6.7. The absorbance of each eluted fraction (total volume 1ml) was analyzed at 280nm and plotted against fraction number to give an elution profile. Fractions within the peak were dialyzed against PBS.

Figure 3.1.5 Analysis of expression and purification of SLT 1 wt by SDS polyacrylamide gel electrophoresis

Figure 3.1.5 shows the binding and subsequent elution of wild type SLT 1 on a 1 ml Gb_3-Sepharose analogue affinity column. Lane 2 shows *Escherichia coli* JM105 periplasm following expression of pSLTwt, Lane 3 shows proteins which do not bind to the affinity matrix (flow through) and Lanes 4-8 show proteins eluted with 6M GuHCl pH6.7 and dialysed against PBS i.e. fractions from the peak shown in figure 3.1.4. Lanes 1 and 9 are molecular weight markers. The arrows indicate the positions of SLT 1 A chain (32kDa) and SLT 1 B chain (7.7 kDa). Molecular masses are given in kDa.

Lane 1 molecular weight markers

Lane 2 precolumn periplasm (10μl)

Lane 3 flow though (20μl)

Lane 4 fraction 10 (30μl)

Lane 5 fraction 11 (30μl)

Lane 6 fraction 12 (30μl)

Lane 7 fraction 13 (30μl)

Lane 8 fraction 14 (30μl)

Lane 9 molecular weight markers

Figure 3.1.5 Analysis of expression and purification of SLT 1 wt by SDS polyacrylamide gel electrophoresis

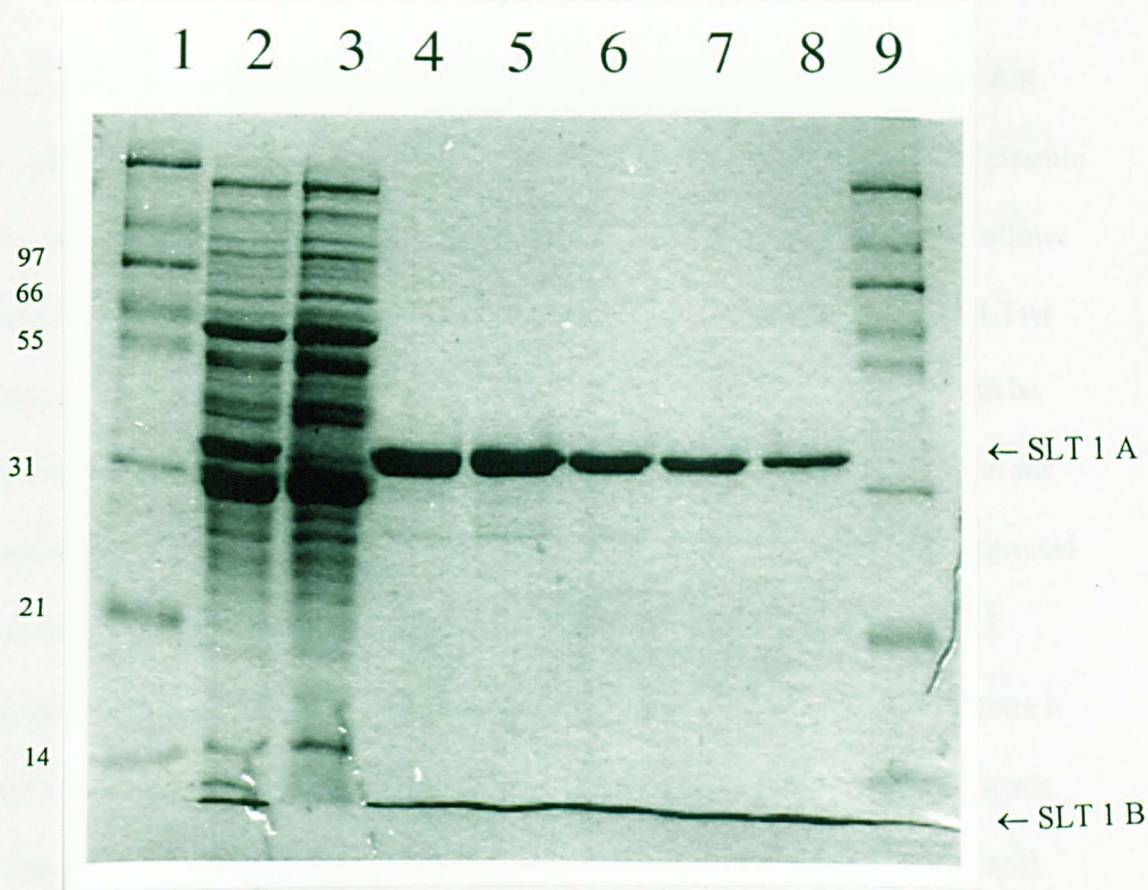

3.1.3 Discussion.

The aim of these experiments was two fold, firstly an expression system was to be designed which would facilitate the rapid expression of wild-type SLT 1(wt) which would could easily be modified for the expression of mutant forms of SLT 1. Secondly the aim was to test and optimize a novel receptor analogue affinity chromatography matrix.

The former was achieved by creating two plasmids both of which contain the full length coding sequence for SLT 1 and its associated Shine-Dalgarno and periplasmic targeting sequences. M13SLTwt contains this sequence in M13 mp18 which allows easy production of single stranded DNA for sequencing and mutagenesis. pSLTwt contains this sequence in the expression plasmid pUC19 where expression can be driven by the *lac* Z promoter. These two plasmids provide a simple method for the production of mutant toxins since mutant DNA made in the M13SLTwt background can easy be substituted into pSLTwt for expression. The results in figure 3.1.5 clearly show that pSLTwt allows the expression of SLT 1 holotoxin, furthermore it can be seen that the recombinant protein is being targeted to the periplasmic space. Periplasmic targeting is designed to allow physiological assembly of the A and B chains in a compartment analogous to that in natural producing strains of *Escherichia coli.* It is also thought that targeting to the periplasm would allow correct disulphide

bond production and hence gives the best chance of producing correctly folded soluble holotoxins. This expression system circumvents the separate expression of A and B chains with its associated technical problems. The single disadvantage of the current method is that all manipulations involving the SLT containing plasmids in bacterial cells, including expression, must be conducted under category III biological containment conditions. The reason for this is that this plasmid contains a holotoxin gene under the control of a strong promoter.

The method of purification described is a modification of the method of Ryd *et* al (1989). In addition to the change in the analogue affinity matrix 0.5M NaCl was added to the wash buffer to prevent the small amount of non-specific protein/column matrix interactions. Small amounts of contaminating proteins had previously been seen in guanidine-eluted fractions.

By SDS PAGE analysis of pre-column periplasm, flow though and eluted protein fractions (figure 3.1.5) it can be seen that the new Gb_3-Sepharose matrix effectively binds toxin. The binding capacity of this matrix was not investigated, however since at least 1mg of pure toxin can be eluted from a 1ml column and no toxin is detected in the flow-though fractions the capacity must be in excess of 1mg per ml matrix. The cost of the previously commercially available Gb_3-Fractogel matrix precluded the purchasing of large quantities of this material. Although this matrix could be regenerated and used several times, its ability to bind toxin was reduced with

repeated use. In contrast Gb_3-Sepharose appears to be extremely stable and tolerates reuse well.

In summary the new expression and purification system described provide a cheap and rapid method for the production of large quantities of biochemically pure SLT 1. The expression system can easily be adapted for the production of mutant SLT provided that the integrity of the receptor binding sites in SLT 1 B chain is maintained and that the mutant A chain is capable of association with the B chain.

Chapter 2

3.2 Cloning, expression and purification of mutant Shiga-like toxin 1 proteins.

Introduction

The role of proteolytic processing of SLT 1 in susceptible eukaryotic cells is the main area of investigation in this study. Current literature involving processing of SLT 1 and other bacterial toxins is covered in section 1.6. The results presented in chapter 2 show the strategy used to clone and express five mutant proteins which were designed to address further, the question of proteolytic processing of SLT 1 in eukaryotic cells.

The expression and purification methods used for the production of these mutant molecules are based on the findings presented in chapter 1 where a system for the expression and purification of wild type recombinant SLT 1 is described.

Four holotoxins, mutant in potential processing sites within the A chain, were made.

1. pSLTP1 codes for SLT 1 Arg248→Gly / Arg251→Gly
2. pSLTP2 codes for SLT 1 Ala246→Gly / Ser247→Ala / Ala 253→Gly / Ser 254→Ala

3. pSLTP3 codes for SLT 1 Arg248→Gly / Arg251→Gly / Ala246→Gly / Ser247→Ala / Ala 253→Gly / Ser 254→Ala (A combination of pSLTP1 and pSLTP2)

4. pSLTP4 codes for SLT 1 Arg248→Gly / Arg251→Gly / Ala246→Gly / Ser247→Ala / Ala 253→Gly / Ser 254→Ala / Arg220→Gly / Arg 223→Gly (pSLTP3 with a second arginine rich site disrupted)

5. A fifth mutant was made for translation *in vitro* which has a stop codon inserted in place of Arg 223.

pGEM223stop codes for SLT 1 Arg223→stop

3.2.1 Cloning of mutant Shiga-like toxins.

pSLTP1, pSLTP2 and pSLTP3 were all produced by oligonucleotide-site-directed mutagenesis (SDM) (2.3.12) of SLT 1 coding DNA in an M13mp18 background followed by subcloning of the mutant sequence into pUC19.

M13SLTP1 and M13SLTP2 were created by SDM of M13SLTwt (section 3.1) with the oligonucleotide P1 or P2i and P2ii (figure 3.2.1). M13SLTP3 was created by SDM of M13SLTP2 DNA with the oligonucleotide P3 (figure 3.2.1). Following mutagenesis, single stranded DNA was screened for mutation by sequencing (2.3.13). Double stranded DNA was made from the appropriate M13 phage clone

(2.3.8) and digested with *EcoR*I and *Pst*I to release a fragment of approximately 1300 base pairs. This fragment was gel isolated (2.3.9) and subcloned into pUC19 to create pSLTP1, pSLTP2 and pSLTP3 by ligation into pUC19 previously cut with *EcoR*I and *Pst*I gel isolated and treated with CIP. The resulting ligation was transformed into TG2 and mini prep plasmid DNA was screened for insert by *Hind*III digestion. Digestion of pSLTP1, pSLTP2 and pSLTP3 with *Hind*III releases a fragment of 580 base pairs. The amino acid changes introduced to SLT 1 coded in pSLTP1, pSLTP2 and pSLTP3 are shown in figure 3.2.3. Plasmid maps are given in figures 3.2.4, 3.2.5 and 3.2.6 respectively.

Site directed mutagenesis methods were also attempted to make two further mutants pSLTP4 and pGEM223stop. However, repeated attempts to produce mutations in this region of the SLT 1 sequence by conventional methods failed. The reasons for this are not clear, but since production of both of these mutants required binding of an oligonucleotide to the same region in the SLT 1 sequence it is considered that DNA secondary structure in this region may prevent efficient binding of a mutagenic primer. Four primer mutagenic recombinant PCR was used in place of SDM to create these two mutants.

Four primer PCR involves three separate PCRs. In the first and second reactions two DNA fragments are produced which have the sequence of the 3' and the 5' ends of the template sequence, both DNA fragments also contain a small region of

homology. In the third round of PCR the gel isolated products of the first two reactions are combined with outside 3' and 5' primers to amplify a single full length product. Taq DNA polymerase often adds a 3' adenine base following amplification of the template DNA. This would produce a single base insertion in the third PCR described. However Vent DNA polymerase has an exonuclease activity and hence does not insert an additional A. For this reason Vent DNA polymerase was used in all four primer recombinant PCRs in place of Taq DNA polymerase.

pSLTP4 was produced by recombinant PCR using the outside primers ESTO3' and PSTO5' (figure 3.1.1) and mutagenic primers P4 and P4r (figure 3.2.1). pGEM223stop was produced by recombinant PCR using the primers ESTO3' and PSTO5' (figure 3.1.1) and mutagenic primers 223stop and 223stopr (figure 3.2.1). The steps involved in producing 223stop and SLTP4 PCR fragments are shown schematically in figure 3.2.2.

PCR and cloning of 233stop:

reaction 1: 1X Vent DNA polymerase buffer, 0.2mM dNTPs, 10ng dsM13SLTwt (template DNA), 50pmoles PSTO5', 50pmoles 223stopr, 0.02U/µl Vent DNA polymerase. Final volume 50 µl. 94°C 1 min, 40°C 1 min, 72°C 1.5 min.

Reaction 2: 1X Vent DNA polymerase buffer, 0.2mM dNTPs, 10ng dsM13SLTwt (template DNA), 50pmoles ESTO3', 50pmoles 223stop, 0.02U/μl Vent DNA polymerase. Final volume 50 μl. 94°C 1 min, 38°C 1 min, 72°C 1.5 min.

Reaction 3: 1X Vent DNA polymerase buffer, 0.2mM dNTPs, 0.25 μl gel isolated fragment from reaction 1, 0.5 μl gel isolated fragment from reaction 2, 100pmoles ESTO3', 100pmoles PSTO5', 0.02U/μl Vent DNA polymerase. Final volume 100 μ l. 94°C 1 min, 44°C 1 min, 72°C 1.5 min for 3 cycles followed by 94°C 1 min, 40°C 1 min, 72°C 1.5 min for 12 cycles.

This series of PCR resulted in a DNA fragment of the correct size approximately 1300 base pairs. This fragment was phenol extracted, gel isolated and cut with *Pst*I and *EcoR*I. Plasmid DNA, pGEM2, was digested with *Pst*I and *EcoR*I gel isolated and treated with CIP. Cut PCR fragment was then ligated into cut pGEM2 to produce pGEM223stop. Mutation was confirmed by plasmid sequencing. The changes made to the primary amino acid sequence of SLT 1 coded in pGEM223stop are shown in figure 3.2.3. A plasmid map is given in figure 3.2.8

PCR conditions for the production of SLTP4:

reaction 1: 1X Vent DNA polymerase buffer, 0.2mM dNTPs, 10ng dsM13SLTP3 (template DNA), 50pmoles PSTO5', 50pmoles P4r, 0.02U/μl Vent DNA polymerase. Final volume 50 μl. 94°C 1 min, 40°C 1 min, 72°C 1.5 min.

Reaction 2: 1X Vent DNA polymerase buffer, 0.2mM dNTPs, 10ng dsM13SLTP3 (template DNA), 50pmoles ESTO3', 50pmoles P4, 0.02U/μl Vent DNA polymerase. Final volume 50 μl. 94°C 1 min, 50°C 1 min, 72°C 1.5 min.

Reaction 3 1X Vent DNA polymerase buffer, 0.2mM dNTPs,0.25 μl gel isolated fragment from reaction 1, 0.25 μl gel isolated fragment from reaction 2, 100pmoles ESTO3', 100pmoles PSTO5', 0.02U/μl Vent DNA polymerase. Final volume 100 μ l. 94°C 1 min, 72°C 1.5 min, 3 cycles followed by 94°C 1 min, 40°C 1 min, 72°C 1.5 min.

This series of PCR resulted in a DNA fragment of the correct size approximately 1300 base pairs. This fragment was phenol extracted, gel isolated and cut with *Pst*I and *EcoR*I. Plasmid DNA, dsM13mp18, was digested with *Pst*I and *EcoR*I gel isolated and treated with CIP. Cut PCR fragment was then ligated into cut M13mp18 to produce M13SLTP4. Following full sequencing to confirm mutation a 1300 base pair fragment was released from M13SLTP4, by digestion with *EcoR*I and *Pst*I, gel isolated and ligated into pUC19, cut previously with *EcoR*I and *Pst*I gel isolated and treated with CIP, to produce pSLTP4. The resulting ligation was transformed into TG2 and mini prep plasmid DNA screened for insert by *Hind*III digestion. pSLTP4 releases a 580 base pair fragment following digestion with *Hind*III. The amino acid changes made to the SLT 1 primary sequence coded in pSLTP4 are shown in figure 3.2.3. A plasmid map is given in figure 3.2.7.

Figure 3.2.1 Oligonucleotide sequences of primers used for the construction of SLT 1 mutant toxins.

Figure 3.2.1 shows the sequence of primers used for site directed mutagenesis and recombinant PCR of mutant Shiga-like toxins. Primers P1, P2i, P2ii, and P3 were used for the SDM of SLT 1 DNA in M13mp18. The primers P4, P4r, 223stop and 223stopr were used in four primer PCRs to create mutant molecules.

Mismatch bases are underlined, numbering denotes the position at which the primer anneals in the sequence published by Calderwood *et al* (1987) (see appendix 5). The sequences of primers ESTO3' and PSTO5' also used in recombinant PCR are shown in figure 3.1.1

Figure 3.2.1 Oligonucleotide sequences of primers used for the construction of SLT 1 mutant toxins.

P1 5'-^{1130}CAT GCA TCG GCA GTT GCC GGA ATG GCA^{1156}-3'

P2i 5'-^{1125}AT CAT CAT GGA GCG CGA^{1144}-3'

P2ii 5'-^{1147}C AGA ATG GGA GCT GAT GAG T^{1166}-3'

P3 5'-^{1131}AT GGA GCG GCA GTT GCC GGA ATG GGA^{1156}-3'

P4 5'-^{1046}GAC TCT GTT GGT GTA GGA GGA ATT TCT T ^{1073}-3'

P4r 5'^{1073}A AGA AAT TCC TCC TAC ACC AAC AGA GTC^{1046}-3'

223stop 5'-^{1056}GT GTA GGA TGA ATT TCT^{1072}-3'

223stopr 5'-^{1072}AGA AAT TCA TCC TAC AC^{1056}-3'

Figure 3.2.2. Recombinant mutagenic PCR used for the production DNA coding for SLTP4 and 223stop mutant SLT 1s.

Reaction 1 : In the first reaction a single outside primer (1) and a mutagenic primer (2) were combined in a PCR which amplifies the 5' portion of the template sequence. This fragment incorporates the mutation present in the mutagenic primer (2) and a restriction site coded in the 5' primer (1).

Reaction 2: In the second reaction a single outside primer (4) and a second mutagenic primer (3) (which is complementary to primer (2)) were combined with template in a PCR which amplifies the 3' portion of the template sequence. The resulting fragment incorporates a restriction site coded in primer (4) and the mutation from primer (3).

Reaction 3: In the final reaction the products from reaction 1 and reaction 2 (products A and B), after removal of primers by gel isolation (2.3.9), are combined in a third reaction where the a region of homology anneals and extends to produce full length PCR product (dotted lines). Both outside primers (1) and (4) are also included in this reaction to amplify the final PCR product.

Figure 3.2.2. Recombinant mutagenic PCR used for the production DNA coding for SLTP4 and 223stop mutant SLT 1s.

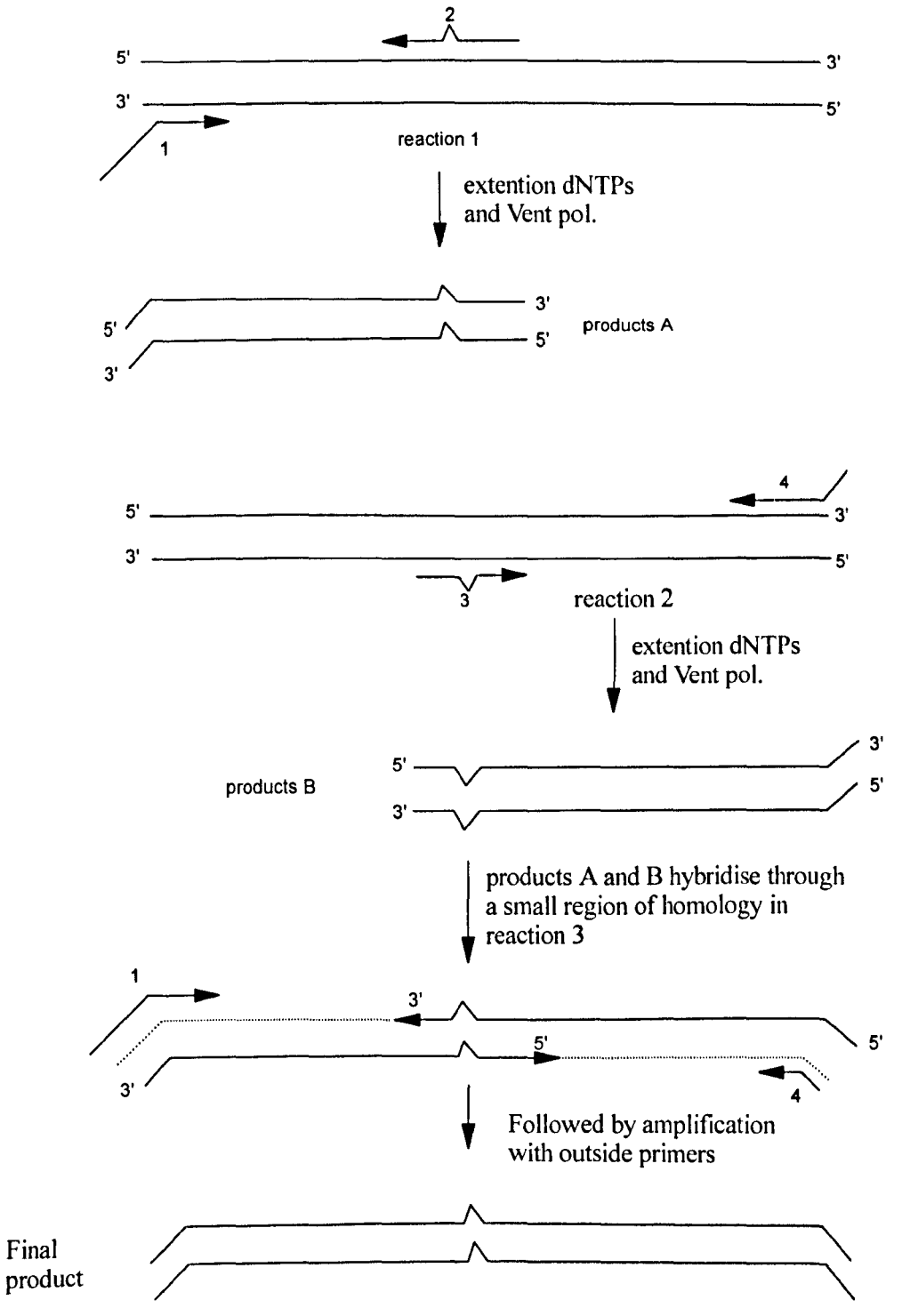

Figure 3.2.3 Amino acid changes made to the primary sequence of SLT 1 as result of mutagenesis.

Figure 3.2.3 shows the portion of the primary sequence of SLT 1 A chain between residues 217 and 256 where amino acid changes were introduced by site directed mutagenesis and recombinant PCR. Changes to the wild type sequence are shown in bold. Numbering of amino-acyl residues is from Calderwood *et al* (1987) (see appendix 5). Residue numbering refers to the mature signal sequence-cleaved protein.

Figure 3.2.3 Amino acid changes made to the primary sequence of SLT 1 as result of mutagenesis.

SLT 1 wt

^{217}D S V R V G R I S F G S I N A I L G S V A L I L N C H H H A S R V A R M A S D E^{256}

SLTP1

^{217}D S V R V G R I S F G S I N A I L G S V A L I L N C H H H A S **G** V A **G** M A S D E^{256}

SLTP2

^{217}D S V R V G R I S F G S I N A I L G S V A L I L N C H H H **G A** R V A R M **G A** D E^{256}

SLTP3

^{217}D S V R V G R I S F G S I N A I L G S V A L I L N C H H H **G A G** V A **G** M **G A** D E^{256}

SLTP4

^{217}D S V **G** V G **G** I S F G S I N A I L G S V A L I L N C H H H **G A G** V A **G** M **G A** D E^{256}

SLT 223stop

^{217}D S V R V G **STOP**

Figure 3.2.4 Plasmid pSLTP1

Construction of pSLTP1 allowed expression of mutant SLTP1 protein in *Escherichia coli* JM105. The plasmid was constructed by ligation of a *EcoR*I / *Pst*I mutant DNA fragment coding for the full length SLTP1 holotoxin and its associated Shine-Dalgarno and periplasmic targeting sequences from M13SLTP1 into *EcoR*I / *Pst*I cut pUC19. Transcription is under control of the inducible *lac*Z promoter.

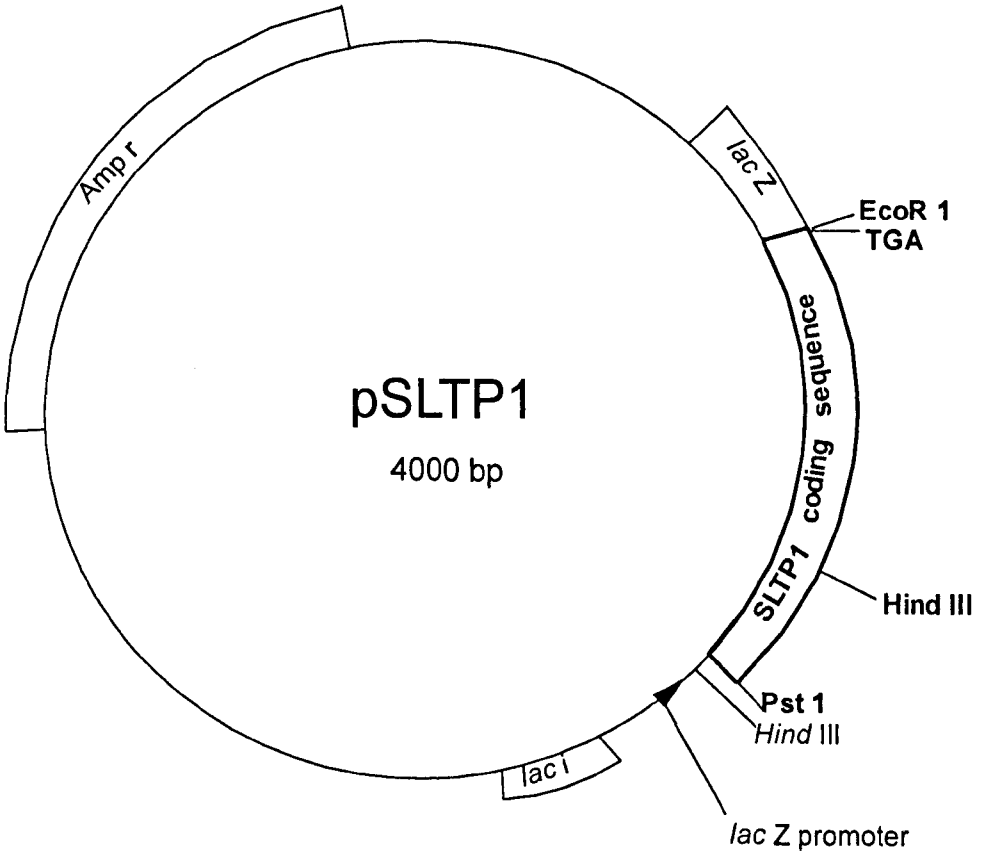

Figure 3.2.5 Plasmid pSLTP2

Construction of pSLTP2 allowed expression of mutant SLTP2 protein in *Escherichia coli* JM105. The plasmid was constructed by ligation of a *EcoR*I / *Pst*I mutant DNA fragment coding for the full length SLTP2 holotoxin and its associated Shine-Dalgarno and periplasmic targeting sequences from M13SLTP2 into *EcoR*I / *Pst*I cut pUC19. Transcription is under control of the inducible *lac*Z promoter.

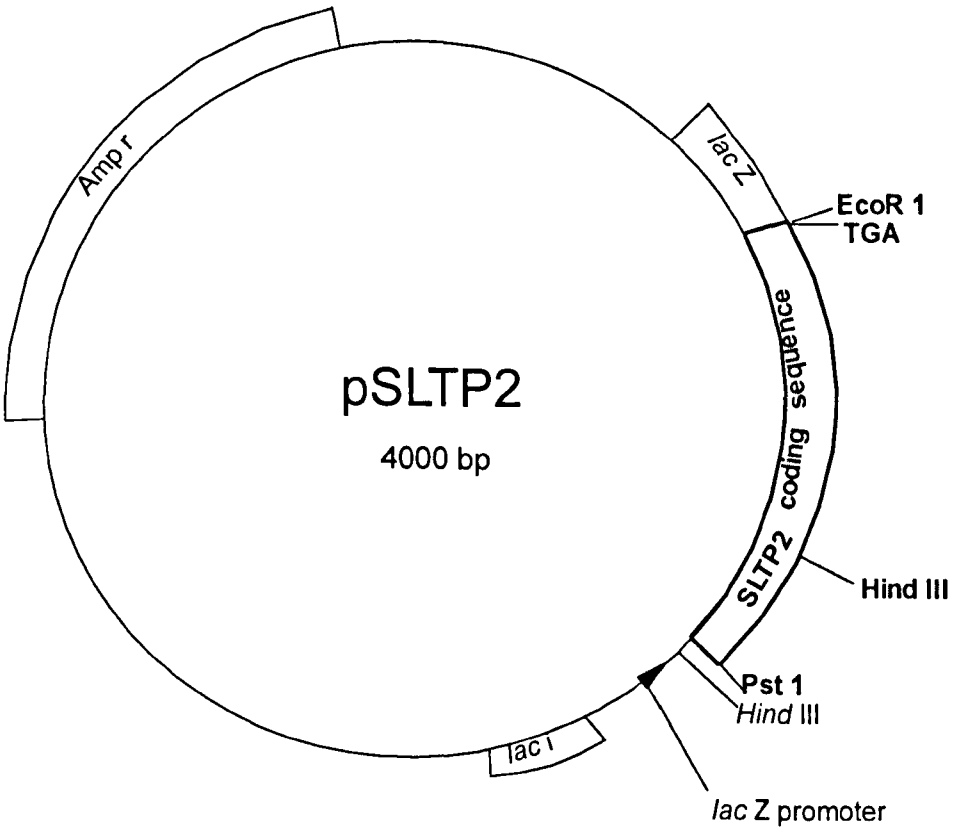

Figure 3.2.6 plasmid pSLTP3

Construction of pSLTP3 allowed expression of mutant SLTP3 protein in *Escherichia coli* JM105. The plasmid was constructed by ligation of a *EcoR*I / *Pst*I mutant DNA fragment coding for the full length SLTP3 holotoxin and its associated Shine-Dalgarno and periplasmic targeting sequences from M13SLTP3 into *EcoR*I / *Pst*I cut pUC19. Transcription is under control of the inducible *lac*Z promoter.

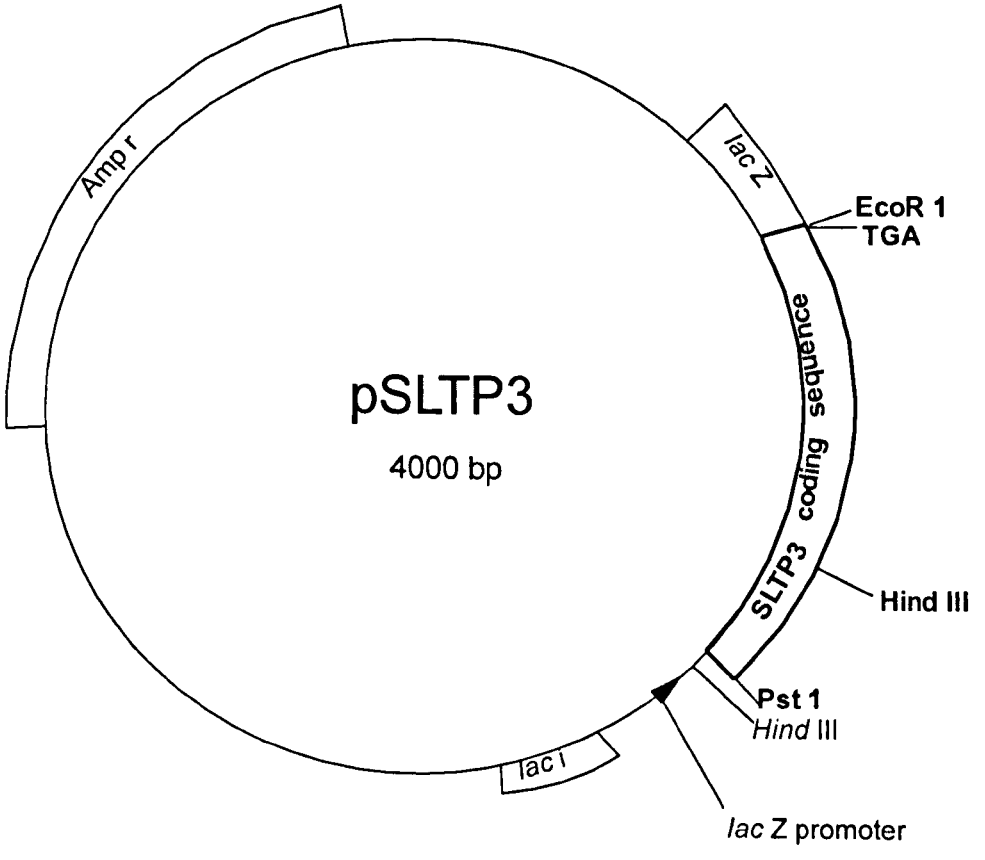

Figure 3.2.7 plasmid pSLTP4

Construction of pSLTP4 allowed expression of mutant SLTP4 protein in *Escherichia coli* JM105. The plasmid was constructed by ligation of a *EcoR*I / *Pst*I mutant DNA fragment coding for the full length SLTP4 holotoxin and its associated Shine-Dalgarno and periplasmic targeting sequences from M13SLTP4 into *EcoR*I / *Pst*I cut pUC19. Transcription is under control of the inducible *lacZ* promoter.

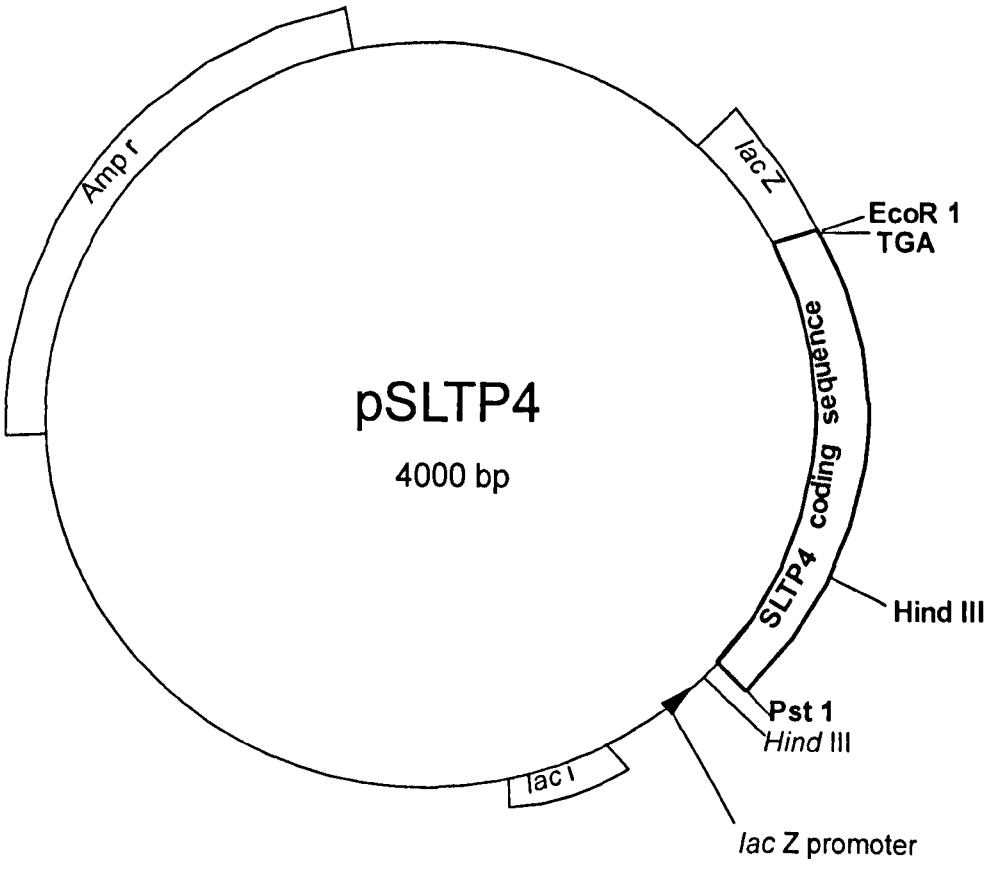

Figure 3.2.8 plasmid pGEM223stop

Construction of pGEM223stop allowed expression *in vitro* of a truncated N-terminal 222 amino acid SLT 1 A chain. The insertion of a stop codon TGA allows premature termination of translation following residue Gly 222. The plasmid was constructed by ligation of a 1300 base pair fragment produced by mutagenic PCR cut with *EcoR*I / *Pst*I into pGEM2 similarly digested with *EcoR*I / *Pst*I. Transcription is controlled by the viral T7 promoter.

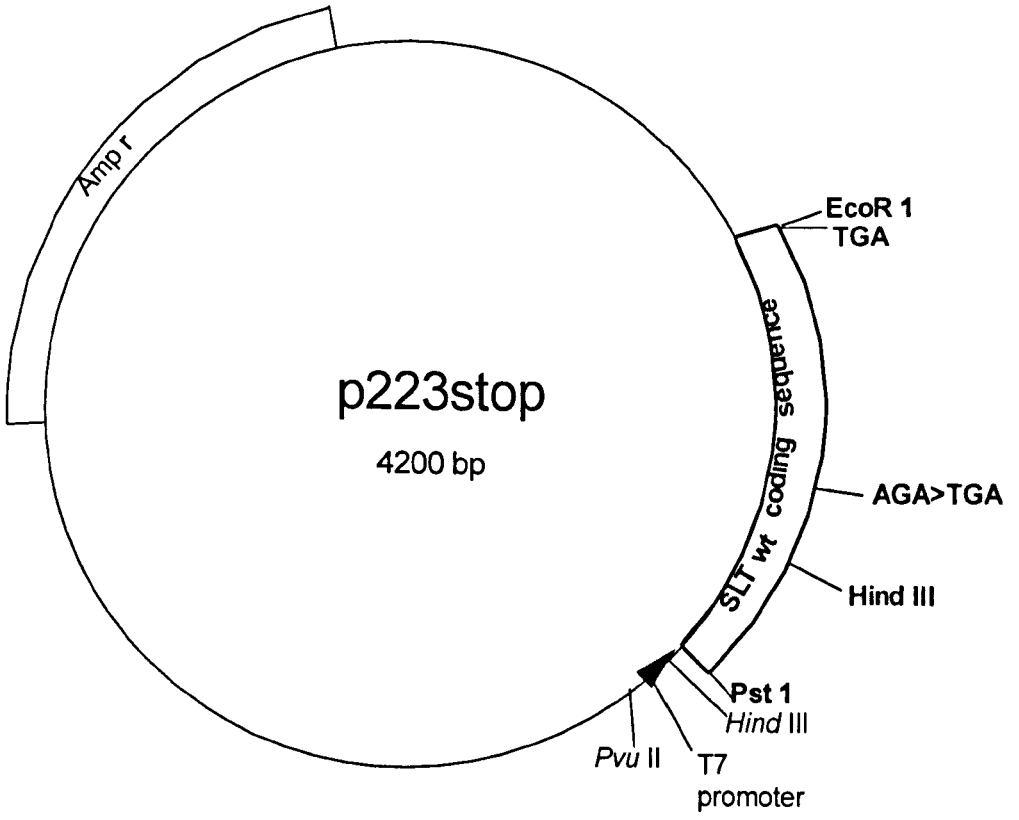

3.2.2 Expression and purification of Mutant Shiga-like toxins *in vivo*.

The expression system and method of purification used for the production of mutant forms of SLT 1, cloned into the pUC19 expression vector, was identical to that used for the expression and purification of SLT 1 wild type (section 3.1.2)

SLTP1, SLTP2, SLTP3 and SLTP4 were expressed using the expression plasmids pSLTP1, pSLTP2, pSLTP3 and pSLTP4 respectively transformed into *Escherichia coli* JM105. Purification of toxins from *Escherichia coli* periplasm was achieved by binding to fresh Gb_3-Sepharose affinity matrix columns described previously (3.1.2).

In all four cases expression and purification using the protocols described yielded recombinant holotoxins with the expected molecular weight as analyzed by SDS PAGE (2.7.7). Approximately 1mg of pure toxin was obtained for each mutant from a starting culture of 1 liter. The results of expression and purification of recombinant mutant holotoxins are shown in figures 3.2.9 - 3.2.12. Recombinant proteins were stored for short periods of time (approximately 1 month) at 4°C in PBS, proteins kept for longer periods of time were stored in small aliquots at -70°C in PBS.

Figure 3.2.9 Analysis of expression and purification of SLTP1 by SDS polyacrylamide gel electrophoresis.

Figure 3.2.9 shows the expression and subsequent purification of mutant SLTP1 protein analyzed on a coomasie G250 stained 15 % SDS PAG. Protein coded in pSLTP1, under the transcriptional control of the *lac*Z promoter, was expressed in *Escherichia coli* JM105. Lane 2 shows the precolumn periplasm extracted from transformed *Escherichia coli.* Lanes 3-6 show eluted fractions of pure mutant protein from a 1 ml Gb_3-Sepharose affinity column with 6M guanidine hydrochloride pH6.7. The arrows indicate the positions of SLT A chain (32kDa) and SLT B chain (7.7kDa). Molecular masses are indicated in kDa.

Lane 1 Molecular weight markers

Lane 2 precolumn periplasm (5μl)

Lane 3 eluted fraction 2 (30μl)

Lane 4 eluted fraction 3 (30μl)

Lane 5 eluted fraction 4 (30μl)

Lane 6 eluted fraction 5 (30μl)

Lane 7 eluted fraction 6 (30μl)

Lane 8 molecular weight markers

Figure 3.2.9 Analysis of expression and purification of SLTP1 by SDS polyacrylamide gel electrophoresis.

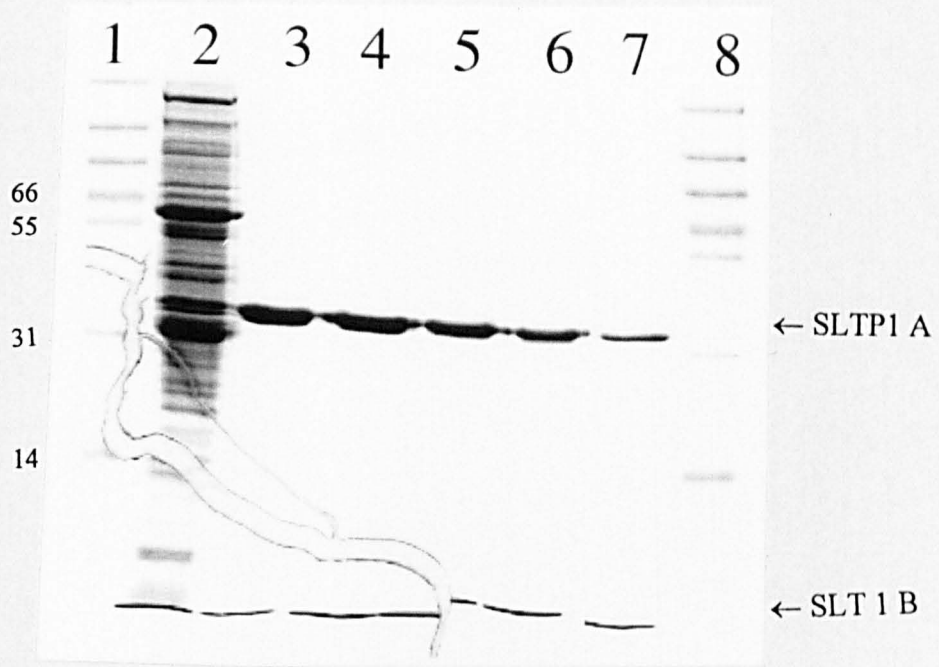

Figure 3.2.10 Analysis of expression and purification of SLTP2 by SDS polyacrylamide gel electrophoresis.

Figure 3.2.10 shows the expression and subsequent purification of mutant SLTP2 protein analyzed on silver stained 15 % SDS PAGE. Protein coded in pSLTP2, under the transcriptional control of the *lac*Z promoter, was expressed in *Escherichia coli* JM105. Lane 2 shows the precolumn periplasm extracted from transformed *Escherichia coli.* Lanes 3-7 show eluted fractions of mutant protein from a 1 ml Gb_3-Sepharose affinity column with 6M guanidine hydrochloride pH6.7. The arrows indicate the positions of SLT A chain (32kDa) and SLT B chain (7.7kDa). Molecular masses are indicated in kDa.

Lane 1 Molecular weight markers

Lane 2 precolumn periplasm (5μl)

Lane 3 eluted fraction 8 (30μl)

Lane 4 eluted fraction 9 (30μl)

Lane 5 eluted fraction 10 (30μl)

Lane 6 eluted fraction 11 (30μl)

Lane 7 eluted fraction 12 (30μl)

Figure 3.2.10 Analysis of expression and purification of SLTP2 by SDS polyacrylamide gel electrophoresis.

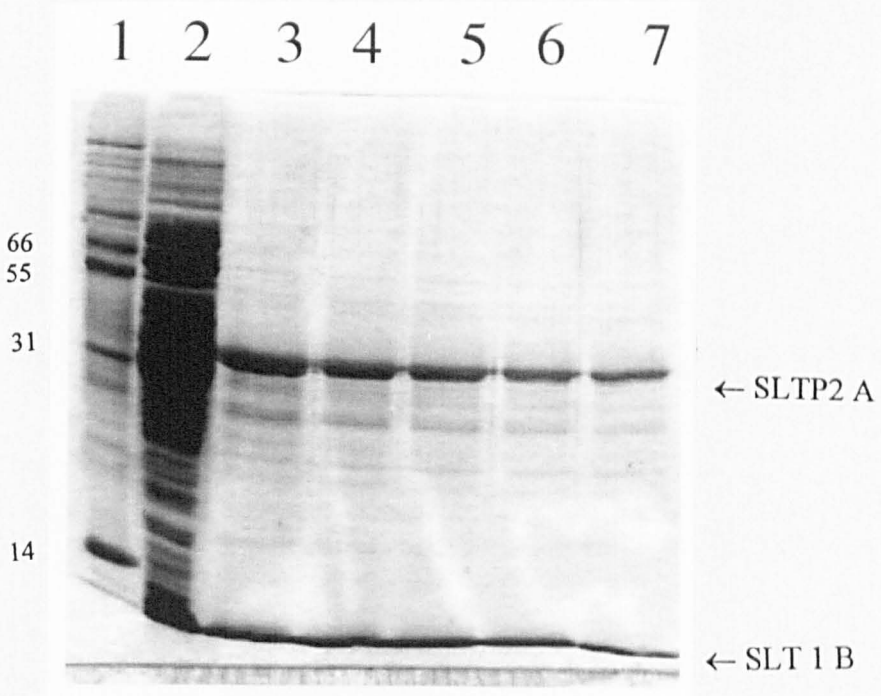

Figure 3.2.11 Analysis of expression and purification of SLTP3 by SDS polyacrylamide gel electrophoresis.

Figure 3.2.11 shows the expression and subsequent purification of mutant SLTP3 protein analyzed on a Coomasie G250 stained 15 % SDS PAG. Protein coded in pSLTP3, under the transcriptional control of the *lacZ* promoter, was expressed in *Escherichia coli* JM105. Lane 2 shows the precolumn periplasm extracted from transformed *Escherichia coli.* Lane 3 shows proteins which do not bind to the column. Lanes 4-8 show eluted fractions of pure mutant protein from a 1 ml Gb_3-Sepharose analogue column with 6M guanidine hydrochloride pH6.7. The arrows indicate the positions of SLT A chain (32kDa) and SLT B chain (7.7kDa). Molecular masses are indicated in kDa.

Lane 1 Molecular weight markers

Lane 2 precolumn periplasm (5μl)

Lane 3 flow through 15 (μl)

Lane 4 eluted fraction 4 (30μl)

Lane 5 eluted fraction 5 (30μl)

Lane 6 eluted fraction 6 (30μl)

Lane 7 eluted fraction 7 (30μl)

Lane 8 eluted fraction 8 (30μl)

Lane 9 molecular weight markers

Figure 3.2.11 Analysis of expression and purification of SLTP3 by SDS polyacrylamide gel electrophoresis.

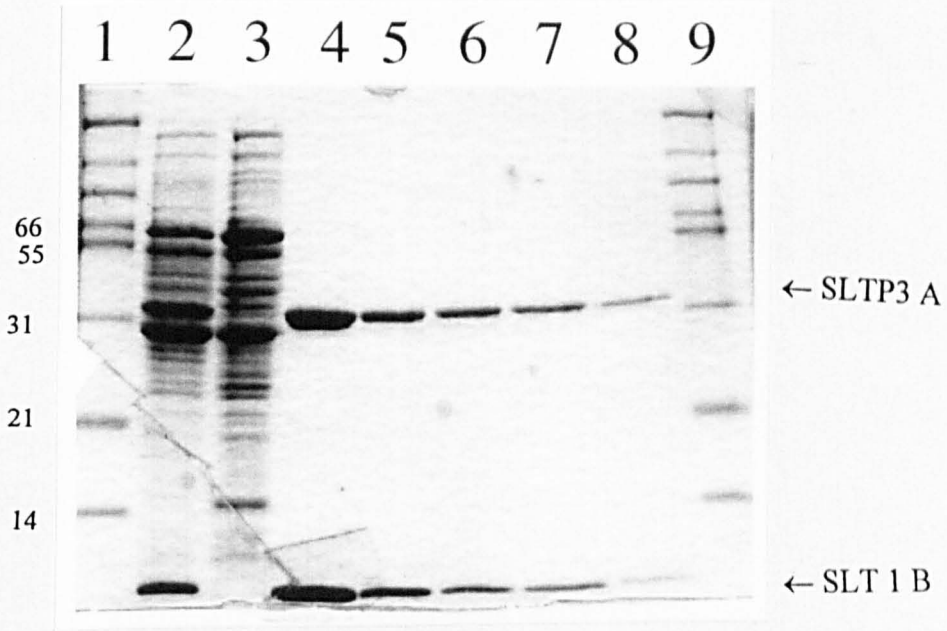

Figure 3.2.12 Analysis of expression and purification of SLTP4 by SDS polyacrylamide gel electrophoresis.

Figure 3.2.12 shows the expression and subsequent purification of mutant SLTP4 protein analyzed on a Coomasie G250 stained 15 % SDS PAG. Protein coded in pSLTP4, under the transcriptional control of the *lac*Z promoter, was expressed in *Escherichia coli* JM105. Lane 2 shows the precolumn periplasm extracted from transformed *Escherichia coli.* Lanes 3-6 show eluted fractions of pure mutant protein from a 1 ml Gb_3-Sepharose affinity column with 6M guanidine hydrochloride pH6.7. The arrows indicate the positions of SLT A chain (32kDa) and SLT B chain (7.7kDa). Molecular masses are indicated in kDa.

Lane 1 Molecular weight markers

Lane 2 precolumn periplasm (5μl)

Lane 3 eluted fraction 6 (30μl)

Lane 4 eluted fraction 7 (30μl)

Lane 5 eluted fraction 8 (30μl)

Lane 6 eluted fraction 9 (30μl)

Lane 7 molecular weight markers

Figure 3.2.12 Analysis of expression and purification of SLTP4 by SDS polyacrylamide gel electrophoresis.

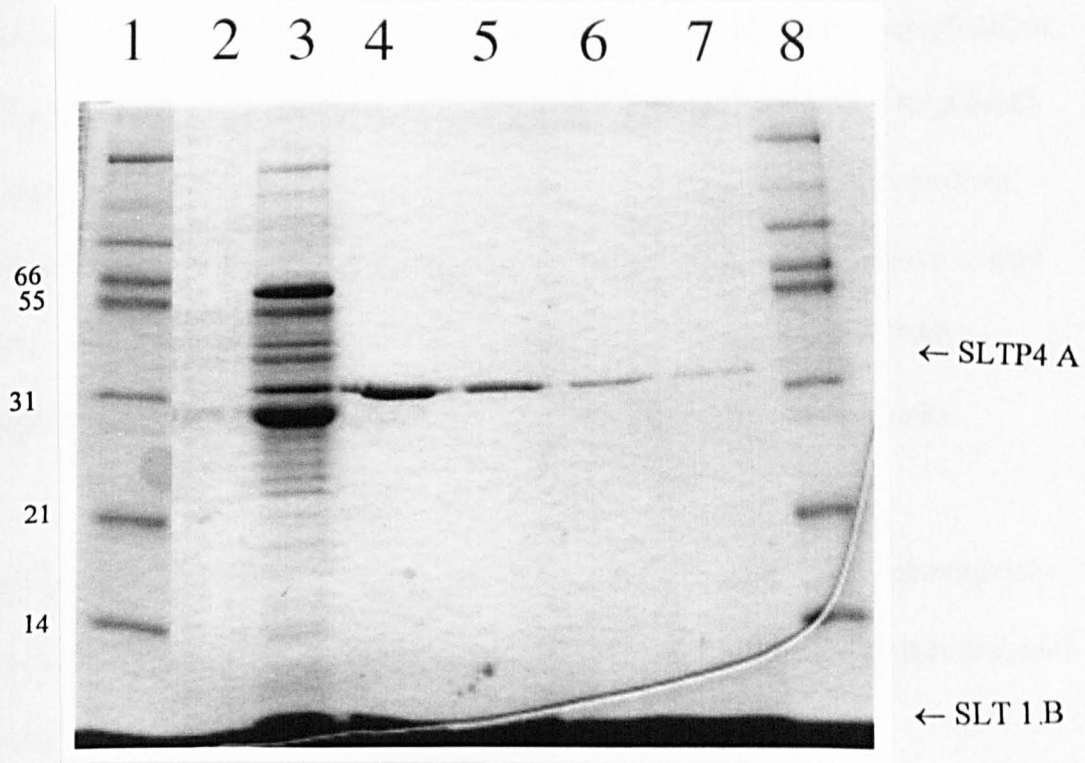

3.2.3 *In vitro* expression of SLT223stop.

RNA transcribed, under control of the viral T7 promoter, in pGEM223stop linerised by digestion with *PvuI* (2.4.1), was expressed *in vitro* using a wheat germ translation system in the presence of [^{35}S]-methionine (2.4.2). Control translation reactions were also carried out in order to check that the translation reactions were working and to aid the sizing of the translation product. The controls used were SLT 1 A1 (an SLT 1 protein truncated by insertion of a stop codon in place of the codon for Arg248 approximately 27kDa in size) and SLT 1 A chain (a full length clone containing the entire SLT 1 A chain coding sequence approximately 32kDa in size) kind gifts from Dr Beverley Burgess (Warwick). Both of these SLT 1 constructs are in the pGEM2 background under control of the viral T7 promoter. PAP R3 (a pGEM2 construct transcriptionally controlled by the T7 promoter) which codes for an inactive mutant of the type I ribosome inactivating protein pokeweed anti-viral protein (PAP) approximately 30kDa in size a kind gift from Dr John Chaddock (Warwick).

Translation of pGEM223stop transcribed RNA results in a protein of approximately 25 kDa as analyzed by SDS PAGE. Expression of SLT223stop and controls is shown are figure 3.2.13.

Figure 3.2.13 *In vitro* translation of SLT223stop protein in wheat germ lysate.

Figure 3.2.13 shows the separation of translated transcripts in a wheat germ cell free system on a 15% polyacrylamide gel. 1μg of each transcript coding for rSLT 1 A chains or a mutant form of poke weed anti-viral protein was translated using a cell free wheat germ lysate in the presence of [^{35}S]-methionine (3.2.3). Molecular masses are indicated in kDa.

Lane 1 [^{14}C]-molecular weight markers

Lane 2 translated pGEMA1 transcript

Lane 3 translated pGEMSLTwt transcript

Lane 4 translated pGEM223stop transcript

Lane 5 translated pGEM2PAPR3 transcript

Figure 3.2.13 *In vitro* Translation of SLT223stop protein in wheat germ lysate.

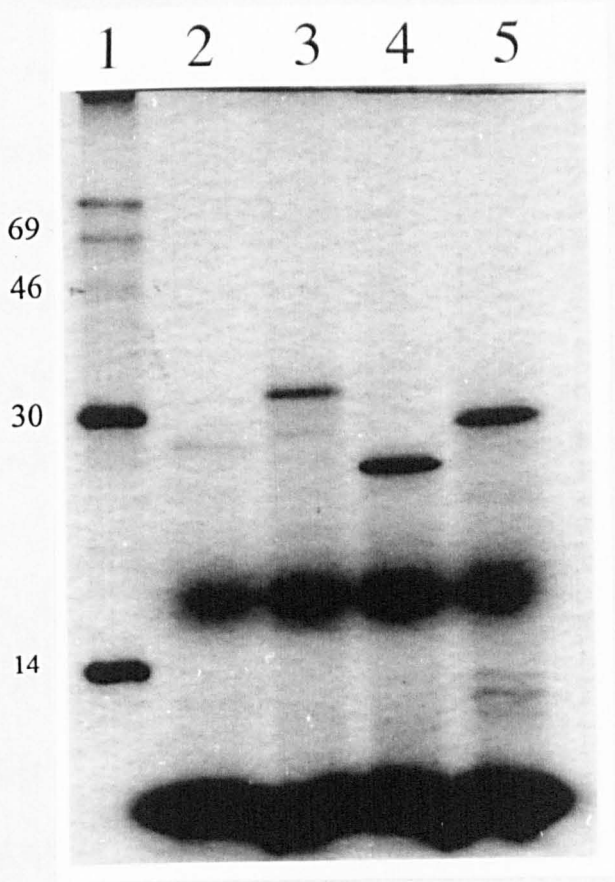

3.2.4 Discussion

Cloning of the SLT 1 operon sequence into the bacteriophage M13mp18 afforded a rapid and simple method for the production of mutant coding sequences for SLT 1. DNA coding for the proteins SLTP4 and 223stop could not be made by standard SDM methods. The reasons for this are not clear. Recombinant PCR provided an effective yet costly alternative to SDM here. By the engineering of unique cloning sites at the 3' and 5' terminal ends of the operon sequence by PCR (3.1.1), mutant coding sequences could be subcloned into the multiple cloning site of pUC19 directly. DNA cloned in this manner was then ideally placed for expression under the transcriptional control of the *lac*Z promoter. The associated Shine-Dalgarno sequence was also included in these constructs as it is considered that this sequence is probably optimally positioned in relation to the translational start site.

The resulting expression constructs were all able to mediate expression of mutant forms of SLT 1 in quantities more than adequate for the purposes of this study approximately 1mg in each case. All mutant proteins expressed were in the form of soluble holotoxins which were able to bind to the trisaccharide globotriose linked via a spacer to cyanogen bromide-activated Sepharose 4B. Binding to this matrix allowed the purification of these toxins to single A and B chain bands on SDS polyacrylamide gels with migration rates as predicted.

pGEM223stop was constructed by cloning a full length SLT 1 coding sequence into which a stop codon had been introduced at the position coding for the amino acid Arg223 into the polylinker region of pGEM2. The resulting construct is able to mediate the transcription and translation of a truncated form of SLT 1 A chain when transcribed and translated in a wheat germ cell free system.

The resulting translation product has an apparent molecular weight of 25.1kDa by measurement of migration on a 15 % polyacrylamide gel (figure 3.2.13). This figure compares with a predicted molecular weight of 24.5kDa for this protein. This small discrepancy may be explained by aberrant migration in this gel system since SLT A1 also shown in figure 3.2.13 appears to have a molecular weight of 28.2kDa compared with the predicted molecular weight of 27.3kDa.

In summary the expression systems and where appropriate purification systems presented in this chapter allow the production of biochemically pure mutant proteins. In the case of potential processing mutant proteins, large quantities were prepared for subsequent biochemical analysis.

Chapter 3

3.3 Characterisation of SLT1 and potential processing mutants.

Introduction

The aim of this study is to investigate the proteolytic processing requirements for SLT 1 during uptake into eukaryotic cells (section 1.6). To achieve this aim several mutant proteins were made with specific amino acid changes at residues likely to be involved in proteolytic processing. In this chapter, the five mutant proteins described in chapter 2 are characterised with respect to their susceptibility to proteolytic processing both *in vitro* and *in vivo*. The effects of several membrane permeable reagents are also investigated. Brefeldin A is a fungal metabolite which is known to disrupt the Golgi stack with consequent peturbation of Golgi to ER trafficking. Brefeldin A-treated Vero cells are not able to transport SLT 1 from the TGN to the Golgi and ER where it is thought that translocation to the cytosol occurs (section 1.6). Ammonium chloride is a reagent which increases lysosomal pH. This reagent was used to inhibit proteolysis of toxin which might occur in the lysosome. Calpain inhibitor I is a potent inhibitor of the proteolytic enzymes known collectively as the calpains. Pretreatment of cells with calpain inhibitor I inhibits the activity of the intracellular calpain thought to play a role in alternative proteolytic processing of SLT 1 (section 1.6).

3.3.1 N-glycosidase activity of SLT 1 and potential processing mutants.

The N-glycosidase activities of SLT 1 wild-type and the processing mutants described in chapter 2 towards isolated rabbit reticulocyte ribosomes were compared *in vitro* using the aniline assay (section 2.7.3). Rabbit reticulocyte ribosomes were incubated with three decreasing amounts of recombinant SLT 1, SLTP1, SLTP2, SLTP3 and SLTP4 (1000ng, 100ng, 10ng) prior to treatment with aniline. The resulting aniline-treated RNA was run on a 1.2% denaturing agarose gel (section 2.3.4). Separated RNA was subjected to northern blot analysis (section 2.3.17) using a DNA probe specific for the 5' end of rabbit 28S ribosomal RNA. Figure 3.3.1 shows an autoradiograph of a northern blot prepared in this manner. Depurination of rRNA followed by treatment with acetic aniline results in cleavage of the rRNA backbone at position 4324 releasing an RNA fragment of 394 bases from the 5' end of 28S rRNA. The presence of this short fragment is diagnostic for the action of ribosome inactivating proteins. The northern blot in figure 3.3.1 clearly demonstrates that all five proteins investigated using the aniline assay possess N-glycosidase activity. This activity is not apparently altered as a result of the mutations made, though from such non-quantitative analyses it isn't possible to totally exclude slight changes in catalytic activity.

Figure 3.3.1 Comparison of N-glycosidase activity of SLT 1 and potential processing mutants using the aniline assay and visualized by northern blot analysis.

Figure 3.3.1 shows a autoradiograph of a rRNA transferred to a nitrocellulose filter by northern blotting followed by hybridization of a DNA oligonucleotide [^{32}P]-γ ATP labelled probe, designed to hybridize to the 5' end of the 28S rRNA from rabbit. Rabbit reticulocyte ribosomes were treated with decreasing amounts of toxin at 30°C for 30 min. The resulting RNA was isolated and treated with acetic-aniline at 60°C for 2 min. Aniline treated RNA was separated on a 1.2% denaturing formamide agarose gel before transfer to nitrocellulose. Specific depurination due to the action of SLT 1 followed by aniline treatment leads to release of a 394 base RNA fragment indicated by an arrow.

Lane 1 1000ng rSLT wild-type

lane 2 100ng rSLT wild-type

Lane 3 10ng rSLT wild-type

Lane 4 1000ng rSLTP1

Lane 5 100ng rSLTP1

Lane 6 10ng rSLTP1

Lane 7 1000ng rSLTP3

Lane 8 100ng rSLTP3

Lane 9 10ng rSLTP3

Lane 10 1000ng rSLTP4

Lane 11 100ng rSLTP4

Lane 12 10ng rSLTP4

Lane 13 1000ng rSLTP2

Lane 14 100ng rSLTP2

Lane 15 10ng rSLTP2

Figure 3.3.1 Comparison of N-glycosidase activity of SLT 1 and potential processing mutants using the aniline assay and visualized by northern blot analysis.

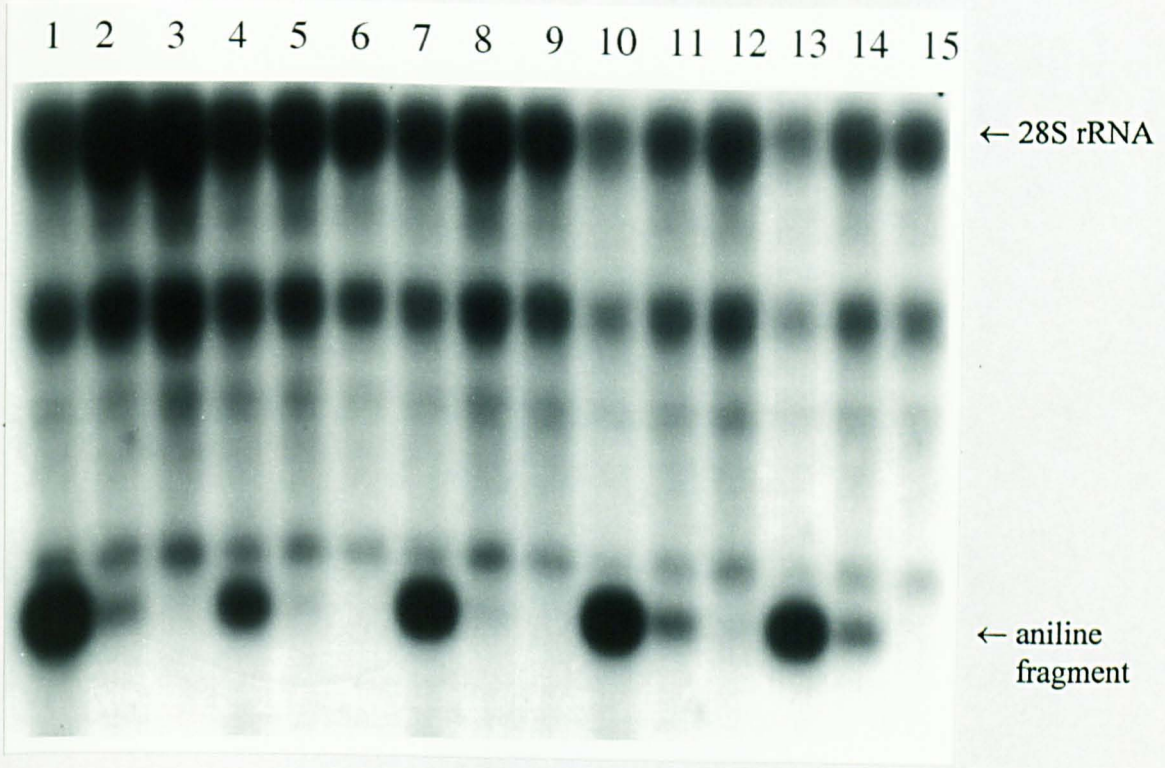

The N-glycosidase activity of the protein 223stop described in Chapter 2 was assessed by its ability to depurinate rabbit reticulocyte ribosomes during *in vitro* translation (2.4.3ii). The 223stop construct was made in order to determine whether an SLT 1 A chain truncated at residue 223 had N-glycosidase activity. To preclude the need for purification of this protein, the coding DNA sequence was cloned into a *in vitro* expression vector where resulting transcrips could be translated and N-glycosidase activity assessed directly on the translating ribosomes. The construction and subsequent expression of pGEM223 in a wheat germ lysate cell free system are described in chapter 2.

To assess whether 223stop maintained N-glycosidase activity, the *in vitro* transcript from pGEM223stop was translated in a non-nuclease treated rabbit reticulocyte lysate system. All transcripts were translated for 1 hour at 30°C. Following translation, rRNA was extracted from this reaction and subjected to hydrolysis with acetic-aniline. The extent of ribosome depurination was then determined by separation of isolated rRNA on a denaturing 1.2% formamide agarose gel. The appearance of a 394 base fragment following acetic-aniline cleavage is diagnostic of ribosome depurination. Figure 3.2.2 shows the results of such an assay. Control transcripts shown in chapter 2 were also translated in non-nuclease treated rabbit reticulocyte lysate. From the assay described the truncated protein, 223stop does not appear to have N-glycosidase activity. The positive controls SLT wt and SLTA1 both display activity in this assay whereas the inactive PAP mutant, PAPR3, does not

show activity. In addition to the three controls described a fourth control was used in which an *in vitro* transcript was omitted from the translation reaction, in its place, 100ng of ricin A chain were added. As expected the ribosomes in this reaction also show characteristic modification.

Figure 3.3.2 Depurination of rabbit reticulocyte ribosomes during *in vitro* translation of pGEM223stop *in vitro* transcript in a non-nuclease treated rabbit reticulocyte lysate.

Figure 3.2.2. shows rRNA extracted from *in vitro* translation reactions in which potential ribosome inactivating proteins have been translated. *In vitro* transcripts coding for toxins were translated in a rabbit reticulocyte lysate system for 1 hour at 30°C. Extracted rRNA was then subjected to hydrolysis with acetic-aniline and separated on a 1.2% denaturing formamide agarose gel. The separated RNA was visualized by ethidium bromide staining. Release of a 394 base RNA fragment (indicated by the arrow) is characteristic of ribosome depurination. In addition to two positive controls (SLTA1 and SLTwt) which possess N-glycosidase activity and a negative control (PAPR3) which lacks N-glycosidase activity, a reaction in which mRNA was replaced with 100ng RTA was included.

Lane 1 Ribosomes translating pGEM223stop transcript

Lane 2 Ribosomes translating pGEMSLTA1 transcript

Lane 3 Ribosomes translating pGEMSLTwt transcript

Lane 4 Ribosomes translating pGEMPAPR3 transcript

Lane 5 100ng RTA no transcript

Figure 3.3.2 Depurination of rabbit reticulocyte ribosomes during *in vitro* translation of pGEM223stop *in vitro* transcript in a non-nuclease treated rabbit reticulocyte lysate.

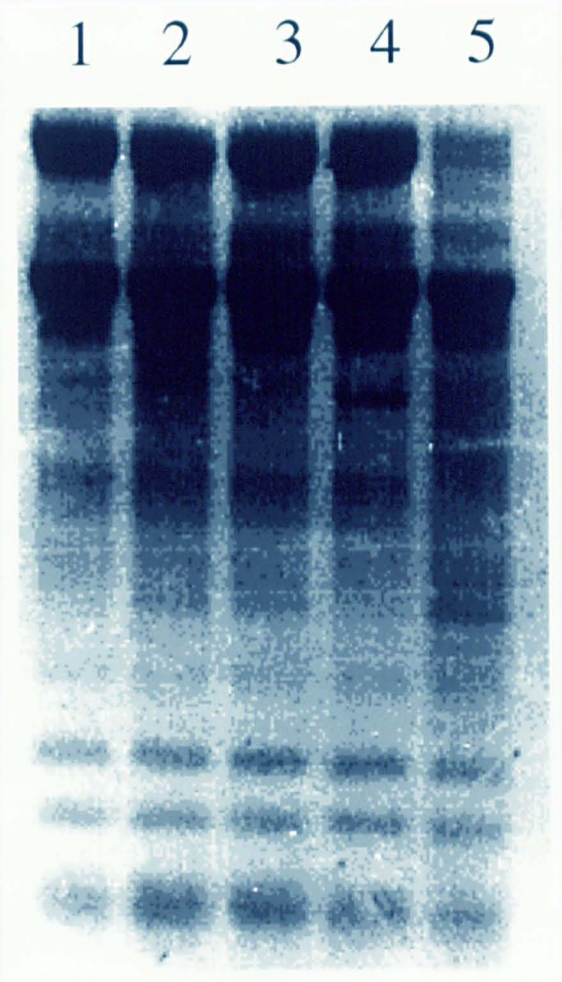

3.3.2 *In vitro* trypsin sensitivity of SLT 1 and potential processing mutants

The sensitivity of SLT 1 and the processing mutants to trypsin was used to assess the effects of mutations made to trypsin-sensitive amino acyl residues. The trypsin-sensitive loop of wild-type SLT 1 contains two arginine residues. Treatment of SLT 1 wt with trypsin *in vitro* results in cleavage of the toxin A chain to two fragments of molecular weight approximately 27kDa and 4kDa, the smaller of these fragments not being resolved on standard 15% SDS PAGE. Removal of exposed arginine residues within the loop should reduce sensitivity to this protease. The use of trypsin treatment of mutant proteins is also used as a measure of the degree of malfolding induced in proteins as a result of mutation. Figure 3.3.3 and 3.3.4 shows the separation by 15% PAGE of mutant and wild-type toxins treated with increasing concentrations of trypsin run under reducing and non-reducing conditions respectively. Under the conditions used wild-type toxin appears to be completely cleaved to the A1 sized fragment at both 0.1 and 5μg/ml trypsin as is the SLTP2 mutant. SLTP1 and SLTP3 are mostly resistant to trypsin at the concentrations used. SLTP4 also remains mostly resistant to trypsin since no A1-sized fragment is generated. However a larger fragment of approximately 29kDa occurs. All fragments generated from the A chains of wild-type and mutant proteins are generated from within the disulphide bonded loop since when the same samples are run under non-reducing conditions these bands are absent (figure 3.3.4).

Figure 3.3.3 Reducing 15% SDS polyacrylamide gel electrophoresis of trypsin-treated SLT 1 and potential processing mutants.

1μg of wild-type and mutant toxins were treated with 0.1 and 5μg/ml of sequencing grade trypsin in a 30μl reaction for 7 min at 37°C. Reactions were stopped by addition of 1μl of TLCK 1mg/ml in 0.05M sodium acetate-acetic acid pH5.0 and incubation on ice for 5 min prior to boiling in sample loading buffer. The resulting protein was separated on a 15% SDS PAG under reducing conditions and protein visualized by silver staining.

Lane 1 SLT 1 wt -trypsin

Lane 2 SLT 1 wt 0.1μg/ml trypsin

Lane 3 SLT 1 wt 5μg/ml trypsin

Lane 4 SLTP1-trypsin

Lane 5 SLTP1 0.1μg/ml trypsin

Lane 6 SLTP1 5μg/ml trypsin

Lane 7 SLTP2-trypsin

Lane 8 SLTP2 0.1μg/ml trypsin

Lane 9 SLTP2 5μg/ml trypsin

Lane 10 SLTP3 -trypsin

Lane 11 SLTP3 0.1μg/ml trypsin

Lane 12 SLTP3 5μg/ml trypsin

Lane 13 SLTP4 -trypsin

Lane 14 SLTP4 0.1μg/ml trypsin

Lane 15 SLTP4 5μg/ml trypsin

Lane 16 MW markers

Figure 3.3.3 Reducing 15% SDS polyacrylamide gel electrophoresis of trypsin-treated SLT 1 and potential processing mutants.

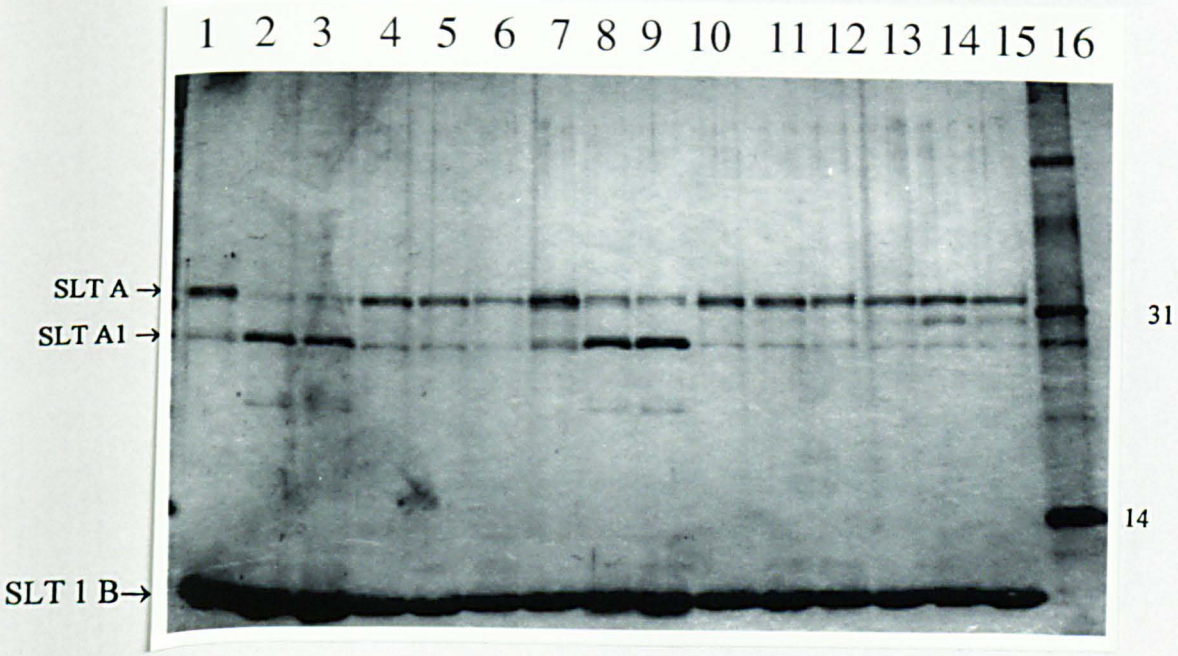

Figure 3.3.4 Non-reducing 15% SDS polyacrylamide gel electrophoresis of trypsin-treated SLT 1 and processing mutants.

1μg of wild-type and mutant toxins were treated with 0.1 and 5μg/ml of sequencing grade trypsin in a 30μl reaction for 7 min at 37°C. Reactions were stopped by addition of 1μl of TLCK 1mg/ml in 0.05M sodium acetate-acetic acid pH5.0 and incubation on ice for 5 min prior to boiling in sample loading buffer. The resulting protein was separated on a 15% SDS PAG under non-reducing conditions and protein visualized by coomasie blue G250 staining.

Lane 1 molecular weight markers

Lane 2 SLT 1 wt -trypsin

Lane 3 SLT 1 wt 0.1μg/ml trypsin

Lane 4 SLT 1 wt 5μg/ml trypsin

Lane 5 SLTP1-trypsin

Lane 6 SLTP1 0.1μg/ml trypsin

Lane 7 SLTP1 5μg/ml trypsin

Lane 8 SLTP2-trypsin

Lane 9 SLTP2 0.1μg/ml trypsin

Lane 10 SLTP2 5μg/ml trypsin

Lane 11 SLTP3 -trypsin

Lane 12 SLTP3 0.1μg/ml trypsin

Lane 13 SLTP3 5μg/ml trypsin

Lane 14 SLTP4 -trypsin

Lane 15 SLTP4 0.1μg/ml trypsin

Lane 16 SLTP4 5μg/ml trypsin

Lane 17 MW markers

Figure 3.3.4 Non-reducing 15% SDS polyacrylamide gel electrophoresis of trypsin-treated SLT 1 and potential processing mutants.

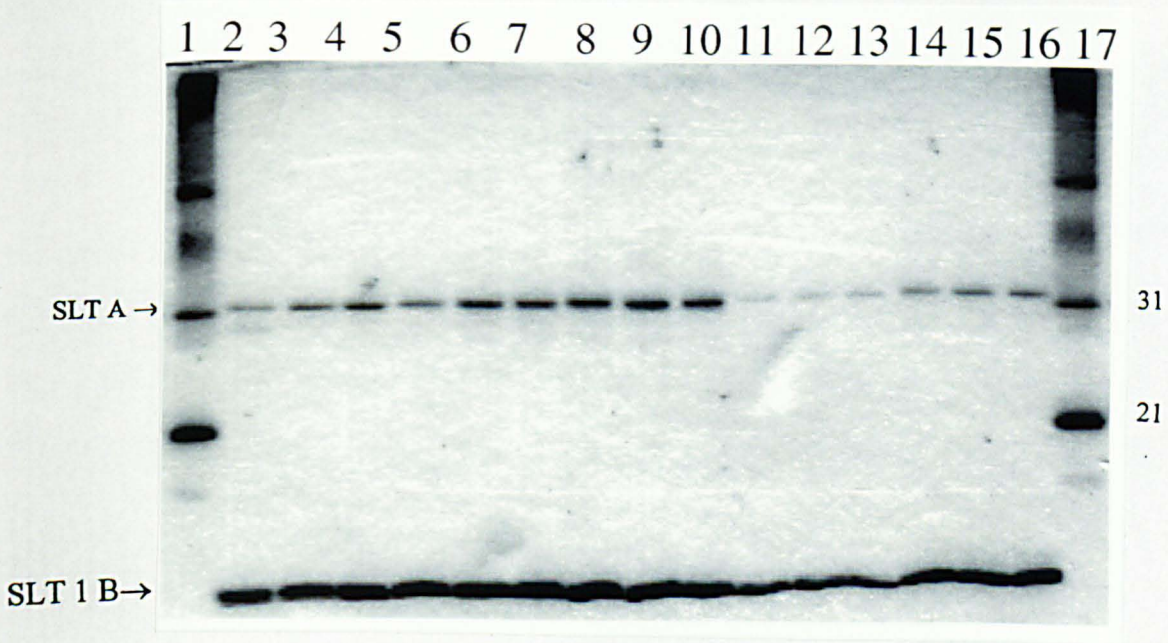

3.3.3 Cytotoxicity of SLT 1 and the potential processing mutants.

The cytotoxicity of wild-type SLT 1 and the processing mutants described in chapter 2 was determined using Vero cells (section 2.7.4). IC_{50} (the concentration of toxin required to reduce protein synthesis by 50%) values were calculated for the toxins described both on untreated Vero cells and also on Vero cells which had been treated with certain reagents, by analyzing protein synthesis inhibition as a function of toxin concentration. The kinetics of intoxication were also determined by analysing protein synthesis inhibition as a function of time. The results of these cytotoxicity experiments are shown in figures 3.3.5-3.3.10.

Over a three hour toxin incubation on untreated Vero cells a large reduction in cytotoxicity between the wild-type toxin and the processing mutants lacking either the loop arginines (SLTP1 and SLTP3) or the loop arginines and the upstream furin consensus motif (SLTP4) can be seen. The mutants SLTP1 and SLTP3 are 25 fold less toxic than wild-type and SLTP4 is 132 fold less toxic than the wild-type protein. The toxicity of the SLTP2 mutant protein is identical to wild type toxin. After a longer (6 hour) incubation, the toxicity of SLTP1 and SLTP3 are identical to that of the wild-type protein, however the mutant SLTP4 remains 62 fold less toxic than the wild-type toxin.

Where the cells are pretreated for 30 minutes with NH_4Cl no effect on the toxicity of the wild-type protein or the mutants SLTP1 and SLTP3 is seen, however the toxicity of SLTP4 appears to be increased by a factor of 3 when compared with the same toxin in untreated Vero cells. Calpain inhibitor I has little effect on the wild-type protein and indeed appears to increase wild-type toxicity by a factor of 2. Calpain inhibitor I does however reduce the toxicity of the mutants SLTP1 and SLTP3 by a factor of 4.5 and 6 respectively. Brefeldin A at a concentration of 2μg/ml protects cells from intoxication with wild-type toxin completely under the conditions tested here. From kinetic measurements wild-type toxin is able to reduce protein synthesis by 50% more quickly than the mutants described giving a t_{50} of 53 minutes. SLTP1 and SLTP4 both have t_{50} values of 75 minutes followed by SLTP3 with a t_{50} of 82 minutes. It is considered that the subtle differences between SLTP1, SLTP4 and SLTP3 are probably not significant as these figures are the result of just two experiments

Figure 3.3.5 Cytotoxicity of SLT 1 wild-type and potential processing mutants: 3 hour incubation of toxin.

$1x10^{-4}$ to 10 ng/ml of each recombinant holotoxin, diluted in DMEM, was incubated with 1.2 to 1.5 $x10^4$ Vero cells plated in 96 well tissue culture plates for 2.5 hours at 37°C in a 5% CO_2 incubator. Following incubation with toxin the cell monolayers were washed once with PBS and 100µl of PBS containing 1µCi of [^{35}S]-methionine was added to each well. Cells were incubated for a further 30 min. Monolayers were then washed three times with 5% ice cold trichloroacetic acid and neutralized by a single wash with PBS. Acid-precipitated protein was then released with 100µl of 0.5M NaOH and incorporated radioactivity was quantified by liquid scintillation counting.

All values are the mean of four replicate samples. Protein synthesis inhibition was calculated as the percentage incorporation of radioactivity compared with the mean of six no toxin controls.

Toxin	IC_{50} ng/ml
rSLT 1 wt	0.019
SLTP1	0.469
SLTP2	0.019
SLTP3	0.469
SLTP4	2.509

Figure 3.3.5 Cytotoxicity of SLT 1 wild-type and potential processing mutants: 3 hour incubation of toxin.

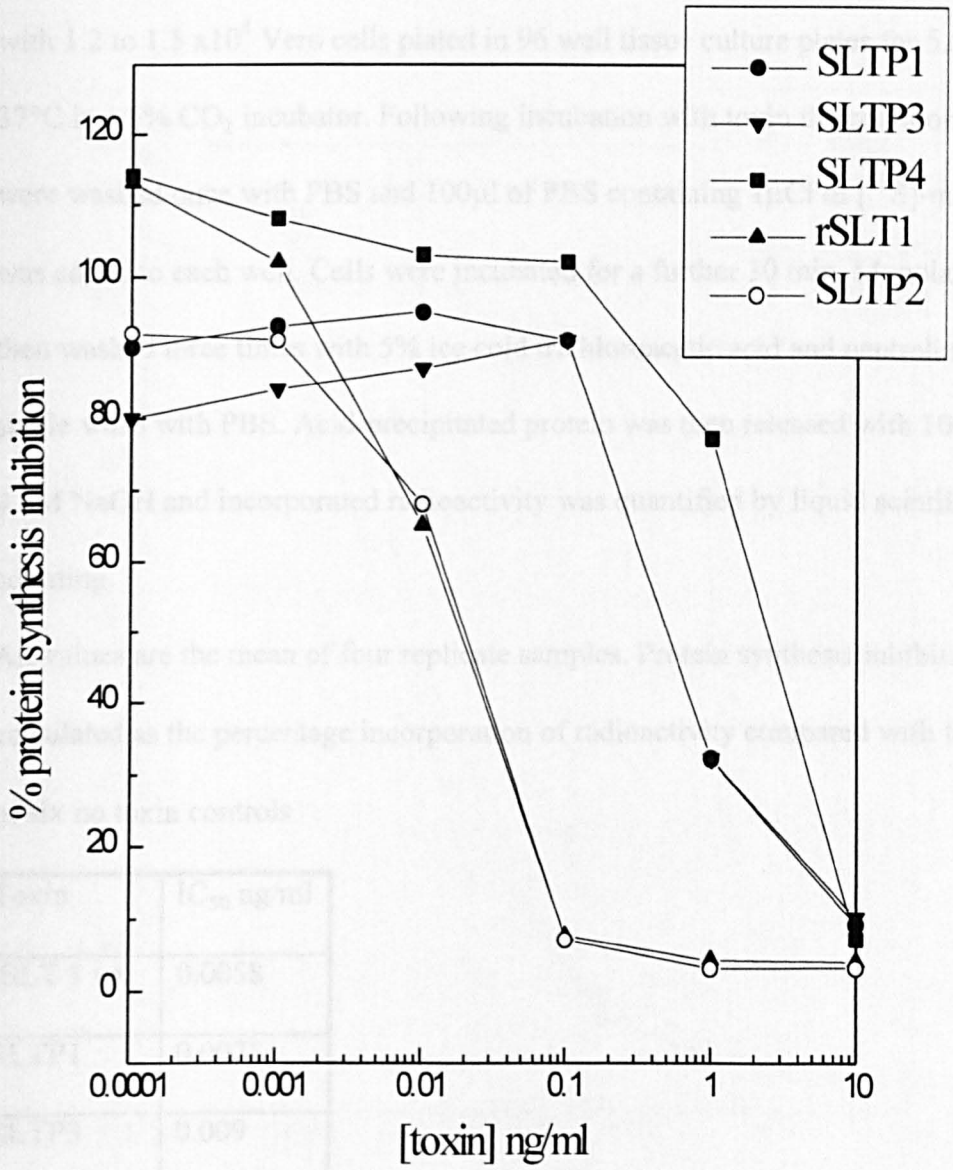

Figure 3.3.6 Cytotoxicity of SLT 1 wild-type and potential processing mutants: 6 hour incubation of toxin.

$1x10^{-4}$ to 10 ng/ml of each recombinant holotoxin, diluted in DMEM, was incubated with 1.2 to 1.5 $x10^4$ Vero cells plated in 96 well tissue culture plates for 5.5 hours at 37°C in a 5% CO_2 incubator. Following incubation with toxin the cell monolayers were washed once with PBS and 100µl of PBS containing 1µCi of [^{35}S]-methionine was added to each well. Cells were incubated for a further 30 min. Monolayers were then washed three times with 5% ice cold trichloroacetic acid and neutralized by a single wash with PBS. Acid-precipitated protein was then released with 100µl of 0.5M NaOH and incorporated radioactivity was quantified by liquid scintillation counting.

All values are the mean of four replicate samples. Protein synthesis inhibition was calculated as the percentage incorporation of radioactivity compared with the mean of six no toxin controls.

Toxin	IC_{50} ng/ml
rSLT 1 wt	0.0058
SLTP1	0.0071
SLTP3	0.009
SLTP4	0.361

Figure 3.3.6 Cytotoxicity of SLT 1 wild-type and potetial processing mutants: 6 hour incubation of toxin.

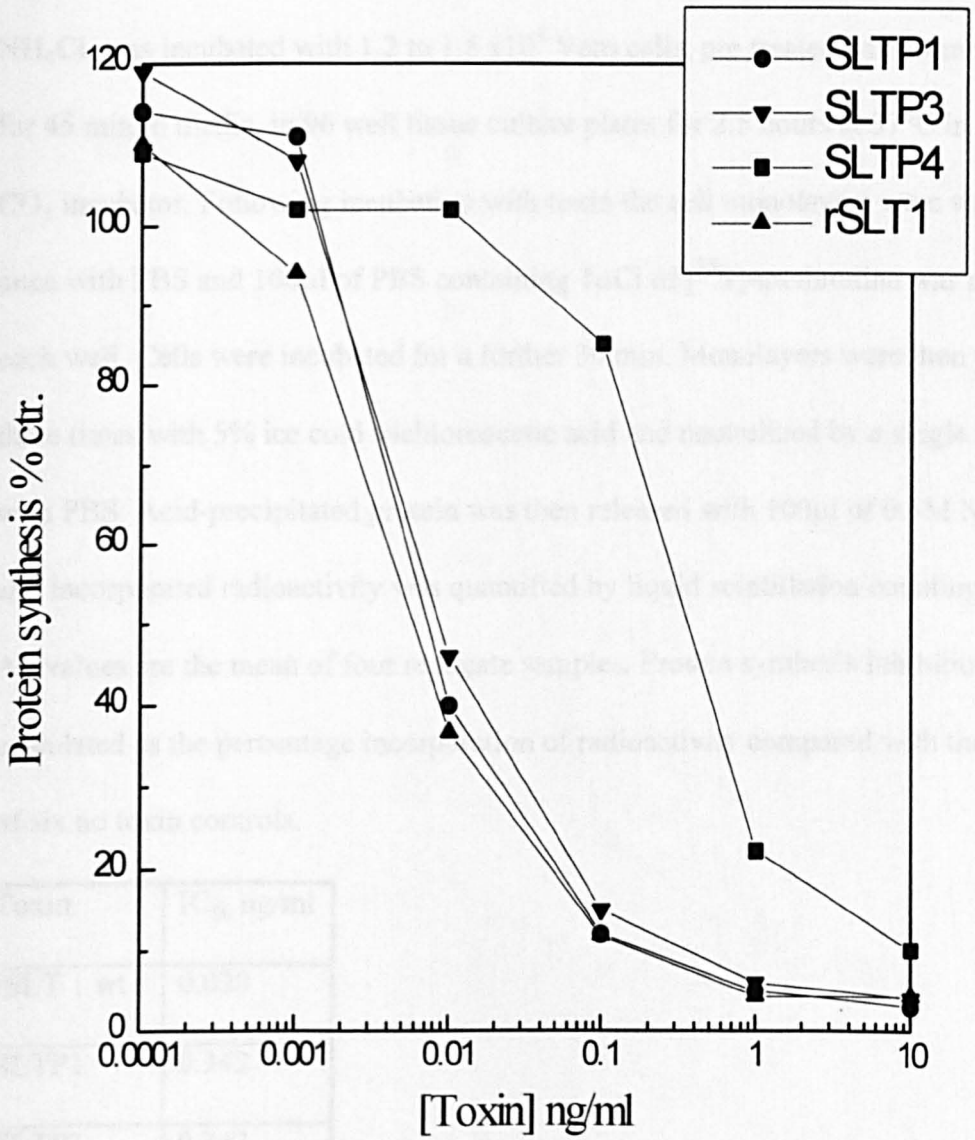

Figure 3.3.7 Cytotoxicity of SLT 1 wild-type and potential processing mutants to Vero cells pretreated with 10mM NH_4Cl: 3 hour incubation of toxin.

$1x10^{-3}$ to 100 ng/ml of each recombinant holotoxin, diluted in DMEM plus 10mM NH_4Cl, was incubated with 1.2 to 1.5 $x10^4$ Vero cells, pre treated with 10mM NH_4Cl for 45 min in media, in 96 well tissue culture plates for 2.5 hours at 37°C in a 5% CO_2 incubator. Following incubation with toxin the cell monolayers were washed once with PBS and 100µl of PBS containing 1µCi of [^{35}S]-methionine was added to each well. Cells were incubated for a further 30 min. Monolayers were then washed three times with 5% ice cold trichloroacetic acid and neutralized by a single wash with PBS. Acid-precipitated protein was then released with 100µl of 0.5M NaOH and incorporated radioactivity was quantified by liquid scintillation counting.
All values are the mean of four replicate samples. Protein synthesis inhibition was calculated as the percentage incorporation of radioactivity compared with the mean of six no toxin controls.

Toxin	IC_{50} ng/ml
rSLT 1 wt	0.020
SLTP1	0.342
SLTP3	0.342
SLTP4	0.774

Figure 3.3.7 Cytotoxicity of SLT 1 wild-type and potential processing mutants to Vero cells pretreated with 10mM NH_4Cl: 3 hour incubation of toxin.

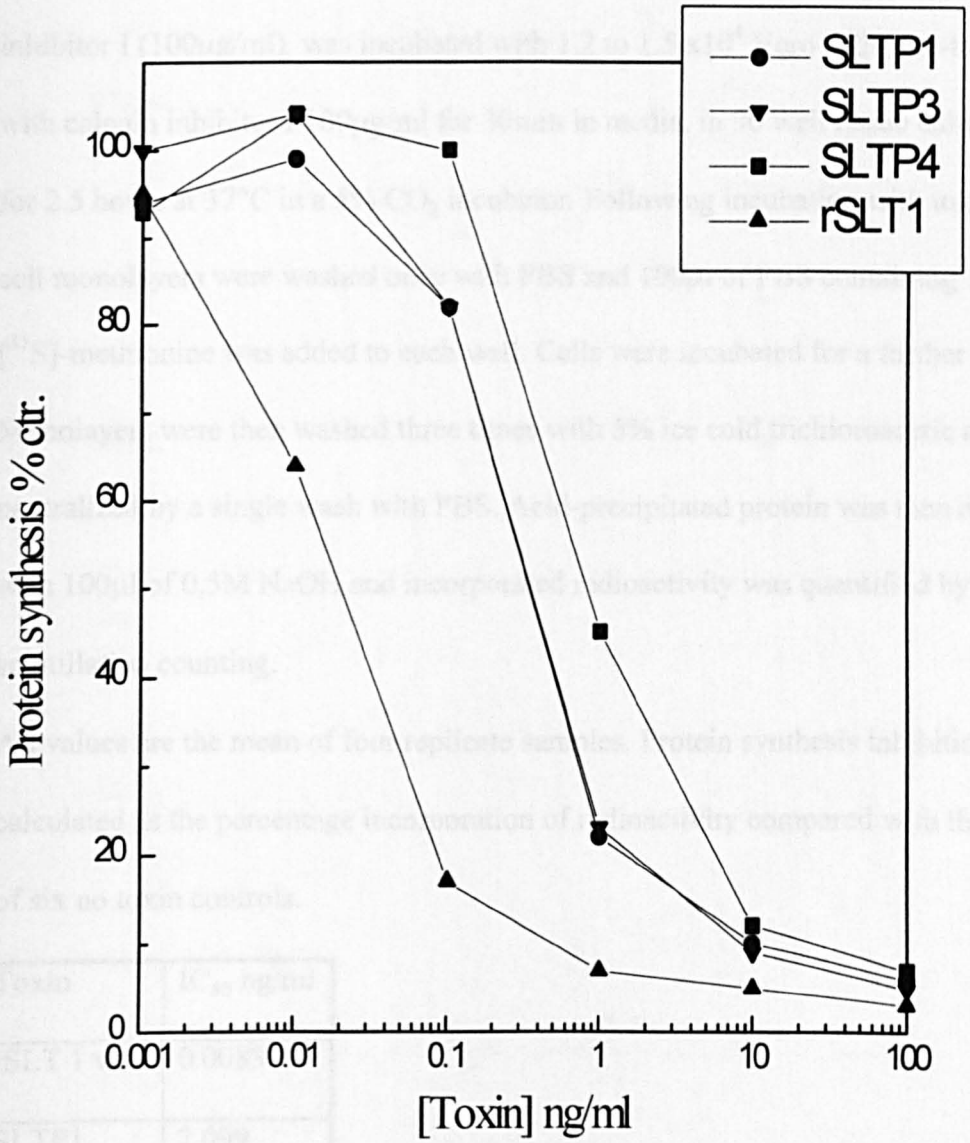

Figure 3.3.8 Cytotoxicity of SLT 1 wild-type and potential processing mutants to Vero cells pretreated with calpain inhibitor I (100μg /ml): 3 hour incubation of toxin.

$1x10^{-4}$ to 10 ng/ml of each recombinant holotoxin, diluted in DMEM plus calpain inhibitor I (100μg/ml), was incubated with 1.2 to 1.5 $x10^4$ Vero cells, pre-treated with calpain inhibitor I 100μg/ml for 30min in media, in 96 well tissue culture plates for 2.5 hours at 37°C in a 5% CO_2 incubator. Following incubation with toxin the cell monolayers were washed once with PBS and 100μl of PBS containing 1μCi of [^{35}S]-methionine was added to each well. Cells were incubated for a further 30 min. Monolayers were then washed three times with 5% ice cold trichloroacetic acid and neutralized by a single wash with PBS. Acid-precipitated protein was then released with 100μl of 0.5M NaOH and incorporated radioactivity was quantified by liquid scintillation counting.

All values are the mean of four replicate samples. Protein synthesis inhibition was calculated as the percentage incorporation of radioactivity compared with the mean of six no toxin controls.

Toxin	IC_{50} ng/ml
rSLT 1 wt	0.0083
SLTP1	2.099
SLTP3	2.845

Figure 3.3.8 Cytotoxicity of SLT 1 wild-type and potential processing mutants to Vero cells pretreated with calpain inhibitor I (100μg /ml): 3 hour incubation of toxin.

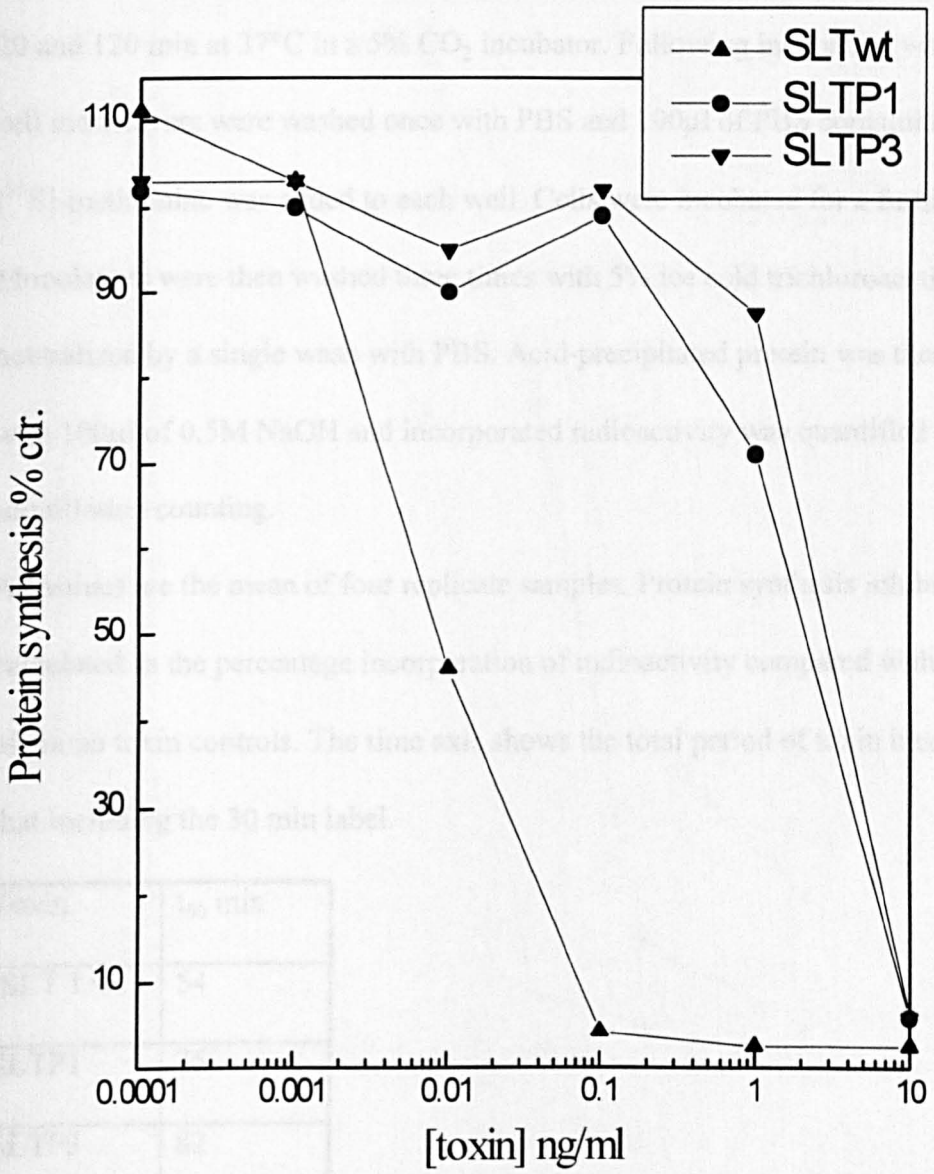

Figure 3.3.9 The kinetics of cytotoxicity of SLT 1 wild-type and potential processing mutants in Vero cells.

100 ng/ml of each recombinant holotoxin, diluted in DMEM, was incubated with 1.2 to 1.5 x10^4 Vero cells plated in 96 well tissue culture plates for time periods between 20 and 120 min at 37°C in a 5% CO_2 incubator. Following incubation with toxin the cell monolayers were washed once with PBS and 100µl of PBS containing 1µCi of [^{35}S]-methionine was added to each well. Cells were incubated for a further 30 min. Monolayers were then washed three times with 5% ice cold trichloroacetic acid and neutralized by a single wash with PBS. Acid-precipitated protein was then released with 100µl of 0.5M NaOH and incorporated radioactivity was quantified by liquid scintillation counting.

All values are the mean of four replicate samples. Protein synthesis inhibition was calculated as the percentage incorporation of radioactivity compared with the mean of six no toxin controls. The time axis shows the total period of toxin incubation i.e. that including the 30 min label.

Toxin	t_{50} min
rSLT 1 wt	54
SLTP1	75
SLTP3	82
SLTP4	75

Figure 3.3.9 The kinetics of cytotoxicity of SLT 1 wild-type and potential processing mutants in Vero cells.

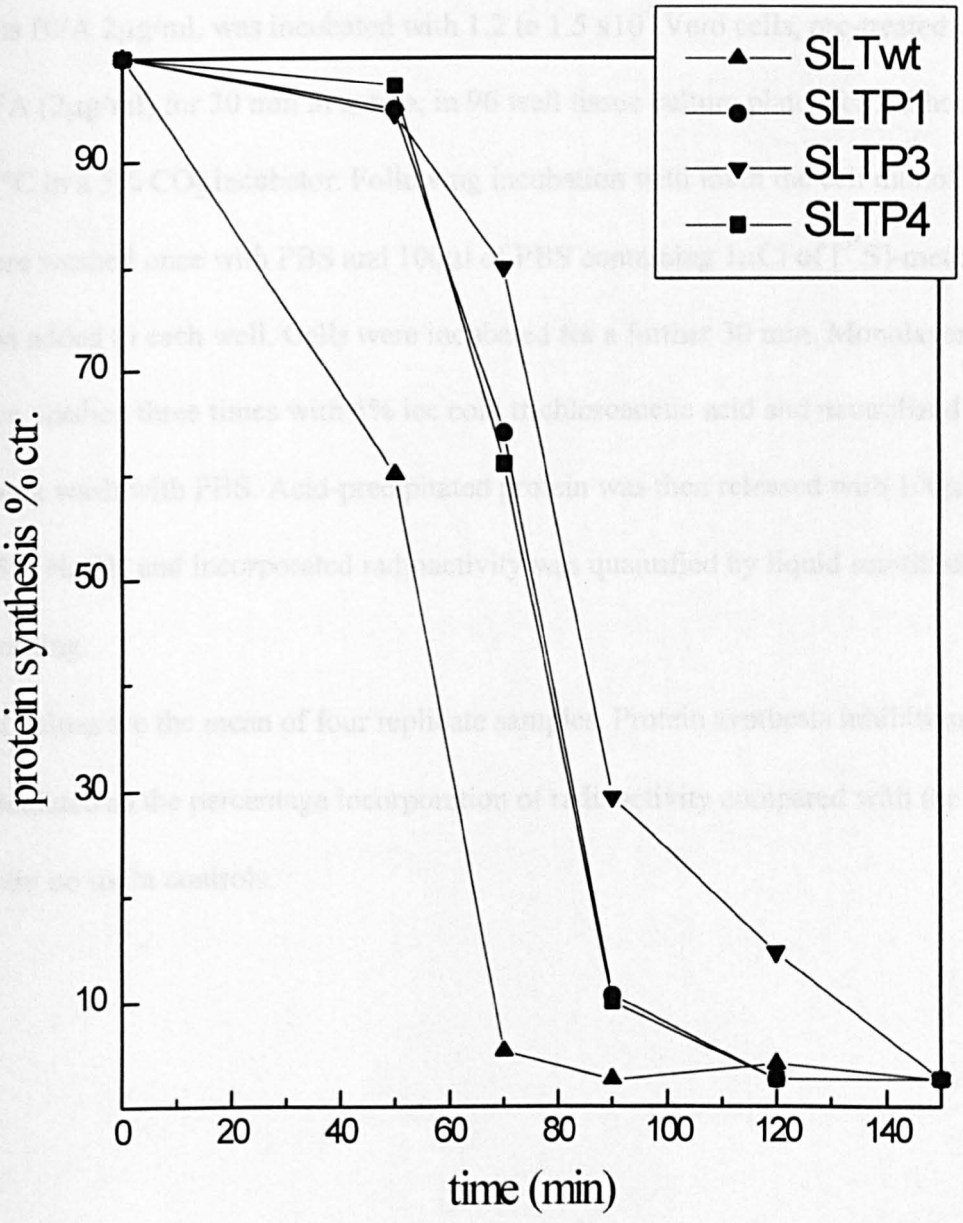

Figure 3.3.10 Cytotoxicity of SLT 1 wild-type to Vero cells pretreated with brefeldin A 2μg/ml: 3 hour incubation of toxin.

$1x10^{-4}$ to 10 ng/ml of recombinant SLT 1 wild-type holotoxin, diluted in DMEM plus BFA 2μg/ml, was incubated with 1.2 to 1.5 $x10^4$ Vero cells, pre-treated with BFA (2μg/ml) for 30 min in media, in 96 well tissue culture plates for 2.5 hours at 37°C in a 5% CO_2 incubator. Following incubation with toxin the cell monolayers were washed once with PBS and 100μl of PBS containing 1μCi of [^{35}S]-methionine was added to each well. Cells were incubated for a further 30 min. Monolayers were then washed three times with 5% ice cold trichloroacetic acid and neutralized by a single wash with PBS. Acid-precipitated protein was then released with 100μl of 0.5M NaOH and incorporated radioactivity was quantified by liquid scintillation counting.

All values are the mean of four replicate samples. Protein synthesis inhibition was calculated as the percentage incorporation of radioactivity compared with the mean of six no toxin controls.

Figure 3.3.10 Cytotoxicity of SLT 1 wild-type to Vero cells pretreated with brefeldin A 2μg/ml: 3 hour incubation of toxin.

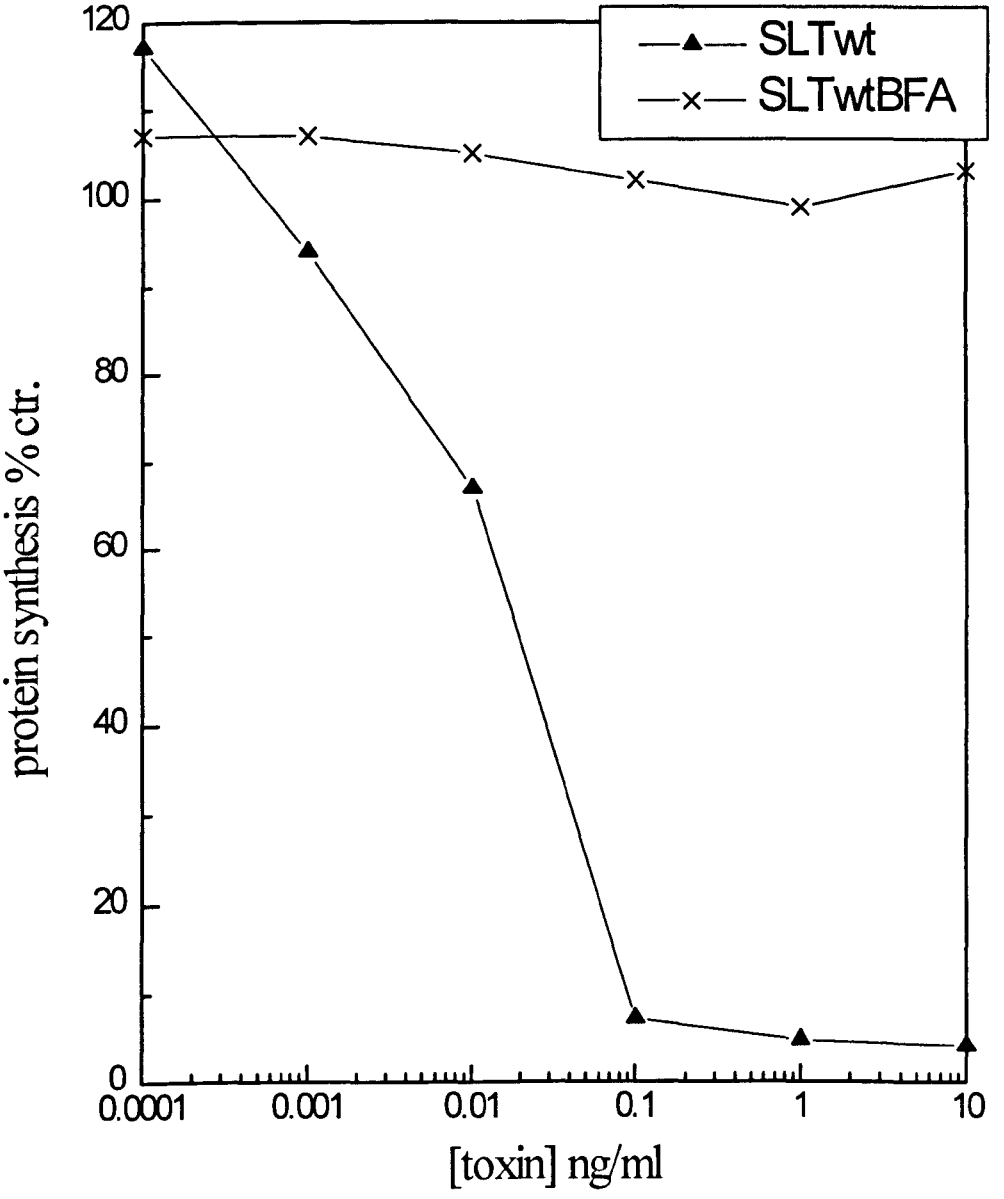

3.3.4 *In vivo* processing of SLT 1 and potential processing mutants.

The sensitivity of mutant toxins to proteolytic processing during target cell intoxication was analysed using recombinant mutant and wild-type toxins radioactively labelled with ^{125}Iodine. 50μg of the mutant holotoxins SLTP1, SLTP3, SLTP4 and the wild-type toxin were labelled with ^{125}I using the non-harsh Iodogen method (section 2.6.4). All proteins were efficiently labelled to specific activities of approximately 25 000cpm/ng in each case (Figure 3.3.11). Susceptibility of mutant and wild type toxins was measured over a time course of 2 hours with samples taken at 30 min, 1 hour and 2 hours. Following intoxication of cells with [^{125} I]-toxin for the specified period of time, cells were lysed in the presence of a cocktail of protease inhibitors before precipitation and separation of protein on 15% SDS PAGs (section 2.7.5). The conditions used in previous cytotoxicity experiments were repeated with the aim of visualizing intracellular proteolytic processing of toxin. The results of *in vivo* proteolytic processing experiments are shown in figures 3.3.12 to 3.3.15. Whether proteolytic cleavage occurs within the extracellular medium, either by proteases present in DMEM or by proteases secreted by Vero cells, was also addressed. 20 ng of each iodinated toxin was incubated at 37°C for 2 hours with 100 μl DMEM removed from a confluent flask of Vero cells. Following incubation total protein was precipitated from the reaction with acetone. The resulting protein pellets

were resuspended in reducing sample loading buffer and separated on 15% SDS polyacrylamide gels. The results from this experiment are shown in figure 3.3.16.

Wild-type toxin was efficiently processed to the A1 subunit size in untreated Vero cells and in cells pretreated with calpain inhibitor I and brefeldin A. The two mutant toxins SLTP1 and SLTP3 are processed in untreated Vero cells albeit more slowly. However, in contrast to the wild-type toxin, SLTP1 and SLTP3 are not processed or are processed more slowly to the A1 subunit size in Vero cells pretreated with either calpain inhibitor I or brefeldin A. SLTP4 apparently remains intact in both untreated Vero cells and in Vero cells treated with calpain inhibitor I and brefeldin A. When the incubation period for SLTP4 is extended to 6 hours in untreated Vero cells there is still no evidence of processing of this mutant toxin. The results obtained from Vero cells pre-treated with NH_4Cl were not conclusive and time did not allow repetition of this particular experiment. From figure 3.3.15 it appears none of the toxins tested are processed in NH_4Cl treated cells. As with all other conditions tested SLTP4 is not processed at all in Vero cells pre-treated with NH_4Cl. Non of the toxins tested were processed by media removed from growing cells showing that all the observed processing events take place in target cells and not in the extracellular medium.

Figure 3.3.11. 15 % reducing SDS polyacrylamide gel electrophoresis of ^{125}I-labelled SLT 1 and potential processing mutants.

Recombinant SLT 1 and the processing mutants described in chapter 2 were labelled with ^{125}Iodine using the iodogen method. The resulting proteins were separated on a 15% SDS polyacrylamide gel under reducing conditions. All proteins were labelled to a specific activity of approximately 25 000 cpm/ng. The positions of SLT A chain and SLT B chain are marked, molecular masses are given in kDa.

Lane 1 8ng [^{125}I]-SLT 1 wt

Lane 2 8ng [^{125}I]-SLTP1

Lane 3 8ng [^{125}I]-SLTP3

Lane 4 8ng [^{125}I]-SLTP4

Lane 5 [^{14}C]-molecular weight markers

Figure 3.3.11. 15 % reducing SDS polyacrylamide gel electrophoresis of ^{125}I-labelled SLT 1 and potential processing mutants.

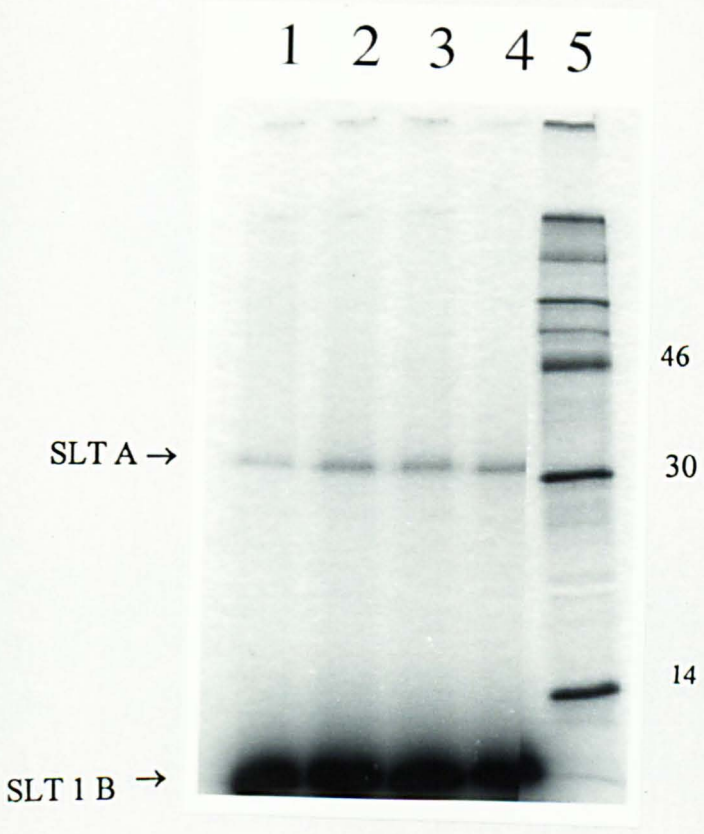

Figure 3.3.12 Proteolytic processing of SLT 1 and potential processing mutants in untreated Vero cells.

Vero cells, grown to a confluent monolayer in 3 cm tissue culture dishes, were incubated at 37°C in a 5% CO_2 incubator with ^{125}I-labelled toxins at a final concentration of 100ng/ml for the specified period of time. Following incubation the toxin was washed off and cells lysed in cell lysis buffer. Cell lysates were centrifuged to remove cell debris and nuclei and protein was precipitated with acetone. The resulting protein pellets were resuspended in reducing sample loading buffer and separated on 15% SDS polyacrylamide gels. The positions of full length SLT A chain and SLT A1 are indicated by arrows. The extent of cleavage to the A1 sized subunit was quantified by scanning densitometry and is plotted against time of incubation in (B).

Lanes labelled M contain [^{14}C]-molecular weight markers. Lanes labelled 30 contain protein precipitated from cells after 30 minutes incubation, Lanes labelled 1 contain protein precipitated from cells after 1 hour incubation lanes labelled 2 contain protein precipitated from cells after 2 hours incubation. The lane labelled 6 contains protein precipitated from cells after 6 hours incubation.

Figure 3.3.12 Proteolytic processing of SLT 1 and potential processing mutants in untreated Vero cells.

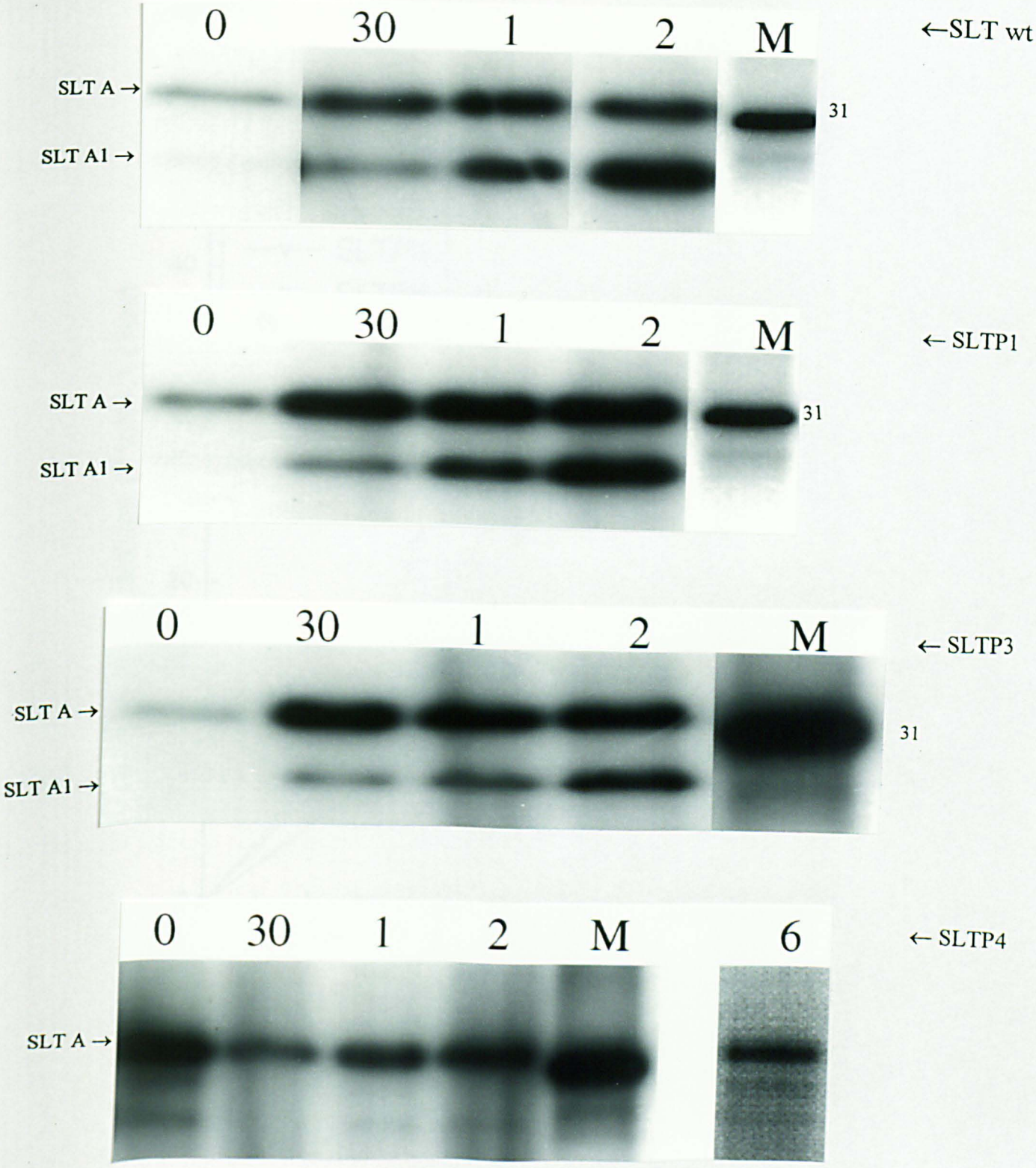

Figure 3.3.12 (B) Proteolytic processing of SLT 1 and potential processing mutants in untreated Vero cells.

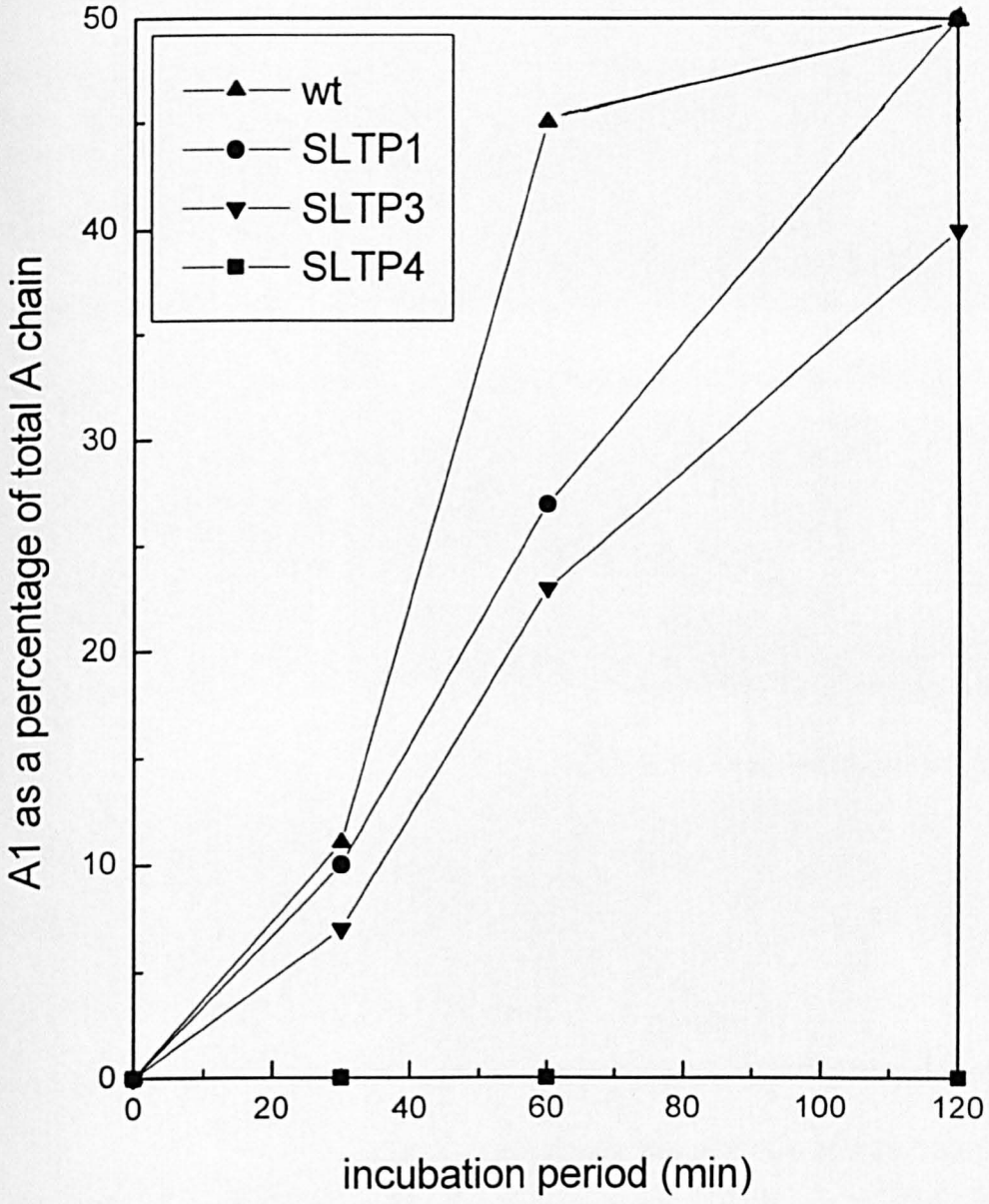

Figure 3.3.13 Proteolytic processing of SLT 1 and potential processing mutants in Vero cells pretreated with calpain inhibitor 1 (100μg/ml)

Vero cells, grown to a confluent monolayer in 3 cm tissue culture dishes, were preincubated with 100μg/ml calpain inhibitor I for 30 min prior to incubation at 37°C in a 5% CO_2 incubator with ^{125}I-labelled toxins at a final concentration of 100ng/ml for the specified period of time. Following incubation the toxin was washed off and cells lysed in cell lysis buffer. Cell lysates were centrifuged to remove cell debris and nuclei and protein was precipitated with acetone. The resulting cell pellets were resuspended in reducing sample loading buffer and separated on 15% SDS polyacrylamide gels. The positions of full length SLT A chain and SLT A1 are indicated. Molecular masses are given in kDa. The extent of cleavage to the A1 sized subunit was quantified by scanning densitometry and is plotted against time of incubation in (B).

Lanes labelled M contain [^{14}C]-molecular weight markers, Lanes labelled 30 contain protein precipitated from cells after 30 minutes incubation, Lanes labelled 1 contain protein precipitated from cells after 1 hour incubation and lanes labelled 2 contain protein precipitated from cells after 2 hours incubation.

Figure 3.3.13 Proteolytic processing of SLT 1 and potential processing mutants in Vero cells pretreated with calpain inhibitor 1 (100μg/ml)

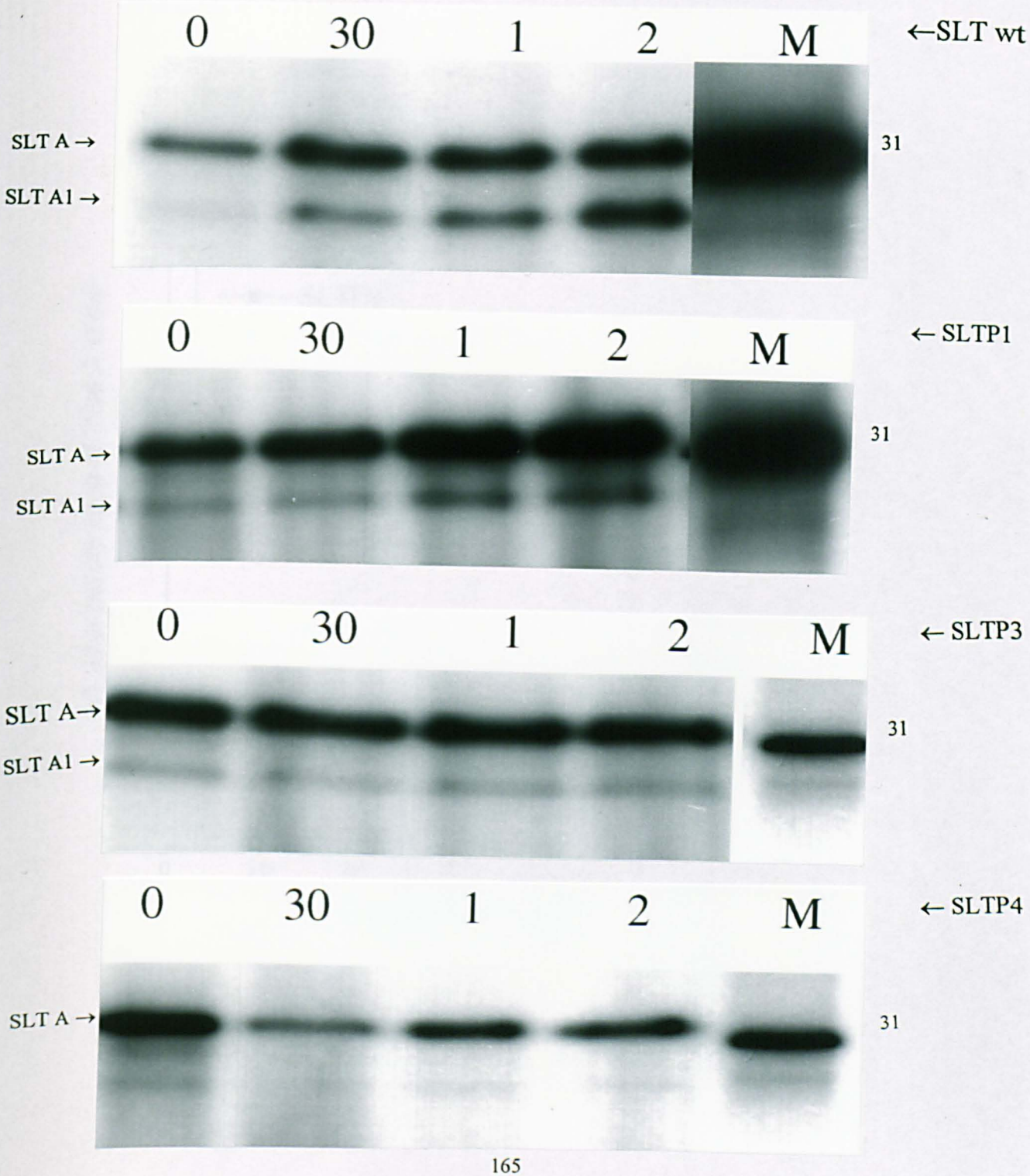

Figure 3.3.13 (B) Proteolytic processing of SLT 1 and potential processing mutants in Vero cells pretreated with calpain inhibitor 1 (100μg/ml)

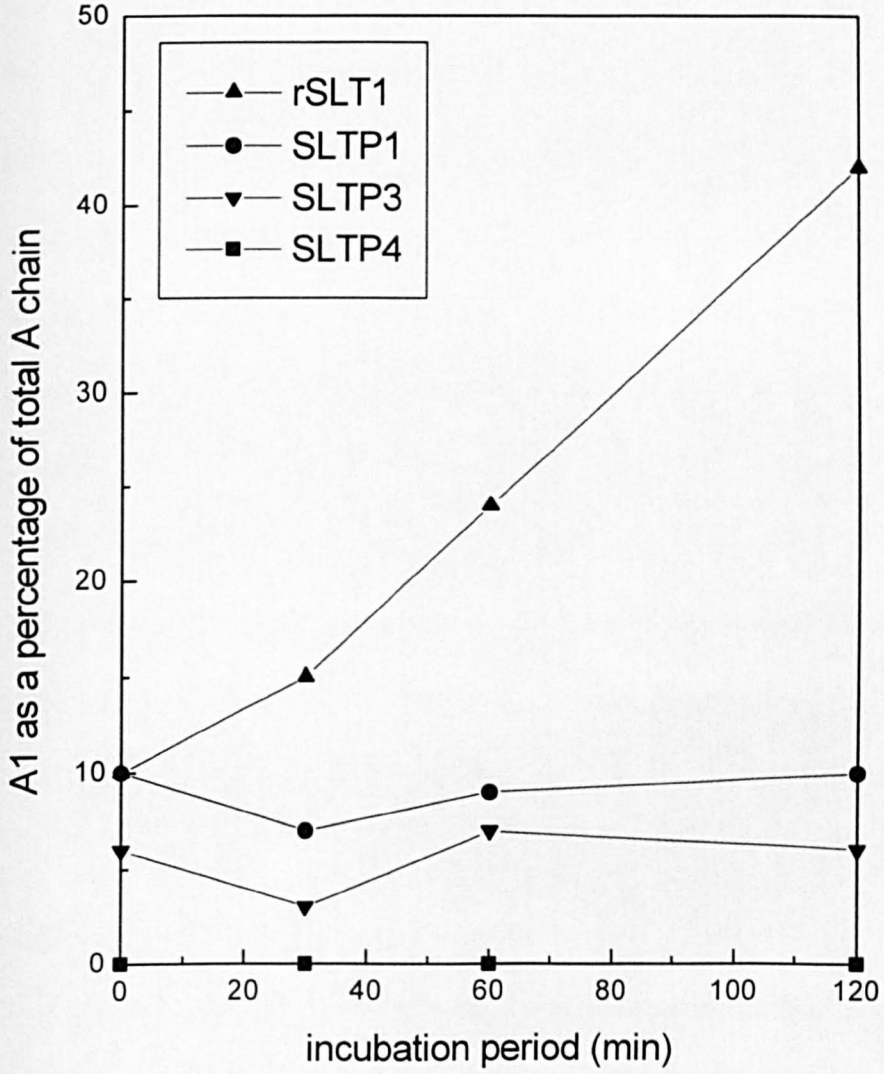

Figure 3.3.14 Proteolytic processing of SLT 1 and potential processing mutants in Vero cells pretreated with brefeldin A (2μg/ml).

Vero cells, grown to a confluent monolayer in 3 cm tissue culture dishes, were preincubated with brefeldin A (2μg/ml) for 30 min prior to incubation at 37°C in a 5% CO_2 incubator with ^{125}I-labelled toxins at a final concentration of 100ng/ml for the specified period of time. Following incubation the toxin was washed off and cells lysed in cell lysis buffer. Cell lysates were centrifuged to remove cell debris and nuclei and protein was precipitated with acetone. The resulting cell pellets were resuspended in reducing sample loading buffer and separated on 15% SDS polyacrylamide gels. The positions of full length SLT A chain and SLT A1 are indicated. Molecular masses are given in kDa. The extent of cleavage to the A1 sized subunit was quantified by scanning densitometry and is plotted against time of incubation in (B).

Lanes labelled M contain [^{14}C]-molecular weight markers, Lanes labelled 30 contain protein precipitated from cells after 30 minutes incubation, Lanes labelled 1 contain protein precipitated from cells after 1 hour incubation and lanes labelled 2 contain protein precipitated from cells after 2 hours incubation.

Figure 3.3.14 Proteolytic processing of SLT 1 and potential processing mutants in Vero cells pretreated with brefeldin A (2μg/ml).

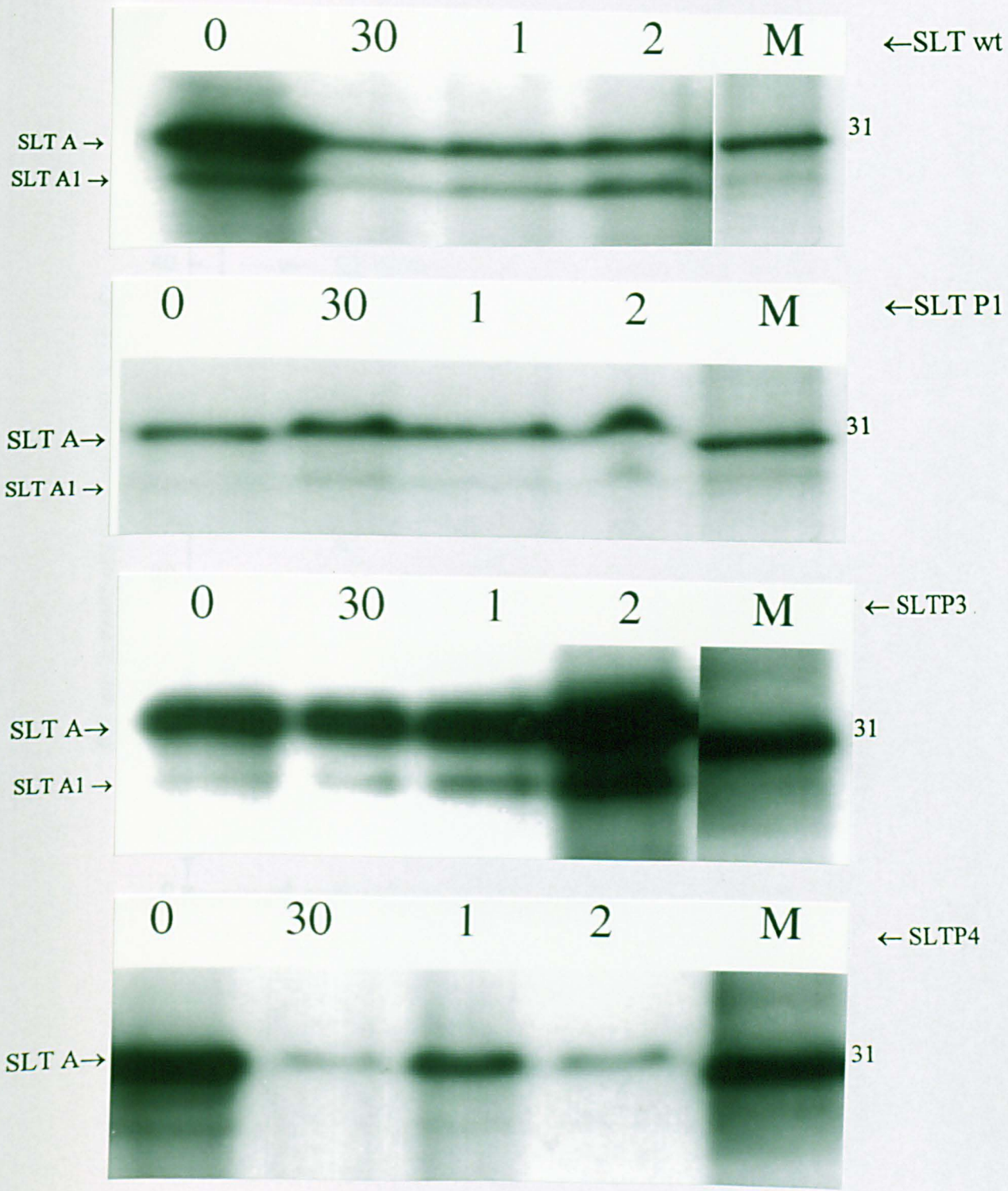

Figure 3.3.14 (B) Proteolytic processing of SLT 1 and potential processing mutants in Vero cells pretreated with brefeldin A (2μg/ml).

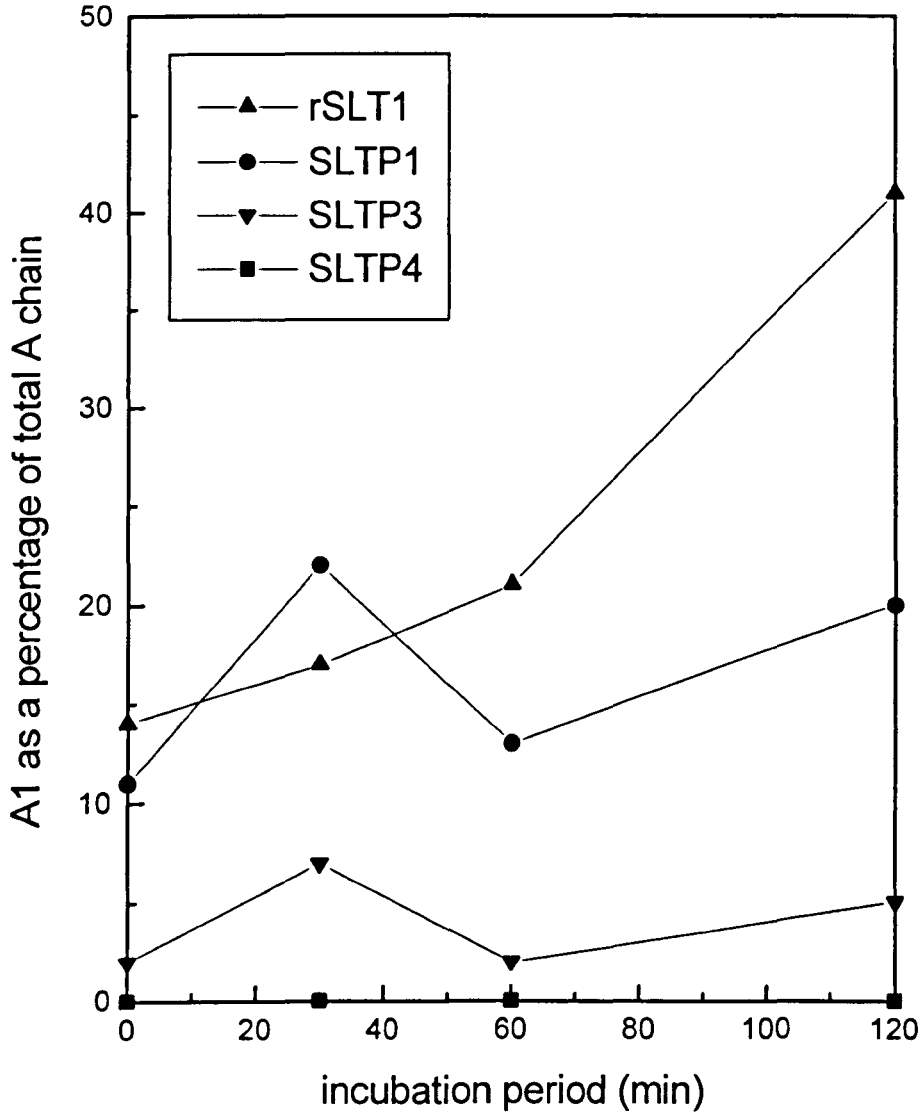

Figure 3.3.15 Proteolytic processing of SLT 1 and potential processing mutants in Vero cells pretreated with 10mM NH_4Cl.

Vero cells, grown to a confluent monolayer in 3 cm tissue culture dishes, were preincubated with 10mM NH_4Cl for 45 min prior to incubation at 37°C in a 5% CO_2 incubator with ^{125}I-labelled toxins at a final concentration of 100ng/ml for the specified period of time. Following incubation the toxin was washed off and cells lysed in cell lysis buffer. Cell lysates were centrifuged to remove cell debris and nuclei and protein was precipitated with acetone. The resulting cell pellets were resuspended in reducing sample loading buffer and separated on 15% SDS polyacrylamide gels. The positions of full length SLT A chain and SLT A1 are indicated. Molecular masses are given in kDa. The extent of cleavage to the A1 sized subunit was quantified by scanning densitometry and is plotted against time of incubation in (B).

Lanes labelled M contain [^{14}C]-molecular weight markers, Lanes labelled 30 contain protein precipitated from cells after 30 minutes incubation, Lanes labelled 1 contain protein precipitated from cells after 1 hour incubation and lanes labelled 2 contain protein precipitated from cells after 2 hours incubation.

Figure 3.3.15 Proteolytic processing of SLT 1 and potential processing mutants in Vero cells pretreated with 10mM NH_4Cl.

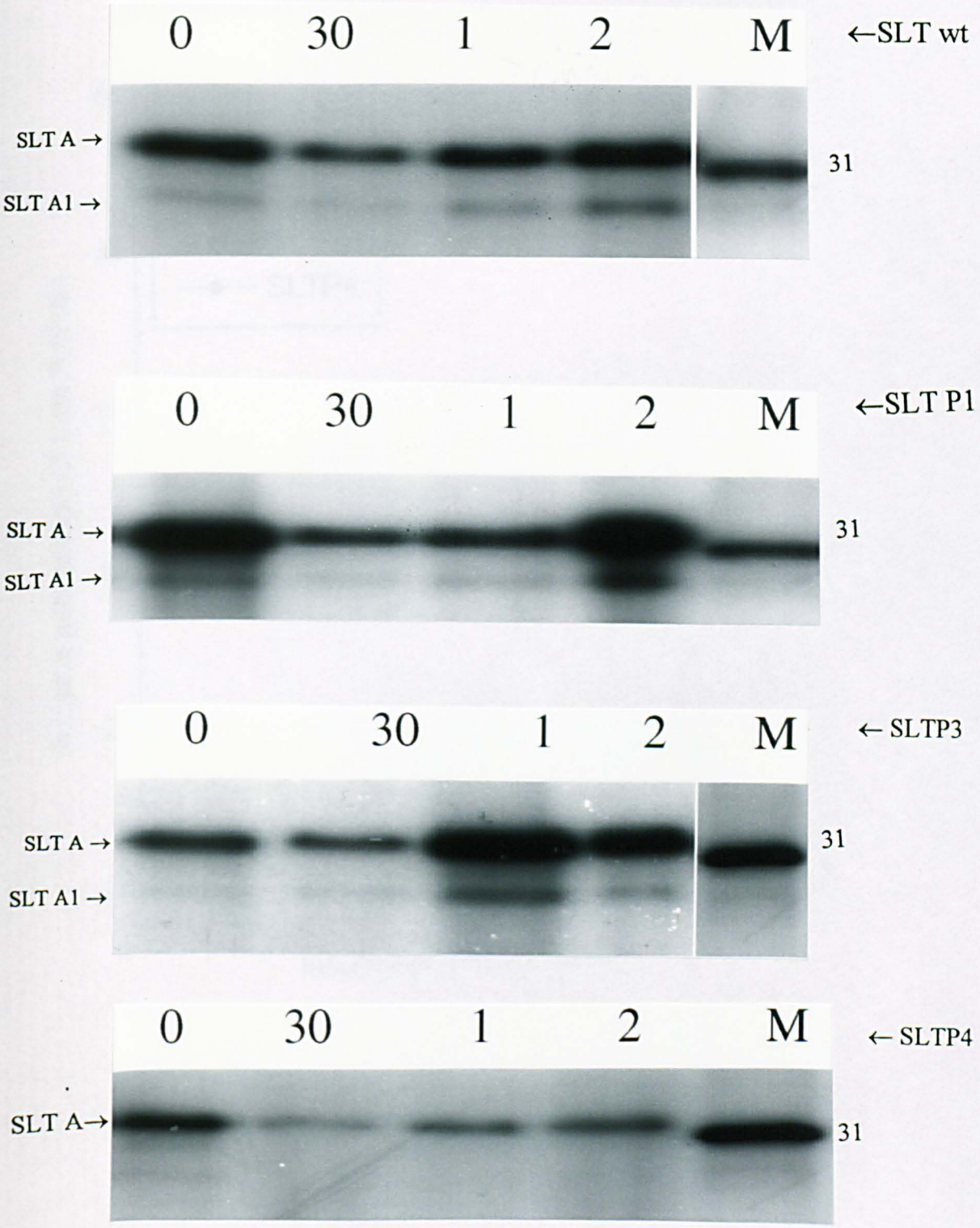

Figure 3.3.15 (B) Proteolytic processing of SLT 1 and potential processing mutants in Vero cells pretreated with 10mM NH_4Cl.

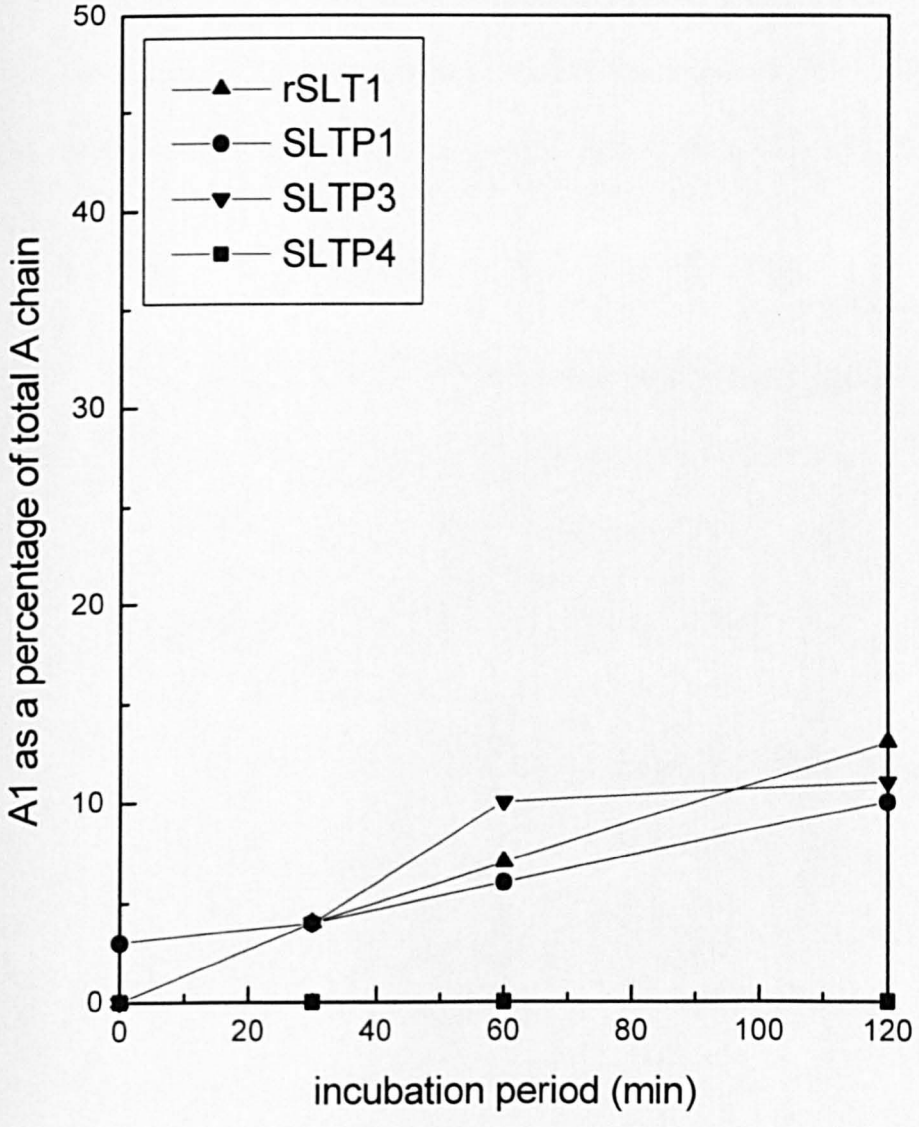

Figure 3.3.16 Proteolysis of SLT 1 and potential processing mutants by extracellular proteases.

100µl of DMEM removed from a confluent flask of Vero cells was incubated with 20ng of iodinated SLT 1 or processing mutants SLTP1, SLTP3 and SLTP4 for 2 hours at 37°C. Protein was precipitated with acetone and separated by reducing 15% SDS PAGE. The position of SLT 1 A chain is indicated, molecular masses are given in kDa.

Gel loading.

Lane 1 SLT 1 wt -media.

Lane 2 SLT 1 wt +media.

Lane 3 SLTP1 -media.

Lane 4 SLTP1 +media.

Lane 5 SLTP3 -media.

Lane 6 SLTP3 +media.

Lane 7 SLTP4 -media.

Lane 8 SLTP4 +media.

Lane 9 [^{14}C]-molecular weight markers.

Figure 3.3.16 Proteolysis of SLT 1 and potential processing mutants by extracellular proteases.

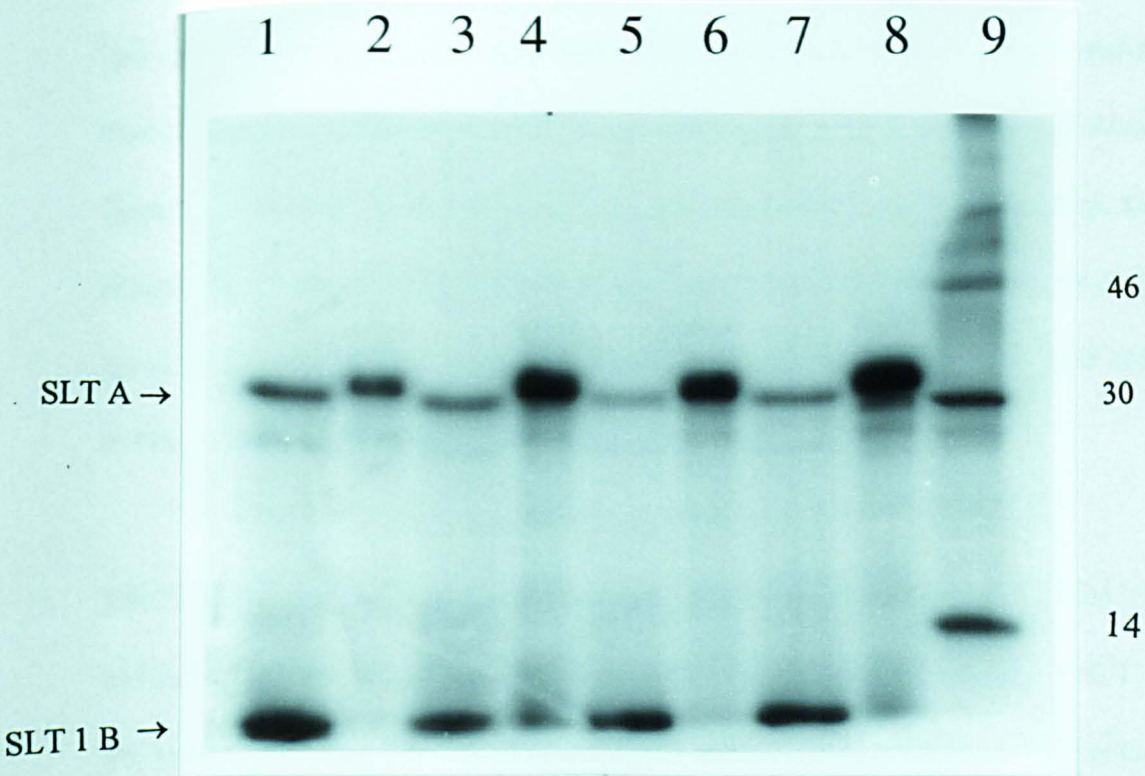

3.3.4 Discussion

The mutants described in chapter 2 were made in order that the proteolytic processing requirements for SLT 1 could be investigated. In total, five mutant toxins were constructed and their biological properties investigated. Following expression (described in chapter 2) the enzymatic properties of these mutant toxins was examined. There are no published data regarding the enzyme kinetics of SLT 1. For this reason the N-glycosidase activities of the mutant proteins were simply related to that of the wild-type toxin preparation made in this study. The northern blot shown in figure 3.3.1 clearly shows that, from a titration of toxin incubated with susceptible ribosomes, all the mutant proteins expressed in *Escherichia coli* have comparable N-glycosidase activity. This allows direct comparisons of cytotoxicity data to be made between mutant and wild-type toxins.

The N-glycosidase activity of a truncated SLT 1 A chain was also investigated by translation *in vitro* of a transcript coding for the N-terminal 222 residues of SLT 1. The reason for doing this was to determine whether an A chain fragment potentially generated by proteolytic processing at the upstream furin consensus motif 220ArgXXArg223 would have any enzymatic activity responsible for a cell killing effect. A previous report by Haddad *et al* (1993) had shown that residues 1-223 of Shiga toxin retained the ability to inhibit protein synthesis in a rabbit reticulocyte

lysate translation reaction. However the construct described was translated in fusion with up to thirty vector encoded amino acid residues. The findings in the present study are in contradiction to the findings of Haddad *et al.* Translation of the N-terminal 222 amino acid residues of SLT 1 did not result in modification of rabbit reticulocyte ribosomes. The reasons for these conflicting results are not known though there are two possible explanations. Firstly, in the present study, although a translation product was produced in a wheat germ system (figure 3.2.13) no such product could be detected in a rabbit reticulocyte lysate translation system. Hence there is no evidence that the 223stop transcript was translated to protein in the experiment shown in figure 3.3.2. However it is apparent that the control transcripts coding for SLTA1 and SLTwt, produced in an identical manner, do translate well. Secondly, the incorporation of thirty vector encoded residues in the construct used by Haddad *et al* may stabilise this truncated protein and allow ribosome depurination to occur. The results presented in this study suggest a fragment generated by processing at the upstream furin site would have no enzymatic activity, though clearly further control experiments should be carried out to confirm these findings.

Trypsin sensitivity is often used as a measure of the stability and accuracy of folding in mutant proteins. Relative to the wild-type toxin additional fragments generated on proteolysis using trypsin, can be indicative of misfolding. The reasons for analysing the trypsin sensitivity of the mutant toxins produced in this study however are two-fold. In addition to assessing the accuracy of folding, digestion with trypsin was used

to demonstrate resistance to trypsin of the mutant proteins in which trypsin-sensitive amino acids had been mutated. Since the disulphide-bonded loop region of SLT 1 contains just two trypsin sensitive arginine residues, mutation to glycines should render the proteins SLTP1, SLTP3 and SLTP4 resistant to trypsin-mediated proteolysis within this loop region. From figure 3.3.3 it can be seen that SLT 1 wild-type and the mutant SLTP2, which retains the two arginine residues in the trypsin-sensitive loop, are indeed sensitive to this protease. Both wild-type and SLTP2 produce an A1 sized subunit on trypsin treatment. In contrast, neither of the mutants SLTP1 and SLTP3 produce an A1 sized subunit as a result of trypsin treatment. Furthermore no additional fragments are generated, indicating that these proteins are correctly folded. The mutant toxin SLTP4 also appears largely resistant to trypsin treatment, with no A1 sized fragment being generated. However a small amount of a higher molecular weight fragment is produced, a possible indication that a degree of misfolding has occurred in this protein. Since this protein apparently retains N-glycosidase activity and retains its ability to assemble into a holotoxin it is considered that perturbations to the structure are probably minor. Figure 3.3.4 shows an SDS polyacrylamide gel of the same samples as those in figure 3.3.3 run under non-reducing conditions. This gel indicates that the fragments produced by the wild-type and SLTP2 proteins are generated from within the disulphide-bonded loop as was expected. The small amount of fragment produced by trypsin treatment of the SLTP4 toxin also appears to be generated from within the disulphide-bonded loop as the fragment is not seen on the non-reducing gel. This result is inexplicable since

there are no arginine or lysine residues within the region subtended by the disulphide bond in SLTP4. We can interpret this finding only by concluding that the batch of trypsin is impure.

The cytotoxic action of SLT 1 and processing mutants SLTP1, SLTP3 and SLTP4 was investigated on Vero cells. In two previous studies using mutations identical or similar to the SLTP1 mutation used in the present study (Burgess and Roberts (1994); Garred *et al* (1995a)) a 10 fold reduction in cytotoxic activity between wild-type and the double arginine mutant was observed. In the present study, a 25 fold reduction in toxicity between SLT 1 wild-type and SLTP1 was observed following a 3 hour incubation of toxin (figure 3.3.1). SLTP3 also gave an IC_{50} 25 fold greater than that of wild-type over the same time period. Following a longer exposure of toxin (6 hours), SLT 1 wild-type, SLTP1 and SLTP3 all give similar IC_{50} values 0.0019, 0.0071, 0.009 ng/ml respectively (figure 3.3.6). These results indicate that whilst an intact furin consensus motif is necessary for rapid intoxication, these mutant proteins can be highly toxic after longer incubations with intact cells.

Since the previous study by Garred *et al* showed that the A1 subunit generated by *in vivo* processing was produced as a result of proteolytic cleavage within the disulphide-bonded loop (by comparison of samples run on reducing and non-reducing PAG) a search was made for amino acyl residues in this region which might constitute a known site for proteolysis other than Arg 248 andArg251, no such site

was identified. However a report by Takao *et al* (1988) showed that SLT 1 was fragmented between Ala 253 and Ser 254. Such a fragment could have been generated during toxin extraction from *E.coli* or extracellulary during purification either way, it suggests such sites are exposed and susceptible to some form of nicking. Such nicking might also occur during uptake into eukaryotic cells and since Garred *et al* showed alternative processing in the loop region which generated a fragment indiscernible in size to wild-type A1, the site of nicking *in vivo* must be very close to the natural furin site. It was decided to mutate the two nearby Ala/Ser pairs to Gly and Ala. Mutation of these two pairs of residues (SLTP2) resulted in a protein identical to that of the wild-type toxin. Therefore the mutations did not perturb enzymatic or translocation activities. In SLTP3 where the Ala/Ser pair mutations are together with the double arginine mutation (SLTP1) the additional mutations do not appear to be important for toxicity since the cytotoxicity of SLTP3 is identical to SLTP1.

By visualization of iodinated toxin in Vero cells, the reason for the transient reduction in cytotoxicity of the mutants SLTP1 and SLTP3 can be explained. Figure 3.3.12 shows protein precipitated from Vero cells exposed to iodinated wild-type and mutant proteins. As previously shown (Garred *et al* 1995a) SLT 1 wild-type is processed to the A1 subunit size. Similarly SLTP1 and SLTP3 are also processed to the A1 size although this occurs more slowly. These data show that in the absence of the wild-type furin consensus motif, proteolytic processing can still occur. This

alternative processing occurs more slowly than processing in the presence of the furin consensus and results in an increased lag period prior to full cytotoxicity of these mutant toxins. The kinetics of the cytotoxic action of SLTP1 and SLTP3 are shown in figure 3.3.9. Wild-type toxin gives a t_{50} of 53 minutes compared to SLTP1 and SLTP3 of 75 and 82 minutes respectively. To conclude, the rate at which an A1 sized fragment is generated appears to be related to the cytotoxic nature of these mutant toxins i.e. the small increase in resistance to cellular proteases is probably responsible for the small transient reduction in the toxicity of these proteins.

Garred *et al* (1995a) showed that in Vero cells pretreated with brefeldin A, the proteolytic processing of the wild-type protein and the mutant Shiga-His was very different. They found that the mutant Shiga-His was not processed to the A1 size in cells pretreated with brefeldin A and concluded that proteolytic processing of Shiga-His occurs in an earlier compartment of the secretory pathway which the mutant does not reach in cells treated with brefeldin A. In a similar manner the effect of brefeldin A was investigated with regard to the proteolytic processing of SLTP1 and SLTP3. In both cases these toxins remained largely unprocessed in BFA treated Vero cells (figure 3.3.14). These data indicate that SLTP1 and SLTP3 both require trafficking to an earlier compartment of the secretory pathway in order for proteolytic processing to occur. No difference between SLTP1 and SLTP3 was observed. Figure 3.3.10 shows the results of SLT 1 wt intoxication of BFA treated Vero cells. These data

were collected simply to ensure that the preparation of BFA used in this study did protect Vero cells from the cytotoxic action of SLT 1.

Garred *et al* (1995a) observed that the mutant Shiga-His remained intact when incubated with Vero cell pretreated with the membrane permeable protease inhibitor calpain inhibitor I. They were also able to correlate these findings with cytotoxicity data in which Vero cells pretreated with calpain inhibitor I were protected from intoxication by the mutant toxin Shiga-His by a factor of 10. In similar experiments carried out with the mutants SLTP1 and SLTP3, a protective effect of 4.5 and 6 fold respectively was also seen (figure 3.3.8) the wild-type toxin however was unaffected by this treatment. When the proteolytic processing of SLTP1 and SLTP3 was visualized in Vero cells treated with calpain inhibitor I no cleavage to the A1 size was seen (figure 3.3.13). These data collectively indicate that SLTP1 and SLTP3 can be proteolytically processed in Vero cells but that the proteolytic enzyme responsible is different to that which normally cleaves wild-type toxin. Together with the results obtained with BFA treated cells this alternative processing enzyme occurs in a different cellular compartment (Golgi stack, ER, cytosol) to the primary processing enzyme assumed to be TGN-located furin.

SLTP1 and SLTP3 both generate a fragment in cells when the proposed primary cleavage site in the disulphide bonded loop is mutated. The fragment is of very similar size to that of wild-type toxin, suggesting that a calpain specific site lies close

to the loop furin site. The specificity of calpain is unclear and no single motif has been identified as forming recognition or cleavage sites for these enzymes. The reason for this maybe that calpain recognises structural elements rather than specific primary amino acid sequences. The changes made here to the primary sequence (Ala/Ser pairs and Arg 248/Arg251) and combinations of the two clearly do not effect proteolytic processing by a calpain like enzyme.

The cellular location of the calpains is generally believed to be cytosolic. The intoxication time course (2,4 hours) used by Garred *et al* when ^{125}I toxins were visualized for processing did not exclude the possibility that such alternative processing occured in the cytosol after translocation. The $t_{1/2}$ of SLT 1 in Vero cells is 54 minutes (figure 3.3.9). After two hours the physiologically active fraction of toxin would be in the cytosol. In the present study therefore, time points of 30 minutes and 1 hour were included. Since nicking of toxin occurs within the toxin lag this may be an indication that the nicking occurs in the endomembrane system. However the possibility that toxin is cleaved in the cytosol can not be rulled out.

Control experiments were carried out in order to exclude proteolytic processing which may occur in the external medium prior to uptake of toxin. Figure 3.3.16 shows toxin incubated with media in which a confluent monolayer of Vero cells was grown. No cleavage of toxin is seen on treatment of toxin with media thus ruling out the possibility that proteases present in the medium or secreted from cells are

responsible for cleavage of toxin. Preincubation of cells with NH_4Cl was used to exclude the role of lysosomal and endosomal proteolytic enzymes in toxin cleavage. The pattern of toxin cleavage in Vero cells was not as expected when cells were pretreated with NH_4Cl (figure 3.3.15). All toxins including the wild-type remain largely unprocessed. This experiment however was only carried out once for each toxin. This experiment also coincided with a period in which old stocks of Vero cells were being used. As a result this experiment needs repeating in order to try to interpret these data. The precise pleiotropic effects of NH_4Cl are ill defined and for this reason the results of this assay are probably flawed. NH_4Cl did appear to increase the toxicity of SLTP4 by a small amount, the reasons for this are not clear.

Since the additional mutations made to the paired Ala/Ser residues did not result in increased resistance to proteolytic processing *in vivo*, further mutations were introduced into a second arginine rich region upstream of the proposed nicking site. Residues Arg220 and Arg223 were mutated to glycine residues in the SLTP3 framework. The resulting mutant toxin was called SLTP4. SLTP4 was assayed under the same conditions as the mutants SLTP1 and SLTP3. SLTP4 is 134 fold less toxic than SLT 1 wild-type after 3 hours incubation on Vero cells and remains 62 fold less toxic after a 6 hour exposure. These results are in contrast to those for SLTP1 and SLTP3 where wild-type cytotoxicity was observed after prolonged exposure of cells to toxin. Visualization of *in vivo* processing of SLTP4 reveals that the toxin remains intact in untreated Vero cells and under all other conditions tested. An additional

time point of 6 hours was included in *in vivo* processing experiments to exclude the possibility that SLTP4 is processed after longer incubation with Vero cells. This is clearly not the case. Since the A1 subunit generated from SLTP3 in Vero cells appears identical in size to that of wild-type A1, it seems unlikely that Arg220 or Arg 223 would constitute an alternative nicking site. It would seem that the additional mutation in SLTP4 results in a downstream steric effect rendering the protease-sensitive loop refractory to cleavage by calpian or other proteases. In spite of the apparent lack of cleavage, the SLTP4 IC_{50} of 0.36 ng/ml towards Vero cells suggests that the separation of the A2 moiety of SLT 1 away from the catalytic A1 domain is not essential for cytotoxicity. However using the methods descibed here one would not be able to detect very small amounts of nicked toxin. Hence the residual toxicity of the SLTP4 mutant may be explained by very small amounts of nicked toxin. The implication of these results is discussed in more detail in chapter 6.

In summary,

1: The role of proteolytic processing of the bacterial toxin SLT 1 during the intoxication of Vero cells was examined using site directed mutagenesis to introduce specific mutations into the A chain.

2: SLTP1 and SLTP3 containing mutations within the disulphide bonded loop of SLT 1 are as toxic as the wild-type SLT 1 after prolonged exposure to Vero cells. Both mutant proteins are cleaved in Vero cells to a fragment apparently identical in size to the A1 fragment generated from the wild-type toxin. In combination with the

data of Garred *et al* (1995a) the alternative cleavage site must lie within the disulphide-bonded loop and the present study confirms that a calpain enzyme may be responsible for this nicking.

3: An SLT 1 A chain truncated at residue 223 and translated in a rabbit reticulocyte lysate did not exhibit N-glycosidase activity a finding which is in contrast to that of Haddad *et al* (1993) in which a similarly truncated ST A chain retained 41% of its activity relative to the full length A chain. Fragments of this size generated intracellularly (eg a fragment generated from Arg220-Arg223) will therefore be enzymatically inactive and are predicted to have no toxicity *in vivo*.

4: The mutations introduced upstream of the proposed nicking site of SLT 1 at a second putative furin site (SLTP4) resulted in a toxin which is apparently refractory to nicking in target cells. In spite of this apparent lack of cleavage, SLTP4 has a IC_{50} of 0.36 ng/ml. This may suggest for the first time that proteolytic processing of SLT 1 A chain is not essential for cytotoxicity. However the possibility that a small amount of toxin becomes nicked but is not detected remains.

Chapter 4

3.4.1 Cloning and expression of a ricin A chain-Shiga-like toxin 1 fusion protein (RASTA2).

Introduction.

A ricin a chain-Shiga-like toxin 1 fusion protein was constructed by gene fusion for expression in *Escherichia coli.* The final construct contains two open reading frames, the first of which codes for the bacterial ompF periplasmic targeting sequence in fusion with the full length ricin A chain sequence, followed by the coding region of SLT A2. The second codes for a wild-type SLT 1 B chain with its natural periplasmic coding sequence. The plasmid pKH206 containing the coding sequence of ricin A chain fused with the ompF signal sequence was a kind gift from R.Argent (Warwick, UK) a plasmid map of pKH206 is included in the appendix 3.

For the purpose of this study, SLT 1 A2 was defined as residues 262-293. It is these residues which are included in the construct described here. It was predicted that the chimeric A chain of RASTA2 would be able to associate with the B chain pentamer of SLT 1 since the A2 portion of SLT 1 is responsible for the major interactions between SLT 1 A chain and the SLT 1 B chains. It was rationalized that the resulting holotoxin could be purified in an identical manner to that of wild-type SLT 1 via its interaction with a Gb_3-receptor-affinity matrix (Gb_3-Sepharose).

This fusion protein was used to further investigate the processing requirements of SLT 1. Since properly folded ricin A chain (RTA) is known to be very resistant to protease (Walker *et al* 1996) and since reports that RTA is proteolytically processed during cell entry (Fiani *et al* (1993)) could not be repeated in our laboratory in spite of intensive efforts to identify specific proteolytic products, it is considered that the ricin portion of this fusion should be highly resistant to intracellular nicking. It is also known that ricin A chain is tolerant of C-terminal extentions (Cook *et al* (1993); O'Hare *et al* (1990)). The RASTA2 fusion protein contains only the A2 portion of SLT 1 where the protease sensitive loop region is not included. It was predicted that the chimeric A chain should be insensitive to protease either *in vitro* or *in vivo*. If this is the case, the effects of the A2 extension can be investigated. For example if this fusion protein remains toxic then the A2 portion is presumably able to translocate from an intracellular compartment to the cell cytosol i.e. the A2 portion of SLT 1 does not form a block to membrane translocation. These results would be additional to evidence presented in chapter 3 that processing of SLT 1 to remove A2 moiety is not essential in order for SLT 1 to be cytotoxic.

3.4.2 Cloning of RASTA2.

The ricin A chain-SLT A2 chimera was constructed by three rounds of recombinant four primer PCR using $Vent_R$ DNA polymerase. In the first round, a fragment was

generated from pKH206 (ricin A chain with an ompF periplasmic signal sequence in pKK223.2). The 5' primer (PSDO) contained a *Pst*1 site, the Shine-Dalgarno sequence from SLT 1 A and a region complementary to the 5' end of the omp F signal sequence. The 3' primer (RTAF2) contained sequence complementary to the 3' end of the ricin A chain sequence figure (3.4.1). This PCR reaction was phenol extracted (2.3.3) and the product gel isolated (2.3.9). In a second round of PCR a fragment containing the coding sequence of SLT 1 A2 SLT 1 B (DNA coding for residues Pro 262 of SLT A2 to Arg 69 of SLT B) was amplified. The 3' primer (ESTO3') contained sequence complementary to the 3' end of SLT 1 B chain followed by an *Eco*R1 site. The 5' primer (RASTA2) contained sequence complementary to the 3' region of ricin A chain followed by sequence complementary to the A2 portion of SLT 1 (figure 3.4.1). This PCR reaction was phenol extracted (2.3.3) and the product gel isolated (2.3.9). Small amounts of each PCR product were then combined with the outside primers PSDO and ESTO3' in order to amplify the full length product. This reaction however did not produce product of the expected size, probably because of the large difference between the Tm values of the two primers used. To get round this problem larger quantities of the two products were combined in a third PCR reaction without primers with Vent DNA polymerase to create the full length coding sequence for the chimeric protein. This PCR produced enough PCR product for gel isolation and cloning, after suitable restriction, into the *Eco*R1 and *Pst*1 sites of M13 mp18 to create M13RASTA2. Following full sequencing of the insert in M13mp18 (2.3.13), a *Pst*1/*Eco*R1 fragment

was released and ligated into similarly restricted pUC19 to create pRASTA2. The RASTA2 DNA fragment generated by PCR contains a *Bgl* II site 590 bp from the 3' end, therefore digestion of pRASTA2 with *EcoR* I and *Bgl* II results in release of a 590 bp fragment. This digest was used to confirm the identity of the clone pRASTA2. This clone was used to express recombinant chimeric protein. A schematic diagram in figure 3.4.2 shows the strategy used to amplify the RASTA2 coding sequence by PCR. A plasmid map is shown in figure 3.4.3.

PCR reaction conditions

reaction 1: 1X Vent DNA polymerase buffer, 0.2mM dNTPs, 10ng pKH206 (template DNA), 100pmoles PSDO, 100pmoles RTAF2, 0.02U/μl Vent DNA polymerase. Final volume 100 μl. 94°C 1 min, 56°C 1 min, 72°C 1 min for 25 cycles.

reaction2: 1X Vent DNA polymerase buffer, 0.2mM dNTPs, 10ng dsM13SLTwt (template DNA), 100pmoles RASTA2, 100pmoles ESTO3', 0.02U/μl Vent DNA polymerase. Final volume 100 μl. 94°C 1 min, 50°C 1 min, 72°C 1 min for 25 cycles.

reaction 3: 1X Vent DNA polymerase buffer, 0.2mM dNTPs, 10μl gel isolated product A, 10μl gel isolated product B, 0.02U/μl Vent DNA polymerase. Final volume 100μl. 94°C 1 min, 57°C 1 min, 72°C 1 min for 10 cycles.

Figure 3.4.1. Oligonucleotide sequences of primers used for the construction of the RASTA2 coding sequence.

Figure 3.4.1 shows the sequence of primers used for the construction of the coding sequence of RASTA2 by recombinant PCR. Primer PSDO contains the complementary sequence of a *Pst*1 site followed by the SLT 1 Shine-Dalgarno sequence and a portion of the ompF sequence. ESTO3' contains sequence complementary to the 3' sequence of SLT 1 B chain followed by an *EcoR* 1 site. RTAF2 contains the sequence of the 3' portion of ricin A chain. RASTA2 contains the sequence of a 3' portion of ricin A chain followed by the 5' portion of SLT 1 B chain (including its Shine-Dalgarno sequence).

Figure 3.4.1. Oligonucleotide sequences of primers used for the construction of the RASTA2 coding sequence.

PSDO

Pst 1 SD ompF complementary sequence

5'-TAT GCT CTG CAG AGG AGT ATT GTG TAA TAT GAT GAA

GCG CAA TAT TCT-3'

ESTO3'

*EcoR*I SLT 1 B complementary sequence

5'-GCT AGA ATT CTC AAC GAA AAA TAA CTT-3'

RASTA2

ricin A chain complementary sequence SLT A2 complementary

5'-CTC CAC CAT CGT CAC AGT TTC CGG CAG ATG

sequence

GAA GAG TC-3'

RTAF2

ricin A chain complementary sequence

5'-AAA CTG TGA CGA TGG TGG AG-3'

Figure 3.4.2 Recombinant mutagenic PCR used for the production of DNA coding for a ricin A chain SLT A2 fusion protein (RASTA2).

Reaction 1: In the first reaction the pre ricin A chain sequence is amplified using the primers PSDO and RTAF2. This reaction produces DNA coding for pre ricin A chain with additional *Pst* 1 and Shine-Dalgarno sequences at the 5' end coded in the primer PSDO (product A).

Reaction 2: In the second reaction the SLTA2 and SLT B chain sequences are amplified. In addition to this sequence a small portion of RTA sequence is included in the primer RASTA2. An *EcoR* 1 site is included in the primer ESTO3' which adds an *EcoR* 1 site to the 3' end of this amplified fragment (product B).

Reaction 3: In the final reaction the first two PCR products A and B are combined in the absence of any primers (removed by gel isolation). The small region of homology between product A and product B facilitates annealing of the two fragments and extension is catalysed by Vent DNA polymerase.

Dotted lines represent DNA generated from the SLT 1 template sequence. The closed lines represent DNA generated from the pre RTA sequence.

Figure 3.4.2 Recombinant mutagenic PCR used for the production of DNA coding for a ricin A chain SLT A2 fusion protein.

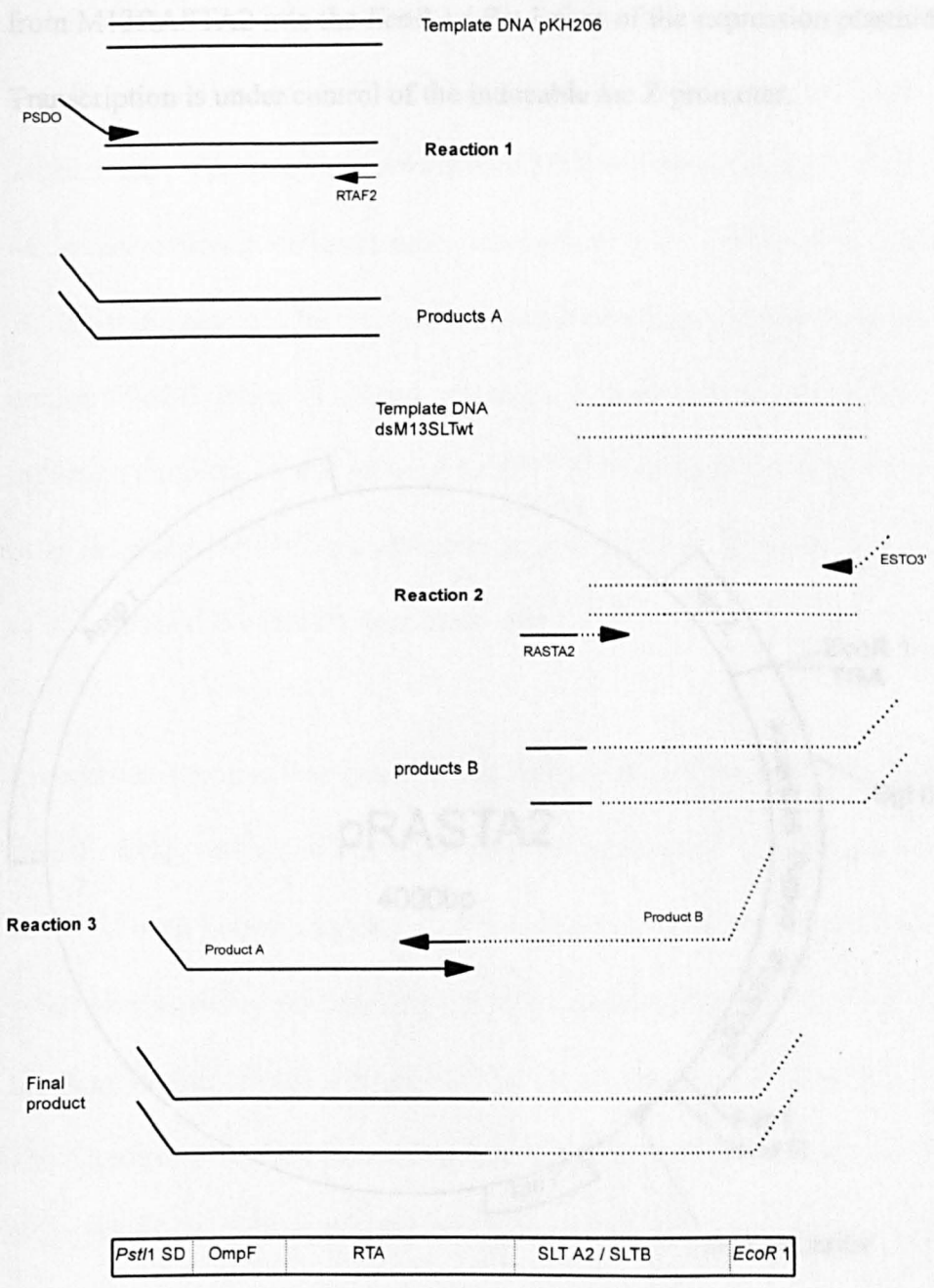

Figure 3.4.3 Plasmid pRASTA2.

Construction of pRASTA2 allowed expression of chimeric protein in *Escherichia coli* JM105. The plasmid was constructed by ligation of an *EcoR* 1 / *Pst* 1 fragment from M13RASTA2 into the *EcoR* 1 / *Pst* 1 sites of the expression plasmid pUC19. Transcription is under control of the inducable *lac* Z promoter.

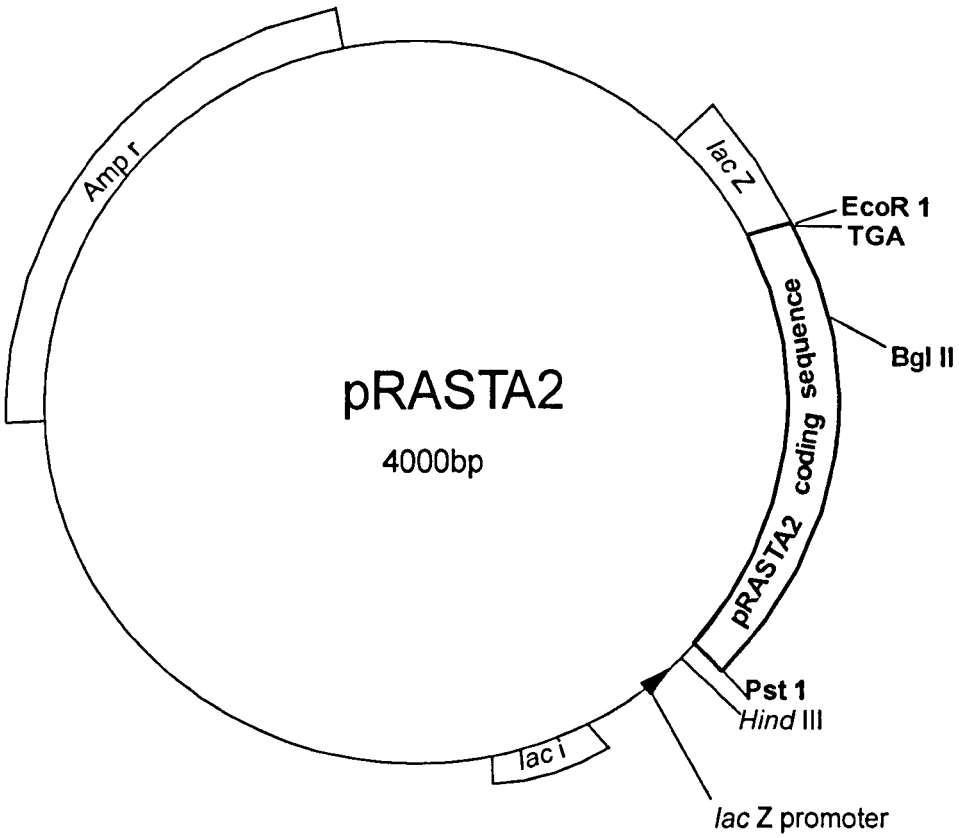

3.4.2 Expression and purification of RASTA2.

The expression system and the method of purification used for the production of RASTA2 in pUC19 expression vector was identical to that used for the expression and purification of SLT 1 wild-type section 3.1.2. The only change to the protocol was the temperature at which the induction of expression was performed. In earlier experiments induction, was performed at 37°C. However the yield of total recombinant protein in this instance was extremely low (< 10μg/l starting culture) and the toxin obtained by this method contained a disproportionate amount of unassembled B chains. A second expression experiment was carried out where the induction temperature was reduced to 30°C. Expression at this temperature resulted in an increased yield of approximately 30μg / l starting culture. A thirty fold excess of unassociated B chain remained however.

Recombinant protein was quantified in terms of the holotoxin concentration rather than the total protein concentration. This was achieved by comparing aliquots of RASTA2 with known amounts of ricin A chain on silver stained polyacrylamide gels, using scanning densitometery. Recombinant protein was stored at 4°C in PBS for short periods of time. Protein kept for longer periods was stored at -70°C in PBS. The excess of SLT 1 B chain was quantified by comparing the ratio of A and B chain in the wild-type SLT preparation with that of RASTA2 using scanning densitometry of silver stained polyacrylamide gels.

The result of expression of pRASTA2 using the method described is shown in figure 3.4.4. Expression of pRASTA2 resulted in the production of a chimeric protein with the predicted molecular mass. The yield of total holotoxin was lower than the yield of wild-type SLT produced in the same system. The yield was increased by a factor of 3 when the temperature was reduced to 30°C (the temperature at which ricin A chain is routinely expressed). At both 37°C and at 30°C the holotoxin preparation obtained after purification on a Gb_3-Sepharose column was contaminated with a thirty fold excess of SLT 1 B chain when compared with a SLT wild-type holotoxin preparation.

Several attempts to label RASTA2 with ^{125}I yielded very low levels of radiolabelled A chain. Metabolic labelling was used as an alternative to iodination, the method for which is described in section 2.6.6. RASTA2 was expressed in the presence of 1000μ Ci [^{35}S]-methionine in defined M9 media minus methionine. Radiolabelled recombinant protein was purified in an identical manner to that of the non-labelled protein using a 1ml Gb_3-Sepharose affinity matrix column. The results of expression of radiolabelled RASTA2 are shown in figure 3.4.5. The procedure described resulted in a small amount of radiolabelled holotoxin as shown in figure 3.4.5. Due to the scarcity of material produced by this procedure the amount of [^{35}S]-RASTA2 was not quantified in terms of protein concentration. 2.5 ml of purified [^{35}S]-methionine labelled RASTA2 was obtained with specific activity of 650cpm/μl. The calculated specific activity includes the excess labelled B chain.

Figure 3.4.4 Analysis of expression and purification of RASTA2 by 15% SDS polyacrylamide gel electrophoresis and Western blot analysis.

Figure 3.4.4 shows the expression and subsequent purification of the chimeric protein RASTA2 separated on a 15% SDS polyacrylamide gel followed by Western blot analysis (1° antibody sheep anti RTA). Protein coded in pRASTA2 under transcriptional control of the *lacZ* promoter, was expressed in *Escherichia coli* JM105. Lane 1 shows precolumn periplasm extracted from transformed *Escherichia coli.* Lanes 3-7 show purified chimeric protein eluted from a 1ml Gb_3-Sepharose analogue affinity column with 6M GuHCl pH 6.7. each track contains 100µl of dialysed protein precipitated with TCA. Lane 8 shows the position of ricin A chain. Lane 9 shows molecular mass markers.

Lane 1 Precolumn periplasm

Lane 2 eluted fraction15 (100 µl)

Lane 3 eluted fraction 16 (100 µl)

Lane 4 eluted fraction 17 (100 µl)

Lane 5 eluted fraction 18 (100 µl)

Lane 6 eluted fraction 19 (100 µl)

Lane 7 eluted fraction 20 (100 µl)

Lane 8 1µg ricin A chain (ICI)

Lane 9 Molecular mass markers

Figure 3.4.4 Analysis of expression and purification of RASTA2 by 15% SDS polyacrylamide gel electrophoresis and Western blot analysis.

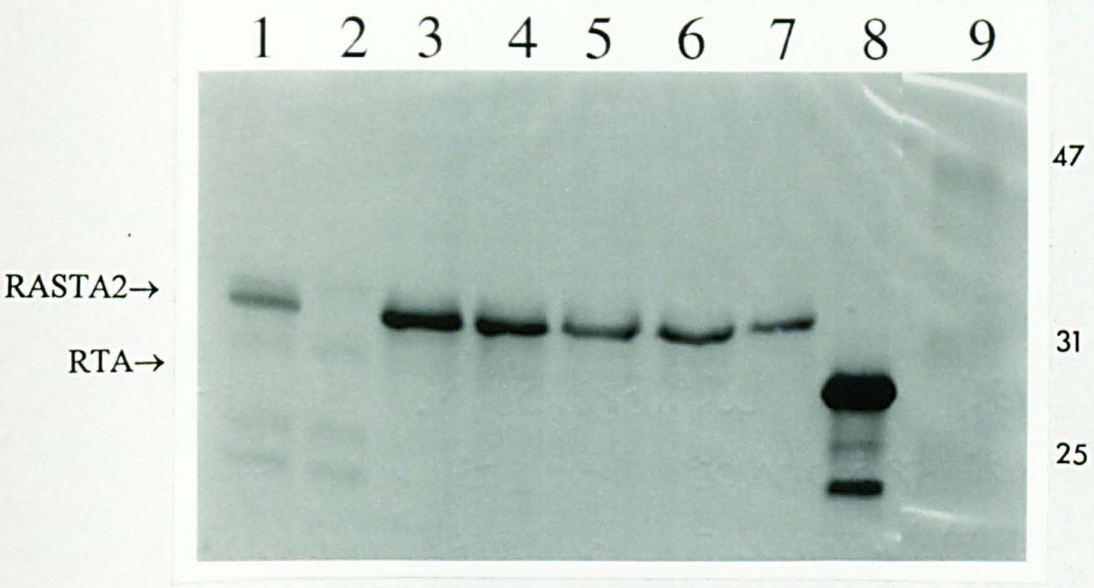

Figure 3.4.5 Analysis of expression and purification of metabolically labelled RASTA2 by 15% SDS polyacrylamide gel electrophoresis.

pRASTA2 coding for chimeric RASTA2 protein under transcriptional control of the *lac* Z promoter in *Escherichia coli* JM105, was grown in methionine free M9 minimal media. Protein expression was induced in the presence of [^{35}S]-methionine. Lane 1 shows molecular mass markers. Lane 2 shows precolumn periplasm extracted from induced, transformed *Escherichia coli.* Lane 3 shows 30µl of purified [^{35}S]-RASTA2 protein. The positions of the chimeric A chain and the SLT 1 B chain are indicated.

Lane1 Molecular mass markers

Lane 2 Precolumn periplasm (5µl)

Lane 3 eluted purified RASTA2 (30µl)

Figure 3.4.5 Analysis of expression and purification of metabolically labelled RASTA2 by 15% SDS polyacrylamide gel electrophoresis.

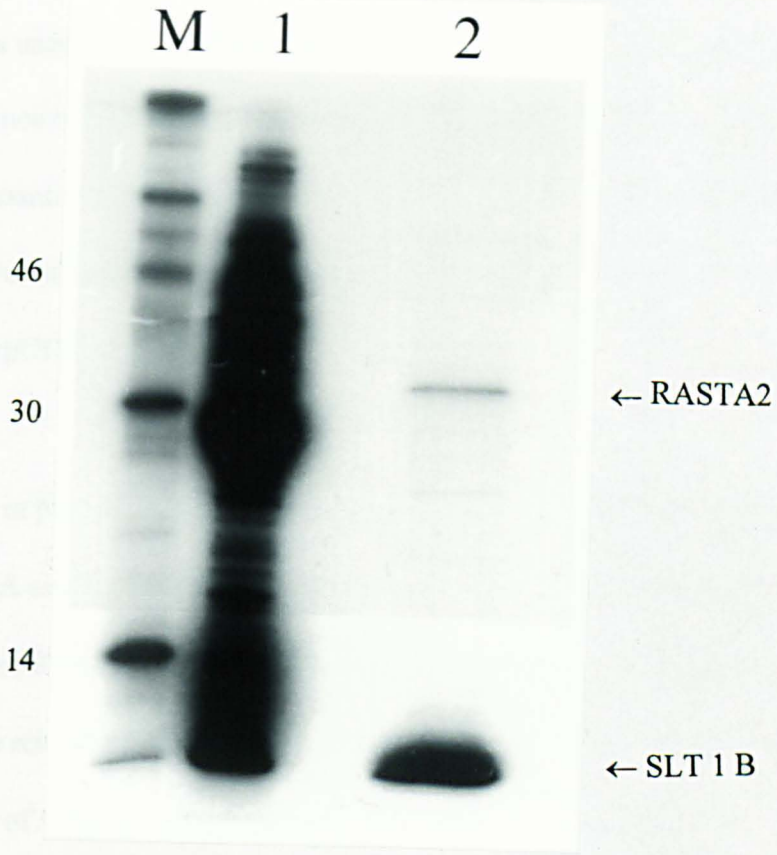

3.4.3 Discussion.

The use of four primer recombinant PCR allowed the production of a gene fusion between the coding region of ricin A chain with an omp F signal sequence with the A2 B chain coding region of the SLT 1 operon. The conventional method whereby the resulting full length PCR product produced in the third round of PCR is amplified using outside 3' and 5' primers did not produce product of the correct size. This was probably due of the large difference in annealing temperatures between the two primers used. Combination of large quantities of the first two reaction products in the presence of nucleotides and Vent DNA polymerase however, did result in a sufficient quantity of DNA fragment for subsequent cloning into M13mp18. DNA sequencing confirmed the sequence of this fragment in M13mp18 which was then cloned into pUC19 for expression.

Expression in pRASTA2 at 37°C resulted in a very poor yield of chimeric holotoxin. Since ricin A chain is routinely expressed at 30°C this temperature was applied to the expression of RASTA2 protein. Induction of expression by IPTG at the lower temperature resulted in a slightly increased yield of holotoxin approximately 30μg from 1 liter of starting culture. At both temperatures the quantity of SLT 1 B chain present in the periplasm extract was disproportionate (in thirty fold excess) with that of the chimeric A chain. Since the A and B chains of RASTA2 are transcribed as a single polycistronic mRNA the reason for the excess B chain is presumably due

either to the efficiency at which the A chain is transported to the periplasm or that the chimeric A chain is unstable and undergoes degradation in *in vivo.*

Repeated efforts to iodinate RASTA2 with [^{125}I] were unsuccessful. Efficient labelling of the B chain was seen, however no labelling of the A chain could be detected on polyacrylamide gels. Analysis of the crystal structure of SLT 1 B chain reveals an abundance of exposed tyrosine residues on the surface of the B chain pentamer making SLT 1 B an extremely good substrate for the iodination reaction. Presumably, during iodination of RASTA2, the large excess of SLT 1 B acts as a sink for the iodine and prevents efficient labelling of the A chain. Since labelled RASTA2 is essential for subsequent analysis of this protein, metabolic labelling was used as an alternative approach. Metabolic labelling with [^{35}S]-methionine resulted in a small quantity of radiolabelled purified protein. The concentration of this preparation was not determined because such a small quantity was obtained. Its activity by volume was calculated by liquid scintillation counting to be 650cpm/μl.

Two previous reports have highlighted the importance of the A2 subdomain for interaction with the B chain pentamer in addition to the crystal structure (Haddad and Jackson (1993); Austin *et al* (1994)). Both of these studies however report the production of C-terminal deletion mutants of SLT 1or ST. The portion responsible for holotoxin assembly being defined as those residues,which when deleted, preclude holotoxin assembly. These are rather indirect methods and the potential negative

effects of gross structural changes can not be ruled out in these studies. Evidence presented in chapter 4 clearly demonstrates that the A2 portion (defined as residues 262 to 293) alone is capable of association with the B chain pentamer. Since RASTA2 A chain can be purified by its interaction with the receptor analogue affinity matrix via the B subunit pentamer the A chain must be associated with the B chains. This data provides the first evidence that the C terminal 31 amino acids of SLT 1 A are sufficient for holotoxin assembly. Despite reports that a proportion of the A-B contacts are made with the A1 portion of SLT 1 clearly these contacts are not essential for holotoxin assembly or maintenence of toxin integrity under the conditions tested.

The characterisation of RASTA2 is described in chapter 5. Despite the very low level expression of RASTA2 in *Escherichia coli* sufficient material was obtained to use in cytotoxicity and *in vitro* proteases sensitivity studies. The radiolabelling of RASTA2 was very dissapointing. Only a minute quantity of radiolabelled A chain was obtained. It was considered that this material might be adequate for a single experiment which is described in chapter 5. The results of this experiment however were unsatisfactory.

Chapter 5

3.5 Characterization of a ricin A chain SLT A2 fusion protein RASTA2.

Introduction

The fusion protein RASTA2 (cloning and expression are described in chapter 4) was produced to predict whether processing of SLT 1was actually necessary or not. The chimeric A chain of RASTA2 was designed to remain intact during endocytosis and subsequent trafficking in sensitive eukaryotic cells. The reasons for our assumption of a protease-resistant RASTA2 are discussed in section 1.6. The fusion protein RASTA2 contains a full length ricin A chain, with an N-terminal periplasmic signal sequence, fused with the C-terminal 31 residues of SLT A2. The resulting A chain has catalytic activity comparable with ricin A chain and is able to associate with the SLT 1 B chain pentamer to form a chimeric holotoxin. The toxic A chain does not however contain the loop region (residues 242-261) known to be the site of proteolytic activation of wild-type SLT 1/ST (Burgess and Roberts (1993); Garred *et al* (1995a)). In this study, the biological characteristics of this fusion protein will be investigated both *in vitro* and *in vivo*. Any relevance to the proteolytic processing requirements of SLT 1 will then be discussed.

3.5.1 N-glycosidase activity of RASTA2.

The N-glycosidase activity of RASTA2 towards isolated rabbit reticulocyte ribosomes was compared with that of ricin A chain *in vitro* using the aniline assay (section 2.7.3). Rabbit reticulocyte ribosomes were incubated with four decreasing amounts of recombinant RASTA2 protein (1000ng, 500ng, 100ng, 10ng) prior to treatment with acetic-aniline. The resulting acetic-aniline treated RNA was run on a denaturing formamide 1.2% agarose gel (section 2.3.4). Separated RNA was visualized by ethidium bromide staining. Figure 3.5.1 shows a gel prepared in this manner. Depurination of rRNA followed by treatment with acetic-aniline results in cleavage of the RNA backbone at position 4324 releasing an RNA fragment from the 5' end of 28S rRNA of 394 bases which is diagnostic for the action of ribosome inactivating proteins. The gel shown in figure 3.5.1 clearly demonstrates that the recombinant chimeric protein RASTA2 has N-glycosidase activity. Although this assay was not performed in order to quantify precisely the level of activity of this protein, comparison of the extent of depurination using scanning densitometry shows that at 100ng RASTA2 is comparable with that of 100ng RTA. Therefore it can be assumed that RASTA2 has roughly the same activity to that of recombinant ricin A chain.

Figure 3.5.1 N-glycosidase activity of RASTA2

Figure 3.5.1 shows ethidium bromide stained rRNA separated on a denaturing 1.2% agarose gel. Rabbit reticulocyte ribosomes were treated with decreasing amounts of toxin at 30°C for 30 min. The resulting RNA was isolated and treated with acetic-aniline at 60°C for 2 min. Aniline treated RNA was separated by denaturing agarose gel electrophoresis. Specific depurination due to the action of SLT 1 followed by acetic-aniline treatment leads to release of a 394 base RNA fragment indicated by an arrow.

Lane 1 1000ng RASTA2 - aniline

Lane 2 1000ng RASTA2 + aniline

Lane 3 500ng RASTA2 + aniline

Lane 4 100ng RASTA2 + aniline

Lane 5 10 ng RASTA2 + aniline

Lane 6 100ng RTA + aniline

Figure 3.5.1 N-glycosidase activity of RASTA2

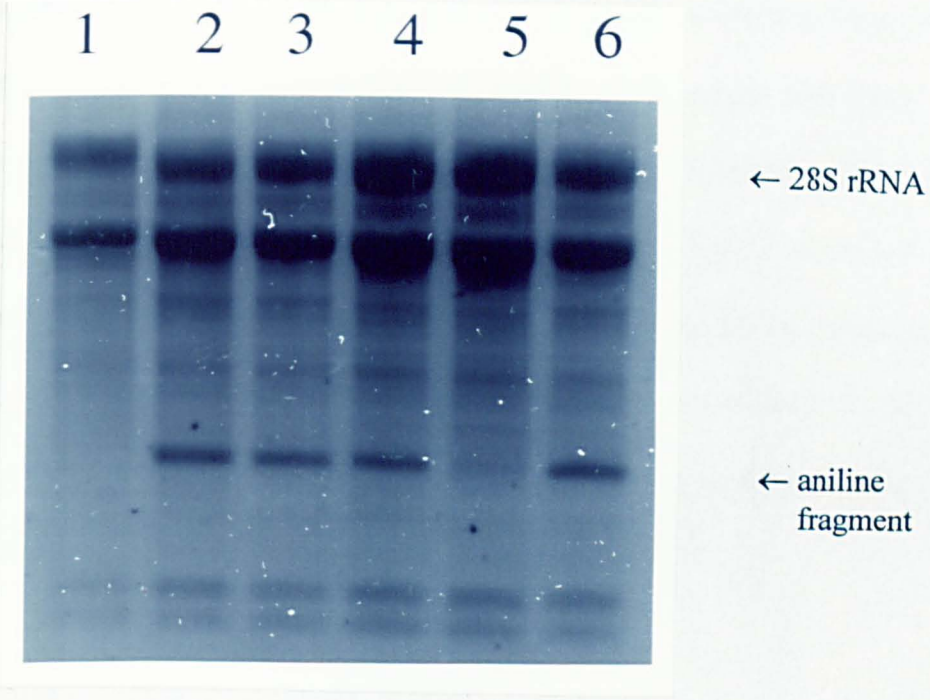

3.5.2 *In vitro* sensitivity of RASTA2 to proteinase K and trypsin.

The sensitivity of RASTA2 to trypsin and proteinase K was compared to that of ricin A chain. RTA is, like several other ribosome inactivating proteins, characteristically insensitive to proteases. SLT however is very sensitive to trypsin (section 3.3.2). The chimeric RASTA2 A chain was designed to be refractory to proteolysis. Addition of endogenously added protease provides a quick and simple assessment of protease sensitivity. Figure 3.5.2 shows a western blot, probed with sheep anti RTA antibodies, of RTA and RASTA2 treated with the proteases trypsin and proteinase K. As expected, ricin A chain is almost totally resistant to digestion with either proteinase K or trypsin. Only where RTA is treated with 10μg/ml proteinase K at 37°C for 7 min is there any sign of reduction in the 30 kDa band. Some low level degradation is seen on treatment of RTA with 10 μg/ml trypsin for 7 mins and with proteinase K at 0°C for 40 min also. RASTA2 is also highly resistant to protease. Only when treated with 10 μg/ml proteinase K at 37°C can A chain degradation be detected.

Figure 3.5.2 Reducing 15% SDS polyacrylamide gel electrophoresis followed by Western blot analysis of proteinase K-and trypsin-treated ricin A chain and RASTA2.

RTA and RASTA2 were treated with trypsin or proteinase K at 0.1 and 10 μg/ml at 37°C for 7 min. In addition both RTA and RASTA2 were treated with proteinase K at 10μg/ml at 0°C for 40 min. Tryptic digests were stopped by addition of 1μl of TLCK 1mg/ml in 0.05M sodium acetate acetic acid pH5.0. Proteinase K digests were boiled for 5 min prior to addition of sample loading buffer. The resulting proteins were separated on a 15% SDS PAG under reducing conditions. Protein was visualized by western blot analysis using sheep anti RTA as primary antibody.

1) RTA - protease

2) RTA + Proteinase K 0.1μg/ml

3) RTA + Proteinase K 10μg/ml

4) RTA + Trypsin 0.1 μg/ml

5) RTA + Trypsin 10 μg/ml

6) RTA + Proteinase K 10μg/ml 0°C

7) RASTA2 - protease

8) RASTA2 + Trypsin 0.1μg/ml

9) RASTA2 + Trypsin 10μg/ml

10) RASTA2 + proteinase K 0.1μg/ml

11) RASTA2 + proteinase K 10μg/ml

12) RASTA2 +proteinase K 10μg/ml 0°C

Figure 3.5.2 Reducing 15% SDS polyacrylamide gel electrophoresis followed by Western blot analysis of proteinase K-and trypsin-treated ricin A chain and RASTA2.

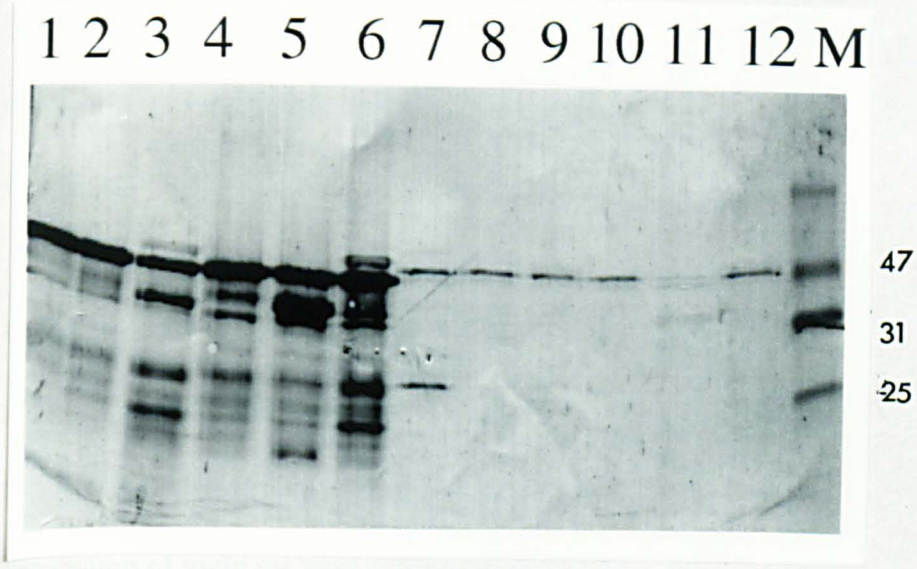

3.5.3 Cytotoxicity of RASTA2 compared with that of ricin and wild-type SLT 1.

The cytotoxicity of RASTA2 was characterized with respect to IC_{50} and to the kinetics of cell killing by plotting percentage protein synthesis inhibition as a function of toxin concentration or time respectively. The method used to determine cytotoxicity is given in section 2.7.4. The results of cytotoxicity experiments are shown in figures 3.5.3, 3.5.4 and 3.5.5. Cytotoxicity curves for SLT 1 wild-type and ricin are also included for comparison. The effect of a thirty fold excess of unassociated SLT 1 B chain was also investigated. This experiment was used to rule out any effects of having such an excess of B chain present in RASTA2 on its cytotoxicity.

In the presence of a thirty fold excess of SLT 1 B chain the cytotoxicity of wild-type SLT 1 remains unchanged. This indicates that the large excess of B chain co-purified with RASTA2 should not significantly effect its cytotoxicity. Over a three hour incubation of toxin on Vero cells, wild-type SLT 1 gave an IC_{50} of 0.019 ng/ml compared to 0.022 ng/ml in the presence of excess B chain (figure 3.5.3). Over a three hour toxin incubation, IC_{50} values for RASTA2, ricin and SLT 1 were 7ng/ml, 19ng/ml and 0.02ng/ml respectively (figure 3.5.4). After a 6 hour incubation of toxin IC_{50} values for RASTA2, ricin and SLT 1 were 0.3ng/ml, 0.35ng/ml and 0.007ng/ml

respectively (figure 3.5.5). From kinetic experiments the $T_{1/2}$ values for RASTA2, ricin and SLT 1 were 133 min, 113 min and 57 min respectively (figure 3.5.6).

Figure 3.5.3 The effect of excess SLT 1 B chain on the cytotoxicity of SLT 1 wild-type: 3 hour toxin incubation.

$1x10^{-4}$ to 10 ng/ml of SLT 1 wild-type and $1x10^{-4}$ to 10 ng/ml of SLT 1 wild-type mixed with a thirty fold molar excess of purified SLT 1 wild-type B chain diluted in DMEM, was incubated with 1.2 to 1.5 $x10^4$ Vero cells plated in 96 well tissue culture plates for 2.5 hours at 37°C in a 5% CO_2 incubator. Following incubation with toxin the cell monolayers were washed once with PBS and 100µl of PBS containing 1µCi of [^{35}S]-methionine was added to each well. Cells were incubated for a further 30 min. Monolayers were then washed three times with 5% ice cold trichloroacetic acid and neutralized by a single wash with PBS. Acid-precipitated protein was then released with 100µl of 0.5M NaOH and incorporated radioactivity was quantified by liquid scintillation counting.

All values are the mean of four replicate samples. Protein synthesis inhibition was calculated as the percentage incorporation of radioactivity compared with the mean of six no toxin controls.

Toxin	IC_{50} ng/ml
SLT 1 wt	0.019
SLT 1 +B	0.022

Figure 3.5.3 The effect of excess SLT 1 B chain on the cytotoxicity of SLT 1 wild-type: 3 hour toxin incubation.

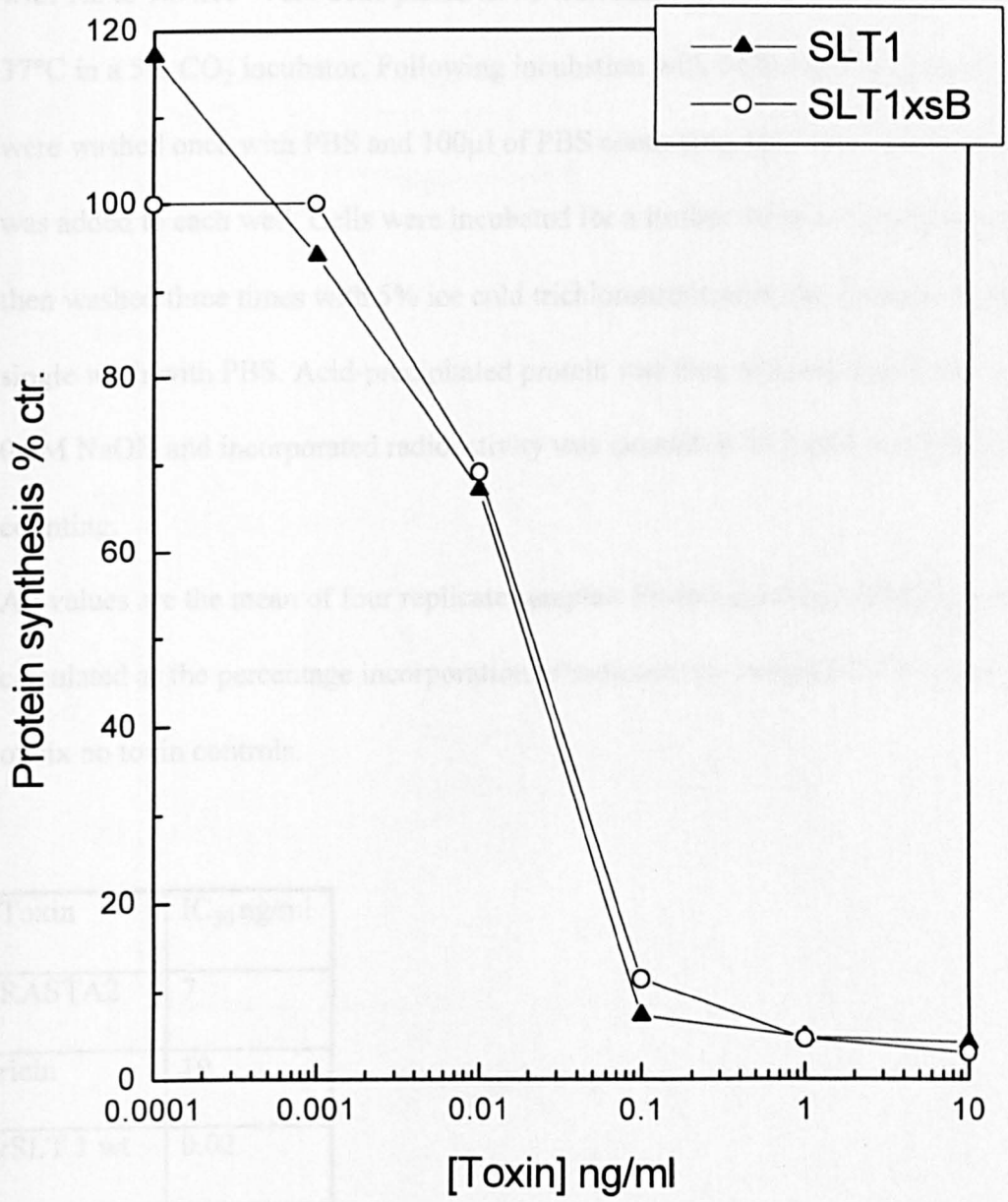

Figure 3.5.4 Cytotoxicity of RASTA2, ricin and SLT 1 wild-type: 3 hour incubation of toxin.

$1x10^{-4}$ to 10 ng/ml of each recombinant holotoxin, diluted in DMEM, was incubated with 1.2 to 1.5 $x10^4$ Vero cells plated in 96 well tissue culture plates for 2.5 hours at 37°C in a 5% CO_2 incubator. Following incubation with toxin the cell monolayers were washed once with PBS and 100µl of PBS containing 1µCi of [^{35}S]-methionine was added to each well. Cells were incubated for a further 30 min. Monolayers were then washed three times with 5% ice cold trichloroacetic acid and neutralized by a single wash with PBS. Acid-precipitated protein was then released with 100µl of 0.5M NaOH and incorporated radioactivity was quantified by liquid scintillation counting.

All values are the mean of four replicate samples. Protein synthesis inhibition was calculated as the percentage incorporation of radioactivity compared with the mean of six no toxin controls.

Toxin	IC_{50} ng/ml
RASTA2	7
ricin	19
rSLT 1 wt	0.02

Figure 3.5.4 Cytotoxicity of RASTA2, ricin and SLT 1 wild-type: 3 hour incubation of toxin.

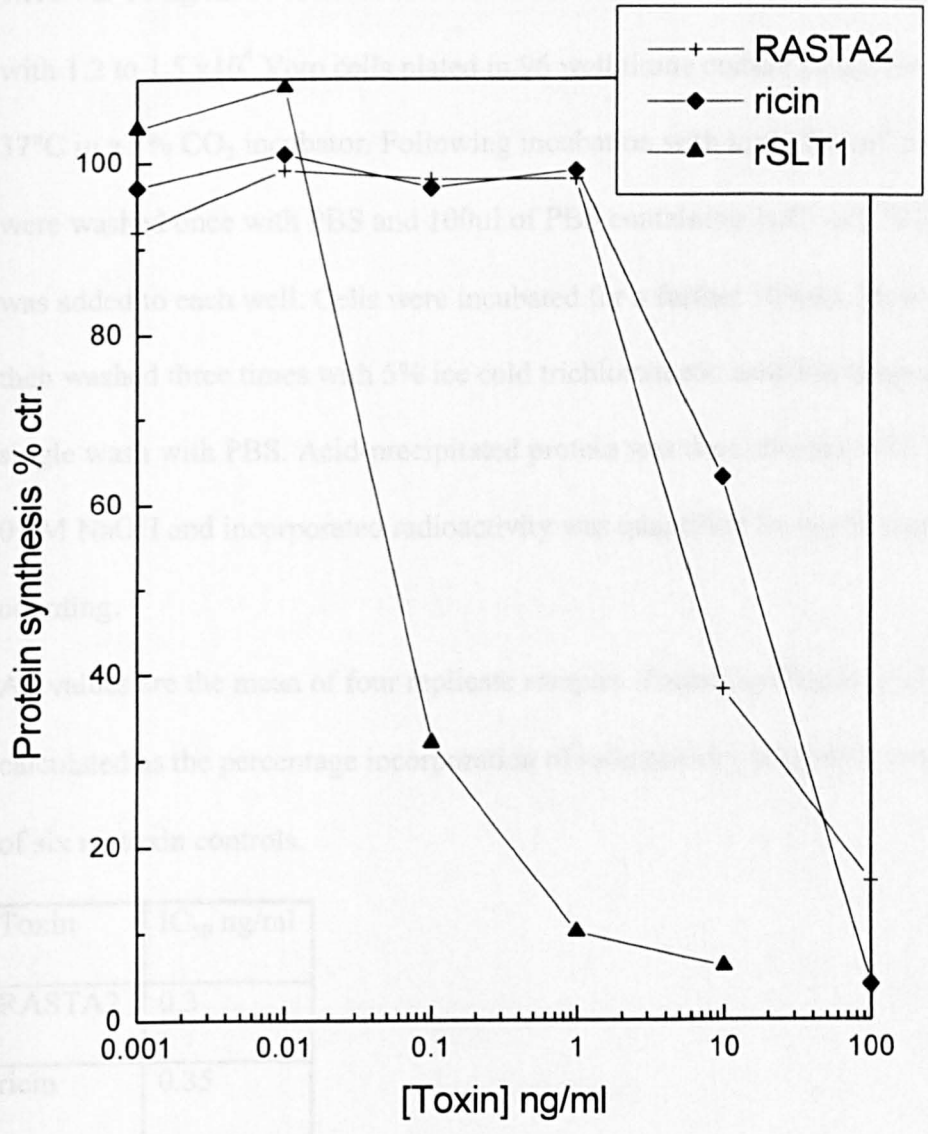

Figure 3.5.5 Cytotoxicity of RASTA2, ricin and SLT 1 wild-type: 6 hour incubation of toxin.

$1x10^{-4}$ to 10 ng/ml of each recombinant holotoxin, diluted in DMEM, was incubated with 1.2 to 1.5 $x10^4$ Vero cells plated in 96 well tissue culture plates for 5.5 hours at 37°C in a 5% CO_2 incubator. Following incubation with toxin the cell monolayers were washed once with PBS and 100µl of PBS containing 1µCi of [^{35}S]-methionine was added to each well. Cells were incubated for a further 30 min. Monolayers were then washed three times with 5% ice cold trichloroacetic acid and neutralized by a single wash with PBS. Acid-precipitated protein was then released with 100µl of 0.5M NaOH and incorporated radioactivity was quantified by liquid scintillation counting.

All values are the mean of four replicate samples. Protein synthesis inhibition was calculated as the percentage incorporation of radioactivity compared with the mean of six no toxin controls.

Toxin	IC_{50} ng/ml
RASTA2	0.3
ricin	0.35
SLT 1 wt	0.007

Figure 3.5.5 Cytotoxicity of RASTA2, ricin and SLT 1 wild-type: 6 hour incubation of toxin.

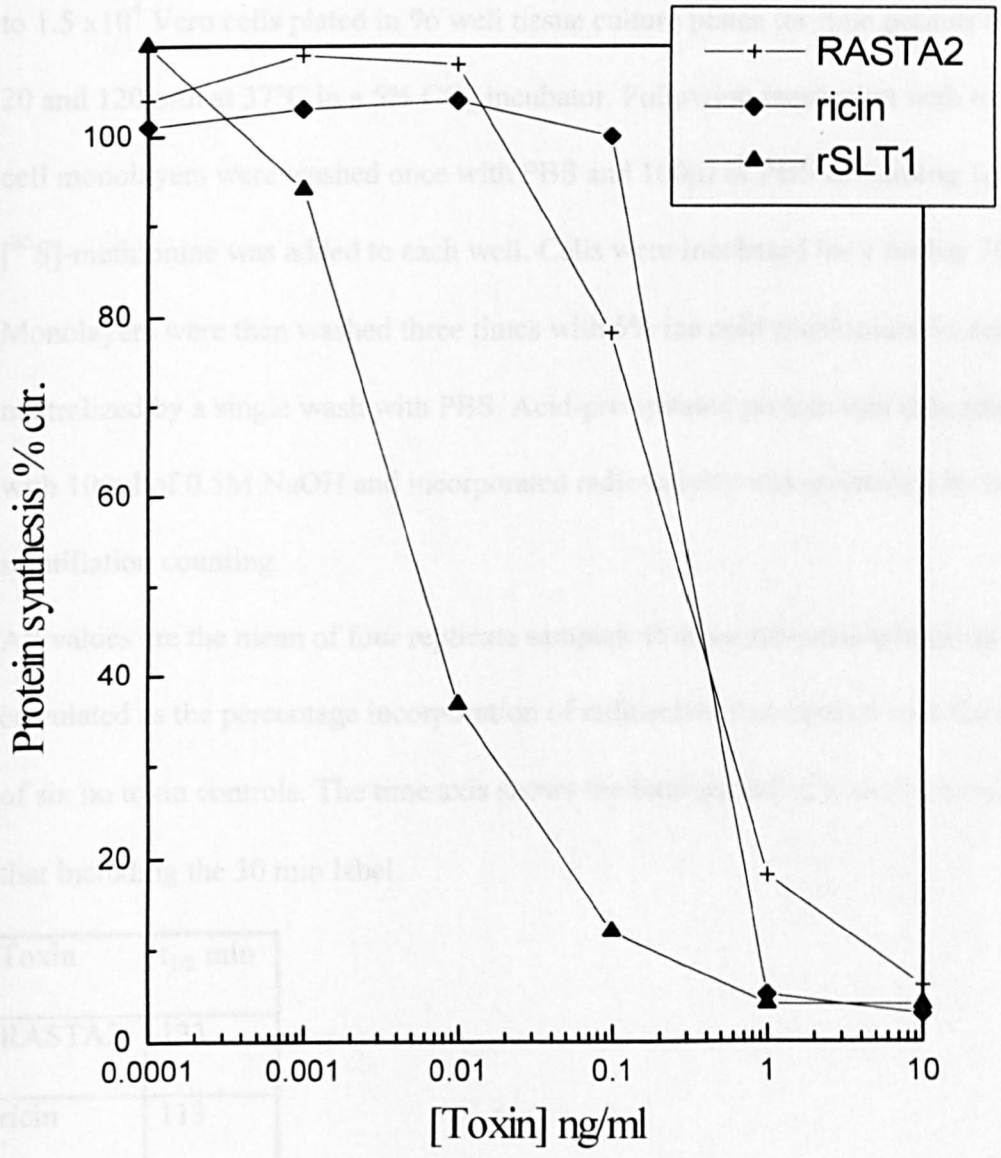

Figure 3.5.6 The kinetics of cytotoxicity of RASTA2, ricin and SLT 1 wild-type in Vero cells.

100 ng/ml of each recombinant holotoxin, diluted in DMEM, was incubated with 1.2 to 1.5 x10^4 Vero cells plated in 96 well tissue culture plates for time periods between 20 and 120 min at 37°C in a 5% CO_2 incubator. Following incubation with toxin the cell monolayers were washed once with PBS and 100µl of PBS containing 1µCi of [^{35}S]-methionine was added to each well. Cells were incubated for a further 30 min. Monolayers were then washed three times with 5% ice cold trichloroacetic acid and neutralized by a single wash with PBS. Acid-precipitated protein was then released with 100µl of 0.5M NaOH and incorporated radioactivity was quantified by liquid scintillation counting.

All values are the mean of four replicate samples. Protein synthesis inhibition was calculated as the percentage incorporation of radioactivity compared with the mean of six no toxin controls. The time axis shows the total period of toxin incubation i.e. that including the 30 min label.

Toxin	$t_{1/2}$ min
RASTA2	133
ricin	113
SLT 1 wt	57

Figure 3.5.6 The kinetics of cytotoxicity of RASTA2, ricin and SLT 1 wild-type in Vero cells.

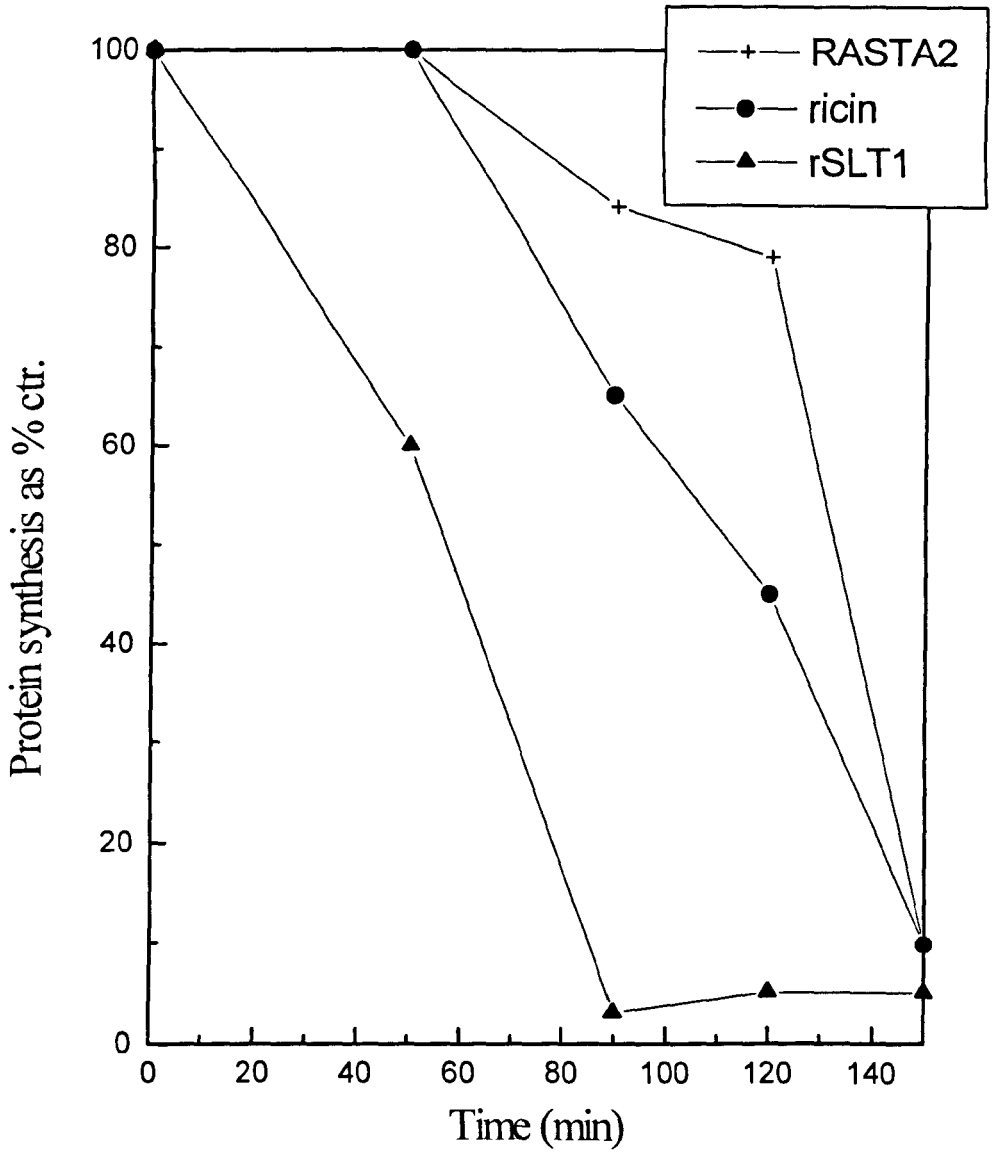

3.5.4 *In vivo* processing of RASTA2 in Vero cells.

In order to determine whether RASTA2 remains intact during trafficking and translocation in Vero cells attempts were made to radioactively label RASTA2. Using an identical protocol used for the iodination of SLT 1 and potential processing mutants no iodinated RASTA2 could be obtained. An alternative method using metabolic labelling was used and is described in section 3.4.2 and 2.6.6.

Metabolic labelling yielded a very small quantity of RASTA2-[^{35}S]-methionine. Due to the scarcity of this material this protein was not quantified, instead the entire preparation was used. *In vivo* proteolytic processing experiments with RASTA2 were carried out in an identical manner to those using iodinated toxin, however time points of four and six hours were used. This experiment yielded a very weak signal from the recovered protein. As a result of the low intensity of the signal, the flurographed gel was exposed to Kodak biomax film for three weeks at -70°C. The results of this experiment are shown in figure 3.5.7. Within the limits of the experiment RASTA2 does not appear to be processed after four hours exposure to Vero cells however after six hours a cleavage fragment of 30kDa can be seen. Since this experiment was carried out on only one occasion and the autoradiograph is so faint the results should be interpreted with caution.

Figure 3.5.7 *In vivo* proteolytic processing of RASTA2 in Vero cells.

Vero cells, grown to a confluent monolayer in 3 cm tissue culture dishes, were incubated at 37°C in a 5% CO_2 incubator with [^{35}S]-methionine labelled RASTA2 for the specified period of time. Following incubation the toxin was washed off and cells lysed in cell lysis buffer. Cell lysates were centrifuged to remove cell debris and nuclei. Protein was precipitated with acetone. The resulting protein pellets were resuspended in reducing sample loading buffer and separated on 15% SDS polyacrylamide gels. The positions of full length RASTA2 A chain is indicated. The position of the 30kDa molecular mass marker is indicated.

Lane M	Molecular mass markers
Lane 0	Untreated RASTA2
Lane 4	Four hours toxin exposure
Lane 6	Six hours toxin exposure

Figure 3.5.7 ***In vivo*** **proteolytic processing of RASTA2 in Vero cells.**

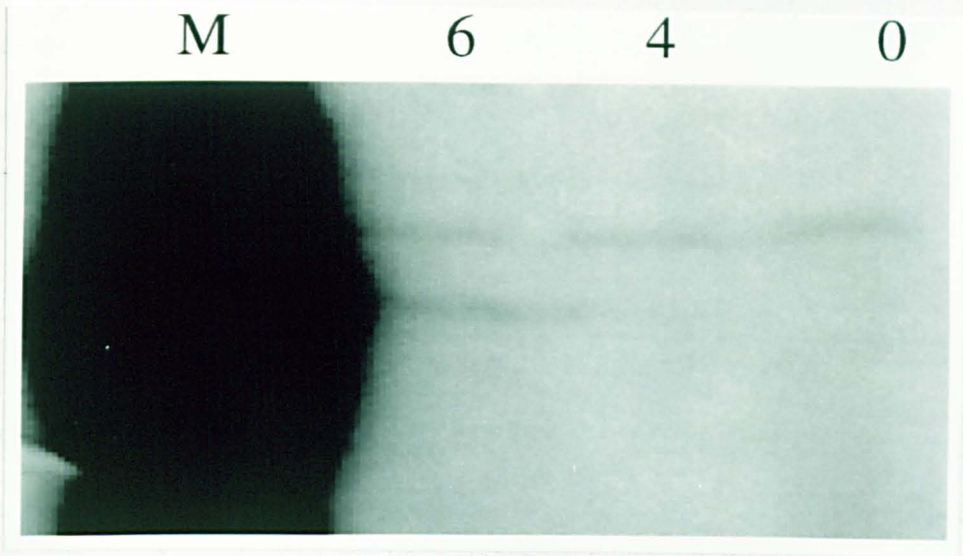

3.5.5 Discussion

The chimeric toxin described in chapter 4 was made in an attempt to determine whether the presence of A2 could prevent toxicity of RTA (perhaps by blocking its translocation). Should no such block in toxicity arise then it might be assumed that A2 need not in fact be cleaved from A1 in cells lacking the furin enzyme or with mutant SLT A chains which are refractory to proteolysis. Evidence is presented in chapter 4 which clearly demonstrates assembly of RASTA2 into a holotoxin and that the integrity of the receptor binding site is maintained. In the current chapter the biological characteristics of this protein are investigated.

The N-glycosidase activity of RASTA2 was investigated by the aniline assay. Although this assay was not performed in a quantitative manner the results which are obtained can be considered semi-quantitative. From a simple titration of RASTA2 it appears that this protein has comparable activity to that of ricin A chain. This result is to be expected if the A2-B chain portion of the protein does not prevent access to the active site. The activity of RTA is greater than that of intact SLT 1, presumably because wild-type SLT 1 has its active site specifically obscured by the side chain of Met 260. RASTA2 therefore has elevated N-glycosidase activity to that of SLT 1 since Met 260 is unlikely to be correctly positioned to interfere with the active site of the RTA moiety.

Since the RASTA2 preparation used for these experiments was contaminated with a large excess of SLT 1 B chain, the effect of additional B chain on the cytotoxicity of SLT 1 wt was investigated. It was considered that such a large amount of unassociated B chain might compete for receptors on the surface of Vero cells and thus provide at least a partial protection against the toxin. However no difference in IC_{50} values was detected between toxin applied in the absence or presence of excess B chain (figure 3.5.3). Presumably Vero cells have such a large quantity of SLT 1 binding sites that the portion occupied by toxin in these experiments is negligible. Alternatively SLT 1 holotoxin may have an increased affinity for Gb_3 compared to that of SLT 1 B chain alone and thus effectively competes for binding to the receptor. Since it appears that the excess B chain does not interfere with cytotoxicity measurements, direct comparisons between RASTA2, SLT 1 and ricin can be made. Since SLTP4 (described in chapter 3) was toxic to Vero cells despite its apparent resistance to proteolytic processing, it was predicted that in the absence of any proteolytic processing, RASTA2 too would also be cytotoxic. The increased cytotoxicity of SLT 1 compared to that of ricin is probably a result of receptor-mediated targeting via the B chains. For this reason it was expected that RASTA2 would show similar IC_{50} and $t_{1/2}$ values to that of SLT 1. RASTA2 is potently toxic to Vero cells giving an IC_{50} of 7ng/ml after three hours and 0.3 ng/ml after six hours. However these figures more closely resemble ricin than SLT 1 (ricin IC_{50} 19ng/ml, 0.35 ng/ml SLT 1 0.02 ng/ml, 0.007 ng/ml after three and six hours respectively).

Likewise the kinetics of entry are also more like ricin than SLT 1 (RASTA2 133min, ricin 113min, SLT 1 57min).

The sensitivity of RASTA2 to protease *in vitro* was compared with that of ricin A chain. From figure 3.5.2 it can be seen that the chimeric A chain has similar protease sensitivity characteristics to that of RTA. Only when RASTA2 is treated with proteinase K at 37°C for 7 min at 10μg/ml is degradation seen. This degradation seems to take the form mostly of total fragmentation rather than more specific proteolysis which may represent cleavage around the RTA-A2 junction. The low concentration at which RASTA2 was obtained did not allow more protein to be used in this analysis. These results provide some evidence that RASTA2 is in fact refractory to proteolysis although the conditions tested *in vitro* are very different to those that the toxin may meet *in vivo*.

The *in vivo* protease sensitivity was investigated using metabolically labelled RASTA2. Unfortunately the results from this experiment are rather poor since radiolabelled RASTA2 could not be obtained at a high enough specific activity. However sufficient radiolabelled RASTA2 holotoxin was obtained to carry out a single experiment. The results from this experiment are shown in figure 3.5.7. As previously stated the radio-labelled RASTA2 used for studying the *in vivo*

proteolytic processing had very low specific activity, as a consequence, this experiment yielded very unsatisfactory results which were on the very limits of detection. The results from this experiment however do indicate that RASTA2 does undergo slow proteolytic processing. A cleavage fragment of approximately 30kDa is seen after incubation of RASTA2 with Vero cells after six hours. No fragment is seen after 4 hours. RASTA2 has a $t_{1/2}$ of 133 minutes so that after six hours more than 80% of these cells are dead. Therefore the toxin recovered from cells after six hours has presumably been subjected to a host of cellular proteases not only those within components of the secretory pathway. If this is the case the proteolytic cleavage observed in this experiment might represent proteolytic degradation rather than a specific proteolytic event essential for cytotoxicity.

This data, if correct may be interpreted to mean that RASTA2 is translocationally defective. If RASTA2 were capable of membrane translocation as an intact A chain, the IC_{50} values might be expected to concur with those for wild-type SLT 1 (or indeed be higher due to the enhanced N-glycosidase activity of the hybrid versus SLT A1). The fact that the fusion is not apparently processed in a physiologically relevant time scale and that it displays cytotoxicity closer to that of ricin and SLTP4 is consistent with a model where A2 obstructs membrane translocation or its presence in some other way introduces a rate limiting step. Since the kinetics and cytotoxicity of RASTA2 are so similar to ricin this explanation would infer that ricin

A chain does not need to fully translocate the membrane either, but that it can act on ribosomes on the cytosolic side of the translocating ER membrane.

Chapter 6

3.6.1 Final discussion.

The aims of the present study are listed at the end of section 1. To extend our knowledge of the proteolytic processing requirements for the bacterial toxin *Escherichia coli* Shiga-like toxin 1. The approach adopted was the production of several mutant forms of SLT 1 altered in a region of the A chain primary sequence where the proposed cleavage is thought to occur. In addition to these, a chimeric toxin was created between ricin A chain and the A2 portion of SLT 1, previously thought to be removed by a processing step. Attempts were made to design this fusion (RASTA2) such that it is refractory to proteolytic cleavage *in vivo*.

In chapter 1 a wild-type SLT 1 *Escherichia coli* expression clone and a revised method of toxin purification are described. Once a method for the rapid production of unnicked SLT 1 in quantities sufficient for biochemical analysis was established, the production of a range of mutant toxins was easily afforded by expression and purification using the same protocol. A total of four SLT 1 toxins mutant in the A chain were produced by this method. Since the fusion protein described in chapter 4 incorporates the cell binding B chain pentamer of SLT 1, this toxin was also purified in an identical manner.

SLTP1 is a toxin which has the two disulphide bonded loop arginine residues mutated to glycine residues. It is these two arginines which are thought to form the furin recognition motif responsible for proteolytic cleavage of toxin during target cell intoxication. These mutations were previously reported by Burgess and Roberts (1993) and similar mutations were made by Garred *et al* (1995a). This toxin remains fully toxic to Vero cells although there is a transient reduction in cytotoxicity relative to wild-type when incubated with cells for less than 3 hours. Both Burgess and Roberts (1993) and Garred *et al* (1995a) report a 10 fold reduction in cytotoxicity of an identical or similar mutant compared with wild-type toxin. In the present study a 25 fold reduction is observed.

In the report by Garred *et al* (1995a), the proteolytic processing of this toxin was followed by precipitating iodinated toxin from Vero cells, 2 and 4 hours after exposure to toxin. This approach was also adopted in the present study to trace the proteolytic processing events of the mutants described. In this study however, shorter incubation times were used in case the processing seen by Garred *et al* (1995) was associated with events in the cytosol. However even with incubations of toxin as short as 30 min, when SLT 1 may still be located within the endomembrane system, SLTP1 was seen to be processed in Vero cells. This indicated that the toxin remained sensitive to target cell proteases, most likely contained within the endocytic pathway. The slight reduction in cytotoxicity during short incubations with toxin can probably be accounted for by a rate limiting step, possibly the novel processing step itself, or

perhaps an impediment in translocation. In an identical way to the study of Garred *et al,* the effects of brefeldin A and a membrane permeable protease inhibitor calpain inhibitor I were investigated here. As in the previous study, SLTP1 was not efficiently processed to the A1 size in cells pretreated with either brefeldin A or calpain inhibitor I under the experimental conditions used. These results suggest that SLTP1 undergoes an alternative processing event during toxin uptake into target cells. This processing must occur in a compartment of the early secretory pathway which the toxin cannot reach in cells treated with brefeldin A (a reagent causing reversible collapse of the Golgi in Vero cells (Fujiwara *et al* (1988)) and which therefore prevents trafficking from the TGN to the Golgi and ER). In contrast, the wild-type toxin is processed in cells treated with BFA and thus must be cleaved in a vesicle prior to the BFA-blocked transport step, probably the TGN. Calpain inhibitor I is an inhibitor of the calcium dependent protease calpain. The exact cellular location of calpain is unclear although its thought that it may be cytosolically located (Murachi (1983)). Preincubation of Vero cells with calpain inhibitor I does not affect the potency of wild-type SLT1. However, Vero cells are afforded a protection of almost five fold in the presence of this reagent to SLTP1. These data together suggest that SLTP1 is processed in a earlier compartment of the secretory pathway to that of wild-type toxin and that the alternative cleavage can be inhibited by calpain inhibitor I. This data is in agreement with Garred *et al* (1995a).

Since SLTP1 is clearly still sensitive to target cell proteases further mutant toxins were produced in an attempt to produce a toxin which would not be processed at all. SLTP3 contains the mutations already described in SLTP1. In addition SLTP3 contains four additional mutant residues. The extra mutations introduced to SLTP3 involve two pairs of Ala/Ser residues which lie either side of the loop arginines. These residues were selected as a result of a report by Takao *et al* (1988) in which tryptic digests of SLT 1 were investigated using mass spectrometry. They found that the preparation of SLT 1 used for analysis was already pre-nicked between residues Ala 253 and Ser 254. This cleavage could not have been performed by trypsin. It was rationalized that the propensity of these target sites to cleavage during the preparation of toxin might mean they are accessible to intracellular proteases. Furthermore, since they lie very close to the loop furin-site residues, alternative cleavage at either of the Ala/Ser pairs would generate nicked, disulphide bonded toxin consisting of an A1-like fragment indistinguishable in size (by SDS PAGE) from the the wild-type version. This would fit with the data of Garred *et al*(1995a). To investigate the possible involvement of these residues in *in vivo* proteolytic processing, they were therefore mutated to glycine and alanine. A second pair of Ala/Ser residues on the C-terminal side of the proposed nicking site were also mutated to glycine and alanine residues. Where the two paired Ala/Ser residues were mutated alone (SLTP2), the resulting holotoxin was essentially wild-type in its biological properties. These same Ala/Ser to Gly and Ala mutations were also made within the SLTP1 framework to generate SLTP3. SLTP3 was 6 fold less toxic to

Vero cells after a short toxin incubation and was as toxic as the wild-type after prolonged incubation (more than 3 hours). Furthermore SLTP3 is proteolytically processed at the same rate as SLTP1 and behaves like SLTP1 in the presence of calpain inhibitor 1 and BFA. From these data it appears that the Ala/Ser paired residues do not play any role in toxin processing.

As a final point, the A1 fragment generated from both SLTP1 and SLTP3 appears identical in size to that of the wild-type-generated A1 fragment (within the constraints of the gel system used). In the study by Garred *et al* (1995a), toxins processed *in vivo* and run under reducing and non reducing conditions revealed that the fragment generated from both the wild-type and the mutant toxin (equivalent to SLTP1 in the present study) was produced by cleavage within the disulphide bonded loop. As the A1 fragments from SLTP1 and SLTP3 are also the same size as those from the wild-type (as judged by SDS-PAGE) it would appear that cleavage of these mutants also occurs in the loop, close to the natural cleavage site.

A fourth set of mutations was introduced to SLT 1 at a site which lies upstream of the proposed primary cleavage site. This site (220Arg--Arg223) resembles a minimal recognition sequence for furin. In the protein SLTP4, Arg220 and Arg223 were mutated to glycine residues within the SLTP3 framework. In contrast to the mutants SLTP1 and SLTP3, SLTP4 does not appear to be processed at all under any of the conditions tested here. However this protein remains cytotoxic to Vero cells albeit

with reduced potency. Following a three hour incubation of toxin SLTP4 is 134 fold less toxic than wild-type and remains 62 fold less toxic after prolonged incubation. These data provide the first evidence that SLT 1 does not require any proteolytic cleavage for toxicity.

Since the fragments generated *in vivo* from SLTP1 and SLTP3 (and Garred *et al* 1995a) seem to be generated from within the disulphide loop, it seems unlikely that the Arg220--Arg223 (mutated in SLTP4) constitutes the site of any alternative cleavage and certainly no visualisation of a truncated A1 fragment was ever seen *in vivo*. It is proposed that the additional mutations in SLTP4 result in a downstream steric effect which renders the alternative cleavage site refractory to proteolysis.

To further test the hypothesis that SLT 1 does not have an absolute requirement for proteolytic processing, a ricin A chain SLT 1 fusion protein was engineered. The creation of the fusion protein RASTA2 by PCR is described in Chapter 4. Ricin A chain is thought to remain intact during target cell intoxication and is characteristically insensitive to proteolysis *in vitro* (Chaddock *et al* (1995); Walker *et al* (1996)). The chimeric holotoxin produced in this study incorporates a full length ricin A chain followed by the A2 portion of SLT 1 excluding the protease sensitive loop region. The fused A chain is transcribed as a bicistronic message with SLT 1 B chain, the two translation products being targeted to the *Escherichia coli* periplasm where they associate to form holotoxin. In addition to information about proteolytic

processing this experiment provides the first direct evidence that the C-terminal 31 residues of SLT 1 A chain are sufficient for B chain association. The fact that the chimeric A chain can be purified using affinity chromatography specific for the B chain interaction shows that the A chain is associated with the B chain pentamer. In a similar manner to the experiments conducted using cholera toxin A2 fused with enzymatic markers such as maltose binding protein and bacterial alkaline phosphatase (Jobling and Holmes (1992)), the portion of SLT 1 A2 required for holotoxin assembly was identified.

Since the mutant toxin SLTP4 was cytotoxic in spite of protease resistance during intoxication it was predicted that the RASTA2 protein, designed to be refractory to proteolysis, would also be cytotoxic. This was the case, RASTA2 was an effective toxin giving an IC_{50} value of 7ng/ml after 3 hours and 0.3ng/ml after 6 hours.

The *in vivo* proteolytic processing of RASTA2 was examined using protein metabolically labelled with [^{35}S]-methionine. However the results from this experiment were rather poor since RASTA2 could not be obtained at a high specific activity. Figure 3.5.7 shows radio-labelled RASTA2 protein recovered from Vero cells after four and six hours. No cleavage of protein is seen over four hours. However there is evidence of cleavage after six hours. Unfortunately these results were obtained at the detection limits of the experiment (the autoradiograph pictured in figure 3.5.7 represents a three week exposure on hypersensitive film) and time

allowed the assay to be performed only once. However from these data it appears that RASTA2 is processed albeit slowly to a fragment of approximately 30kDa. This cleavage is only detected between four and six hours, a time point at which its likely that there is more than 80% cell death. If this is the case, the cleaved toxin recovered may be a result of exposure to a host of cellular proteases as the cell dies rather than proteolytic enzymes contained within the endocytic pathway. The observed cleavage of RASTA2 might therefore be a result of degradation rather than a specific proteolytic processing event leading to the production of a translocationally competent fragment. Finally, the chimeric A chain may be structurally unstable since its expression in *Escherichia coli* yields very small quantities of A chain but very large quantities of B chain with which it is co-expressed. This potential instability may account for its proteolysis.

To conclude it appears that SLT 1 does not require proteolytic processing in order to be cytotoxic. However the possibility remains that a very small fraction of both SLTP4 and RASTA2, which cannot be detected using the assays performed here becomes nicked during intoxication. Since the enzymatic activity of RASTA2 is greater than that of SLTP4 it was expected that this protein would have greater cytotoxicity. However this was not the case. One possible explanation of these data is that in the absence of proteolytic processing membrane translocation is impaired. If time had allowed further experiments, subcellular fractionation might have been

possible to see if these proteins are associated with membrane after time points where toxicity is seen. Again if time had allowed, isolation of proteolytic fragments from SLTP1 and SLTP3 followed by protein sequencing might have enabled the exact site of alternative processing to be assertained. The absence of a model *in vitro* translocation assay makes the study of the exact translocation requirements of SLT 1 difficult. One possible method of studying these cleavage-defective proteins *in vivo* might be to examine whether there is a preference for modification of bound ribosomes over free ribosomes. A differential preference for bound ribosomes might indicate that the toxin remains membrane associated. This is an assay under development at Warwick and may yield interesting information in the future. Precise evaluation of the enzymatic differences between SLT 1 and RASTA2 and ricin would also be useful in this study. For example, if the greater enzymatic activity of RASTA2 could be confirmed the lower cytotoxicity (even when RASTA2 is imported by the ST Gb_3 receptors) would suggest that membrane translocation of RASTA2 is severly impaired. Perhaps therefore A2 inhibits this process, or perhaps therefore RA translocation is less efficient than that of SLT *in vivo*.

The expression problems encoutered with RASTA2 might be overcome by a variety of methods. Substitution of the OmpF signal sequence with that of wild-type SLT 1 would be likely to increase the efficiency of targeting expressed protein to the periplasm in *Escherichia coli.* If RASTA2 is indeed structurally unstable then the use of a non-structured spacer arm between the folding domains of the RTA and SLT

components might help improve stability and as a result improve the yield of protein after expression. Since the large excess of SLT 1 B chain appears to drastically reduce the efficiency of iodination of the chimeric A chain, its removal by gel filtration would probably allow RASTA2 to be labelled to a specific activity which would allow *in vivo* proteolytic processing experiments to be carried out since RTA is routinely labelled with [^{125}I].

In the present study, attempts to demonstrate furin and calpain cleavage of SLT 1 and the mutants were also made. However the prepartions of furin and calpain used were old and seemingly inactive since cleavage of the wild-type SLT 1 could not be demonstrated. However with more time, investigation of the roles of these proteolytic enzymes *in vitro* could yield interesting information.

The study of proteolytic processing in several bipartite bacterial toxins such as PE and DT has led to the general conclusion that these toxins require proteolytic processing prior to translocation to the cytosol where they act on their cytosolic targets. It was previously considered that like PE and DT, SLT 1 / ST also required proteolytic activation as an essential step to render it cytotoxic. Studies where the protease-sensitive site of PE is disrupted, showed that toxicity is dramatically reduced. Jinno *et al* (1989) mutated arginine-276 and 279 of PE which resulted in reduction of cytotoxicity of 3-4 and 2.5 logs respectively. The cell binding, endocytosis and catalytic activities of these mutant toxins apparently remained the

same. Thus the lack of a toxic effect was thought to be a result of a block in proteolytic processing..In a later study, PE proteolytic processing was seen to be mediated between residues 279 and 280 (Ogata *et al* (1990)). Therefore it appears that mutation of residues 276-279 causes an effective block in an essential proteolytic activation step.

DT likewise has an absolute requirement for proteolytic processing (Sandvig and Olsnes (1981)). Cleavage after residue Arg-190 is probably the site at which proteolytic activation occurs (Moskaug *et al* (1988)). As previously discussed in section one, there are several other examples of bacterial toxins which must be activated by proteolysis. This activation can occur either during secretion from the producing organism or during transport within a target cell in order to be cytotoxic. In the present study, results are presented which suggest that unlike many other bacterial toxins SLT 1 does not require proteolytic activation in order to be cytotoxic. A protease-insensitive mutant toxin (SLTP4) described here, remains a potent toxin giving IC_{50} values just 65 fold less than the wild-type toxin. Since no cleavage fragment can be visually detected even after six hours of toxin exposure to Vero cells, it appears that SLT 1 can remain cytotoxic in the absence of proteolytic activation. This study provides the first evidence of a toxin with a bipartite A chain which is not seen to require proteolytic processing for cytotoxicity. The implication from this work is that a full length A chain (or possibly holotoxin) has the ability to translocate a membrane to gain entry to the cytosol (thought to be the ER, Sandvig *et*

al (1992)). The reduction in cytotoxicity seen may reflect a reduced competence for translocation.

Appendix 1

Alignment of the active site residues of SLT 1 A subunit (residues 138-210) with that of ricin A subunit (residues 149-218). Generated from the ALIGN program from Intelligenics. (Window length 20, word length 1, density at less, gap penalty 3) Identical residues are indicated by a closed circle chemically similar residues are indicated by a closed rectangle, dashes indicate gaps introduced into the sequence of ricin A chain. Calderwood *et al* (1990).

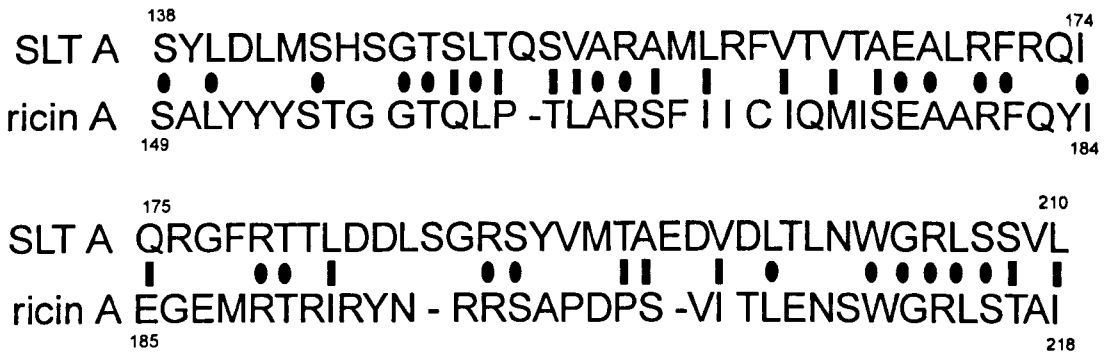

Appendix 2

The structure of Gb_3-Sepharose receptor analogue affinity matrix. Gb_3-Sepharose contains the trissacharide globotriose linked via a 6 carbon spacer arm to activated Sepharose-4B. The hatched line represents solid Sepharose support. Gb_3-Sepharose was a kind gift from Dr D. Muller (Warwick, UK).

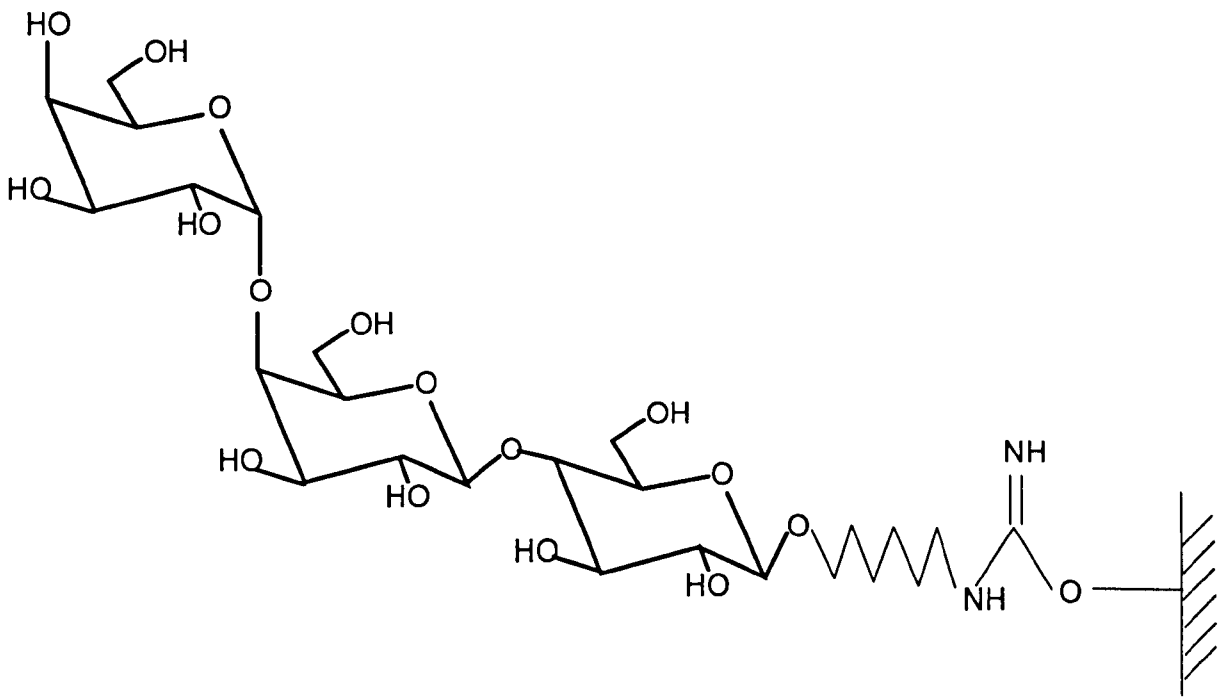

Appendix 3

Plasmid pKH206. Plasmid pKH206 contains the coding sequence of ricin A chain fused to the Omp F periplasmic signal sequence in the high level expression vector pKK223.3. Plasmid pKH206 was a kind gift from R. Argent (Warwick, UK). Argent *et al* (1994)

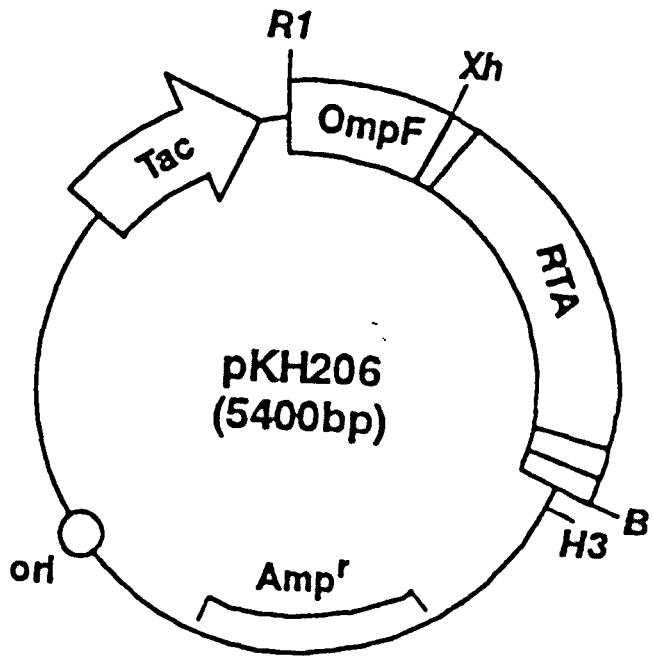

Appendix 4

Plasmid pSBC32. Plasmid pSBC32 contains the coding sequence of SLT 1 B chain in the high level expression vector pKK223.3. This plasmid was a kind gift from Dr SB Calderwood. Calderwood *et al* (1990)

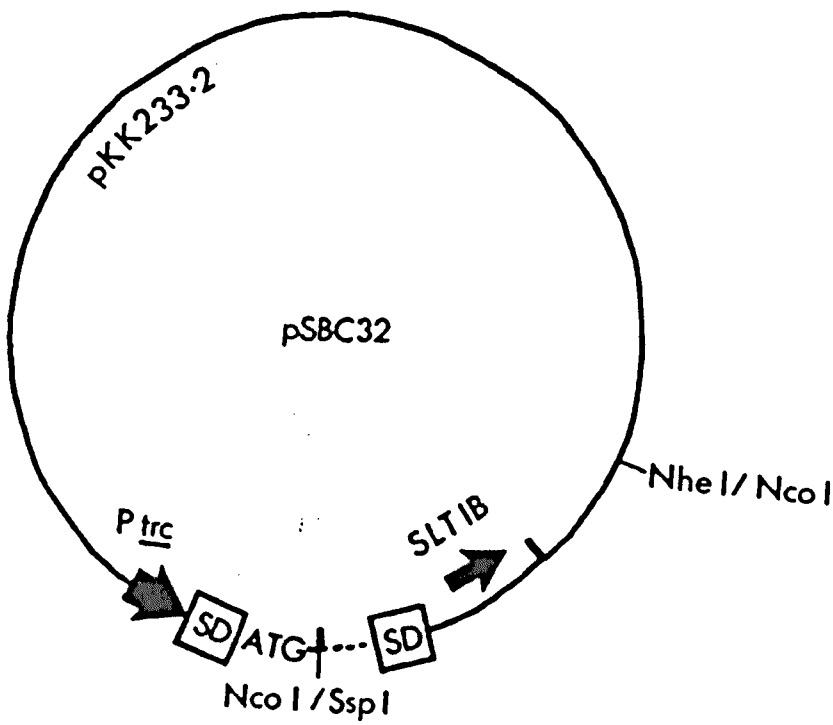

Appendix 5

DNA and amino acid sequences of the Shiga-like toxin 1 operon from *Escherichia coli* phage H19B. The Shine-Dalgarno sequences are indicated with diamonds. The proposed signal peptide cleavage sites are indicated by arrows. Numbers on the right of each row indicate amino acids those on the left indicate DNA bases. Active site residues are blocked. Calderwood *et al* (1990).

```
313
GCT CAA GGA GTA TTG TGT AAT ATG AAA ATA ATT ATT TTT AGA
                           Met Lys Ile Ile Ile Phe Arg -19
355
GTG CTA ACT TTT TTC TTT GTT ATC TTT TCA GTT AAT GTG GTG
Val Leu Thr Phe Phe Phe Val Ile Phe Ser Val Asn Val Val
- - - - - - - - - - - - - - - - - - - - - - - - - - - - -
GCG AAG GAA TTT ACC TTA GAC TTC TCG ACT GCA AAG ACG TAT
Ala Lys Glu Phe Thr Leu Asp Phe Ser Thr Ala Lys Thr Tyr  13
- - -
GTA GAT TCG CTG AAT GTC ATT CGC TCT GCA ATA GGT ACT CCA
Val Asp Ser Leu Asn Val Ile Arg Ser Ala Ile Gly Thr Pro  27
418
TTA CAG ACT ATT TCA TCA GGA GGT ACG TCT TTA CTG ATG ATT
Leu Gln Thr Ile Ser Ser Gly Gly Thr Ser Leu Leu Met Ile  41
523
GAT AGT GGC TCA GGG GAT AAT TTG TTT GCA GTT GAT GTC AGA
Asp Ser Gly Ser Gly Asp Asn Leu Phe Ala Val Asp Val Arg  55
565
GGG ATA GAT CCA GAG GAA GGG CGG TTT AAT AAT CTA CGG CTT
Gly Ile Asp Pro Glu Glu Gly Arg Phe Asn Asn Leu Arg Leu  69
607
ATT GTT GAA CGA AAT AAT TTA TAT GTG ACA GGA TTT GTT AAC
Ile Val Glu Arg Asn Asn Leu Tyr Val Thr Gly Phe Val Asn  83
649
AGG ACA AAT AAT GTT TTT TAT CGC TTT GCT GAT TTT TCA CAT
Arg Thr Asn Asn Val Phe Tyr Arg Phe Ala Asp Phe Ser His  97
691
GTT ACC TTT CCA GGT ACA ACA GCG GTT ACA TTG TCT GGT GAC
Val Thr Phe Pro Gly Thr Thr Ala Val Thr Leu Ser Gly Asp 111
733
AGT AGC TAT ACC ACG TTA CAG CGT GTT GCA GGG ATC AGT CGT
Ser Ser Tyr Thr Thr Leu Gln Arg Val Ala Gly Ile Ser Arg 125
775
ACG GGG ATG CAG ATA AAT CGC CAT TCG TTG ACT ACT TCT TAT
Thr Gly Met Gln Ile Asn Arg His Ser Leu Thr Thr Ser Tyr 139
817
CTG GAT TTA ATG TCG CAT AGT GGA ACC TCA CTG ACG CAG TCT
Leu Asp Leu Met Ser His Ser Gly Thr Ser Leu Thr Gln Ser 153
859
GTG GCA AGA GCG ATG TTA CGG TTT GTT ACT GTG ACA GCT GAA
Val Ala Arg Ala Met Leu Arg Phe Val Thr Val Thr Ala Glu 167
901
GCT TTA CGT TTT CGG CAA ATA CAG AGG GGA TTT CGT ACA ACA
Ala Leu Arg Phe Arg Gln Ile Gln Arg Gly Phe Arg Thr Thr 181
943
CTG GAT GAT CTC AGT GGG CGT TCT TAT GTA ATG ACT GCT GAA
Leu Asp Asp Leu Ser Gly Arg Ser Tyr Val Met Thr Ala Glu 195
985
GAT GTT GAT CTT ACA TTG AAC TGG GGA AGG TTG AGT AGC GTC
Asp Val Asp Leu Thr Leu Asn Trp Gly Arg Leu Ser Ser Val 209
1027
CTG CCT GAC TAT CAT GGA CAA GAC TCT GTT CGT GTA GGA AGA
Leu Pro Asp Tyr His Gly Gln Asp Ser Val Arg Val Gly Arg 223
1069
ATT TCT TTT GGA AGC ATT AAT GCA ATT CTG GGA AGC GTG GCA
Ile Ser Phe Gly Ser Ile Asn Ala Ile Leu Gly Ser Val Ala 237
1111
TTA ATA CTG AAT TGT CAT CAT CAT GCA TCG CGA GTT GCC AGA
Leu Ile Leu Asn Cys His His His Ala Ser Arg Val Ala Arg 251
1153
ATG GCA TCT GAT GAG TTT CCT TCT ATG TGT CCG GCA GAT GGA
Met Ala Ser Asp Glu Phe Pro Ser Met Cys Pro Ala Asp Gly 265
1195
AGA GTC CGT GGG ATT ACG CAC AAT AAA ATA TTG TGG GAT TCA
Arg Val Arg Gly Ile Thr His Asn Lys Ile Leu Trp Asp Ser 279
1237
TCC ACT CTG GGG GCA ATT CTG ATG CGC AGA ACT ATT AGC AGT
Ser Thr Leu Gly Ala Ile Leu Met Arg Arg Thr Ile Ser Ser 293
1279
TGA GGG GGT AAA ATG AAA AAA ACA TTA TTA ATA GCT GCA TCG
                Met Lys Lys Thr Leu Leu Ile Ala Ala Ser -10
1321
CTT TCA TTT TTT TCA GCA AGT GCG CTG GCG ACG CCT GAT TGT
Leu Ser Phe Phe Ser Ala Ser Ala Leu Ala Thr Pro Asp Cys   4
- - - - - - - - - - - - - - - - - - - - - - - - - - - - -
GTA ACT GGA AAG GTG GAG TAT ACA AAA TAT AAT GAT GAC GAT
Val Thr Gly Lys Val Glu Tyr Thr Lys Tyr Asn Asp Asp Asp  18
1405
ACC TTT ACA GTT AAA GTG GGT GAT AAA GAA TTA TTT ACC AAC
Thr Phe Thr Val Lys Val Gly Asp Lys Glu Leu Phe Thr Asn  32
1447
AGA TGG AAT CTT CAG TCT CTT CTT CTC AGT GCG CAA ATT ACG
Arg Trp Asn Leu Gln Ser Leu Leu Leu Ser Ala Gln Ile Thr  46
1489
GGG ATG ACT GTA ACC ATT AAA ACT AAT GCC TGT CAT AAT GGA
Gly Met Thr Val Thr Ile Lys Thr Asn Ala Cys His Asn Gly  60
1531
GGG GGA TTC AGC GAA GTT ATT TTT CGT TGA CTC AGA ATA GCT
Gly Gly Phe Ser Glu Val Ile Phe Arg ---
1573
CAG TGA AAA TAG CAG GCG GAG
```

References

Allured VS, Collier RJ, Carroll SF, McKay DB 1986 **Structure of Exotoxin A of *Pseudomonas aeruginosa* at 3.0 Angstrom resolution.** Proc Natl Sci USA **83** 1320-1324.

Argent R.1995 Personal communication.

Argent RH, Roberts LM, Wales R, Robertus JD, Lord JM. 1994 **Introduction of a disulphide bond into ricin A chain decreases the cytotoxicity of the ricin holotoxin.** J Biol Chem **269** 26705-26710.

Austin PR, Jablonski PE, Bohach GA, Dunker AK and Hovde CJ. 1994 **Evidence that the A2 fragment of Shiga-like toxin type 1 is required for holotoxin integrity.** Infect.Immum. **62** 1768-1775.

Barr PJ 1991 **Mammaliain subtilisins: the long-sought dibasic processing endoproteases** Cell **66** 1-3

Barr PJ, Mason OB, Landsberg KE, Wong PA, Kiefer MC, Brake AJ. 1991 **cDNA and gene structure for a human subtlisin-like protease with cleavage specificity for paired basic amino acid residues.** DNA and Cell Biol **10** 319-328.

Baldini MM, Kaper JB, Levine MM, Candy DCA, Moon HW 1983 **Plasmid-mediated adhesion in enteropathogenic *Escherichia coli*** J Pediatr Gastroenterol Nutr **2** 534-538.

Bennett MJ, Choe S, Eisenberg D 1994 **Refined structure of dimeric Diphtheria toxin at 2.0 angstrom resolution.**Protein Sci **3** 1444-1463.

Booth BA, Finkelstein MB, Finkelstein RA 1984 ***Vibrio cholerae* hemagglutinin/protease nicks cholera enterotoxin** Infec Immun **45** 558-560.

Bopp CA, Greene KD, Downes F,Sowers EG, Wells JG, Wachsmuth IK 1987 **Unusual verotoxin producing *Escherichia coli* associated with hemorrhagic colitis.**J clin Microbiol **25**. 1485-1489

Brennan SO, Peach RJ 1991 **The processing of the human proinsulin and chicken proalbumin by rat hepatic vesicles suggests a convertase specific for X-Y-Arg-Arg or Arg-X-Y-Arg sequences.** J biol Chem **266** 21504-21508.

Bresnaham PA, Leduc R, Thomas J, Thorner HL, Gibson AJ,Braake P, Barr J, thomas G. 1990. **Human fur gene encodes a yeast KEX2-like endoprotease that cleaves pro-beta-NGF in vivo.** J Cell Biol **111** 2851-2859.

Brown EJ, Ussery MA, Leppla SH, Rothman SW 1980 **Inhibition of protein synthesis by Shiga toxin.** FEBS lett **117** 84-88.

Burgess BJ and Roberts LM. 1993 **Proteolytic cleavage at arginine residues within the hydrophilic disulphide loop of the *Escherichia coli* Shiga-like toxin 1 A subunit is not essential for cytotoxicity.** Mol Microbiol **10** 171-179.

Calderwood SB, Auclair F, Donohue-Rolfe A,Keusch GT, Mekalanos JJ(1987) **Nucleotide sequence of the Shiga-like toxin genes of *Escherichia coli*** . Proc Natl Acad Sci USA **84** 4364-4368.

Calderwood SB, Acheson DW, Goldberg MB, Boyko SA, Donohue-Rolfe A. (1990) **A system for the production and rapid purification of large amounts of Shiga toxin / Shiga-like toxin 1 B subunit**. Infect Immun **58** 2977-2982.

Cater AO, Borczyk AA, Carlson JAK, Harvey B, Hockin JC, Karmali MA, Krishnan C, Kron DA, Lior H,(1987) **A severe outbreak of *Escherichia coli* 0157:H7 associated hemorragic colitis in a nursing home.** N. Engl J Med **317** 1496-1500

Carrol SF and Collier RJ 1987 **Active site of *Pseudomonas aeruginosa* exotoxin A. Glutamic acid 553 is photolabelled by NAD and shows functional homology with glutamic acid 148 of Diphtheria toxin.** J Biol Chem **262** 8707-8711.

Cavanagh, JB, Howard JG, Whitby JL 1956 **The neurotoxin of *Shigella shigae*. A comparative study of the effects produced in various laboratory animals.** Br J Exp Med **37** 272-278.

Chaddock JA, Roberts LM, Jungnickel B, Lord M. 1995 **A hydrophobic region of ricin A chain which may have a role in membrane translocation can function as**

an efficient noncleaved signal peptide. Biochem Biophys Reaseach Comm. **217** 68-73.

Chaudhary VK, Jinno Y, Fitzgerald D, Pastan I. 1990 ***Pseudomonas*** **exotoxin A contains a specific sequence at the carboxyl terminus that is required for cytotoxicity.** Proc Natl Acad Sci **87** 308-312.

Choe S, Bennett MJ, Fujii G, Curmi PMG, Kantardjeff KA, Collier RJ Eisenburg D 1992 **The crystal structure of diphtheria toxin.** Nature **357** 216-222.

Clements JD and Finkelstein RA 1979. **Isolation and characterization of homogenous heat labile enterotoxins with high specific activity from *Escherichia coli* cultures.** Infect Immun **24** 760-769.

Cohen A, Hannigan GE, Williams BRG, Lingwood CA. 1987 **Roles of globotriosyl- and galabiosylceramide in verotoxin binding and high affinity interferon receptor.**J Biol Chem **262** 17088-17091.

Collier RJ and Kandel J 1971 **Structure and activity and Diphtheria toxin** J Biol Chem **246** 1496-1503.

Cook JP, Savage PM, Lord M, Roberts LM. 1993 **Biologically active interleukin 2-ricin A chain fusion proteins may require intracellular proteolytic cleavage to exhibit a cytotoxic effect.** Bioconjugate Chem. **4** 440-447.

Coradi H (1903) **Ueber Iosliche durch asseptisch Autolyse erhltene Giftstoffe Von Ruhur- und Typhusbazillen.** Dtsch Med Wochenschr **29** 26-28.

Dallas WS and Falkow SLT 1980. **Amino acid sequence homology between cholera toxin ans *Escherichia coli* heat labile entero toxin.** Nature London **288** 499-501.

DeLange RJ, Drazin RE, Collier RJ 1976 **Amino acid sequence of fragment A, an enzymatically active fragment from Diphtheria toxin.** Proc Natl Sci USA **73** 69-72.

Deresiewicz RL, Calderwood SB, Robertus JD, Collier RJ 1992 **Mutations affecting the activity of the Shiga-like toxin 1 A chain.** Biochem **31** 3272-3280.

Deresiewicz RL, Austin PR, Hovde CJ 1993 **The role of tyrosine 114 in the enzymatic activity of Shiga-like toxin A chain.** Mol Gen Genet **241** 467-473.

van Deurs B, Sandvig K, Peterson OW, Olsnes S, Simons K, Griffiths G. 1988. **Estimation of the amount of internalized ricin that reaches the *trans*-Golgi network.** J Cell Biol. **106** 253-267.

van Deurs B, Peterson S, Olsnes S, Sandvig K. 1987. **Delivery of internalized ricin from endosomes to cisternal Golgi elements is a discontinuous temperature-sensitive process.** Exp Cell Res **171** 137-152

van Deurs B, Tonnessen TI,Peterson OW, Sandvig K, Olsnes S. (1986) **Routing of internalized ricin and ricin conjugates to the Golgi complex** J Cell Biol. **102** 37-47

Donohue-Rolfe A, Acheson D, Kane AV, Keusch GT 1989 **Purification of Shiga toxin and Shiga-like toxins I and II by receptor analog affinity chromatography with immobilized P1 glycoprotein and production of cross reactive monoclonal antibodies.** Infec Immun **57** 12 3888-3893.

Donohue-Rolfe A, Keusch GT, Edson C, Thorley-Lawson D, Jacewicz M, 1984 **Pathogenesis of shigella diarrhea IX Simplified high yeild purification of shigella cytotoxin and charaterisation of subunit composition and function by the use of subunit specific monoclonal and polyclonal antibodies.** J Exp Med **160** 1767-1781.

Donta ST, Poindexter NJ, Ginsberg BH 1982. **Comparison of the binding of cholera and *Escherichia coli* enterotoxins to Y1 adrenal cells.** Biochem **21** 660-664

DubosRJ, Geiger JW 1946 **Preparation and properties of Shiga toxin and toxoid.** J Exp Med **84** 143-156.

Dummont ME and Richards FM. 1988 **The pH dependent confirmational change of diphtheria toxin.** J Biol Chem **263** 2087-2097.

Endo Y, Mitsui K, Motizuki M, Tsutugi K 1987 **The mechanism of action of ricin and related toxins on eukaryotic ribosomes.** J Biol Chem **262** 5908-5912.

Endo Y, Tsurugi K, Yutsudo T Takeda Y, Ogasawara T, Igarashi K.1988 **Site of action of a vero toxin VT2 from *Escherichia coli* 0157:H7 and of Shiga toxin on**

eukaryotic ribosomes.RNA N-glycosidase activity of the toxins. Eur J Biochem **171** 45-50.

Falnes PO, Choe S, Madshus IH, Wilson BA, Olsnes S. 1994 **Inhibition of membrane translocation of diphtheria toxin A fragment by internal disulphide bridges.** J Biol Chem **269** 8402-8407.

Fiani ML, Blum JS, Stahl PD 1993 **Endosomal proteolysis precedes ricin A chain toxicity in macrophages.** Arch Biochem Biophys **307** 225-230

Finkelstein RA 1988 **Cholera, the cholera enterotoxins, and the cholera enterotoxin-related enterotoxin family** 85-101 In P. Owen and T. J. Foster (ed), Immunochemical and molecular genetic analysis of bacterial pathogens. Elsevier/North-Holand Science Publishing (Biomedical Division), Amsterdam.

Fisherman PH 1982. **Internalization and degradation of cholera toxin by cultured cells: relationship to toxin action.** J Cell Biol **93** 860-865.

Fontaine A, Arondel J, Sasonetti PJ 1988 **The role of Shiga toxin in the opathogenosis of bacilliary dysentry studied using a tox- mutant of *Shigella dysenteriae* 1** Infect Immun **56** 3099-3109.

Fraser ME, Chernaia MM, Kozlov YV, James MNG (1994) **Crystal structure of the holotoxin from *Shigella dysenteriae* at 2.5 A resolution.** Struc Biol **1** 59-64.

Fredlander AM. 1986 **Macrophages are sensitive to anthrax lethal toxin through an acid-dependant process.** J Biol Chem **261** 7123-7126.

Freedman RB, 1989 **Protein disulphide Isomerase: multiple roles in the modification of nascent secretory proteins.** Cell **57** 1069-1072.

Fryling C, Ogata M, FitzGerald D. 1992 **Characterisation of a cellular protease that cleaves *Pseudomonas* exotoxin** Infect Immun **60** 497-502.

Furutani M, Kashiwagi K, Ito K, Endo Y, Igarashi K 1992 **Comparison of the modes of action of a Vero toxin (a Shiga-like toxin) from *Escherichia coli* , of ricin and of α-sarcin.** Arch Biochem Biophys **239** 1 140-146

Fujiwara T, Oda K, Yokota S, Takatski A, Ikehara Y 1988 **Brefeldin A causes disassembly of the Golgi complex and accumulation of secretory proteins in the ER.** J Biol Chem **263** 18545-18552

Garred O, Dubinina Escherichia coli, Holm KP, Olsnes S, Deurs BV, Kozlov J, Sandvig K. 1995a **Role of processing and intracellular transport for optimal toxicity of Shiga toxin and toxin mutants.** Exp Cell Res **218** 39-49.

Garred O, Deurs B, Sandvig K. 1995b. **Furin-induced cleavage and activation of Shiga toxin.** J Biol Chem **270** 10817-10821.

Gething MJ and Sambrook, J 1992 **Protein folding in the cell** Nature **355** 33-45.

Gill DM and Dinius LL 1971 **Observations on the structure of Diphtheria toxin.**J Biol Chem **246** 1485-1491

Gilman AG 1984 **Guanine nucleotide-binding regulatory proteins and dual control of adenylate-cyclase.** J Clin Invest **73** 1-4

Gordon VM, Klimple KR, Arora N, Henderson MA, Leppla SH. 1995 **Proteolytic activation of bacterial toxins by eukaryotic cells is performed by furin and by additional cellular proteases.** Infect Immun **63** 1 82-87.

Gordon VM, Leppla SH, Hewlett EL 1988. **Inhibitors of receptor-mediated endocytosis block entry of *bacillus anthracis* adenylate cyclase toxin but not *Bordetella pertussis* adenylate cyclase toxin** Infect Immun **56** 1066-1069.

Grant CCR, Messer RJ, Cieplak W Jr.1994 **Role of trypsin like cleavage at arginine 192 in the enzymatic and cytotoxic activities of *Escherichia coli* heat labile enterotoxin.** Infect Immun **62** 4270-4278.

Guidi-Rontani C 1992 **Cytotoxic activity of recombinant chimeric protein between *Pseudomonas aeruginosa* exotoxin A and *Corynebacterium diphtheriae* diphtheria toxin** Mol Microbiol **6** 1281-1287.

Haddad JE, Jackson MP 1993 **Identification of the Shiga toxin A subunit residues required for holotoxin assembly.**J Bacteriol. **175** 7652-7657

Haddad JE, Al-Jaufy A, Jackson MP 1993 **Minimum domain of the Shiga toxin A subunit required for enzymatic activity.** J Bacteriol. **175** 4970-4978

Hart JP, Monzingo AF, Donohue-Rolfe A, Keusch GT, Caldwerwood SB, Robertus JD 1991 **Crystallization of the B chain of Shiga-like toxin 1 from *Escherichia coli.*** J Mol Biol **218** 691-694.

Hovde CJ, Calderwood SB, Mekalanos JJ, Collier RJ 1988 **Evidence that glutamic acid 167 is an active-site residue of Shiga-like toxin 1** Proc Natl Acad Sci **85** 2568-2572.

Howard JG 1955 **Observations on the intoxication produced in mice and rabbits by the neurotoxin of *Shigella shigae.*** Br J Exp pathol **36** 439-446.

Hunt CM, Harvey JA, Youngs ER, Irwin ST, Reid TM 1989 **Clinical and pathological variability of infection by enterhaemorrhagic (Vero cytotoxin producing) *Escherichia coli* .** J Clin Pathol **42** 847-852.

Hwang J, FitzGerald DJ, Adhya S, Pastan I 1987 **Functional domains of *Pseudomonas* exotoxin identified bydeletion analysis of the gene expressed in *E.coli*** Cell **48** 129-136.

Inocencio NM, Moehring JM, Moehring TJ.1994 **Furin activates *Pseudomonas* exotoxin by specific cleavage *in vivo* and *in vitro.*** J Biol Chem **269** 50 31831-31835.

Jacewicz M, Clausen H, Nudelman E, Donohue-rolfe A, Keusch GT 1986 **Pathogenesis of *Shigella* diarrhea.XI. Isolation of a *Shigella* toxin-binding**

glycolipid from rabbit jejunum and HeLa cells and its identification as globotriaosylceramide. J Exp Med **163** 1391-1404.

Jackson MP, Neil RJ, Obrien AD, Holmes RK, Newland JW 1987 **Nucleotide sequence analysis and comparison of the structural genes for Shiga-like toxin I and Shiga-like toxin II encoded by bacteriophages from *Escherichia coli* 933.** FEMS Microbiol Lett **44** 109-114.

Jackson MP,Wadolkowski EA, Weinstein DL, Holmes RK, O'Brien AD 1990 **Functional analysis of the Shiga toxin and Shiga-like toxin type II variant binding subunits by using site directed mutagenesis.** J Bact **172** 2 653-658.

Jiang JX, Abrams FS, London Escherichia coli. 1991 **Folding changes in membrane -inserted DT that may play important roles in it's translocation.** Biochemistry **30** 3857-3864.

Johnson WM, Lior H, Bezanson GS, 1983 **Cytotoxic *Escherichia coli* 0157:H7 associated with haemorrhagic colitis in Canada.** Lancet **1** 76

Johnson VG, Nicholls PJ, Habig WH, Youle RJ.1993 **The role of proline 345 in diphtheria toxin translocation.** J Biol Chem **268** 3514-3519.

Jobling MG and Holmes RK. 1992 **Fusion proteins containing the A2 domain of cholera toxin assemble with B polypeptides of cholera toxin to form immunoreactive and functional holotoxin-like chimeras.** Infec Immun **60** 11 4915-4924.

Karmali MA, Steele BT, Petric M, Lim C 1983 **Sporadic cases of hemolytic uremic syndrome associated with fecal cytotoxin and cytotoxin producing bacteria *Escherichia coli.*** Lancet **1** 619-620.

Keenan KP, Sharpnack DD, Collins H, Formal SB, O'Brien AD 1986 **Morphologic evaluation of the effects of Shiga toxin and *Escherichia coli* Shiga-like toxin on the rabbit intestine .** Am J Pathol **125** 69-80.

Keusch GT, Grady GF, Mata LJ, Mclver J 1972 **The pathogenesis of *Shigella* diarrhea.1. Enterotoxin production by *Shigella dysenteriae* 1** J Clin Invest **51** 1212-1218.

Kiarash A, Boyd B, Lingwood CA 1994 **Glycospingolipid receptor function is modified by fatty acid content.**J Biol Chem. **269** 111138-111146.

Klimple KR, Molly SS, Thomas G, Leppla SH. 1992 **Anthrax toxin protective antigen is activated by a cell surface protease with the sequence specificity and catalytic properties of furin.** Proc Natl Sci USA **89** 10277-10281.

Kongmuang U, Honda T, Miwatini T. 1988 **Effect of nicking on Shiga-like toxin 1 of Enterhaemorrhagic *Escherichia coli*** FEMS Microbiol letts **56** 105-108.

Konowalchuk J, Speirs JI, Stavric S 1977 **Vero response to a cytotoxin of *Escherichia coli* .** Infect Immun **18** 775-779.

Laemmeli 1970 **Cleavage of structural proteins during assembly of the head of bacteriophageT4** Nature **227** 680-685.

Leppla SH, Martin OC, Muehl LA 1978 **The exotoxin of *P. Aeruginosa*: A proenzyme having an unusual mode of activation.** Biochem Biophys Res Commun **81** 532-538.

Leppla SH, Friedlander AM, Cora E. 1988 **Proteolytic activation of anthrax toxin bound to cellular receptors**. Bacterial protein toxins. Gustav Fisher, New York. *In* Fehrenbach F, Alouf JE, Falmaagene P, Goebel W, Jeljaszewicz J, Jurgen D and Rappouli R,(ed). 111-112

Leppla SH. 1991 **The anthrax toxin complex** Sourcebook of bacterial protein toxins. Acedemic Press London *In* J Escherichia coli Alouf and J H freer (ed.).

Lewis MJ and Pelham HRB 1990 **A human homologue of the yeast HDEL receptor** Nature **348** 162-163

Lewis MJ and Pelham HRB 1992 **Sequence of a second Human KDEL receptor.** J Mol Biol **226** 913-916.

Lewis MJ, Sweet DJ, Pelham HRB 1990 **The *ERD2* gene determines the specificity of the luminal ER protein retention system.** Cell **61** 1359-1363

Lingwood CA, Law H, Richardson S, Petric M, Brunton J, De Grandis S, Karmali M. 1987 **Glycolipid binding of purified and recombinant *Escherichia coli* produced vero toxin *in vitro*.** J Biol Chem **262** 8834-8839.

Lippincott-Schwartz J, Yuan LC, Bonifacino JS, Klausner RD. 1989 **Rapid redistribution of Golgi proteins into the ER in cells treated with brefeldin A :Evidence for membrane cycling from Golgi to ER.** Cell **56** 801-813.

Lord JM, Roberts LM, Robertus JD.1994 **Ricin: structure, mode of action, and some current applications.** FASEB J **8** 201-208

Lory S and Collier RJ. 1980 **Expression of enzymatic activity by exotoxin A from *Pseudomonas aeruginosa.*** Infect Immun **28** 494-501.

Ljungh A, Erickson M, Erickson O, Henter JI, Wadstrom T 1988 **Shiga-like toxin production and connective tissue protein binding in *Escherichia coli* isolated from a patient with ulcerative colitis.** Scand J Infect Dis **20** 443-446

Maniatis T, Fritsch ES, Sambrook J, 1989 **Molecular cloning: A laboratory manual.** Cold Spring Harbor Laboratory, NY.

May MJ, Hartley MR, Roberts LM, Krieg PA, Osborn RW, Lord JM. 1989 **Ribosome inactivation by ricin A chain: a sensitive method to assess the activity of wild-type and mutant polypeptides.** EMBO J **8** 301-308.

Mekalanos JJ, Collier RJ, Romig WR 1979 **Enzymic activity of cholera toxin. II. Relationships to proteolytic processing, disulphide bond reduction, and composition.** J Biol Chem **254** 5855-5861.

Merril CR, Goldman D, Sedman SA, Ebert MH. 1981 **Ultrasensitive stain for proteins in polyacrylamide gels shows regional variation in cerebrospinal fluid proteins.** Science **211** 1437-1438.

Michel A, Zanen J, Monier C, Crispeels C, Dirkx J 1972 **Partial characterization of Diphtheria toxin and its subunits.** Biochem Biophys Acta **257** 249-256.

Milne JC and Collier RJ. 1993 **pH-dependant permiabilization of the plasma-membrane of mammalian-cells by anthrax toxin protective antigen.** Mol Microbiol **10** 647-653.

Misumi Y, Oda K, Fujiwara T, Takami N, Tashiro K, Ikehara Y 1991. **Functional expression of furin demonstrating its intracelluar localisation and endoprotease activity for processing of proalbumin and complement pro-C3.**J Biol Chem **266** 16954-16959

Moehring JM, Inocencio NM, Robertson BJ, Moehring TJ. 1993 **Expression of mouse furin in a Chinese hamster cell resistant to *Pseudomonas* exotoxin A and viruses complements the genetic lesion.** J Biol Chem **268** 4 2590-2594.

Montford W, Villafranca JE, Monzingo AF, Ernst SR, Katzin B, Rutenber E, Xuong NH, Hamlin R, Robertus JD 1987 **The three dimensional structure of ricin at 2.8 A.** J Biol Chem **262** 5398-5403.

Morris RE, Gerstein AS, Bonventre PF, Saelinger CB 1985 **Receptor mediated entry of DT into monkey kidney (Vero) cells : Electron microscopic evaluation** Infect Immun **50** 721-727.

Moskaug JO, Stenmark H, Olsnes S. 1991 **Insertion of Diphtheria toxin B-fragment into the plasma membrane at low pH.** J Biol Chem **266** 2652-2659.

Munro S and Pelham HRB. 1987 **A C-terminal signal prevents secretion of luminal ER proteins.** Cell **48** 899-907.

Murachi T. 1983 **Calpain and calpastatin** TIBS May 167-169.

Newton DL, Wales R, Richardson PT, Walbridge S, Saxena sk, Acherman EJ, Roberts LM, Lord JM, Youle RJ. 1992 **Cell surface and intracellular functions for ricin galactose binding** J Biol Chem **267** 11917-11922.

O'Brien AD, Newland JW, Miler SF, Holmes RK, Smith HW, FormalSB 1984 **Shiga-like toxin-coverting phages from *Escherichia coli* strains that cause hemorrhagic colitis or infantile diarrhea.** Science **226** 694-696.

O'Brien AD, Lively TA, Chen ME, Rothman SW, Formal SB 1983 ***Escherichia coli* 0157:H7 strains associated with haemorrhagic colitis in the United States produce *Shigella dysenteriae* 1 (Shiga) like cytotoxin.** Lancet **1** 702.

O'Brien AD and La Veck GD 1982 **Immunochemical and cytotoxic activities of *Shigella dysenteriae* (Shiga) and Shiga-like toxins.** Infect immun **35** 1151-1154.

O'Brein AD, LaVeck GD, Thompson MR, Formal SB 1982b **Production of *Shigella dysenteriae* type 1-like cytotoxin by *Escherichia coli*.** J Infect Dis **146** 763-769.

Ogata M, Chaudhary VK, Pastan I, FitzGerald DJ 1990 **Processing of *Pseudomonas* exotoxin by a cellular protease results in the generation of a 37,000Da toxin fragment that is translocated to the cytosol.** J Biol Chem **265** *20678-20685.*

O'Hare M, Brown AN, Hussain K, Gebhardt A, Watson G, Roberts LM, Vitetta ES, Thorpe PE, Lord MJ. **Cytotoxicity of recombinant ricin A-chain fusion protein containing a proteolytically-cleavable spacer sequence.** FEBS **273** 200-204.

Olsnes S, and Pihl A 1976 **Abrin, ricin and their associated agglutinins**, in the specificity of the action of animal, bacterial and plant toxins (Cuatrecases P, ed), 129-173 Chapman and Hall, London.

Olsnes S and Sandvig K. 1985 in Endocytosis (Pastan I and Willingham MC eds.) Plenum press New York 195-234.

Olsnes S and Pihl 1982 **Toxic lectins and related proteins, in molecular action ot toxins and viruses** (Cohen and van Heyringen eds.), 51-105 Elevier, Amsterdam.

Olsnes S, Reisbig R, Eiklid K 1981 **Subunit structure of shigella cytotoxin.** J biol Chem **256** 8732-8738

Osborn RW and Hartley MR 1990 **Dual effects of ricin A chain on protein synthesis in rabbit reticulocyte lysate.** Eur J Biochem **193** 401-407.

Pelham HRB 1988 **Evidence that luminal ER proteins are sorted from secreted proteins in a post-ER compartment.** EMBO **7** 913-918

Pelham HRB.1990 **The retention signal for soluable proteins of the endoplasmic reticulum.** TIBS **15** 483-486.

Pelham HRB, Roberts LM, Lord JM. 1992 **Toxin entry: how reversible is the secretory pathway?** TICBs **2** 183-185.

Pellizzari A, Pang H, Lingwood CA 1992 **Binding of Verocytotoxin 1 to its receptor is influenced by differences in receptor fatty acid content.** Biochem **31** 1363-1370.

Peter F, Van P,Soling H-D. 1992 **Different sorting of Lys-Asp-Glu-Leu proteins in rat liver.** J Biol Chem. **267** 10631-10637.

Phaedria M, Hilaire St., Boyd MK, Toone EJ 1994 **Interaction of the Shiga-like toxin type 1 B-subunit with its carbohydrate receptor.** Biochemistry **33** 14452-14463.

Pickett CL, Twiddy EM, Cokes C, Holmes RK. 1989 **Cloning, nucleotide sequence and hybridization studies of the type II heat-labile enterotoxin gene of *Escherichia coli.*** J Bacteriol **171** 5180-5187.

Prior TI, Fitzgerald DJ, Pastan I. 1992 **Translocation mediated by domain II of *Pseudomonas* exotoxin A: Transport of barnase into the cytosol.** Biochem **31** 3555-3559.

Rappaport RS, Sagin JF, Pierzchala WA, Bonde G, Rubin BA, Tint H 1976 **Activation of heat labile *Escherichia coli* enterotoxin by trypsin.** J Infect Dis **133** (suppl.) 41-54.

Reisbig R, Olsnes S, Eiklid K 1981 **The cytotoxic activity of *Shigella* toxin.**J Biol Chem **256** 8739-8744.

Riley LW, Remis RS, Helgerson SD, McGee HB, Wells JG, Davis BR, Herbert RJ, Olcott ES, Johnson LM, Hargrett NT, Blake PA, Cohen ML 1983 **Hemorrhagic colitis associated with a rare *Escherichia coli* serotype.** N Engl J Med **308** 681-685.

Rutenber Escherichia coli, Katzin BJ, Ernst S, Collins EJ, Mlsna D, Ready MP and Robertus JD 1991 **Crystallographic refinement of ricin to 2.5 A.** Proteins **10** 240-250.

Ryd M, Alfredson H, Blomberg L, Anderson A, Lindberg AA 1989 **Purification of Shiga toxin by α-D-galactose-(1→4)-β-D-galactose-(1→4)-β-D-gucose-(1→) receptor ligand-based chromatography** FEBS **258** 2 320-322.

Samuel JE and Gordon VM 1994 **Evidence that proteolytic separation of Shiga-like toxin type IIv A subunit into A1 and A2 subunits is not required for toxin activity.** J Biol Chem **269** 4853-4859.

Sandvig K and Olsnes S 1980 **Diphtheria toxin entry into cells is facilitated by low pH.**J Cell Biol **87** 828-832.

Sandvig K and Olsnes S 1981 **Rapid entry of nicked diphtheria toxin into cells at low pH. Characterisation of the entry process and effects of low pH on the toxin molecule.** J Biol Chem **256** 9068-9076.

Sandvig K, Sudan A, Olsnes S. 1984 **Evidence that diphtheria toxin and modeccin enter the cytosol from different vesicular compartments** J Cell Biol. **98** 963-970.

Sandvig K, Ryd M, Garred O, Schweda E, Holm PK, van Deurs B 1994 **Retrograde transport from the Golgi complex to the ER of both Shiga toxin and the nontoxic Shiga B-fragment is regulated by butyric acid and cAMP.** J Cell Biol **126** 53-64

Sandvig K, Olsnes S, Brown EJ, Peterson OW, Deurs B. 1989 **Endocytosis from coated pits of Shiga toxin: A glycolipid-binding protein from *Shigella dysenteriae* 1** J Cell Biol. **108** 1331-1343.

Sandvig K and Olsnes 1982. **Entry of the toxic proteins abrin, modeccin, ricin and diphtheria toxin into cells. Effect of pH, metabolic inhibitors and ionophores and evidence for toxin penetration from endocytotic vesicles** J Biol Chem **257** 7504-7513.

Sandvig K, Tonnessen TI, Olsnes S. 1986 **Ability of inhibitors of glycosylation and protein synthesis to sensitize cells to abrin, ricin shigella toxin and pseudomonas toxin.** Cancer Res **46** 6418-6422.

Sandvig K, Prydz K, Hansen SH, van Deurs B.1991 **Ricin transport in BFA-treated cells : Correlation between Golgi structure and toxic effect.** J Cell Biol. **115** 971-981.

Sandvig K, Prydz K, Ryd M, van Deurs B. 1991b **Endocytosis and intracelluar transport of the glycolipid-binding ligand Shiga toxin in polarized MDCK cells.** J Cell Biol. **113** 553-562.

Sandvig K, Garred O, Prydz K, Koziov JV, Steen, Hansen H, van Deurs B. 1992 **Retrograde transport of endocytosed Shiga toxin to the endoplasmic reticulum.** Nature **358** 510-511.

Sansonetti PJ, 1991 **Genetic and molecular basis of epithelial cell invasion by *Shigella* species** Rev Infect Dis [Suppl 4] S285-S292.

Schalken JA, Roebroek AJM, Oomen PPCA, Wagenaar SS, Debruyne FMJ, Bloemers HPJ, van de Ven WJM 1987 **Fur gene expression as a discriminatory marker for small cell and nonsmall cell lung carcinomas.** J Clin Invest **80** 1545-1549.

Scotland SM, Smith HR, Rowe B.1985 **Two distinct toxins active on Vero cells from *Escherichia coli* 0157** [letter] Lancet **2** 885-886.

Semenza JC, Harwick KG, Dean N, Pelham HRB 1990 ***ERD2*, a yeast gene reqired for the receptor-mediated retrieval of luminal ER proteins from the secretory pathway.** Cell **61** 1349-1357

Shen WH, Choe S, Eisenberg D, Collier RJ 1994 **Participation of lysine 516 and phenylananine 530 of diphtheria toxin in receptor recognition.** J Biol Chem **269** 29077-29084.

Siegall CB, Ogata M, Pastan I, FitGerald D 1991 **Analysis of sequences in domain II of *Pseudomonas* exotoxin A which mediate translocation.** Biochem **30** 7154-7159.

Simpson JC, Lord JM, Roberts LM 1995 **Point mutations in the hydrophobic C-terminal region of ricin A chain indicate that Pr 250 plays a key role in membrane translocation** Eur J Biochem **232** 458-463.

Simpson JC, Dascher C, Roberts LM, Lord JM, Balch WE. 1995 **Ricin cytotoxicity is sensitive to recycling between the endoplasmic recticulum and the Golgi complex.** J Biol Chem **270** 20078-20083.

Singh Y, Chaudhary VK, Leppla SH 1989 **A deleted variant of *Bacillus anthracis* protective antigen is non-toxic and blocks anthrax toxin action *in vivo*.** J Biol Chem **264** 19103-19107.

Sixma TK, Pronk SE Kalk KH, van Zanten BAM, Berghuls AM, Hol WGJ 1992 **Lactose binding to heat-labile enterotoxin revealed by X-ray crystallography.** Nature **355** 561-564.

Sixma TK, Pronk SE, Kalk KH, Wartna ES, van Zanten BAM, Witholt B, Hol WGJ 1991 **Crystal structure of a cholera toxin-related heat-labile enterotoxin from *E.coli*.** Nature **351** 371-377.

Sixma TK, Stein PE, Hol WGJ,Read RJ 1993 **Comparison of the B-pentamers of heat-labile enterotoxin and verotoxin-1: Two structures with remarkable similarity and dissimilarity.** Biochem **32** 191-198.

Spangler BD and Westbrook EM 1989 **Crystallization of isoelectrically homogenous cholera toxin.** Biochem **28** 1333-1340.

Stein PE, Boodhoo A, Tyrrell GJ, Brunton JL, Read RJ (1992) **Crystal structure of the cell-binding B oligomer of verotoxin 1 from *Escherichia coli*** . Nature **355** 748-750.

Stillmark H 1888 **Uber ricin, eine gifiges ferment aus den samen von Ricinus communis L. und anderen euphorbiaceen.** Inaugural dissertation, University of Dorpat, Estonia.

Strockbine NA, Jackson MP, Sung LM, Holmes RK, O'Brien AD 1988 **Cloning and sequencing of the genes for shiga toxin from *Shigella dysenteriae* type 1** J Bacteriol **170** 1116-1122.

Strockbine NA, Marques LRM, Newland JW, Smith HW, Holes RK, O'Brien AD 1986 **Two toxin converting phages from *Escherichia coli* 0157:H7 strain 933**

encode antigenically distinct toxins with simlar biological activities. Infect Immun **53** 135-140.

Takao T, Tanabe T, Hong Y-M, Shimonishi Y, Kurazono H, Yutsudo T, Sasakawa C. 1988 **Identity of molecular structure of Shiga-like toxin 1 (VT1) from *Escherichia coli* 0157:H7 with that of Shiga toxin.** Microbial Patho **5** 357-369.

Thompson MR, Steinberg MS, Gemski P, Formal SB, Doctor BP 1976 **Inhibition of *in vitro* protein synthesis by *Shigella dysenteriae* 1 toxin.** Biochem Biophys Res Commun **71** 783-788.

Tsuji T, Honda T, Miwatani T. 1984 **Comparison of the effects of nicked and unnicked *Escherichia coli* heat labile enterotoxin on Chinese hamster ovary cells.** Infect Immun **46** 1 94-97.

Tsuneoka M, Nakayama K, Hatsuzawa K, Komada M, Kitamura N, Mekada E. 1993 **Evidence for the involvement of furin in the cleavage and activation of Diphtheria toxin.** J Biol Chem **268** 26461-26465.

Tyrrell GJ, Ramotar K, Toye B, Lingwood CA, Brunton JL 1992 **Alteration of the carbohydrate binding specificity of vero toxins from Galα1-4Gal to GalNAcβ1-3Galα1-4Gal and vice versa by site directed mutagenesis of the binding subunit.** Proc Natl Acad Sci **89** 524-528

Van Ness BG, Howard JB, Bodley JW 1980 **ADP-ribosylation of elongation factor 2 by Diphtheria toxin.** J Biol Chem **255** 10710-10716

Vitetta ES 1986 **Synergy between immunotoxins prepared with native ricin A chain and chemically modified ricin B chains.** J Immunol **136** 1880-1887.

Von Wolfen H, Russmann H, Karch H, Meyer T, Bitzan M, Kohrt TC, Aleksic S 1989 **Vero cytotoxin-producing *Escherichia coli* 02:H5 isolated from patients with ulcerative colitis** Lancet **1** 1449-1450

Waddell T,Head S, Petric M, Cohen A, Lingwood C 1988 **Globotriosyl ceramide is specifically recognised by the *Escherichia coli* vero cytotoxin 2.** Biochem Biophys Res Commun **152** 674-679.

Wales R, Chaddock JA, Roberts LM, Lord JM. 1992 **Addition of an ER retention signal to the ricin A chain increases the cytotoxicity of the holotoxin.** Exp Cell Res **203** 1-4.

Wales R, Roberts LM, Lord JM 1993 **Addition of an endoplasmic reticulum retrieval sequence to ricin A chain significantly increases its cytotoxicity to mammalian cells.** J Biol Chem **268** 23986-23990.

Walker D, Chaddock AM, Chaddock JA, Roberts LM, Lord MJ, Robinson C. 1996 **Ricin A chain fused to a chloroplast-targetting signal is unfolded on the chloroplast surface prior to import across the envelope membranes.** J Biol Chem **271** 1-4

Watanabe T,Murakami K, Nakayama K 1993 **Positional and additive effects of basic amino acids on processing of precursor proteins within the constitutive secretory pathway.** FEBS lett **320** 215-218

Well JG, Davis BR, Wachsmuth IK, Riley LW, Remis Rs, Sokolow R, Morris GK 1983 **Laboratory investigation of hemorrhagic colitis outbreaks associated with a rare *Escherichia coli* serotype** J Clin Microbiol **18** 512-520.

Youle RJ and Neville DM 1982 **Kinetics of protein synthesis inactivation by ricin-anti-Thy 1 antibody hybrids.** J Biol Chem **157** 1598-1600.

Youle RJ and Colombatti 1987 **Hybridoma cells containing intracellular anti ricin antibodies show ricin meets secretory antibody before entering the cytosol.** J Biol Chem **262** 4676-4682.

Yoshida T, Chen C, Zhang M, Wu HC. 1991 **Disruption of the Golgi apparatus by brefeldin A inhibits the cytotoxicity of ricin, modeccin and *Pseudomonas* exotoxin.** Exp Cell Res **192** 389-395.

Zhang R, Scott D, Westbrook M, Nance S, Spangler B, Shipley G, Westbrooke E. 1995 **The three-dimensional crystal structure of Cholera toxin.** J Mol Biol **251** 563-573.